Characterizing Permafrost in the Entire European Alps: Spatial Distribution and Ice Content

Dissertation
zur
Erlangung der Naturwissenschaftlichen Doktorwürde
(Dr. sc. nat.)

vorgelegt der
Mathematisch-naturwissenschaftlichen Fakultät
der
Universität Zürich

von

Lorenz Böckli
von
Winterthur

Promotionskomitee
Prof. Dr. Wilfried Haeberli (Vorsitz)
Dr. Stephan Gruber (Leitung der Dissertation)
Dr. Jeannette Nötzli
Prof. Dr. Alexander Brenning

Zürich 2013

Summary

Permafrost is a subsurface phenomenon existing in cold mountain regions. It influences ecosystems, hydrology, mechanical properties of the subsurface and sediment transport. The practical relevance of permafrost research in the European Alps is given by the construction and maintenance of infrastructure in permafrost zones and the assessment and prevention of permafrost-related natural hazards. Permafrost is generally invisible at the terrain surface and direct observation via satellite imagery is impossible. Therefore, modeling approaches are required to spatially map permafrost and analyze its characteristics. However, mountain permafrost is characterized by a high spatial variability caused by topography, surface and subsurface characteristics, which make observation and modeling of permafrost challenging.

The aim of this thesis is to characterize permafrost for the entire Alps using widely applicable methods, which allow comparable permafrost analyses, which are compatible between regions. This requires an Alpine-wide collection of permafrost evidence data, where local data sets are compiled in a standardized database. Based on that, a permafrost distribution model was developed that a) distinguishes between different surface types, b) accounts for the spatial extrapolation of model results to settings (topography and surface characteristics) where no calibration data is available, and c) addresses scaling issues, which are required if different sub-models rely on different spatial resolutions or if the model prediction is performed for another resolution than the model calibration. This modeling approach was used to provide the first fully consistent permafrost distribution map for the European Alps. Additionally, the total permafrost ice content in the Alps was estimated as a first step towards the understanding of permafrost hydrology in a changing climate.

Currently, the Alpine permafrost evidence inventory contains 408 evidence points and polygon information of 4795 rock glaciers. The compiled point evidence is biased towards permafrost existence and unbalanced with respect to surface and ground characteristics. However, it allows new insights because large environmental gradients are covered that cannot be analyzed using local inventory data. The rock glacier inventories provide a comprehensive source indicating permafrost absence/presence. The

permafrost distribution model is based on a statistical approach that distinguishes between the two surface domains debris cover and steep bedrock. For each domain a regression model was developed with the explanatory variables mean annual air temperature, incoming solar radiation and precipitation. Temperature offset terms are used to extrapolate to other spatial domains, where no calibration data is available. The predicted permafrost index values describe qualitatively the probability of permafrost occurrence in a permafrost map. Low index values represent locations where permafrost only occurs in very favorable condition, whereas high index values represent grid cells with permafrost in nearly all conditions. Local modifying variables and processes such as the effect of the snow cover on the thermal regime of the ground can not all be accounted for in such a modeling approach. Therefore, we designed an interpretation key that allows the map-user to account for these and to refine the shown estimate of permafrost index values on the map. The map has a grid spacing of approximately 30 m and covers the entire Alps. The results reveal that the area underlain by permafrost is larger than the glacial coverage in the Alps and is estimated to be in the order of 6000 km^2.

The estimation of the permafrost ice content for an entire mountain range is challenging because information of subsurface characteristics is rare and needs to be spatially extrapolated. According to our analysis, the total water content of permafrost ice in the European Alps is about 26 km^3, which is approximately one quarter of the total water equivalent of the glacier ice in 2003.

In order to enhance the possibilities for model calibration and quantitative evaluation, further efforts are required to coordinate permafrost observations in the European Alps and to compile local permafrost observations into an Alpine-wide database. The combination of statistical-empirical and physically-based modeling approaches offers new possibility for applying complex models to an entire landscape and thus, to enhance the possibilities of mapping and characterizing permafrost for large areas.

Zusammenfassung

Permafrost ist ein weit verbreitetes Untergrundphänomen in Gebirgen wie den europäischen Alpen und beeinflusst Ökosysteme, hydrologische und mechanische Eigenschaften des Untergrunds sowie den Sedimenthaushalt. Permafrost ist relevant für die Planung und den Erhalt von Infrastrukturbauten, und die Beurteilung sowie Prävention von Naturgefahren. Da das Untergrundphänomen nicht direkt an der Erdoberfläche sichtbar ist, sind Untersuchungen dazu im Gelände mit grossem Aufwand verbunden. Zudem ist die räumliche Variabilität von Permafrost in Gebirgen sehr gross, was die Extrapolation von Beobachtungen und Messungen erschwert.

Das Ziel dieser Arbeit war es, die Verbreitung von Permafrost mit einem einheitlichen Modellansatz für die gesamten europäischen Alpen abzuschätzen. Dazu wurden lokale Messungen und Beobachtungen in einem alpenweiten Inventar zusammengefasst. Basierend auf diesem Inventar konnte ein Modell zur Verbreitung von Permafrost erstellt werden. Der in dieser Arbeit entwickelte Modellansatz berücksichtigt a) die Unterscheidung verschiedener Oberflächentypen, b) die räumliche Extrapolation von Modellvorhersagen in Gebiete, wo keine Kalibrierungsdaten vorhanden sind, und c) skalenabhängige Lösungsansätze. Letztere werden benötigt, wenn die einzelnen Teilmodelle auf unterschiedlichen räumlichen Auflösungen basieren oder die Modellkalibrierung mit einer anderen Auflösung durchgeführt wurde als die Modellanwendung. Das im Rahmen dieser Arbeit erstellte Modell bildet die Grundlage für die erste Permafrostkarte für den gesamten Alpenraum. Basierend auf dieser Karte wurde zudem der totale Eisgehalt des Permafrosts in den Alpen abgeschätzt. Diese Abschätzung entspricht einem ersten wichtigen Schritt, um die hydrologischen Aspekte von Permafrost für eine gesamte Gebirgsregion besser zu verstehen.

Das alpenweite Inventar für Permafrostdaten, welches im erweiterten Rahmen dieser Arbeit zusammengestellt wurde, beinhaltet Daten von insgesamt 408 Punktbeobachtungen und Polygonen von 4795 Blockgletschern. Insgesamt gibt es mehr Beobachtungen über die Präsenz von Permafrost als über dessen Absenz, und die Verteilung der Beobachtungen mit Blick auf die Oberflächeneigenschaften ist unausgewogen. Trotzdem liefert dieses Inventar wertvolle neue Erkenntnisse, da erstmals einheitliche Analy-

sen über den gesamten Alpenraum möglich sind. Insbesondere die Blockgletscherinventare bieten flächendeckend einen relativ guten Hinweis zur Verbreitung von Permafrost.

Das statistische Permafrostmodell differenziert zwischen den zwei Oberflächentypen Schutt und steiler Fels. Für beide Oberflächen wurde ein Regressionsmodell gerechnet mit den folgenden erklärenden Variablen: mittlere jährliche Lufttemperatur, einfallende kurzwellige Solarstrahlung und jährliche Niederschlagsmenge. Temperaturoffsets werden verwendet, um die Modellergebnisse auf Gebiete, wo keine Kalibrierungsdaten vorhanden sind, zu extrapolieren. Die Permafrostkarte verwendet Indexwerte, welche qualitativ die Wahrscheinlichkeit von Permafrostvorkommen beschreiben. Kleine Indexwerte beschreiben Flächen, wo Permafrost nur unter sehr günstigen Bedingungen vorkommt. Hohe Indexwerte beschreiben Geländezellen, wo Permafrost unter fast allen Bedingungen existiert. Nicht alle lokalen Effekte, die einen Einfluss auf den Permafrost ausüben, konnten im Modell berücksichtigt werden (z.B. Einfluss der Schneedecke). Die Legende und der Interpretationsschlüssel versuchen dem Rechnung zu tragen, indem die wichtigsten lokalen Einflüsse erklärt werden, was dem Kartennutzer erlaubt, die geschätzten Indexwert in der Karte den lokalen Gegebenheiten entsprechend anzupassen. Die Abschätzung des Eisgehalts im Permafrost für eine komplette Gebirgskette ist anspruchsvoll, da die wenigen Informationen, die es zu Untergrundeigenschaften gibt über grosse Regionen extrapoliert werden müssen. Hinzu kommt die grosse Unsicherheit der räumlichen Verbreitung von Permafrost. Basierend auf unseren Modellrechnungen, beträgt das Wasseräquivalent von Permafrosteis in den europäischen Alpen 24–28 m^3, was ungefähr einem Viertel des Wasseräquivalents der Gletscher entspricht.

Um in Zukunft die Möglichkeiten für die Kalibrierung und Validierung von Permafrostmodellen zu verbessern, ist eine gute Koordination zwischen den verschiedenen Forschergruppen in den Alpen wichtig. Die Kombination von statistisch-empirischen und physikalisch basierten Modellansätzen ermöglicht neue Ansätze, um komplexe Modelle auf eine ganze Region anzuwenden und deshalb den Permafrost für eine grosse Region besser zu charakterisieren.

Contents

Part I Synopsis

Part II Research papers

Part III Appendix

List of figures

List of tables

Abbreviations

ALT	Active Layer Thickness
APIM	Alpine Permafrost Index Map
ASTER GDEM	ASTER Global DEM
AUROC	Area Under the Receiver Operating Characteristic Curve
BTS	Bottom Temperature of Snow (normally refers to a method, cf. *Haeberli*, 1973)
DEM	Digital Elevation Model
GCM	Global Circulation Model
GCS	Geographic Coordinate System
GIS	Geographic Information System
GLM	Generalized Linear Model
GLMM	Generalized Linear Mixed Model
GST	Ground Surface Temperature
MAAT	Mean Annual Air Temperature
MAGT	Mean Annual Ground Temperature
MAGST	Mean Annual Ground Surface Temperature
MARST	Mean Annual Rock Surface Temperature
PISR	Potential Incoming Solar Radiation
RCM	Regional Climate Model
RMSE	Root Mean Square Error
TTOP	Temperature at the Top Of Permafrost
TWE	Total Water Equivalent

Part I

Synopsis

1 Introduction

1.1 Motivation

Permafrost is a widespread phenomenon not only in high-latitude regions, but also at high elevations in mountain areas such as the European Alps (*Haeberli et al.*, 2011). It affects ecosystems (*Yang et al.*, 2010), the hydrology (*Hinzman et al.*, 2003) and the mechanical properties of the subsurface (*Arenson and Springman*, 2005). The high sensitivity of mountain permafrost to climate change (*Haeberli et al.*, 2011) leads to changes in permafrost conditions, which can affect river runoff, water supply, and landscape stability (*IPCC*, 2007). Among the most important implications for human beings in mountainous areas are a) problems in engineering of infrastructure in seasonally or perennially frozen ground (e.g., *Bommer et al.*, 2010), b) permafrost related natural hazards (e.g., *Haeberli*, 1992), and c) river runoff and water supply (e.g., *Woo et al.*, 2008). In a mountain range, it is therefore desirable to know where permafrost is present and what its thermal condition and ice content is. Permafrost as a thermal subsurface phenomenon is invisible and field evidence is generally rare or expensive. Therefore, suitable modeling tools are essential to analyze the spatial, thermal and mechanical characteristics of permafrost.

Permafrost studies in the European Alps usually focus on single countries or regions, but large parts of the Alps have not been addressed yet. The related modeling ap-

proaches are regionally calibrated and applied and rely on differing methods, which makes it impossible to compile them into an Alpine-wide characterization of permafrost. Therefore, a uniform characterization of permafrost in the Alps is required to make permafrost analyses comparable and compatible between regions.

1.2 Objectives and related research questions

This thesis focuses on permafrost characterization in the entire European Alps. The aim is to obtain a spatially continuous estimate of permafrost distribution using uniformly applicable methods and to provide the first Alpine permafrost distribution map. Additionally, the permafrost ice content of the European Alps is estimated, which is important to further analyze the relevance of permafrost on river runoff and water supply in a changing climate. The following three objectives were defined to achieve this:

A Assemble existing permafrost evidence for the European Alps in order to characterize permafrost for a large area and to provide a uniform Alpine-wide database for model calibration and evaluation.

B Model the spatial distribution of permafrost in the European Alps and provide an Alpine permafrost map.

C Estimate total permafrost ice content in the European Alps.

For each objective research questions are formulated. Objective A is important because an Alpine-wide collection of permafrost data is missing and it forms the basis to reach objective B and C. The main research question for objective A is:

> *A1: What are the most relevant evidence types and which information per evidence type is required for an Alpine-wide permafrost inventory, which serves to a) increase knowledge of spatial permafrost distribution, and b) provide a solid basis for model calibration and evaluation?*

Because permafrost is generally invisible, modeling is required to map its spatial distribution. The research questions for objective B are:

> *B1: How can the permafrost distribution be estimated for the entire European Alps?*
>
> *B2: What kind of legend and interpretation key is suitable to communicate the estimated permafrost distribution and its uncertainties in a map-based product?*

The estimation of total water equivalent of Alpine permafrost requires a simple but robust framework that deals with the involved assumptions and uncertainties. The following research question is defined for objective C:

> *C1: What is the permafrost ice content of the European Alps and which are the most important parameters of such an estimation?*

1.3 Structure of thesis

This thesis is divided into three parts:

Part I provides a synopsis of the entire thesis. After this introduction, the relevant scientific background is reviewed in Chapter 2, where an overview of the main characteristics of permafrost is given, permafrost field evidence are introduced and main modeling approaches are described. At the end of Chapter 2, needs, which are identified based on reviewing the permafrost literature are formulated. Chapter 3 describes the main methods that were applied and Chapter 4 summarizes the most important results. Both, Chapters 3 and 4 summarize the research conducted in the journal papers (*Part II*). A generic discussion of the applied methods and the obtained results is given in Chapter 5. Finally, Chapter 6 concludes *Part I*. Here the research questions from the Introduction are revisited, the main findings are drawn and an outlook is given.

Part II contains the four journal papers, which constitute the main research of this thesis. For each journal paper the main contributions of the author are summarized at the beginning. *Publication I* describes the compilation of the Alpine permafrost evidence inventory. In *Publication II* the uniform statistical framework to estimate permafrost distribution in the Alps is introduced. *Publication III* applies the permafrost distribution model to the Alps and presents the final Alpine Permafrost Index Map. In the last *Publication (IV)*, the total permafrost ice content for the European Alps is estimated.

Part III consists of a personal bibliography, curriculum vita and acknowledgments.

2 Background

2.1 Definition and relevance of permafrost

Permafrost is defined as ground that remains at or below $0\,^{\circ}\mathrm{C}$ for at least two consecutive years (*van Everdingen*, 1998), irrespective of the presence or absence of ice. Problems of the definition of permafrost arise especially in continental climates where the distinction of permafrost and glacier is not always obvious, because transitions of cold/polythermal glaciers, ice-cored moraines and perennially frozen sediments are possible (*Kneisel et al.*, 2000a, *Haeberli et al.*, 2006). In mountain areas such as the European Alps, permafrost is characterized by a high spatial variability, caused by effects of mountain topography (e.g., *Gruber and Haeberli*, 2007), surface characteristics (e.g., *Gubler et al.*, 2011, *Schneider et al.*, 2012) and ground properties (e.g., *Hanson and Hoelzle*, 2005, *Schneider et al.*, 2012). Topography and surface characteristics largely control microclimate and snow cover characteristics, which both influence the thermal regime of the ground significantly (*Hanson and Hoelzle*, 2005, *Luetschg et al.*, 2004, *Haeberli et al.*, 2011, *Apaloo et al.*, 2012) and thus contribute to the spatial variability of permafrost characteristics.

The uppermost ground layer above permafrost is the *active layer*. Here, the ground thaws during summer due to seasonal air temperature variations. By definition, this layer does not belong to the *permafrost*, which starts directly underneath the active layer

and reaches from the *permafrost table* to the *permafrost base*. Detailed overviews of permafrost related terms are given by *Williams and Smith* (1989), *Osterkamp and Burn* (2003).

The phenomenon of permanently frozen ground has been known in the arctic for many centuries, but the first written reference dates back to 1598 (*Danilov* 1990, cited in *Dobinski* 2011). The expansion of infrastructure (e.g., military installations, petroleum exploration, mining) resulted in an increased understanding of basic and engineering knowledge from polar and arctic permafrost studies (e.g., *Black*, 1954, *French*, 2007). In the late 1970s, the Proceedings of the International Permafrost Conferences started to contain papers about permafrost in mid-latitude/high-altitude mountain regions (e.g., *Barsch*, 1978, *Gorbunov*, 1978, *Haeberli*, 1978, *Harris and Brown*, 1978), which signaled the essential beginning of systematic research on permafrost in high-mountain areas (*Haeberli et al.*, 2011). Since then, permafrost research in mountain regions was rapidly intensified.

Permafrost is relevant in many high-mountain regions. The main points are summarized below (partly based on *Noetzli*, 2008):

- Permafrost is an important landscape feature in the Alps that alters the sediment transfer budget (*Nyenhuis*, 2005, *Etzelmüller and Frauenfelder*, 2009) and influences geomorphic processes. Important geomorphological features in the Alps that are related to permafrost are a) rock glaciers (e.g., *Barsch*, 1977, *Haeberli et al.*, 2006), b) push-moraines (e.g., *Haeberli*, 1979, *Kneisel*, 2004), and c) ice faces and hanging glaciers (*Alean*, 1985, *Haeberli and Alean*, 1985).
- Construction and maintenance of infrastructure in high-alpine environments requires special adaptation to perennially frozen ground (*Keusen and Haeberli*, 1983, *Haeberli*, 1992, *Phillips*, 2006, *Wu et al.*, 2008, *Bommer et al.*, 2010). Changes in ground conditions, caused by the degradation of permafrost, can induce differential settlement by soil creep and deformation (*Harris et al.*, 2009) and lead to high maintenance costs (*Bommer et al.*, 2010).
- The main permafrost related concerns with respect to natural hazards are a) the destabilization of debris slopes by warming or degrading permafrost that possibly increase the amount of erodible ground material for debris slopes (*Haeberli*, 1992, *Rebetez et al.*, 1997, *Kneisel et al.*, 2007), and b) permafrost related slope instabilities of steep bedrock and related rock fall activity (*Fischer et al.*, 2006, *Gruber and Haeberli*, 2007, *Ravanel et al.*, 2010, *Fischer et al.*, 2012).
- The hydrological significance of permafrost and the related effects of climate change on the changing discharge of large rivers is important (*Ballantyne*, 1978, *Woo and Winter*, 1993, *Woo et al.*, 2008, *Ye et al.*, 2009, *Niu et al.*, 2011) and alters the sediment transfer budget of high-alpine catchments (*Etzelmüller and Frauenfelder*, 2009).

- Current permafrost temperatures or geomorphological landscape features can be used to estimate past climatic conditions (*Frauenfelder et al.*, 2001, *Mottaghy and Rath*, 2006). The interpretation of borehole temperature in mountainous terrain, however, is challenging because the climatic signal can be disturbed by three-dimensional topographical and transient effects (*Kohl*, 1999, *Gruber et al.*, 2004b, *Noetzli and Gruber*, 2009). Additionally, changes and variations in local surface conditions make it difficult to link directly changes in permafrost temperatures to changes in climate (*Smith and Riseborough*, 1996).

2.2 Controlling variables and processes of permafrost

Permafrost and its characteristics are governed by a variety of processes and their interactions at and below the Earth's surface. The **thermal regime at the surface** is controlled by the energy balance that involves incoming and outgoing short-, longwave radiation, sensible heat flux, latent heat flux, ground heat flux and latent heat (details are given by *Oke*, 1988, *Williams and Smith*, 1989). Besides regional patterns, air temperature in mountain areas is generally a function of elevation and mainly influences the sensible heat flux and the longwave radiation. The spatial distribution of mountain permafrost is strongly related to slope, aspect and shading effects, which primarily control incoming shortwave radiation and lead to strong spatial heterogeneity (e.g., *Allen et al.*, 2009). In steep bedrock, differences in north-south exposed slopes result in differences in mean annual ground surface temperatures (MAGST) similar to those of 1000 m elevation change (*Gruber et al.*, 2004a). For shallow slopes, the effect of aspect angle is much less pronounced due to a smaller differentiation of the incoming solar radiation.

Surface characteristics, such as the albedo (e.g., *Williams and Smith*, 1989, *Hall et al.*, 2005), the vegetation coverage (*Dingman and Koutz*, 1974, *Luthin and Guymon*, 1974, *Yi et al.*, 2007), the grain size of surface material (*Gubler et al.*, 2011) are relevant for the thermal regime at the surface. The latter plays a key role in the thermal regime of many rock glaciers and talus slope, where a coarse blocky surface layer leads to a cooling effect of the ground (e.g., *Humlum*, 1997, *Harris and Pedersen*, 1998, *Gorbunov et al.*, 2004, *Delaloye and Lambiel*, 2005, *Hanson and Hoelzle*, 2005, *Haeberli et al.*, 2006, *Gruber and Hoelzle*, 2008). A number of processes may be responsible for the cooling effect of coarse blocks (details are given by *Harris and Pedersen*, 1998, *Gruber and Hoelzle*, 2008, *Juliussen and Humlum*, 2008) and ground temperatures of coarse blocks can be up to 7 °C colder in comparison to finer grained material (*Harris and Pedersen*, 1998).

Additionally, ground surface temperatures are strongly dependent on snow cover parameters such as timing, duration, thickness, accumulation and melting processes (*Good-*

rich, 1982, *Zhang*, 2005). Snow is characterized by a low thermal conductivity and thus acts as an insulator between the atmosphere and the ground. Here, the thickness of the snow cover (cf. *Luetschg et al.*, 2008), the date of first significant snowfall in autumn and the melt-out date in late spring or summer are important and control if the snow cover has a cooling or warming effect on ground surface temperature relative to air temperature. Situations at the foot of slope below avalanche detachment zones are often covered by an insulating snow cover until late spring, which leads to permafrost favorable conditions (*Haeberli*, 1975). The high albedo of snow leads to a reduction in the absorbed solar energy (*Zhang*, 2005). This can cause a cooling effect on the ground's thermal regime for situations with a thin snow cover (*Keller and Gubler*, 1993, *Hasler et al.*, 2011b) or for steep rock walls (*Pogliotti*, 2010). During the snowmelt process, latent heat is released and acts as a heat sink (*Goodrich*, 1982, *Zhang*, 2005). The release of latent heat has also been observed during strong rain events in winter, when rain water percolates to the bottom of the snow pack and refreezes (*Westermann et al.*, 2011). A coarse blocky ground surface layer can lead to the formation of funnels in the snow cover allowing for heat exchange between the active layer and cold winter atmosphere (*Bernhard et al.*, 1998, *Harris and Pedersen*, 1998).

The above summarized effects at the terrain surface are responsible for the surface offset (Fig. 2.1), which is the difference of MAGST and mean annual air temperature (MAAT) (*Smith and Riseborough*, 2002, *Hoelzle and Gruber*, 2008). The variability in MAGST that is related to effects of topography and surface characteristics results in approximately 6 °C (*Gubler et al.*, 2011).

The **thermal regime at depth** is mainly controlled by ground surface temperatures, ground characteristics and the ground heat flux from the earth's interior. In many permafrost-modeling studies, conduction is assumed to be the most important transfer mechanism of heat. If we assume uniform ground conditions, a one-dimensional heat flow from the Earth interior to the surface and a sinusoidal surface temperature variation as upper boundary condition, ground temperature (G_T) at any depth (z) and any time (t) can be approximated using an analytical solution to the heat conduction equation (*Ingersoll et al.*, 1954):

$$G_T(z,t) = Ts + (Q_g/K)z + A_s e^{-z\sqrt{\omega/2\kappa)}} sin\Big[\omega t - \Big(\frac{\omega}{2\kappa}\Big)^{1/2} z\Big], \tag{2.1}$$

where Ts is the surface temperature, Q_g the geothermal heat flux (W m^{-2}), K the thermal conductivity (W K^{-1} m^{-1}), κ the thermal diffusivity ($m^2 s^{-1}$), and t the time in seconds counted from the date in spring when the surface temperature wave passes through its mean annual value. The surface wave is given by the amplitude A_s (°C) of

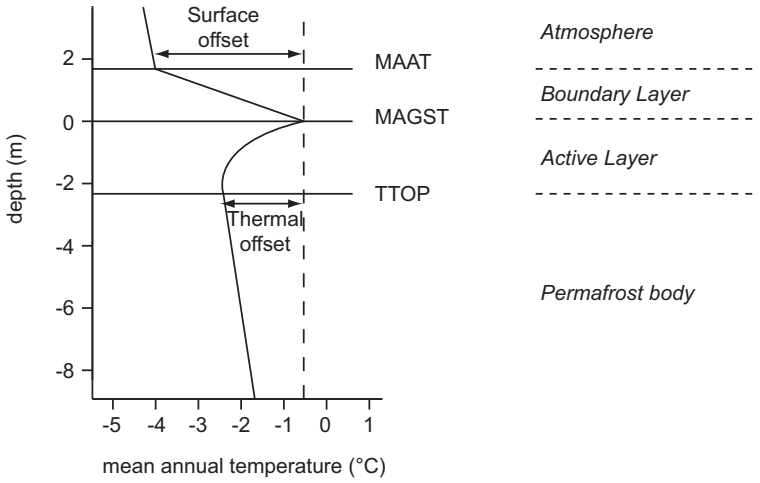

Figure 2.1: *Schematic mean annual temperature profile through the surface boundary layer, showing the relation between air temperature and permafrost temperature (modified from* Smith and Riseborough, *2002). The boundary layer alters the surface offset and is characterized by snow cover, vegetation and surface characteristics.*

the temperature wave, the period of the wave ω (s^{-1}, i.e. $\omega = 2\pi/31536000$ s for one year), and describes the seasonal temperature variations at the surface. In Eq. (2.1), entirely uniform ground conditions are assumed. This condition is rarely met in reality because the thermal properties of a ground normally vary with depth, moisture conditions and temperatures (*Williams and Smith*, 1989). This is especially true in the active layer, where freezing and thawing occurs and thus, the thermal properties of a ground can change significantly with small changes in temperatures.

Another analytical equation that is often used in permafrost modeling is the Stefan Solution (*Lunardini*, 1991) to the moving freezing or thaw front (e.g., *Nelson et al.*, 1997, *Anisimov et al.*, 2002, *Zhang et al.*, 2005). The Stefan Solution is a special case of the Neumann Problem (Neumann 1860 in *Lunardini*, 1991) where phase change position is analyzed in systems with plane interfaces in a homogenous medium close to the melting point (*Lunardini*, 1991). A simplified solution of the Stefan Problem is given by *Hinkel and Nicholas* (1995), where the active layer thickness (ALT) is:

$$ALT = \sqrt{\frac{2K}{L\rho\Theta_o}}\sqrt{ADDT}. \tag{2.2}$$

L is the latent heat of melting of water, ρ is the density of ice, Θ_o is the soil porosity, and $ADDT$ is the accumulated degree-days of thaw. In this model, $ADDT$ is a partial temperature integral over time, calculated by summing the average daily temperatures (°C)

from the beginning of the surface thaw (i.e., 0 °C) in spring to the end of surface thaw in autumn, which ignores possible diurnal thaw events. In the Stefan model (Eq. 2.2) the thickness of the active layer is mainly dependent on thermal conductivity, soil porosity, ice content and the temperature signal from the surface.

The temperature at the top of the permafrost body (TTOP, Fig. 2.1), is widely used to analyze climate-permafrost interactions (*Smith and Riseborough*, 1996, *Juliussen and Humlum*, 2007, *Riseborough*, 2007). The thermal offset (Fig. 2.1) arises because the thermal conductivity of the ground is greater in frozen state than when thawed and is strongly influenced by moisture status (*Smith and Riseborough*, 1996). The effect of latent heat is especially important for ice-rich permafrost because of the required energy for ice-melt. As a consequence, the degradation of ice-rich permafrost close to 0 °C is slowed down significantly (*Romanovsky et al.*, 2010) and thus, the ability to see changes in permafrost from changes in ground temperature is reduced. In addition the temperature at depth is strongly dependent on three-dimensional topographical and transient effects in high mountain environments (*Kohl*, 1999, *Gruber et al.*, 2004b, *Noetzli and Gruber*, 2009). This can result in permafrost conditions at depth, where surface temperatures do not indicate it, and is a relic of colder conditions in the past (e.g., little ice age) and/or colder adjacent ground temperatures. In steep topography, multi-lateral warming (lateral heat flux between different warm mountain sides) accelerates the pace of a surface temperature signal penetrating the subsurface (*Noetzli and Gruber*, 2009). Next to conductive heat transport, advective heat transport caused by the movement of fluids into and within frozen soils can be important to the thermal regime of the ground (*Kane et al.*, 2001, *Scherler et al.*, 2010). In steep bedrock, percolating water in fractures may be significant for the temporal regime of the ground and its stability (*Davies et al.*, 2001, *Gruber and Haeberli*, 2007, *Hasler et al.*, 2011a).

2.3 Evidence and monitoring of permafrost

In general, permafrost evidence can be separated into *direct evidence* and *indirect evidence*. Borehole temperatures are the most common direct permafrost evidence and allow for a given location and time interval to determine permafrost presence or absence, active layer depth (e.g., *Harris and Isaksen*, 2008) and permafrost base (if the borehole is deep enough). If the drilling core is available, information of the internal structure such as volumetric ice content or grain size distribution can be analyzed (*Vonder Mühll et al.*, 2000, *Isaksen et al.*, 2003). In the framework of "Permafrost and climate in Europe" (PACE), six 100 m deep boreholes were drilled on a north-south transect in Europe (*Harris et al.*, 2009). Additionally, several less deep boreholes exist in the Alps (e.g., *Arenson*

et al., 2002, *Luetschg et al.*, 2004, *Hanson and Hoelzle*, 2005, *PERMOS*, 2010, *Schneider et al.*, 2012). Other direct evidence is generally rare and includes natural outcrops, such as detectable ground ice in rock fall detachment zones (an overview for the European Alps is given by *Gruber and Haeberli*, 2007) and outcrops due to human construction work (e.g., *Keusen and Haeberli*, 1983, *Haeberli*, 1992, *Wegmann and Keusen*, 1998).

Indirect evidence includes a) geophysical investigations (reviews are given by *Vonder Mühll et al.*, 2000, *Kneisel et al.*, 2008, *Hauck*, submitted), b) detection of surface movement (e.g., *Kääb et al.*, 1997, *Strozzi et al.*, 2004, *Janke*, 2005, *Kääb*, 2008), c) measurements of proxy variables such as the basal temperature of snow (BTS, *Haeberli*, 1973, *Hoelzle*, 1992, *Lewkowicz and Ednie*, 2004, *Brenning et al.*, 2005) or ground surface temperature (GST, e.g., *Heggem et al.*, 2006, *Hoelzle and Gruber*, 2008, *Gubler et al.*, 2011), and d) mapping and observing of permafrost indicators such as intact rock glaciers (*Barsch*, 1978, *Lilleoren and Etzelmüller*, 2011) or hanging glaciers (*Alean*, 1985, *Haeberli et al.*, 1997, *Gruber and Haeberli*, 2007). Many rock glacier inventories exist in the Alps, from which the most comprehensive data in the scope of permafrost distribution mapping is available. This is because rock glaciers are well visible geomorphological features that can spatially be mapped over large areas using air/satellite imagery (*Janke*, 2001, *Lehmkuhl et al.*, 2003, *Nyenhuis et al.*, 2005, *Brenning et al.*, 2007, *Lilleoren and Etzelmüller*, 2011). In other regions, also other indicators for present or former permafrost exist: pingos (*Gurney*, 1998), palsas (*Gurney*, 2001, *Luoto and Seppälä*, 2002), ice wedges and other periglacial landforms (*Matsuoka*, 2001b, *Grosse et al.*, 2005). Even on Mars, permafrost related features have been mapped by remote sensing (*Mahaney et al.*, 2007).

Long-term permafrost monitoring is important to improve the knowledge-base of current permafrost conditions, related processes and to analyze climate change effects. The global network for permafrost monitoring is the Global Terrestrial Network for Permafrost (GTN-P, `http://www.gtnp.org`) that was initiated by the International Permafrost Association (IPA) and contains amongst others the Circumpolar Active Layer Monitoring Network (CALM, e.g., *Tarnocai et al.*, 2004). In 1995, "Priorities for the Global Geocryological Database", were released by the IPA (Table 1 in *Heginbottom*, 1995): Observation parameters were ranked with different priorities for a) process understanding, b) engineering design, c) global climate model validation, d) change detection, and e) impact evaluation. According to *Heginbottom* (1995), important parameters for monitoring are: permafrost extent, permafrost thickness, active layer thickness, ground ice content, spatial displacement, ground temperature, and moisture content.

2.4 Permafrost distribution modeling

A model is a conceptual or mathematical representation of a phenomenon (*Riseborough et al.*, 2008). The value of a model depends on its applicability for a given purpose and not its sophistication. Thus, complex models are not per se more useful than simple ones, especially when calibration and test data are limited. The choice of a modeling approach depends on the scale of interest (or level of detail), the knowledge and relevance of involved processes, available calibration and evaluation data, and acquirable computational resources.

Permafrost modeling is important because permafrost as a subsurface phenomenon is in general invisible and its detection based on remote sensing (e.g., *Burke et al.*, 2012) is difficult, especially for mountainous areas. Additionally, field evidence is sparse and generally expensive in realization. Where no field evidence is available, models are the only tools to estimate current permafrost conditions. In general, permafrost models can be separated into statistical-empirical and physics-based approaches. Overviews of permafrost models are given by *Etzelmüller et al.* (2001a), *Hoelzle et al.* (2001), *Riseborough et al.* (2008), and *Harris et al.* (2009).

2.4.1 Statistical-empirical models

Statistical-empirical models relate permafrost occurrence to topoclimatic variables, such as elevation, slope angle, aspect angle, MAAT, or potential incoming solar radiation (PISR). The advantage of these models is that in general only a few input parameters are required, the computational requirements are limited and the testing and evaluation of such models is relatively straightforward. As a basis such models require permafrost evidence data for calibration. The statistical and empirical relationships act as proxies for the most important processes of the energy balance at the surface or heat transfer in the ground. In mountainous regions, statistical-empirical models are often used to spatially predict permafrost occurrence.

One of the first empirical permafrost models for mountain permafrost is known as the "rules of thumb" (*Haeberli*, 1975), which are based on a simple energy balance approach and use basic relations of permafrost occurrence to topographic attributes, surface characteristics and snow redistribution. The availability of digital elevation models (DEM) in the early 1990's, allowed the implementation of these rules in a GIS and to spatially predict permafrost over wide areas (PERMAKART, *Keller*, 1992). Additionally, new variables such as PISR (e.g., *Funk and Hoelzle*, 1992) could be computed using DEMs. Based on that, PERMAMAP, which uses linear statistical relationships to predict BTS, was established to estimate the spatial permafrost distribution (*Hoelzle*, 1992, *Hoel-*

zle et al., 1993). PERMAKART and PERMAMAP form the basis for many permafrost distribution-modeling approaches in the Alps (*Keller*, 1992, *Imhof*, 1996, *Frauenfelder et al.*, 1998, *Gruber and Hoelzle*, 2001, *BAFU*, 2005, *Brenning et al.*, 2005, *Ebohon and Schrott*, 2008) and other mountain regions (e.g., *Serrano et al.*, 2001, *Tanarro et al.*, 2001, *Julian and Chueca*, 2007, *Ruiz and Liaudat*, 2012). Further, generalized linear models (GLMs) such as logistic regressions are used to predict permafrost occurrence using binary calibration information (e.g., permafrost absence vs. permafrost presence) in many studies (e.g., *Luoto and Seppälä*, 2002, *Lewkowicz and Ednie*, 2004, *Luoto and Hjort*, 2004, *Heggem et al.*, 2005, *Lewkowicz and Bonnaventure*, 2008, *Ridefelt et al.*, 2008, *Li et al.*, 2009, *Panda et al.*, 2010, *Bonnaventure and Lewkowicz*, 2011, *Bonnaventure et al.*, 2012). Other studies use rock glacier inventories to infer the occurrence of permafrost (*Janke*, 2004), to identify the lower boundary of discontinuous permafrost (*Lambiel and Reynard*, 2001, *Nyenhuis et al.*, 2005) or map past permafrost distributions (*Lambiel and Reynard*, 2001, *Frauenfelder et al.*, 2001). Generalized additive models (GAM) and other statistical approaches such as artificial neural networks or support vector machine have been applied in geomorphological mapping studies (e.g., *Hjort and Marmion*, 2008, *Brenning*, 2009).

The predicted results of permafrost distribution models are typically visualized in map-based products using discrete classification schemata to characterize the spatial distribution of permafrost (cf. *Heginbottom*, 2002). Maps that are based on GLMs provide probabilities of permafrost occurrence or corresponding probability classes (e.g., *Lewkowicz and Ednie*, 2004).

Existing permafrost distribution models are calibrated for a specific spatial domain or surface type (e.g., using BTS measurements in gentle terrain) but subsequently often applied to a whole mountain range. This spatial extrapolation is required for every spatially distributed permafrost model, but corresponding methods or a critical discussion of this issue are often missing in permafrost distribution studies. Additionally, scaling issues are often neglected in permafrost distribution models. However, they are important because permafrost observations are related to a specific spatial scale, depending on the type of observation (e.g., ground surface temperature are mostly representative for a small area in a highly variable environment), which has to be adequately accounted for in a modeling approach when using DEMs with coarse grid resolutions or when different types of permafrost evidence are combined.

An important improvement in permafrost distribution modeling has been established in the permafrost map of Switzerland, provided by the Federal Office for Environment (FOEN, Switzerland, *BAFU*, 2005) by distinguishing between different surface types. Two different modeling approaches were used to map permafrost in steep bedrock and debris areas. In debris areas, the modeling is based on the "rules of thumb", for steep

bedrock corresponding relationships to predict MAGST were extracted from a physically based modeling approach (*Gruber et al.*, 2004a).

2.4.2 Physics-based models

Physics-based or process-based permafrost models use mathematical formulations to solve the relevant equations representing processes in the ground thermal regime (e.g., energy balance, heat conduction). Such models allow for spatio-temporal extrapolation, are suitable to analyze processes, feedbacks and sensitivities and can be used to study transient effects (*Etzelmüller et al.*, 2001a, *Hoelzle et al.*, 2001). Physics-based models require detailed knowledge of the involved physical processes, the geophysical properties of the ground and of the energy balance at the surface.

Simple physics-based models use **analytical solutions** to the general heat flow theory: E.g., Stefan Solution to the freezing or thawing front, Eq. (2.2) (*Lunardini*, 1991, *Anisimov et al.*, 2002, *Shiklomanov and Nelson*, 2003, *Zhang et al.*, 2005), the Kudryavtsev Model for estimating maximal annual thaw propagation and the mean annual temperature at the top of permafrost (Kudryavtsev et al 1974 in *Riseborough et al.*, 2008), and the TTOP model to estimate the mean annual temperature at the top of permafrost (*Smith and Riseborough*, 1996, *Juliussen and Humlum*, 2007, *Riseborough*, 2007). These models are applied predominantly to Arctic regions and often referred to as "equilibrium models" (*Riseborough et al.*, 2008) because they approximate equilibrium permafrost conditions for a given annual regime.

Numerical models that account for transient effects accommodate variable materials, geometries and boundary conditions (*Riseborough et al.*, 2008) and often use gridded data of meteorological parameters, as well as spatial information of surface and subsurface conditions as input variables. The meteorological data is provided either by existing meteo stations or regional/global climate models (*Sazonova et al.*, 2004, *Nicolsky et al.*, 2007, *Stendel et al.*, 2007). One-dimensional numerical models have been applied to Arctic regions to quantify active layer thickness and to assess the effect of climate change on permafrost (*Hinzman et al.*, 1998, *Oelke et al.*, 2003, *Zhang et al.*, 2006, *Marchenko et al.*, 2008, *Burn and Zhang*, 2009, *Etzelmüller et al.*, 2011, *Zhang et al.*, 2012). In mountainous areas, such models have been used to predict ground temperatures (*Gruber et al.*, 2004a, *Farbrot et al.*, 2007, *Engelhardt et al.*, 2010, *Hipp et al.*, 2012) in order to analyze the coupling of the atmosphere and the ground, including snow cover effects (*Luetschg et al.*, 2004, *Luetschg and Haeberli*, 2005). Further the influences of meltwater infiltration (*Scherler et al.*, 2010) and of coarse blocky surface layers (*Gruber and Hoelzle*, 2008) were investigated using numerical modeling approaches. Three-dimensional thermal models have been applied to analyze transient temperature fields in the European Alps (*Kohl et al.*,

2001, *Gruber et al.*, 2004b, *Noetzli*, 2008, *Noetzli and Gruber*, 2009). The distributed hydrological model GEOtop (*Rigon et al.*, 2006, *Endrizzi*, 2007) is a physically-based model that simulates the coupled energy and water balance with phase change in the soil and considers a multilayer physically-based snow-pack model. GEOtop has been designed specifically for application in mountain regions and has been evaluated in the Swiss Alps (*Gubler et al.*, 2013).

For large scale permafrost mapping, numerical models are often not suitable because of a) the large spatial heterogeneity of input variables that needs to be estimated for each grid cell, b) unknown parameterization of surface and ground properties that influence the modeling results significantly, c) challenging evaluation because of the amount of input variables required, the complexity of processes addressed and the parameterization used in the model (cf. *Gubler et al.*, 2013), and d) limited computational power. New methods that are currently developed try to address some of these problems by linking Regional Climate Models (RCMs), topography, and sub-grid variability to efficiently apply physically-based land surface models (*Fiddes and Gruber*, 2012).

2.5 Permafrost in the European Alps

Different monitoring programs exist in the European Alps. Since the early 1990s, permafrost related observations and measurements in Switzerland are compiled in the Swiss Permafrost Monitoring Network (PERMOS, `www.permos.ch`). The observed parameters were chosen according the "Priorities for the Global Geocryological Database" (*Vonder Mühll et al.*, 2008, Sect. 2.3). The aim of PERMOS is the systematic long-term documentation of the current state and changes of mountain permafrost in the Swiss Alps. A similar monitoring network was launched recently in France (*Permafrance*, 2010) and other monitoring programs exist for single mountain regions (e.g., Corvatsch, Switzerland (*Hoelzle et al.*, 2002, *Gubler et al.*, 2011, *Schmid et al.*, 2012); Jungfraujoch and Matterhorn, Switzerland (*Hasler et al.*, 2008, 2011a,b, 2012, *Girard et al.*, 2012); Hoher Sonnblick, Austria (*Schöner et al.*, 2012)). Currently, no systematic collection of permafrost evidence exists that compiles regional and national observations in an Alpine-wide inventory. This would be important to compare permafrost characteristics within different regions and would allow permafrost analyses that span larger environmental gradients than possible with regional permafrost inventories.

The permafrost distribution in the European Alps is analyzed in several studies (*Haeberli*, 1975, *Keller*, 1992, *Imhof*, 1996, *Frauenfelder et al.*, 1998, *Lambiel and Reynard*, 2001, *Guglielmin et al.*, 2003, *BAFU*, 2005, *Nyenhuis et al.*, 2005, *Ebohon and Schrott*, 2008, *Permafrance*, 2010). Currently, a uniform modeling approach for the Entire Alps is miss-

ing and the existing permafrost distribution models cannot easily be compiled into an Alpine-wide permafrost map, because the relevant studies are a) regionally calibrated, b) rely on differing methods, and c) exclude parts of the European Alps. The following rough estimates of permafrost area[1] are available for single Alpine countries: Switzerland: 2000 km^2 (*Keller et al.*, 1998), Austria: 1600 km^2 (*Ebohon and Schrott*, 2008), and France: 1200 km^2 (*Permafrance*, 2010). The permafrost thickness ranges from a few meters to one hundred meters and more (*Haeberli*, 1975, *Lüthi and Funk*, 2001, *PERMOS*, 2010). Ground temperatures measured in boreholes in the Alps are in the range of -3 to 0 °C (*Harris et al.*, 2003, *PERMOS*, 2010) and the thickness of the active layer is around 0.5 to 8 m (*PERMOS*, 2010).

As a simple approximation, permafrost can be expected in vegetation-free areas above about 2500 m in the European Alps (*Haeberli*, 1975, *Hoelzle et al.*, 1993). According to the "rules of thumb"(*Haeberli*, 1975, Sect 2.4.1), permafrost in the Swiss Alps is possible above 2400 m in steep, north-exposed slopes and above 3000 m in steep, south-exposed slopes, respectively. For locations at the base of a slope, where long-lasting snow reduces the warming of the ground in summer, permafrost is possible around 2100 m (*Haeberli*, 1975). Due to fast glacier retreat, dead-ice in recently deglaciated glacier forefields show potential for permafrost occurrence in the European Alps (*Kneisel*, 1998, *Kääb and Kneisel*, 2006, *Kneisel and Kääb*, 2007). In such areas, permafrost is expected to occur in isolated patches. Subglacial permafrost is less relevant in the Alps because only few cold-based glaciers exist that would be conducive to permafrost occurrence at their bed (*Haeberli*, 1976, *Lüthi and Funk*, 2001). Additionally to typical permafrost locations, extra zonal permafrost exists in Europe (e.g., *Christian*, 1987, *Kneisel et al.*, 2000b, *Luetscher et al.*, 2005, *Morard et al.*, 2008, *PERMOS*, 2010).

The ice content of permafrost in the European Alps is largely unknown and so is the relevance of permafrost for water storage. Studies exist in the Alps that analyze the ice content of individual rock glaciers (*Haeberli*, 1985, *Vonder Mühll and Holub*, 1992, *Evin and Fabre*, 1990, *Burger et al.*, 1999, *Arenson et al.*, 2002, *Hausmann et al.*, 2007), talus slopes (*Hauck and Kneisel*, 2008, *Scapozza et al.*, 2011), and moraines (*Keusen and Haeberli*, 1983, *Hauck et al.*, 2003, *Lambiel and Baron*, 2008). At two catchments in the central European Alps, high nickel concentrations (exceeding the limit for nickel in drinking water) were attributed to meltwaters from active rock glaciers (*Thies et al.*, 2007). These high nickel concentrations could not be related to catchment geology and the authors conclude that high mountain runoff could become increasingly impacted by meltwaters from active

[1]Next to the term "permafrost area", the term "permafrost extent" is often used and defines estimates in percent area (*King*, 1986, *Brown et al.*, 1997, *Lawrence and Slater*, 2005, *Zhang et al.*, 2008a, *Bonnaventure and Lewkowicz*, 2011): continuous permafrost: 90–100 %, discontinuous permafrost: 50–90 %, sporadic permafrost: 10–50 %, isolated patches: 0–10 %.

rock glaciers. Similar results were found in a study of an alpine watershed in Colorado (USA), where the observed concentration increases of acidic metal-rich water were attributed to melting of permafrost and dropping water tables (*Todd et al.*, 2012).

2.6 Needs

Based on previous sections in this chapter, needs that arise from the current state of research and are addressed in this thesis are formulated (the sections to which the needs mainly refer to are given in brackets):

- In the European Alps, a uniform Alpine-wide inventory of permafrost evidence is needed in order to a) analyze permafrost characteristics for an entire mountain range, which allows for the inclusion of larger environmental gradients in permafrost analyses than possible with local data sets, and b) develop an Alpine-permafrost distribution model, which requires calibration and evaluation data that spans the environmental gradients of the study area. The compilation of such an Alpine-wide inventory inevitably requires an improved collaboration between different research institutions and companies in the European Alps. (Sect. 2.5)
- In permafrost distribution modeling, three considerations which are only partly addressed in existing studies, require further attention: A) Surface characteristics influence ground temperatures significantly. It is therefore essential to account for that in permafrost distribution modeling by distinguishing the most important surface types. B) The prediction of a permafrost distribution model is spatially restricted to the morphological setting it is calibrated for. Because calibration data is rare and restricted to limited settings, spatial extrapolation of model prediction is an integral part of permafrost distribution modeling, and has to be addressed and discussed in a modeling study accordingly. C) Different types of permafrost observation are related to a specific spatial scale, for which the specific observation method is representative. Thus, scaling issues have to be considered when combing different data and models that rely on different evidence types. (Sect. 2.4.1)
- A consistent Alpine permafrost distribution model and a derived permafrost distribution map are needed in order to make permafrost analyses comparable and compatible between regions, and to derive and describe regional patterns. Uncertainties and assumptions included in the modeling approach should be accounted for in the final permafrost distribution map in order to make these more transparent. (Sect. 2.5)

- Climate change that comes together with different precipitation and runoff patterns highlights the importance of analyzing the hydrological significance of permafrost in the European Alps. Because existing studies are lacking in the European Alps, first the total content of permafrost ice and the related sensitivities of such an estimate need to be addressed. (Sect. 2.5)

3 Methods

3.1 Compilation of Alpine-permafrost evidence

The compilation of the Alpine permafrost inventory is described in *Publication I* (*Cremonese et al.*, 2011) in *Part II* of this thesis. The main aim of this inventory is to collect information on permafrost in order to compile an Alpine-wide permafrost evidence inventory, which serves as a comprehensive data set for permafrost analyses, including model calibration and evaluation.

The establishment of a permafrost evidence inventory requires a design and data structure that allows for efficient acquisition and provision of different permafrost related information. This includes a strategy to homogenize different data in terms of terminologies and spatial reference. For the Alpine permafrost inventory, the following relevant types of evidence are considered: borehole temperature, ground surface temperature, rock fall scar, trench or construction site, surface movement, geophysical prospecting, other indirect evidence and rock glaciers. For all permafrost observations, the information of presence or absence of permafrost is essential to characterize the spatial distribution of permafrost. To assess the quality of this binary information, corresponding certainty levels are used that allow a subjective quality assessment. This helps to exclude evidence with low certainty from a given analyses.

The temperature-based measurements are summarized using annual means. Here, the time period used for averaging is required in order to obtain a temporal reference (Table 3.1). Additionally, for each evidence location, spatial information such as slope angle, aspect angle, surface characteristics and vegetation coverage is given, because this information can only be derived with limited accuracy from digital datasets such as DEMs or satellite images.

Table 3.1: *Relevant information of temperature-based evidence information shown at the example of borehole temperature (more details are given in Publication I).*

keyword	description
name	established local borehole name
depth	maximum depth of the borehole (m)
ALT	mean of maximum annual active layer thickness (m)
ALT years	years used for the calculation of average active layer depth
MAGT min	minimum mean annual temperature in the borehole (°C)
MAGT min depth	depth of the sensor corresponding to the MAGT min (m)
MAGT period	years used for the averaging to obtain the MAGT min
MAGT accuracy	accuracy of the temperature sensors (°C)
GST	mean annual ground surface temperature (°C) at this location
comments	any additional information

Next to point evidence, polygon information of rock glacier occurrence and related status information is useful in the scope of estimating permafrost distribution (Sect. 2.3). For the status information, different terminologies are common in Europe (intact, relict, active, inactive or fossil), which need to be homogenized.

Each country (or region) uses its own spatial reference system and the coordinates of the point locations and the polygon data of the rock glaciers are stored in local projections. This requires the definition of a common uniform spatial coordinate system. Here, geographic coordinates using the geodetic datum WGS1984 are used, as this is a common coordinate system and related transformation methods are available for most local projections. The evaluation of the spatial information is important because a) errors introduced in the data entry process cannot be excluded, and b) the coordinate transformation methods that were applied need to be assessed. For this, a simple approach using the open source visualization possibilities within Google Earth is performed (Fig. 3.1).

The collection of permafrost data was performed by four "calls for evidence", where the most important research institutes and companies that focus on permafrost research in

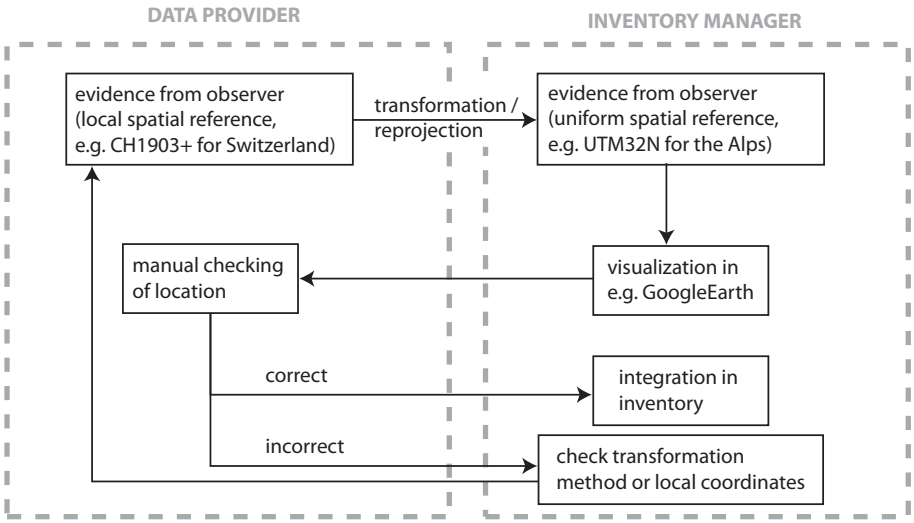

Figure 3.1: *Evaluation process of the spatial information of point evidence in order to avoid errors in spatial positioning introduced during data entry or coordinate transformation (see Publication I for more details).*

the European Alps were contacted via email accompanied by a spreadsheet and detailed instructions.

3.2 Permafrost distribution modeling at the regional scale

The methods to build a statistical permafrost distribution model on for the European Alps are described in *Publication II* (*Boeckli et al.*, 2012a) in *Part II* of this thesis. *Publication III* (*Boeckli et al.*, 2012b) describes the required steps from a permafrost distribution model to a spatially continuous estimate of permafrost occurrence and the compilation of the Alpine Permafrost Index Map (APIM). The overall approach is illustrated in Fig. 3.2 and includes a) the distinction of different surface types that are separately addressed using two sub-models, b) the combination of the sub-models that are based on different type of calibration data (continuous vs. binary), c) the extrapolation of the predicted permafrost distribution to areas where no calibration data is available, and d) the development of a map-based product accompanied by a suitable legend and interpretation guidelines.

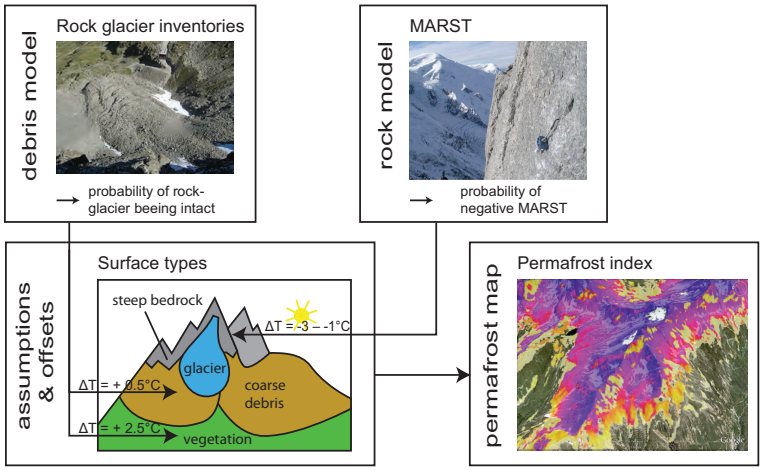

Figure 3.2: *Schematic illustration of the entire modeling approach that results in a spatially continuous estimate of permafrost distribution and a corresponding permafrost map.*

3.2.1 Distinction of different surface types and related sub-models for the European Alps

In permafrost distribution modeling, it is essential to distinguish between different surface types, as they influence the underlying thermal regime significantly (Sect 2.2).

Based on the data compiled in the Alpine permafrost evidence inventory the following two statistical sub-models were developed:

a) The *rock model* is based on mean annual rock surface temperature (MARST) in near-vertical bedrock. This sub-model is chosen because the linkage of near-vertical bedrock and the atmosphere is relatively straightforward, which makes permafrost in steep bedrock a system that is simple enough for attempting an extrapolation of findings to environments not measured (*Gruber*, 2012b).
b) The *debris model* is calibrated using status information of rock glaciers (intact vs. relict). The amount of available rock glaciers polygons and the good spatial coverage of this information in the European Alps make them a unique data source for model calibration.

The other evidence types compiled in the Alpine permafrost evidence inventory could not be used for model calibration because a) they are not sufficient in number to allow consistent statistical analyses, b) the integration and homogenization of heterogeneous permafrost observations is challenging and based on subjective assumptions, which results in a reduced confidence in the data, and c) the remaining observations are strongly biased towards permafrost existence.

The rock model is based on temperature measurements of 57 sensors located in steep bedrock (Fig. 3.3) at 0.1–0.5 m depth (cf. *Gruber et al.*, 2003) and uses a linear regression to predict MARST. MARST values corresponding to single or a few years duration were adjusted to longer-term temperature trends following the approach described by *Allen et al.* (2009). The lateral variability of MARST is mainly controlled by short-wave radiation (*Gruber et al.*, 2004a, *Allen et al.*, 2009). The resolution of Alpine-wide DEMs is too coarse to reproduce this variability and the usage of locally measured terrain variables is preferred instead. PISR was therefore calculated following *Corripio* (2003) based on local measurements of elevation, slope angle and aspect angle. For most of the locations local horizons affecting the obstruction of solar incoming radiation were determined using a camera with a fish eye lens (cf. *Gruber et al.*, 2003) and considered in the PISR calculations. To apply the rock model to the entire Alps using a DEM with a coarse grid resolution, scaling issues have to be considered (details are given in *Publication II*).

The debris model uses status information of rock glaciers for the calibration and predicts the probability of a rock glacier to be intact as opposed to relict. As reviewed in Sect. 2.4.1, generalized linear models (GLMs) are often used in permafrost distribution mapping when binary calibration data is available. In the context of the debris model, an extension of GLM is required that accounts for random inventory effects. Such random effects may be related to different observation techniques and interpretation criteria being applied in the compilation of inventories by different research groups, which may result in an inventory-specific bias. The generalized linear mixed model (GLMM, *Venables and Ripley*, 2002) is able to account for such random effects and is therefore applied here.

3.2.2 Combination of statistical sub-models that base on different calibration data types (continuous vs. binary)

Linear and logistic regressions are common statistical methods in permafrost distribution modeling (Sect. 2.4.1). In order to combine these two approaches, a uniform framework is required that allows for integration of probabilities derived from a linear regression with probabilities derived from a binary regression model. The framework uses a GLM (or GLMM) with a probit link function (*Hosmer and Lemeshow*, 2000, *Gelman and Hill*, 2007) instead of a logistic link function, which is more commonly used. While both are nearly identical (*Aldrich and Nelson*, 1984, *Gelman and Hill*, 2007), a probit link function is preferred because of its relation to the cumulative normal distribution function (*Aldrich and Nelson*, 1984, *Gelman and Hill*, 2007). The probability of permafrost presence is modeled linearly not at the logit scale but at the probit scale, which is obtained from an inverse cumulative distribution function of the standard normal distribution:

Figure 3.3: *Typical location of a sensor measuring near rock surface temperatures shown at the example at Hochkalter, Baverian Alps, Germany (photograph by M. Rieckh).*

$$\text{probit}(p) = \Phi^{-1}(p). \tag{3.1}$$

Φ is the cumulative standard normal distribution function and p the probability of permafrost. Thus, the probit model can be written as

$$\text{probit}(p) = \alpha + \sum_{i=1}^{k} \beta_i x_i, \tag{3.2}$$

where x_i and β_i are the model's k explanatory variables and their coefficients, and α represents the intercept term. With a linear regression, commonly mean annual ground surface temperature $MAGST$ (or any kind of continuous proxy variable) is addressed in permafrost distribution models:

$$MAGST = \alpha + \sum_{i=1}^{k} \beta_i x_i. \tag{3.3}$$

The probability of permafrost occurrence at a given location can be expressed by the probability of $MAGST$ being ≤ 0°C (neglecting the annual variability of $MAGST$). p is then given as

$$p = \Phi(-MAGST/\sigma), \tag{3.4}$$

The negative sign is due to the fact that we are interested in the probability of negative rather than positive temperatures. σ is the prediction standard deviation of the linear regression model. From Eqs. (3.1), (3.2) and (3.4) it becomes evident that a linear regression of $MAGST$ is equivalent to a probit regression of p:

$$-MAGST/\sigma = \alpha + \sum_{i=1}^{k} \beta_i x_i \tag{3.5}$$

Eq. (3.5) allows for conversion of temperature based probabilities into probit-based probabilities and vise versa. In this study, a spatially varying degree of membership of land cover class (m, with values between 0 and 1 that sum up to 1 at each location) was used to combine the two sub-models. The integrated model is then (subscripts indicate: debris $_d$, bedrock $_r$):

$$\mathrm{probit}(p_\mathrm{d}, p_\mathrm{r}; m_\mathrm{d}, m_\mathrm{r}) = m_\mathrm{d}\mathrm{probit}(p_\mathrm{d}) + m_\mathrm{r}\mathrm{probit}(p_\mathrm{r}), \tag{3.6}$$

which accounts for generalization to more than two land cover classes. Probabilities of permafrost occurrence can be obtained from this integrated probit value by applying the inverse probit transformation.

To assess the goodness-of-fit for linear regressions, the R^2 and the root mean square error (RMSE) are used in this thesis. The discrimination of a binary prediction (e.g., permafrost presence versus absence) can be measured by the area under the receiver-operating characteristics curve (AUROC, *Mason and Graham*, 2002). It ranges from 0.5 (random discrimination) to 1 (perfect discrimination), where according to *Hosmer and Lemeshow* (2000):

0.7$\leq$ AUROC$\leq$ 0.8 is an acceptable discrimination
0.8$\leq$ AUROC$\leq$ 0.9 is an excellent discrimination
AUROC $\geq$ 0.9 is an outstanding discrimination

A 10-fold cross-validation is performed to assess how transferrable to independent test dat sets the models are (*Hand*, 1997). Here, the original data set is randomly partitioned into 10 sub-samples. Of these 10 sub-samples, a single sub-sample is retained for testing the model, and the remaining 9 sub-samples are used as training data. This process is repeated 10 times using each of the 10 sub-samples exactly once as the validation data.

3.2.3 Extrapolation to other settings

One main challenge regarding permafrost distribution modeling is that evidence is sparse and their sampling in respect to surface characteristics, unbalanced. Therefore, extrapolation is a distinct part of permafrost distribution modeling. As described in Sect. 3.2.1, our permafrost modeling approach consists of two individual sub-models that are both restricted to a specific spatial domain. The rock model is only intended for use in steep homogenous bedrock, whereas the debris model is restricted to areas with rock glacier occurrence. To provide a spatially continuous map of permafrost distribution we need to infer permafrost conditions in other surface domains. This is addressed by introducing offset terms in the modeling approach (Fig. 3.2).

The *rock model* was calibrated with measurements in homogenous near-vertical bedrock. The model quantifies the effect of topography on MARST and does not account for differing surface and near-surface characteristics. In general, this results in an overestimation of MARST, as temperatures at greater depth are likely to be lower due to effects of snow, debris and fractures in bedrock (*Gruber and Haeberli*, 2007). To account for this, a temperature-based offset is included in the rock model (Δ_R), which is implemented as a linear function of PISR and mainly based on investigations by (*Hasler et al.*, 2011b), details are given in *Publication III*:

$$\Delta_R = O_{min} + PISR\frac{O_{max} - O_{min}}{350\,W\ m^{-2}}, \tag{3.7}$$

where O_{min} is the minimal and O_{max} is the maximal temperature offset for pixels where PISR $= 350\ W\ m^{-2}$. Based on the investigations by *Hasler et al.* (2011b), $O_{\min}$ was set to $-0.5\,°$C and $O_{\max} = -2.5\,°$C. Spatial variation of Δ_R is not considered.

The *debris model* predicts the probability of a rock glacier to be intact as opposed to relict and provides an optimistic estimate (biased towards an overestimation) of permafrost in debris surfaces because of two main rock glacier characteristics: a) cooling effect of coarse blocks (Sect. 2.2), and b) rock glacier movement towards lower elevations (e.g., *Barsch*, 1978). Consequently, it is desirable to find relationships to infer conditions below surfaces other than rock glaciers. Both sources of bias are considered in this study by assuming average, constant temperature offsets that account for the related processes (details are given in *Publication III*) and allow for predicting the occurrence of permafrost probability for debris cover.

In order to apply the two models (debris and rock) as illustrated in Fig. 3.2 and to address the offset terms (Sect. 3.2.3), surface cover information is required. Here, steep bedrock and debris cover are distinguished based on slope angle using an index, which describes the degree of membership in the steep bedrock surface class (Eq. (1) in *Pub-*

lication III). The models could then be integrated using Eq. (3.6). Vegetation cover is derived using Landsat Thematic Mapper images and the soil-adjusted vegetation index (SAVI, *Huete*, 1988). Glacier outlines were provided by *Paul et al.* (2011) and represent glacier extent in the year 2003.

3.2.4 Compilation of a permafrost distribution map

Permafrost distribution maps are often based on discrete classifications schemata (cf. *Heginbottom*, 2002) or probabilities of permafrost occurrence (e.g., *Lewkowicz and Ednie*, 2004). In this thesis, we use *permafrost index values* instead of *probabilities* because the later do not communicate the uncertainties and assumptions that are integrated in our final map-based product. This index represents an indicator of the probability for permafrost occurrence per grid cell e.g., 25 m x 25 m). The map user can further refine the estimate on the map with an interpretation key to the map and enhanced local knowledge of terrain and surface cover information. Such information includes local characteristics that influence permafrost occurrence but could not be addressed in the modeling approach. This local information can be obtained by the interpretation of high-resolution air imagery, detailed topographical or geomorphological maps and field visits. Selected pictures that explain the most important local modifying effects are used in the interpretation key to keep this process straightforward and user-friendly.

3.3 Estimation of permafrost ice content at the regional scale

The methods to estimate the permafrost ice-content for the entire Alps are described in *Publication IV* (*Boeckli et al.*, submitted) in detail in *Part II* of this thesis.

In general, the permafrost ice content (ICE) of a homogenous spatial unit can be defined as:

$$ICE = A(Z_p - Z_{ALD})I_C, \tag{3.8}$$

where A is the planimetric area (m^2), Z_P the depth of the permafrost base (m), Z_{ALD} the active layer depth (m) and I_C the volumetric ice content of the ground (m^3/m^3). The latter three variables are characterized by a large spatial heterogeneity and related field evidence is sparse compared to the large study area. This requires a simple but robust modeling approach that comes along with few input variables and allows for definition of the lower and upper bounds for each variable, in order to analyze the corresponding

sensitivities of these spatially distributed variables. For that, we distinguish between different surface types, respectively ground types, as they differ significantly in potential ice storage. For each surface type an assumed average depth profile is defined including the most important geophysical properties (e.g., thermal conductivity, porosity, relative saturation). Based on mean annual ground surface temperatures, permafrost depth and the thickness of the active layer can be estimated using analytical solutions of the heat conduction equation. In this thesis, we distinguish between coarse debris and steep bedrock, which both are mapped using slope angle thresholds and satellite imagery. Intact rock glaciers are treated separately and their density is estimated using rock glacier inventories. For steep bedrock, ground surface temperatures are calculated based on the rock model introduced in Sect. 3.2.1, and for fine debris cover constant differences of MAGST and MAAT are used to spatially predict MAGST. Based on that, Eqs. (2.1) and (2.2) are applied to calculate permafrost depth and active layer thickness by assuming a two-layered ground profile (Fig. 3.4). The upper layer was considered to be fractured bedrock or debris cover, while the lower layer is considered as unfractured bedrock for both profiles.

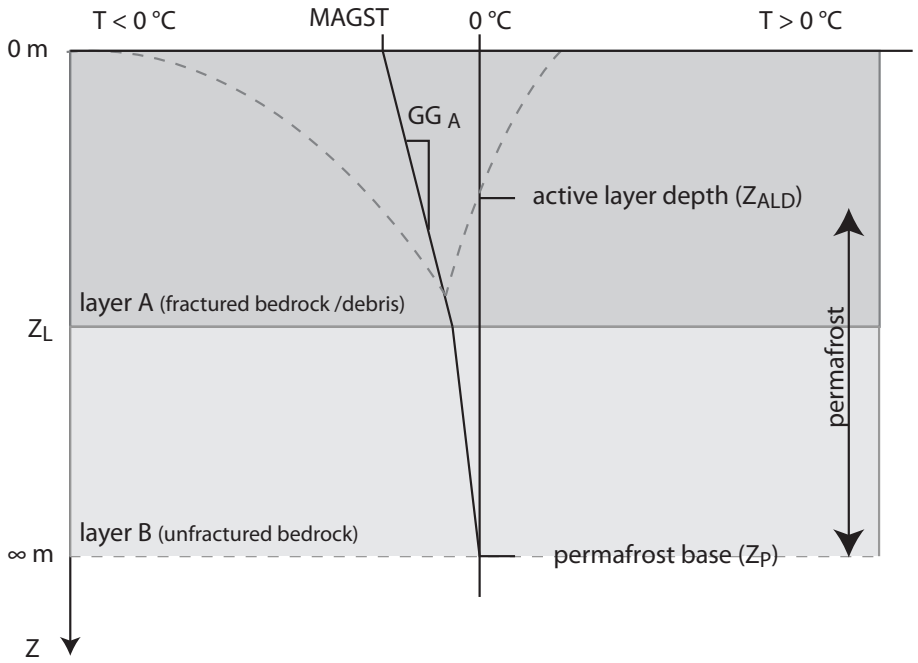

Figure 3.4: *Schematic permafrost profile based on MAGST and a two-layered ground. In each layer (A and B), the temperature gradient (GG) is assumed to be constant (from* Boeckli et al., *submitted).*

The ground properties for unfractured bedrock were defined according to published values (cf. *Cermak and Rybach*, 2012). To calculate the thermal conductivity for fractured bedrock and debris, the approach of *de Vries* (1963) as suggested by *Zhang et al.* (2008b) was adopted. Here, the porosity and the relative saturation are required that are defined based on the literature. For intact rock glaciers, permafrost depth and volumetric ice content were assumed to be constant, irrespective of ground surface temperature and estimated based on published values.

The consideration of the uncertainties that come along with such an estimation is important because the spatial extrapolation of surface and ground conditions is applied over large areas. Therefore, a sensitivity analysis is performed for all involved parameters individually (one-at-a-time sensitivity) by using lower respective upper bounds that were defined for each parameter.

4 Results

4.1 Alpine permafrost evidence inventory

The results of the Alpine permafrost inventory are described in *Publication I* (*Cremonese et al.*, 2011) in *Part II* of this thesis. The inventory was compiled within the framework of the project PermaNET (part of the European Territorial Cooperation in the scope of the Alpine Space Program, `http://www.alpine-space.eu`). In total, 18 different data contributors were involved, permafrost evidence of 408 points was collected and polygon information of 4795 rock glaciers was compiled (Fig. 4.1). The inventory extends from 44.29 to 47.47 °N and from 5.91 to 14.88 °E covering all Alpine countries except Monaco, Liechtenstein and Slovenia. Ground surface temperature, borehole temperature and geophysical prospecting are the most common types of point evidence. Most of the points are located in Switzerland, France and Italy. The elevation of the permafrost evidence ranges from 1000 m in a cold talus slope in central Austria (Toteisboden) to 4120 m for a ground surface measurement location in the Mont Blanc Massif (Grandes Jorasses, France). Most of the points have slope angles in the range 10–45 °C and are located in coarse debris (44 %). Evidence of the absence of permafrost is also relevant: whilst 75 % of the rock glaciers presented in the inventory are relict forms, only 23 % of the point types of evidence indicate the absence of permafrost.

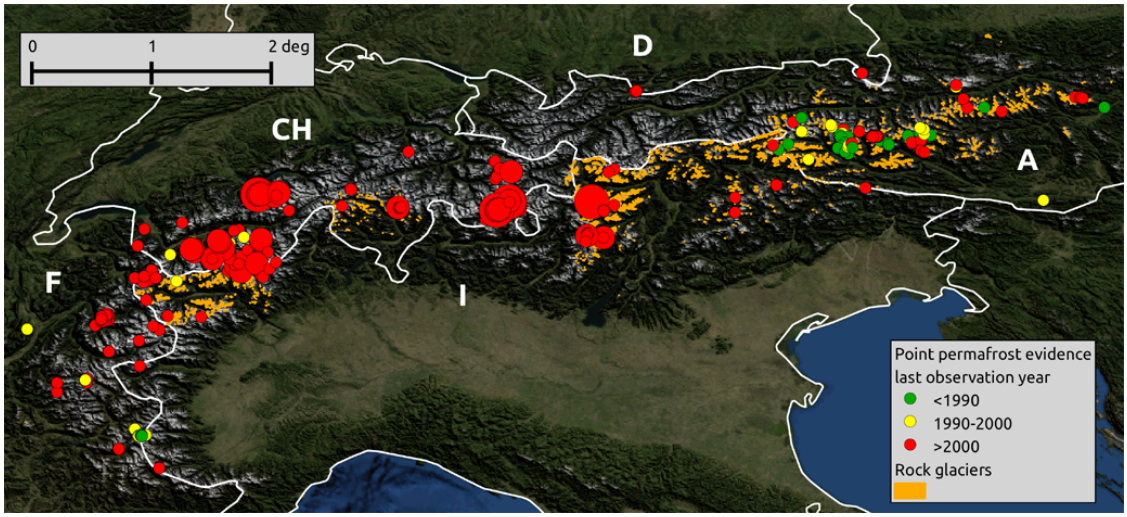

Figure 4.1: *Map of the permafrost evidence compiled for the Alps (from* Cremonese et al., *2011). The dots represent point permafrost evidence. The colors of dots represent the classes of last observation dates confirming permafrost state (before 1990, between 1900 and 2000, after 2000). The size of the dots indicates 3 classes ($\leq$3 years, 3–8 years, $\geq$8 years) representing the length of observations/measured data associated with each evidence. Orange polygons represent rock glacier inventories.*

4.2 Permafrost distribution in the European Alps

The results of the Alpine permafrost distribution map and the underlying modeling approach are described in detail in *Publication II* (*Boeckli et al.*, 2012a) and *Publication III* (*Boeckli et al.*, 2012b) in *Part II* of this thesis.

4.2.1 Statistical sub-models

For both sub-models (debris and rock model) the following potential explanatory variables were investigated: mean annual air temperature (MAAT), potential incoming solar radiation (PISR), mean annual sum of precipitation (PRECIP) and a seasonal precipitation index (SEASONAL). Alpine-wide MAAT data (*Hiebl et al.*, 2009) and Alpine-wide monthly precipitation data (*Efthymiadis et al.*, 2006) are available for the climate standard period 1961–1990. MAAT is based on the GTOPO30 elevation model (*U.S. Geological Survey*, 1997) with an approximate grid resolution of 1000 m. A constant lapse rate of 0.0065 °C m^{-1} (*International Organization for Standardization*, 1975) was used to interpolate the coarse MAAT based on more precise elevation information form the Global

Digital Elevation Model (ASTER G-DEM, *Hayakawa et al.*, 2008). The ASTER G-DEM shows a grid spacing of 1 arc-second (approximately 30 m) and an overall vertical accuracy on a global basis of approximately 20 m at 95 % confidence (*USGS et al.*, 2009). The precipitation data is gridded at 10 arc-minute resolution (approximately 15 km). The index SEASONAL is derived by dividing the mean sum of summer precipitation (May–October) by the mean sum of winter precipitation (November–April). PISR was derived from the ASTER G-DEM and calculated for one year with an hourly temporal resolution and clear sky conditions (100 % atmospheric transmittance).

The debris model (Sect. 3.2.1) is based on status information of 3580 rock glaciers. While MAAT and PISR show a clear relation to the activity status of rock glaciers, the correlation to precipitation is less obvious in a univariate analysis (Fig. 4.2). Nevertheless, precipitation was included in the final model based on the high significance of the Wald test (Table 4.1). The seasonal precipitation index shows no significant contribution within the debris model and was therefore not considered. The debris model achieves an AUROC of 0.91, which is considered as an outstanding discrimination (Sect. 3.2.2).

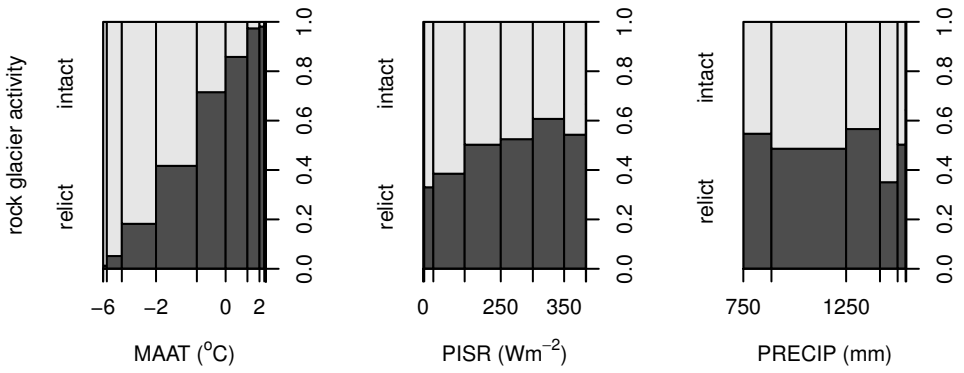

Figure 4.2: *Frequencies of intact as opposed to relict rock glaciers conditional on the explanatory variables MAAT, PISR and PRECIP (from* Boeckli et al., *2012a). Bar widths in these spinogramms are proportional to the empirical frequency of the given interval of values of explanatory variable.*

The rock model (Sect. 3.2.1) is based on MARST measured at 57 locations in steep bedrock. For all locations, MARST is higher than MAAT (mean difference = 4.6 °C) and the difference of MARST and MAAT increases with higher PISR (Fig. 4.3). PRECIP and SEASONAL were omitted from the final model (Table 4.1), because theses variables show no high significance. The model results in an R^2=0.82 and a root mean square error $RMSE$=1.57 °C.

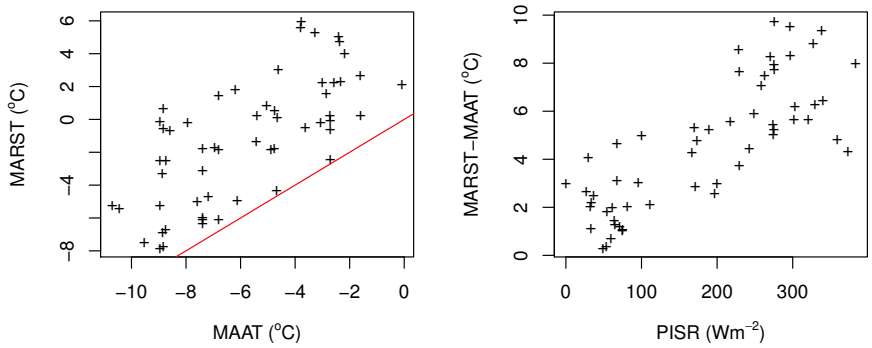

Figure 4.3: *Scatterplots illustrating the relation of MARST to MAAT (left) and of the difference between MARST and MAAT to PISR (right, from* Boeckli et al.*, 2012b). The red line in the left plot represents MAAT=MARST.*

Table 4.1: *Model coefficients (and standard errors in parentheses) for the final debris and rock model. The coefficients can not be compared directly between the models because the debris model is based on a generalized linear mixed model (GLMM) and the rock model on a linear regression. (PRECIP was centered (cPRECIP) by subtracting its mean value of* 1271 *mm.)*

	debris model	rock model
intercept	0.817 (0.192)***	1.677 (0.573) ***
MAAT (°C)	−0.906 (0.046)***	1.096 (0.081) ***
PISR ($\mathrm{W\,m^{-2}}$)	−0.007 (0.001)***	0.019 (0.002) ***
cPRECIP (mm)	0.001 (0.0002)***	-

Significance of Wald test: * < 0.05, ** < 0.01, *** < 0.001

4.2.2 Permafrost map, legend and interpretation key

The Alpine Permafrost Index Map (APIM, an example of Rimpfischhorn is shown in Fig. 4.4, top) should be used together with the provided legend and interpretation key. The final map has a grid resolution of approximately 30 m and covers the entire European Alps. The map is freely available as KML-overlay for Google Earth or as Web Map Service (WMS) to embed in a standard GIS software[1]. For individual regions the APIM is also available in a higher spatial resolution (Bavaria, Germany; Trentino, Italy; South Tyrol, Italy; Valle da Aosta, Italy, Veneto, Italy; and entire Switzerland). An additional map (Fig. 4.4, bottom) that shows the surface types was produced for the application of the model and is necessary in order to comprehend the index value in the map. The legend shows a continuous color gradient from "permafrost in only very favorable conditions" (yellow) to "permafrost in nearly all conditions" (dark violet, Fig. 4.5). The term "permafrost in only very favorable conditions" refers to a situation (topography and ground characteristics) that locally modifies favorably conditions for permafrost presence, while the term "permafrost in nearly all conditions" indicates that the probability of permafrost occurrence is very high irrespective of local modifying factors that are addressed by the interpretation key.

Many processes that influence the permafrost distribution locally are not addressed in the modeling approach, e.g., snow transport by avalanches or wind drift (Sect. 2.2). The aim of the interpretation key is to provide a user-friendly scheme that allows for refinement of the permafrost distribution estimate in the APIM, based on local surface or terrain information. The most important modifying processes are discussed in Sect. 2, visualized in Fig. 4.6 and summarized below:

A A cover of coarse blocks with open voids and no infill of fine material indicates favorable conditions for permafrost due to their effective cooling system.
B Fine-grained soil or soil with coarse blocks but infill of fine material indicates less favorable conditions for permafrost compared to coarse blocks.
C A dense vegetation cover usually indicates the absence of permafrost.
D An intact rock glacier is a reliable visual indicator for permafrost within its creeping mass, but does not allow for direct conclusions on adjacent areas.
E Often, the foot of a talus slope shows favorable conditions for permafrost because most talus slopes show a progressive increase in grain size downslope and long lasting snow depositions are predominantly located at the foot of a slope.
F The top of a slope often contains smaller clasts as well as an infill of fine material resulting in less favorable conditions for permafrost.

[1]Data is available at `http://doi.pangaea.de/10.1594/PANGAEA.784450` or at `http://www.geo.uzh.ch/microsite/cryodata/PFmapexplanation.html`)

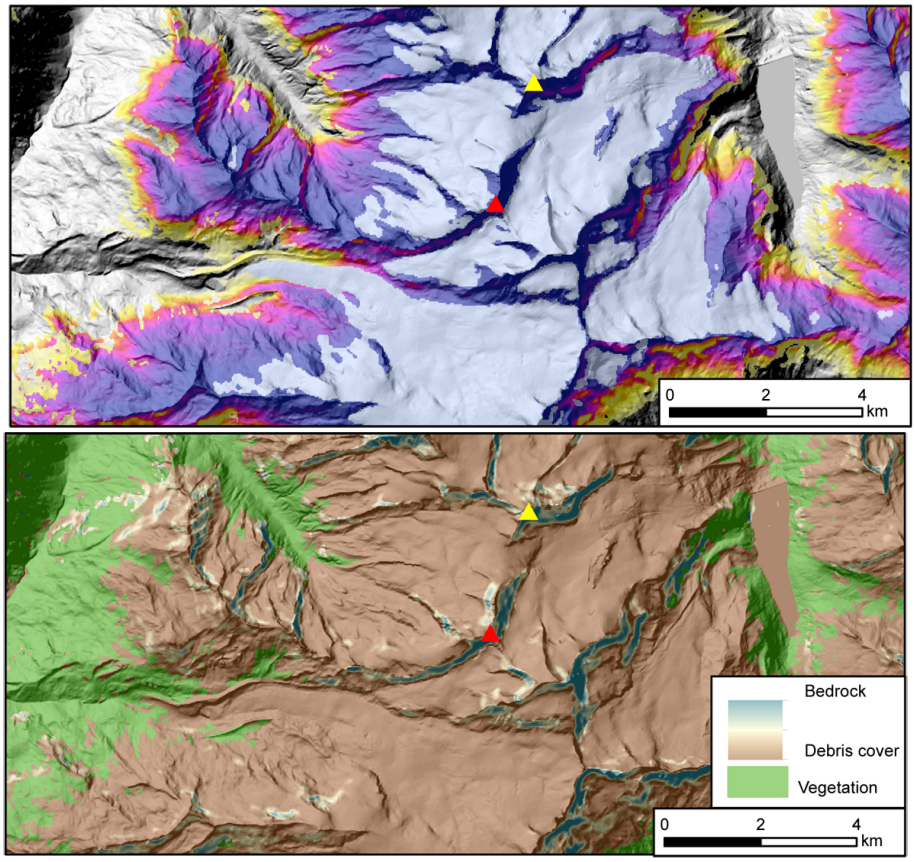

Figure 4.4: *Alpine Permafrost Index Map (APIM, top) and surface cover map (bottom) shown for the area surrounding the Rimpfischhorn (4199 m, red triangle) and the Allalinhorn (4027 m, yellow triangle) in Switzerland (from* Boeckli et al., *2012b).*

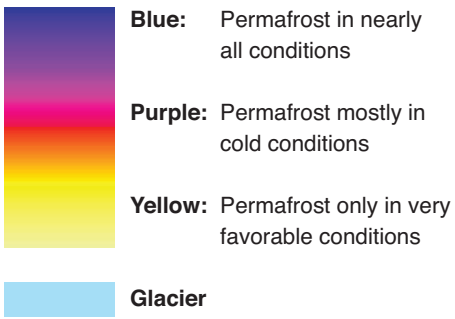

Figure 4.5: *Legend to the Alpine Permafrost Index Map (APIM) showing a qualitative index that describes how likely permafrost exists (from* Boeckli et al., *2012b).*

G Strongly fractured rock with depositions of snow and debris indicates locally colder conditions.

H Near-vertical, largely unfractured and mostly snow-free bedrock is indicative of relatively warm ground conditions, especially for sun-exposed locations.

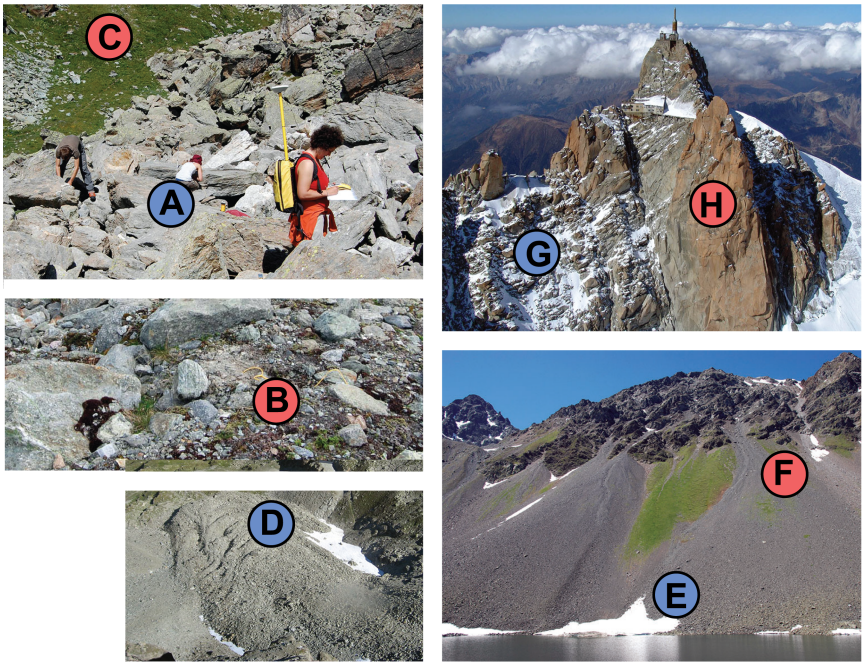

Figure 4.6: *Pictures that are part of the interpretation key and help the map user to identified the most import processes that modify the shown estimate on the map locally.*

4.2.3 Model evaluation and summary statistics

The performance of the APIM in rock glacier areas can be assessed using rock glaciers that were not used for model calibration. The discrimination of rock glaciers status (N=2798) based on predicted permafrost index values results in an AUROC of 0.78. This is an acceptable value according to *Hosmer and Lemeshow* (2000). For other surface types the evaluation is currently not possible even if a lot of data is available and large efforts are being made in developing adequate strategies. This is mainly because of the large spatial heterogeneity of mountain permafrost and related environmental variables, which leads to high requirements in sampling design of test data and strategies to relate coarse grid resolution to permafrost measurements representing sub-gird charact-

eristics. These difficulties in validating permafrost distribution models are an important insight, because it limits the confidence of permafrost distribution maps significantly.

Table 4.2: *Estimated permafrost index areas (km^2) for the Alpine countries using different index values, and comparison to glacier area (CH: Switzerland, IT: Italy, AT: Austria, FR: France, DE: Germany, SLO: Slovenia, FL: Liechtenstein).*

country	index ≥ 0.1	index ≥ 0.5	index ≥ 0.9	glaciers
CH	3710	2163	754	1010
IT	3353	1786	569	441
AT	2907	1557	484	340
FR	1587	703	199	265
DE	44.1	7.6	0.8	0.6
SLO	25.7	3.6	0.1	0.0
FL	0.3	0.0	0.0	0.0
total	11 626	6220	2007	2056

The total area potentially influenced by permafrost in the European Alps ranges from 2000–12 000 km^2, depending on the permafrost index area[2] considered (Table 4.2). The largest extent of permafrost is between 2600 and 3000 m, whereas the largest area of glaciers is above 3000 m (Fig. 9 in *Publication III*). According to this analysis, Switzerland is the country that contains the largest permafrost area. In Italy and Austria also large permafrost areas exist. The analysis of the relative areas shows that above 2800–3700 m (depending on the index values considered) permafrost is present in all area not being covered by glacier (Fig 4.7). In the highest elevation bands, permafrost is restricted to rock faces, crests or peaks.

4.3 Total permafrost ice content in the European Alps

The content of this chapter is presented in more detail in Publication IV (*Boeckli et al.*, submitted). To reduce computational effort and to efficiently apply the sensitivity analysis, the results are calculated for aggregated ground surface temperature classes with an interval of 2 °C. For each surface type (steep bedrock, debris cover, and intact rock

[2]The term "permafrost index area" refers to the area having an index equal to or higher than a specific threshold and is not equal to the term "permafrost area" that would be defined as the surface actually underlain by permafrost (cf. *Zhang et al.*, 2000, *Gruber*, 2012a).

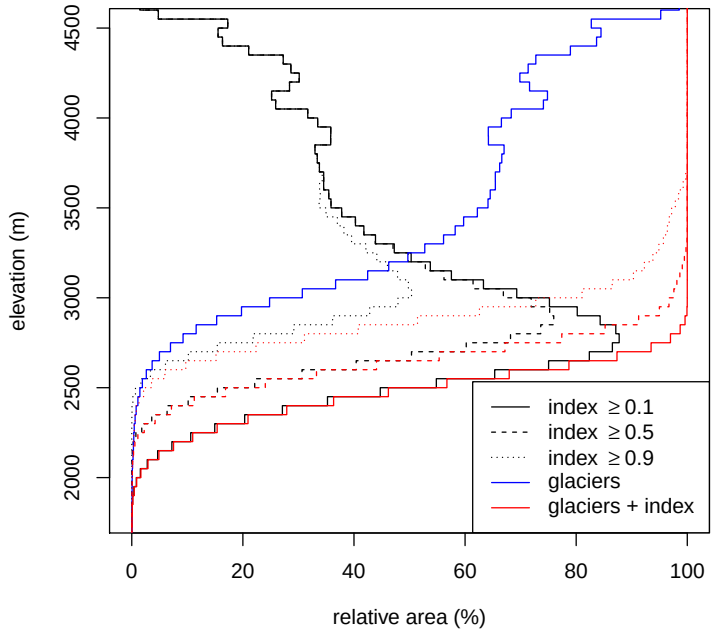

Figure 4.7: *Altitudinal distribution of permafrost index area in relation to the relative area in the Alps per elevation band (calculated for elevation bands of 50 m).*

glacier) the total water equivalent TWE of permafrost ice content was calculated separately and the sensitivity analysis is performed for all parameters individual by using lower respective upper bounds instead of best guess parameterization.

The planimetric area of steep bedrock in the European Alps is approximately 2984 km^2 and the corresponding total water equivalent TWE of permafrost is estimated to be 1.7 km^3. The largest contribution to the TWE originates from MAGST values between -2 and 0 °C. The area covered by coarse debris, whether frozen or unfrozen, is much larger (around 190 044 km^2) and the related TWE is estimated to range from 17.2 to 21.4 km^3. Again, the largest contribution to the TWE originates from MAGST values between -2 and 0 °C. In this MAGST class, mean permafrost thickness is around 65 m and the mean thickness of the active layer is estimated to range from 1.5–2.9 m. For bedrock permafrost, the most sensitive parameters are the thermal conductivity and the porosity of the lower layer, which is assumed to be unfractured bedrock (Fig. 3.4). For debris permafrost the geophysical properties of the upper layer (coarse debris) show larger sensitivities than the properties of the lower layer.

The total area of intact rock glaciers, that is derived based on eight existing rock glacier inventories in the Alps is estimated to be 233 km^2 and the derived TWE of intact rock glacier is 4.86 km^3.

Summing up the three proportions (debris, steep bedrock and intact rock glaciers) results in a TWE of permafrost ice of 24–28 km^3. The uncertainty of this estimate is large, but cannot be quantified with the chosen approach where the individual parameters are represented by extreme estimates in order to quantify the sensitivity of the individual parameters.

5 Discussion

In the following sections of this chapter, the main findings of the previous chapters are discussed in a broader context. More specific discussion to the single topics and detailed modeling aspects can be found in the research papers in *Part II*.

5.1 Permafrost evidence inventory

The observation and measurement of permafrost and related processes in the field is important to increase knowledge about the spatial distribution of permafrost and to have a basis for model calibration and evaluation. The compilation of regional observation and monitoring programs in international frameworks allows for analyses that span larger environmental gradients (e.g., analyze the influence of climatic regions and geological settings on rock glacier occurrence), which provides new insights that are not possible to obtain using local data sets only.

In high mountains, evidence and measurements have to be interpreted with care because of the high spatial heterogeneity in terrain, surface and subsurface characteristics. Here, an appropriate sampling design is required in order to minimize problems typical of observational data in complex terrain (*Brenning et al.*, 2005, *Gubler et al.*, 2011). In the Alpine permafrost evidence inventory such a sampling design is missing because it represents a (arbitrary) collection of available permafrost data in the European Alps:

the spatial distribution in terms of terrain characteristics and surface cover is unbalanced and the collected evidence is strongly biased towards permafrost existence. The total number of observations is small compared to the large area of the European Alps. Additionally, the quality of the data is a major challenge when compiling data from different sources. The reason for that is the missing international standards and protocols for permafrost observations, which lead to high efforts in data homogenization to provide interoperability. Here, well-managed metadata is important and would facilitate the management of such spatial data infrastructures (e.g., *Giles*, 2011).

To improve the current Alpine permafrost inventory it is important to further strengthen the coordination of permafrost observations in the European Alps. This requires a stronger collaboration between research institutes and companies in order to develop and implement a suitable sampling design of evidence for an entire mountain range. The focus of new observations should not only lie on permafrost presence, but also permafrost absence observations at high elevations are important to enhance the understanding of the spatial characteristics of permafrost. Additionally, more permafrost observations in complex terrain (e.g., *Matsuoka*, 2001a, *Hasler et al.*, 2008), are needed to enhance the understanding of permafrost characteristics in terrain where highly-fractured bedrock, debris cover, patchy snow-cover and strong lateral variability of radiation interact with each other. A proper evaluation of the data included in the evidence inventory is currently missing and needs to be addressed in the future with high priority to enhance the confidence of this data set. Here, existing frameworks, which are developed to asses uncertainties in environmental data (e.g., *Goodchild*, 2004, *Leung et al.*, 2004, *Brown and Heuvelink*, 2007) could possibly be applied. To gain the largest benefit for the permafrost community, permafrost observations and other geoscience related data should be fully available for free. Examples which this thesis could benefit from are the freely available ASTER G-DEM (*Hayakawa et al.*, 2008), the Landsat imagery collection[1], or the rock glacier inventories provided in the framework of the 7th International Conference on Permafrost in Yellowknife, Canada (*Delaloye et al.*, 1998, *Frauenfelder*, 1998, *Hoelzle*, 1998, *Imhof*, 1998, *Reynard and Morand*, 1998, *Schoeneich et al.*, 1998).

5.2 Permafrost distribution modeling in high mountains

The permafrost distribution model that is developed in the framework of this thesis is novel because a) it allows for integration of different sub-models that are calibrated for different surface types, b) the extrapolation to locations where no calibration data is available is accounted for by having the possibility to apply corresponding temperature

[1]Landsat scenes are provided by GLOVIS (`http://glovis.usgs.gov`).

offsets, and c) scaling issues that are required when the model prediction is performed for another grid resolution than the model was originally calibrated for (or sub-models that rely on different spatial resolution) are considered. The presented framework is flexible and enables the inclusion of additional sub-models to better account for different surface types. For other mountain regions, such as the rocky mountains, a possible extension would be to include a sub-model that deals with permafrost occurrence in vegetated areas (cf. *Kremer et al.*, 2011). The extrapolation to settings where no calibration data is available is a distinct part of all permafrost distribution models, but has often not been considered adequately. Therefore, our modeling approach represents an important step in permafrost mapping.

An important limitation of all permafrost distribution models is the sparse data for model calibration and evaluation and their unbalanced sampling in respect to topography and surface characteristics. The available data strongly limits the physical processes and the governing factors that can be accounted for in a modeling approach. Additionally, the level of detail (or scale of interest) of a study defines what level of generalization is appropriate. The Alpine permafrost distribution model is developed for a large mountain area and is based on a few explanatory variables only. In the following the most important sources of uncertainties of the model are discussed:

Calibration data. The two sub-models are based on rock glacier inventories and mean annual rock surface temperature (MARST). It is important to highlight the difference of these two calibration sources in terms of temporal characteristics: Most rock glaciers are some centuries to several millennia old (e.g., *Haeberli*, 1985, *Berthling and Etzelmüller*, 2007) and thus reflect past climate conditions. Their response to current surface temperature has been investigated in respect to creep behavior (e.g., *Kääb et al.*, 2007, *Delaloye et al.*, 2008) and degradation of permafrost in rock glaciers is observed in some studies (*Ikeda and Matsuoka*, 2002, *Maurer and Hauck*, 2007). However, the delayed response of rock glaciers to atmospheric forcing and the question of how long intact rock glaciers can survive in a warming climate needs further investigations. On the other hand, MARST are linked relatively directly to the atmosphere and are only marginally influenced by sub-surface temperature. Thus, they hardly reflect current climatic conditions and the influence of past climate conditions is present.

The *rock model* is only based on 57 MARST values in the European Alps, which inevitably requires a strong generalization of the model for application to other environmental settings (such as geology or mean atmospheric humidity that influences the radiation budget). However, absent vegetation, a reduced snow cover and less important active-layer processes make permafrost in steep bedrock a system that is simple enough to attempt an extrapolation of findings to environments not measured (*Gruber*, 2012b). Additonally to spatial extrapolation, also temporal extrapolation is important because

MARST values correspond to different observation years taken for averaging. This was addressed by extrapolating the MARST values to the period 1961–1990 using long-term MAAT measurements from Piz Corvatsch, Switzerland (details are given in *Publication II*). This approach a) assumes that the difference of MAAT to its longer-term mean and the difference of MARST to its longer-term mean are equal and spatially uniform, and b) is representative of inter-annual variability, because some of the measurement series are only one year long. The *debris model* (Sect. 3.2.1) is based on status information of 3580 rock glaciers. The existence of an intact rock glacier not only depends on permafrost but also on suitable debris production and transport mechanisms, implying that permafrost can exist in areas where rock glaciers are absent (*Imhof*, 1996). The exact mapping of rock glaciers extents involves subjective decisions (e.g., how far upslope a rock glacier reaches) and a related inventory-specific bias must be assumed, which is considered by the generalized linear mixed model (GLMM) using random effects. Rock glacier inventories were used in previous studies using logistic regressions (*Nyenhuis*, 2005, *Janke*, 2004). However, these studies do not use different rock glacier inventories and thus random effects are not considered in the statistical modeling. Additionally, no thermal offsets were applied in these studies to infer permafrost conditions for areas, which are not rock glaciers, but the predicted modeling results are presented as permafrost probabilities for an entire landscape.

Explanatory variables. For the Alpine permafrost distribution model, the environmental variables MAAT, PISR and precipitation are considered as explanatory variables. MAAT, or elevation in a local context, describes the altitudinal distribution of permafrost, whereas PISR addresses the lateral variability of topography effects. An important limitation in our PISR calculation is that cloudiness is not considered (e.g., diurnal variations of moisture in the atmosphere resulting in generally higher permafrost limits in east exposed slopes compared to west exposed slopes, *Haeberli*, 1975). The variable "precipitation" can be interpreted as a proxy for regional averaged cloudiness or snow cover characteristics. However, the grid resolution of this variable is coarse and local characteristics are not accounted for. Especially the effect of snow on permafrost distribution is large, but the spatial prediction of average snow cover characteristics (first significant snow fall in autumn, snow depth, melt-out date) is difficult due to regional precipitation patterns and effects of wind and avalanches (*Lehning et al.*, 2006, *Mott et al.*, 2008) and thus, no Alpine-wide data is currently available. This results in a possible overestimation of ground temperatures at the foot of talus slopes, where avalanche deposits are common in many topographical situations and responsible for a net cooling effect (cf. *Haeberli*, 1975, Sect. 2.2).

Surface characteristics and offset terms. The influence of surface characteristics on ground temperature is considered by distinguishing between debris cover, steep bedrock

and vegetation in our modeling approach. This is a strong simplification because various transition zones of these surface types exist and within each surface type the variability (e.g., grain size) is large. Additionally, the estimation of averaged offset terms for a specific surface type for the entire Alps is not an easy task because offset terms are highly variable (cf. *Hoelzle and Gruber*, 2008) and strongly depend on ground and surface characteristics. The offsets that are applied in this study, are based on few observations and include subjective assumptions.

Other limitations. Subsurface conditions, transient, and three-dimensional effects are neglected in our analysis, but are assumed to play a less important role when estimating current permafrost distribution. This can not be assumed when future conditions need to be estimated or changes in permafrost detected. However, the relationship of changing climate and environment on permafrost conditions are complex and partly non-linear (e.g., a reduced snow-cover in winter may result in local cooling effect due to increased albedo and effects of latent heat (Sect. 2.2) but later the warming effect of the absent snow cover will be dominant), which makes predictions of future conditions challenging, even if process-based approaches are applied on a more local scale.

The **evaluation** of a permafrost distribution model is difficult because field evidence of permafrost presence or absence is rare compared to often large study areas. Additionally, the existing evidence is concentrated on few distinct surface types such as rock glaciers, talus slopes and bedrock, but few evidence exists in intermediate slopes characterized by a mixture of bedrock and debris cover (unbalanced sampling of existing permafrost evidence). While the prediction of permafrost distribution models is grid based, observations represent point information within a complex, spatially variable mountain topography (Fig. 5.1), which further complicates the evaluation of gridded permafrost models.

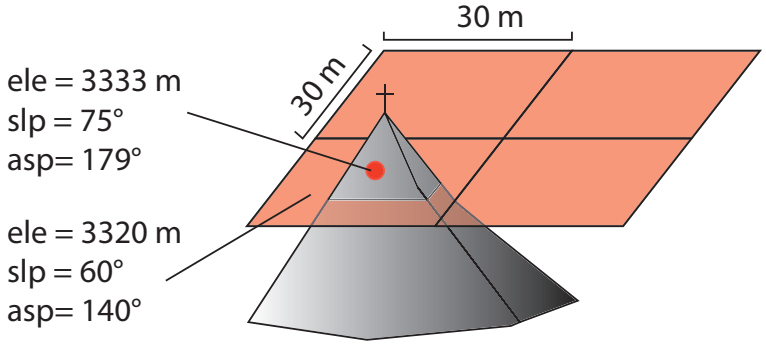

Figure 5.1: *Schematic illustration of sub-grid variability in mountain terrain variables shown for a DEM with a grid resolution of 30 m (ele: elevation, slp: slope angle, asp: aspect angle).*

A promising tool for future large scale modeling of environmental characteristics is TopoSUB, "a tool for efficient large area numerical modeling in complex topography at sub-grid scales" (*Fiddes and Gruber*, 2012). Here, the most important aspects of land surface heterogeneity are sampled through a lumped scheme, which allows numerical modeling of processes at fine grid resolutions over large areas (*Fiddes and Gruber*, 2012). Additionally, grid computing systems allow for handling big numerical simulations and offer new possibilities to evaluate physical-based models for different environmental settings (e.g., *Gubler et al.*, 2013) and thus to possible apply them to an entire landscape in the future.

5.3 Permafrost distribution map

Instead of probabilities, index values are used in the final map of permafrost occurrence because the former does not communicate the underlying subjective assumptions that are part of our modeling approach. Existing permafrost distribution maps mainly use discrete classification schemata to visualize the spatial distribution of permafrost (cf. *Heginbottom*, 2002). These schemata describe the permafrost extent (estimates in percent area) or the probability of permafrost occurrence in distinct classes, which can easily be visualized in a map. The uncertainty of the underlaying permafrost distribution model is then expressed in these permafrost classes. The distinction of discrete classes claims a spatial accuracy of the map-based product that is not supported by the data and does not account for the spatially fuzzy limit of permafrost in reality. The translation of the model output in such classes requires subjective assumptions and often comes along with the extrapolation of the model output to other settings (topography and surface characteristics) than used for model calibration. Often this step has not been described in detail in previous studies, especially the spatial extrapolation to new surface domains is often not accounted for. Permafrost mapping that is based on logistic regression modeling directly predicts the probability of permafrost occurrence (or negative ground temperatures). Here, mainly classified probability ranges are used in corresponding maps (e.g., *Lewkowicz and Ednie*, 2004, *Etzelmüller et al.*, 2006, *Lewkowicz and Bonnaventure*, 2008). However, also these modeling approaches need to account for different surface types and the limited data for model calibration.

The strategy behind the interpretation key to the permafrost map is novel: Here, the map-user has the possibility to improve the predicted permafrost occurrence based on additional information. However, the benefit of this strategy has to be evaluated by local stakeholders and other researchers because it requires an additional effort for the map user. Additionally, no clear boundaries of permafrost classes are provided in our

map and thus common GIS operations such the calculation of the permafrost area or the intersection of the permafrost layer with other data (e.g., natural hazard zonation, cf. *Fischer et al.*, 2012) is complicated. Considering index values ≥ 0.5 is one possible assumption to estimate the permafrost area. However, the definition of exact permafrost areas is not possible with the Alpine permafrost map, but different scenarios can be defined (e.g., conservative vs. anti-conservative estimation of permafrost distribution) depending on the purpose of a analysis. Apart from the modifying local processes that are captured in the interpretation key, the permafrost map has to be interpreted with care in recently deglaciated glacier forefield, because of ongoing fast glacier retreat (*Haeberli et al.*, in press, 2013).

The map is developed an applied for a large mountain region. The interpretation key allows for using the map also in a more local context, but additional studies (e.g., geophysical observation or physically-based modeling) are needed for a detailed assessment of local permafrost characteristics.

5.4 Estimation of permafrost ice content for an entire mountain range

The total water equivalent (TWE) of permafrost ice is estimated to range within 24–28 km^3. The largest contribution to the TWE is contained in debris permafrost (74 %), while intact rock glaciers (19 %) and permafrost in steep bedrock (7 %) are less relevant in the Alps. Thus, the parameterization of the geophysical properties of debris is more important than the corresponding parameterizations of intact rock glaciers and steep bedrock. The estimation of permafrost ice content for an entire mountain range is difficult, because the spatial extrapolation of existing information of subsurface characteristics (e.g., thermal conductivity, porosity and relative saturation) is difficult. This results in high uncertainties of the values presented. However, the aim was to estimate the order of magnitude of permafrost ice content in the Alps and to reveal the underlying uncertainties that come along with the chosen modeling approach. The ranges that are considered by the lower and upper bounds in the sensitivity analysis represent extreme estimates as the overall approach deals with averaged behavior for an entire landscape.

Studies in northern Canada assume averaged "ground ice versus depth" profiles for entire landscapes (*Pollard and French*, 1980, *Couture and Pollard*, 1998), independent of near-surface ground temperatures. This is not possible for the European Alps, because of the high spatial variability of near-surface ground temperatures and their absolute

values, which is often close to 0 °C. Additionally, the spatial characteristics of subsurface conditions are highly variable in the Alps.

In the applied modeling approach, constant differences between MAGST and MAAT were used, which represents a strong assumption neglecting the effects of the snow and the solar radiation. It is assumed that the permafrost area in debris cover is overestimated in our analysis, because talus slopes often show permafrost absence at the top of the slope and permafrost presence at the base of the slope (*Haeberli*, 1975, *Lambiel and Pieracci*, 2008, *Phillips et al.*, 2009, *Scapozza et al.*, 2011), which is not considered in our modeling approach. On the other hand, paleoclimatic effects from past cold periods can significantly influence the thermal regime at depth (*Noetzli and Gruber*, 2009) and thus, our approach based on current surface temperature possible underestimates current permafrost thicknesses and derived ice contents.

Ice stored in permafrost represents a seldom recognized ground water reservoir in alpine terrain (*Clow et al.*, 2003). Permafrost controls runoff processes such as the groundwater storage capacity, which is minimal in spring when the ground is frozen (*Roulet and Woo*, 1986), or the amount of water infiltration into the active layer (*Quinton et al.*, 2011). Existing studies have highlighted the importance of the hydrological significance of permafrost for single catchments and relates an increase in base flow to thawing of permafrost ice (*Ye et al.*, 2009, *Caine*, 2010). The TWE of permafrost in the European Alps found by this study (24–28 km^3) is approximately one quarter of the TWE of Alpine glaciers (90 ± 30 km^3, *Levermann et al.*, 2012). However, in other mountain ranges such as the dry Chilean Andes, the water equivalent of rock glaciers is estimated to be much larger than the glacier water equivalent (*Azócar and Brenning*, 2010) and the contribution of total permafrost (including non-rock glacier areas) is even larger. Loss rates for permafrost ice are hardly known but are certainly much smaller than for glaciers (cf. *Kääb et al.*, 1997). Consequently, the volume of glacier is assumed to vanish much more rapidly with a probable disappearance of most Alpine glaciers during the coming decades (*Haeberli et al.*, in press, 2013). It is possible that in the European Alps already during the second half of the 21st century, more subsurface ice in permafrost may remain than surface ice in glaciers.

6 Conclusions and outlook

Permafrost in high-mountains is heterogeneous and its spatial characterization requires a large amount of suitable field evidence as well as adequate strategies to efficiently calibrate and apply models for a large-scale area. The research questions that have been formulated to address these issues are revisited in the following section (Sect. 6.1). Then, the main products generated in the framework of this thesis are listed (Sect. 6.2). Section 6.3 gives an overview of the main insights gained. Finally an outlook for further potential research is given in Section 6.4).

6.1 Revisiting the research questions

In the following, the research questions that have been formulated in Section 1.2 for the individual objectives are revisited.

A1: What are the most relevant evidence types and which information per evidence type is required for an Alpine-wide permafrost inventory, which serves to a) increase knowledge of spatial permafrost distribution, and b) provide a solid basis for model calibration and evaluation?

For all evidence types the information whether permafrost is present or absent is important to characterize the spatial distribution of permafrost. Rel-

evant evidence types are borehole temperatures, ground surface temperatures, rock fall scars, trench or construction sites, surface movements, geophysical prospecting and other indirect evidence. A qualitative index describing the degree of certainty of the presence or absence of permafrost is needed to later exclude parts of the evidence for specific analyses. Furthermore, the spatial location and its estimated accuracy are required. Meta-data of local terrain and surface characteristics observed in the field is of great value because this information can only be derived with limited accuracy from digital datasets such as DEMs or satellite imagery. Temperature-based observations additionally provide important information by using averaged values, such as mean annual ground surface temperatures, which can be used for calibrating statistical models.
The rock glacier inventories must contain the following information: activity status (intact/relict) for each rock glacier, perimeter of the inventory, specification of the delineation method (e.g., air photo, map) and the mapping strategy used to compile the inventory. Additionally, a subjective measure by the data contributors describing the completeness of the inventory in the defined perimeter is important in order to exclude incomplete inventories from analyses.

B1: How can the permafrost distribution be estimated for the entire European Alps?

To predict the permafrost distribution Alpine-wide, a statistical modeling approach is preferred instead of a process-based model. This is because the evaluation and application of process-based models is currently too challenging to be of direct use for large-scale application. Based on the compiled evidence in the Alpine-wide permafrost inventory, two types of evidence were suitable for statistical model calibration: a) rock glacier inventories and b) mean annual rock surface temperatures measured in steep bedrock. Based on these evidence types, two statistical models were developed, one for debris-covered areas (debris model) that is based on status information of rock glaciers and one for steep bedrock (rock model) using mean annual rock surface temperature for calibration. For both models, mean annual air temperature and incoming solar radiation show a clear relation to the response variable and are therefore used in the statistical models. Additionally, the mean annual sum of precipitation significantly contributes to the debris model and was therefore considered. To infer conditions below debris surfaces other than rock glaciers, temperature offset terms that are based on the

literature but involve some degree of subjective choice during model building were applied to the debris model. Finally, both models are combined based on a linear membership function to the surface types steep bedrock and debris, allowing for a spatially continuous estimation of the permafrost distribution.

B2: What kind of legend and interpretation key is suitable to communicate the estimated permafrost distribution and its uncertainties in a map-based product?

The applied Alpine-wide permafrost model provides probabilities of the occurrence of permafrost. These probabilities are translated into permafrost index values because the term "index" better explains the uncertainties and assumptions that are integrated in the entire modeling approach. To underline this, the legend to the index varies from "permafrost in nearly all conditions" to "permafrost only in very favorable conditions" and describes semi-quantitatively the occurrence of permafrost. Both terms communicate to some degree the involved uncertainties of the model and deliberately allow for further interpretations.
The interpretation key that comes together with the Alpine permafrost index map, summarizes the main local modifying processes that could not be accounted for in the Alpine-wide permafrost model. Selected pictures and brief explanations help the map user to identify such situations (topography and surface characteristics) and to correctly interpret the implications for permafrost presence or absence.

C1: What is the permafrost ice content of the European Alps and which are the most important parameters of such an estimate?

The permafrost ice content in the European Alps is estimated to be in the order of 26 km^3, which is approximately one quarter of the glacier ice volume of the year 2003 in the Alps. The geophysical parameters that most influence this estimate are the thermal conductivity of the ground's material and its porosity. According to the results obtained, most permafrost ice is present underneath debris-covered areas, in loose debris. Consequently, the result is highly sensitive to the predicted ground surface temperature in this domain, but a proper evaluation of the results is currently not possible as only few evidence is available.

6.2 Contributions

This section contains a complete list of the contributions that arise from this thesis, while the explicit author contributions are listed separately in Part II preceding the individual publications.

Alpine permafrost evidence inventory. The first Alpine-wide permafrost evidence inventory provides a collection of permafrost observations and rock glacier inventories in the Alps. The large environmental gradients that are covered in this data collection allow analyses that are not possible with local data sets and offer new possibilities to calibrate and evaluate permafrost models. For each evidence type the relevant information was defined, which allows for collection and homogenization of evidence from different research groups and companies. A simple approach to evaluate the spatial location of the evidence was developed and applied in order to reduce errors during data entry or coordinate transformation.

Permafrost distribution model for an entire mountain range. The statistical modeling approach that has been developed as part of this thesis allows for a) integration of different statistical sub-models that are possibly based on different calibration data types (continuous and binary), b) scaling issues, which are required if the sub-models are based on different grid resolutions or if the model prediction is performed to another resolution than the model calibration, and c) integration of temperature offsets that allow for extrapolation of the model prediction to other settings. The modeling approach was developed in the domain of the European Alps but could be adopted for and applied to any other mountain range.

Alpine permafrost distribution map. For the first time, the permafrost distribution has been mapped Alpine-wide, including regions where no local permafrost map was available previously (e.g., Bavaria, southern Germany). The map has a grid resolution of approximately 30 m and is freely available as Google Earth overlay or as Web Mapping Service (WMS) for integration in a GIS. We developed a legend and interpretation key, which allows the map user to account for local modifying processes, and thus to locally refine the estimate that is shown in the permafrost map. Pictures with the most important situations (topography and surface characteristics) that are not accounted for in the underlying permafrost distribution model help the map user to identify such locations and an accompanying text describes the related implications for the interpretation of permafrost presence or absence.

Estimation of permafrost ice content for the European Alps. The permafrost ice content in the Alps was estimated using a simple framework that distinguishes between

different surface types and corresponding averaged depth profiles that are defined by geophysical parameters. Gridded ground surface temperatures and analytical solutions to the heat conduction equation were used to calculate permafrost depth and active layer thickness. Based on this, the ice-content could be estimated. Rock glaciers, as a geomorphological feature with high volumetric ice content, were treated separately and their spatial density was estimated using existing rock glacier inventories.

6.3 Insights

Quality and sampling of evidence data. The quality of the data and meta-data compiled in the Alpine-wide permafrost inventory is heterogeneous and further efforts are required to improve this. Problems arose in this study because non-uniform international standards with respect to permafrost observations and terminologies were encountered, which need strong efforts to ensure interoperability. Existing evidence is strongly biased towards permafrost presence and less evidence for permafrost absence is available. This is a strong limitation for statistical modeling using permafrost presence and absence as binary calibration source.
Additionally, the sampling is not balanced with respect to surface cover types. Most of the investigations are performed in distinct surface types or geomorphological features such as bedrock, rock glaciers or talus slope. However, large parts of the Alps cannot be attributed to such distinct classes and hardly any evidence is available in these areas.

Evaluation of evidence data. The evaluation of evidence data is important to assess its quality. The visualization of point and polygon locations in their geographic context provides a straightforward approach to detect obvious errors in coordinates introduced during data entry or coordinate transformations. However, small-scale errors in the spatial location of evidence cannot be assessed with this approach.
The meta-data contained in the Alpine evidence inventory offers possibilities to compare topographical variables provided by the data contributor with those derived from an Alpine-wide DEM. This allows for the assessment of parts of the meta-data of the inventory and if necessary to exclude individual evidence from further analyses.

Integration of statistical models that are based on different calibration data types and/or different spatial resolutions. Generalized linear (mixed) models with a probit link function allow to link probabilities derived from binary calibration data with probabilities derived from a linear regression model. This offers the possibility to combine different statistical models that are based on different types of calibration data in a uniform framework.

Direct and indirect evidence of permafrost always is related to a certain spatial scale, for which the specific evidence is representative. By combining statistical models that are based on different evidence types or on situations where the model prediction is performed at another resolution as the model was originally calibrated for, scaling issues need to be considered.

Extrapolation of model's prediction to settings where no calibration data is available. Because for some settings (as defined by topography and surface characteristics), hardly any evidence of permafrost is available, the extrapolation of model predictions outside its calibration domain is an implicit part of permafrost distribution modeling. This issue often has been neglected in previous permafrost mapping efforts, but needs to be adequately addressed. The design of a modeling approach that allows the integration of different temperature offsets, is one possibility to extrapolate model prediction to settings the model is not calibrated for. However, because of the large variability of near-surface ground conditions the estimation of averaged offset terms for different surface cover types and assumed ground profiles includes large uncertainties.

Evaluation of permafrost distribution models. The evaluation of permafrost distribution models is difficult because a) less evidence for model evaluation is available, b) the existing evidence is biased towards permafrost existence and unbalanced in regard to topography and surface characteristics, and c) the prediction of a model is grid based, whereas permafrost evidence is representative for one point within complex mountain topography. Independent polygon information of rock glaciers offers a possibility to evaluate permafrost distribution models in rock glacier areas. However, model assessment in non-rock glacier debris areas is only possible by estimating corresponding transfer approaches.

Permafrost ice in the Alps. The estimation of the permafrost ice content of an entire mountain range includes the difficulties of the estimation of the permafrost distribution. The additional dimension (subsurface) that needs to be accounted for when estimating permafrost ice content, increases the uncertainties further.
Currently, more surface ice exists in glaciers than subsurface ice in permafrost in the European Alps. Due to rapid glacier retreat it is probable that during the second half of the 21st century more permafrost ice than glacier ice may remain.

6.4 Outlook

The following key problems have been identified as warranting future research:

Alpine-wide permafrost evidence database. The coordination of research groups generating and maintaining permafrost evidence and related monitoring programs should be further improved in future in order to obtain a better data base for permafrost analyses. Important next steps are: a) Definition of an Alpine-wide strategy towards a balanced sampling design of permafrost observations in respect to climate, topography, surface and subsurface characteristics, b) establishment and implementation of international standards for acquiring permafrost related data, its processing and storage, c) development and maintenance of a user-friendly solution to provide Alpine-wide permafrost data and its meta-data to the permafrost research community, and d) development and implementation of strategies to assess the quality of the data that is stored in an Alpine-wide database.

Permafrost distribution modeling. The spatial estimation of permafrost could be improved using enhanced surface cover information derived from high-resolution (spatial/spectral) satellite imagery, additional topographical variables (cf. *Etzelmüller et al.*, 2001b) and complex spatial mapping algorithms (e.g., *Brenning*, 2009). The identification of distinct terrain features such as ridges, or slope base locations could help to account for main effects of the snow cover or three-dimensional topography. Further, transient modeling approaches are needed to account for changes in the environment (e.g., glacier coverage). Additional synthetic calibration data for specific situations could possibly be provided by physically-based permafrost models and improve the calibration base for permafrost distribution models. Recently developed downscaling approaches for regional climate model data (cf. *Fiddes and Gruber*, in prep.) could help to provide new data that could be used as explanatory variables in modeling approaches as well as data for future climate scenarios. Finally, the evaluation of permafrost distribution models needs to be improved. One possibility could be to conduct on inter-comparison project of different permafrost models.

Permafrost mapping. Future permafrost mapping products could contain additional information such as estimated permafrost depth, active layer thickness, ice content or transient information of past or future permafrost characteristics. In addition to new modeling approaches, also advanced visualization strategies would be required to provide user-friendly output products.

Permafrost ice and its drainage after melting. In the second half of the 21st century, when surface ice in glaciers is assumed to have mostly disappeared, permafrost ice

could have a more important role as a water reservoir from the European Alps than today. The significance of this or the influence of permafrost on drainage processes requires further attention.

References

Aldrich, J. and Nelson, F. (1984). *Linear probability, logit, and probit models*. Sage Publications, Inc.

Alean, J. (1985). Ice avalanche activity and mass balance of high-altitude hanging glaciers in the Swiss Alps. *Annals of Glaciology*, 6: 248–249.

Allen, S., Gruber, S., and Owens, I. (2009). Exploring steep bedrock permafrost and its relationship with recent slope failures in the Southern Alps of New Zealand. *Permafrost and Periglacial Processes*, 20 (4): 345–356. doi: 10.1002/ppp.658.

Anisimov, O., Shiklomanov, N., and Nelson, F. (2002). Variability of seasonal thaw depth in permafrost regions: a stochastic modeling approach. *Ecological Modelling*, 153 (3): 217–227. doi: 10.1016/S0304-3800(02)00016-9.

Apaloo, J., Brenning, A., and Bodin, X. (2012). Interactions between seasonal snow cover, ground surface temperature and topography (Andes of Santiago, Chile, 33.5^{o}S). *Permafrost and Periglacial Processes*, 23 (4): 277–291. doi: 10.1002/ppp.1753.

Arenson, L., Hoelzle, M., and Springman, S. (2002). Borehole deformation measurements and internal structure of some rock glaciers in Switzerland. *Permafrost and Periglacial Processes*, 13 (2): 117–135. doi: 10.1002/ppp.414.

Arenson, L. U. and Springman, S. M. (2005). Triaxial constant stress and constant strain rate tests on ice-rich permafrost samples. *Canadian Geotechnical Journal*, 42 (2): 412–430. doi: 10.1139/t04-111.

Azócar, G. and Brenning, A. (2010). Hydrological and geomorphological significance of rock glaciers in the dry Andes, Chile (27^o–33^o S). *Permafrost and Periglacial Processes*, 21 (1): 42–53. doi: 10.1002/ppp.669.

BAFU (2005). Hinweiskarte der potentiellen Permafrostverbreitung in der Schweiz. *Swiss Federal Office for the Environment (FOEN)*.

Ballantyne, C. K. (1978). The hydrologic significance of nivation features in permafrost areas. *Geografiska Annaler. Series A, Physical Geography*, 60 (1/2): pp. 51–54.

Barsch, D. (1977). Nature and importance of mass wasting by rock glaciers in alpine permafrost environments. *Earth Surface Processes*, 2 (2): 231–245. doi: 10.1002/esp.3290020213.

Barsch, D. (1978). Active rock glaciers as indicators for discontinuous alpine permafrost. An example from the Swiss Alps. In: *Proceedings of the 3th International Conference on Permafrost. Edmonton, Canada, 10–13 July*, (edited by Brown, R.), pp. 349–352.

Bernhard, L., Sutter, F., Haeberli, W., and Keller, F. (1998). Processes of snow/permafrost-interactions at high mountain site, Murtel/Corvatsch, eastern Swiss Alps. In: *Proceedings of the 7th International Conference on Permafrost. Nordicana, Yellowknife, Canada, 23–27 June*, (edited by Lewkowicz, A. and Allard, M.), pp. 35–41.

Berthling, I. and Etzelmüller, B. (2007). Holocene rockwall retreat and the estimation of rock glacier age, prins karls forland, svalbard. *Geografiska Annaler: Series A, Physical Geography*, 89 (1): 83–93. doi: 10.1111/j.1468-0459.2007.00309.x.

Black, R. (1954). Permafrost: A review. *Geological Society of America Bulletin*, 65 (9): 839–856. doi: 10.1130/0016-7606(1954)65[839:PR]2.0.CO;2.

Boeckli, L. and Noetzli, J. (2011). Wenn die Permafrostverbreitung auch für Laien fassbar wird. *Geosciences Actuel*, 4: 14–16.

Boeckli, L., Brenning, A., Gruber, S., and Noetzli, J. (2012a). A statistical approach to modelling permafrost distribution in the European Alps or similar mountain ranges. *The Cryosphere*, 6 (1): 125–140. doi: 10.5194/tc-6-125-2012.

Boeckli, L., Brenning, A., Gruber, S., and Noetzli, J. (2012b). Permafrost distribution in the European Alps: calculation and evaluation of an index map and summary statistics. *The Cryosphere*, 6 (4): 807–820. doi: 10.5194/tc-6-807-2012.

Boeckli, L., Gruber, S., Noetzli, J., and Brenning, A. (submitted). Estimated permafrost ice content at the regional scale: Method and application to the European Alps. *submitted to Permafrost and Periglacial Processes*.

Bommer, C., Phillips, M., and Arenson, L. (2010). Practical recommendations for planning, constructing and maintaining infrastructure in mountain permafrost. *Permafrost and Periglacial Processes*, 21 (1): 97–104. doi: 10.1002/ppp.679.

Bonnaventure, P. and Lewkowicz, A. (2011). Modelling climate change effects on the spatial distribution of mountain permafrost at three sites in northwest Canada. *Climatic Change*, 105: 293–312. doi: 10.1007/s10584-010-9818-5.

Bonnaventure, P. P., Lewkowicz, A. G., Kremer, M., and Sawada, M. C. (2012). A permafrost probability model for the Southern Yukon and Northern British Columbia, Canada. *Permafrost and Periglacial Processes*, 23 (1): 52–68. doi: 10.1002/ppp.1733.

Brenning, A. (2009). Benchmarking classifiers to optimally integrate terrain analysis and multispectral remote sensing in automatic rock glacier detection. *Remote Sensing of Environment*, 113 (1): 239–247. doi: 10.1016/j.rse.2008.09.005.

Brenning, A., Gruber, S., and Hoelzle, M. (2005). Sampling and statistical analyses of BTS measurements. *Permafrost and Periglacial Processes*, 16: 383–393. doi: 10.1002/ppp.541.

Brenning, A., Grasser, M., and Friend, D. (2007). Statistical estimation and generalized additive modeling of rock glacier distribution in the San Juan Mountains, Colorado, United States. *Journal of Geophysical Research*, 112 (F2): F02S15.

Brown, J., Ferrians, O., Heginbottom, J., and Melnikov, E. (1997). *Circum-Arctic map of permafrost and ground-ice conditions*. Washington, DC: U.S. Geological Survey in Cooperation with the Circum-Pacific Council for Energy and Mineral Resources. Circum-Pacific Map Series CP-45, scale 1:10,000,000.

Brown, J. D. and Heuvelink, G. B. (2007). The Data Uncertainty Engine (DUE): A software tool for assessing and simulating uncertain environmental variables. *Computers & Geosciences*, 33 (2): 172–190. doi: 10.1016/j.cageo.2006.06.015.

Burger, K., Degenhardt, J., and Giardino, J. (1999). Engineering geomorphology of rock glaciers. *Geomorphology*, 31 (1): 93–132. doi: doi:10.1016/S0169-555X(99)00074-4.

Burke, M., Abraham, J., Smith, B., Cannia, J., Voss, C., Jorgenson, M., Walvoord, M., Wylie, B., Anderson, L., Ball, L., *et al.* (2012). Airborne electromagnetic imaging of discontinuous permafrost. *Geophysical Research Letters*, 39: 8 pp. doi: 10.1029/2011GL050079.

Burn, C. R. and Zhang, Y. (2009). Permafrost and climate change at Herschel Island (Qikiqtaruq), Yukon Territory, Canada. *Journal of Geophysical Research: Earth Surface*, 114 (F2): 2156–2202. doi: 10.1029/2008JF001087.

Caine, N. (2010). Recent hydrologic change in a colorado alpine basin: an indicator of permafrost thaw? *Annals of Glaciology*, 51 (56): 130–134. doi: 10.3189/172756411795932074.

Cermak, V. and Rybach, L. (2012). Thermal conductivity and specific heat of minerals and rocks. *Landolt-Börnstein - Group V Geophysics Numerical Data and Functional Relationships in Science and Technology. SpringerMaterials - The Landolt-Börnstein Database*. doi: 10.1007/b20008.

Christian, E. (1987). Composition and origin of underground arthropod fauna in an extrazonal permafrost soil of central Europe. *Biology and Fertility of Soils*, 3 (1): 27–30.

Clow, D., Schrott, L., Webb, R., Campbell, D., Torizzo, A., and Dornblaser, M. (2003). Ground water occurrence and contributions to streamflow in an alpine catchment,

Colorado Front Range. *Ground Water*, 41 (7): 937–950. doi: 10.1111/j.1745-6584.2003.tb02436.x.

Corripio, J. (2003). Vectorial algebra algorithms for calculating terrain parameters from DEMs and solar radiation modelling in mountainous terrain. *International Journal of Geographical Information Science*, 17 (1): 1–23.

Couture, N. and Pollard, W. (1998). An assessment of ground ice volume near Eureka, Northwest Territories. In: *Proceedings of the 7th International Conference on Permafrost. Nordicana, Yellowknife, Canada, 23–27 June*, (edited by Lewkowicz, A. and Allard, M.), pp. 195–200.

Cremonese, E., Gruber, S., Phillips, M., Pogliotti, P., Boeckli, L., Noetzli, J., Suter, C., Bodin, X., Crepaz, A., Kellerer-Pirklbauer, A., Lang, K., Letey, S., Mair, V., Morra di Cella, U., Ravanel, L., Scapozza, C., Seppi, R., and Zischg, A. (2011). Brief Communication: "An inventory of permafrost evidence for the European Alps". *The Cryosphere*, 5 (3): 651–657. doi: 10.5194/tc-5-651-2011.

Danilov, I. (1990). *Podzemnyje l'dy*. Nerda, Moskva (in Russian).

Davies, M. C. R., Hamza, O., and Harris, C. (2001). The effect of rise in mean annual temperature on the stability of rock slopes containing ice-filled discontinuities. *Permafrost and Periglacial Processes*, 12 (1): 137–144. doi: 10.1002/ppp.378.

de Vries, D. A. (1963). Thermal properties of soil. *In Physics of Plant Environment, edited by W. R. van Dijk, pp. 210–235, North Holland Publishing, Amsterdam*.

Delaloye, R. and Lambiel, C. (2005). Evidence of winter ascending air circulation throughout talus slopes and rock glaciers situated in the lower belt of alpine discontinuous permafrost (Swiss Alps). *Norsk Geografisk Tidsskrift - Norwegian Journal of Geography*, 59 (2): 194–203. doi: 10.1080/00291950510020673.

Delaloye, R., Reynard, E., and Wenker, L. (1998). Rock glaciers, Entremont, Valais, Switzerland. *Boulder CO: National Snow and Ice Data Center/World Data Center for Glaciology. Digital Media*.

Delaloye, R., Perruchoud, E., Avian, M., Kaufmann, V., Bodin, X., Hausmann, H., Ikeda, A., Kääb, A., Kellerer-Pirklbauer, A., Krainer, K., Lambiel, C., Mihajlovic, D., Staub, B., Roer, I., and Thibert, E. (2008). Recent interannual variations of rock glacier creep in the European Alps. In: *Proceedings of the 9th International Conference on Permafrost. Fairbanks, Alaska, 30 June–3 July*, (edited by Kane, D. and Hinkel, K.), pp. 343–348.

Dingman, S. L. and Koutz, F. R. (1974). Relations among vegetation, permafrost, and potential insolation in Central Alaska. *Arctic and Alpine Research*, 6 (1): pp. 37–47.

Dobinski, W. (2011). Permafrost. *Earth-Science Reviews*, 108: 158–169. doi: 10.1016/j.earscirev.2011.06.007.

Ebohon, B. and Schrott, L. (2008). Modeling mountain permafrost distribution: A new map of Austria. In: *Proceedings of the 9th International Conference on Permafrost. Fairbanks, Alaska, 30 June–3 July*, (edited by Kane, D. and Hinkel, K.), pp. 397–402.

Efthymiadis, D., Jones, P., Briffa, K., Auer, I., Böhm, R., Schöner, W., Frei, C., and Schmidli, J. (2006). Construction of a 10-min-gridded precipitation data set for the Greater Alpine Region for 1800–2003. *Journal of Geophysical Research*, 110: D01105. doi: 10.1029/2005JD006120.

Endrizzi, S. (2007). Snow cover modellin at the local and distributed scale over complex terrain. Ph.D. thesis, Department of Environmental Engineering, University of Trento.

Engelhardt, M., Hauck, C., and Salzmann, N. (2010). Influence of atmospheric forcing parameters on modelled mountain permafrost evolution. *Meteorologische Zeitschrift*, 19 (5): 491–500. doi: doi:10.1127/0941-2948/2010/0476.

Etzelmüller, B. and Frauenfelder, R. (2009). Factors controlling the distribution of mountain permafrost in the Northern Hemisphere and their influence on sediment transfer. *Arctic, Antarctic, and Alpine Research*, 41 (1): 48–58. doi: 10.1657/1938-4246.

Etzelmüller, B., Hoelzle, M., Heggem, E. S. F., Isaksen, K., Mittaz, C., Mühll, D. V., Odegard, R. S., Haeberli, W., and Sollid, J. L. (2001a). Mapping and modelling the occurrence and distribution of mountain permafrost. *Norsk Geografisk Tidsskrift - Norwegian Journal of Geography*, 55 (4): 186–194. doi: 10.1080/00291950152746513.

Etzelmüller, B., Ødegård, R. S., Berthling, I., and Sollid, J. L. (2001b). Terrain parameters and remote sensing data in the analysis of permafrost distribution and periglacial processes: principles and examples from southern Norway. *Permafrost and Periglacial Processes*, 1: 79–92. doi: 10.1002/ppp.384.

Etzelmüller, B., Heggem, E., Sharkhuu, N., Frauenfelder, R., Kääb, A., and Goulden, C. (2006). Mountain permafrost distribution modelling using a multi-criteria approach in the Hövsgöl area, northern Mongolia. *Permafrost and Periglacial Processes*, 17: 91–104. doi: 10.1002/ppp.554.

Etzelmüller, B., Schuler, T. V., Isaksen, K., Christiansen, H. H., Farbrot, H., and Benestad, R. (2011). Modeling the temperature evolution of Svalbard permafrost during the 20th and 21st century. *The Cryosphere*, 5 (1): 67–79. doi: 10.5194/tc-5-67-2011.

Evin, M. and Fabre, D. (1990). The distribution of permafrost in rock glaciers of the southern Alps (France). *Geomorphology*, 3 (1): 57–71. doi: 10.1016/0169-555X(90)90032-L.

Farbrot, H., Etzelmüller, B., Schuler, T., Guðmundsson, Á., Eiken, T., Humlum, O., and Björnsson, H. (2007). Thermal characteristics and impact of climate change on mountain permafrost in Iceland. *Journal of Geophysical Research*, 112 (F3): F03S90.

Fiddes, J. and Gruber, S. (2012). TopoSUB: a tool for efficient large area numerical modelling in complex topography at sub-grid scales. *Geoscientific Model Development*, 5 (5): 1245–1257. doi: 10.5194/gmd-5-1245-2012.

Fiddes, J. and Gruber, S. (in prep.). Toposcale: An efficient method to downscale surface fluxes from global gridded climate datasets. *to be defined*.

Fischer, L., Kääb, A., Huggel, C., and Noetzli, J. (2006). Geology, glacier retreat and permafrost degradation as controlling factors of slope instabilities in a high-mountain rock wall: the Monte Rosa east face. *Natural Hazards and Earth System Science*, 6 (5): 761–772. doi: 10.5194/nhess-6-761-2006.

Fischer, L., Purves, R. S., Huggel, C., Noetzli, J., and Haeberli, W. (2012). On the influence of topographic, geological and cryospheric factors on rock avalanches and rockfalls in high-mountain areas. *Natural Hazards and Earth System Science*, 12 (1): 241–254. doi: 10.5194/nhess-12-241-2012.

Frauenfelder, R. (1998). Rock glaciers, Fletschhorn Area, Valais, Switzerland. *International Permafrost Association, Data and Information Working Group, NSIDC, University of Colorado at Boulder*.

Frauenfelder, R., Allgöwer, B., Haeberli, W., and Hoelzle, M. (1998). Permafrost investigations with GIS – a case study in the Fletschhorn area, Wallis, Swiss Alps. In: *Proceedings of the 7th International Conference on Permafrost. Nordicana, Yellowknife, Canada, 23–27 June*, (edited by Lewkowicz, A. and Allard, M.), pp. 551–556.

Frauenfelder, R., Haeberli, W., Hoelzle, M., and Maisch, M. (2001). Using relict rock-glaciers in GIS-based modelling to reconstruct Younger Dryas permafrost distribution patterns in the Err-Julier area, Swiss Alps. *Norsk Geografisk Tidsskrift - Norwegian Journal of Geography*, 55 (4): 195–202. doi: 10.1080/00291950152746522.

French, H. (2007). *The Periglacial Environment*. John Wiley and Sons Ltd, Chichester, UK, 458 pp.

Funk, M. and Hoelzle, M. (1992). Application of a potential direct solar radiation model for investigating occurrences of mountain permafrost. *Permafrost and Periglacial Processes*, 3(2): 139–142. doi: 10.1002/ppp.3430030211.

Gelman, A. and Hill, J. (2007). *Data analysis using regression and multilevel/hierarchical models*, vol. 648. Cambridge University Press: Cambridge, UK.

Giles, J. R. (2011). Geoscience metadata–No pain, no gain. *Geological Society of America Special Papers*, 482: 29–33. doi: 10.1130/2011.2482(03).

Girard, L., Beutel, J., Gruber, S., Hunziker, J., Lim, R., and Weber, S. (2012). A custom acoustic emission monitoring system for harsh environments: application to freezing-induced damage in alpine rock walls. *Geoscientific Instrumentation, Methods and Data*

Systems, 1 (2): 155–167. doi: 10.5194/gi-1-155-2012.

Goodchild, M. F. (2004). A general framework for error analysis in measurement-based GIS. *Journal of Geographical Systems*, 6: 323–324. doi: 10.1007/s10109-004-0140-5.

Goodrich, L. (1982). The influence of snow cover on the ground thermal regime. *Canadian Geotechnical Journal*, 19: 421–432.

Gorbunov, A. (1978). Permafrost in the mountains of central Asia. In: *Proceedings of the 3th International Conference on Permafrost. Edmonton, Canada, 10–13 July*, (edited by Brown, R.), pp. 372–377.

Gorbunov, A. P., Marchenko, S. S., and Seversky, E. V. (2004). The thermal environment of blocky materials in the mountains of Central Asia. *Permafrost and Periglacial Processes*, 15 (1): 95–98. doi: 10.1002/ppp.478.

Grosse, G., Schirrmeister, L., Kunitsky, V. V., and Hubberten, H.-W. (2005). The use of CORONA images in remote sensing of periglacial geomorphology: an illustration from the NE Siberian coast. *Permafrost and Periglacial Processes*, 16 (2): 163–172. doi: 10.1002/ppp.509.

Gruber, S. (2012a). Derivation and analysis of a high-resolution estimate of global permafrost zonation. *The Cryosphere*, 6 (1): 221–233. doi: 10.5194/tc-6-221-2012.

Gruber, S. (2012b). A global view on permafrost in steep bedrock. In: *Proceedings of the 10th International Conference on Permafrost, Salekhard, Russia, 25–29 June*, (edited by Hinkel, K.), pp. 131–136.

Gruber, S. and Haeberli, W. (2007). Permafrost in steep bedrock slopes and its temperature-related destabilization following climate change. *Journal of Geophysical Research*, 112: F02S18. doi: 10.1029/2006JF000547.

Gruber, S. and Hoelzle, M. (2001). Statistical modelling of mountain permafrost distribution: local calibration and incorporation of remotely sensed data. *Permafrost and Periglacial Processes*, 12: 69–77. doi: 10.1002/ppp.374.

Gruber, S. and Hoelzle, M. (2008). The cooling effect of coarse blocks revisited: a modeling study of a purely conductive mechanism. In: *Proceedings of the 9th International Conference on Permafrost. Fairbanks, Alaska, 30 June–3 July*, (edited by Kane, D. and Hinkel, K.), pp. 557–561.

Gruber, S., Peter, M., Hoelzle, M., Woodhatch, I., and Haeberli, W. (2003). Surface temperatures in steep Alpine rock faces - a strategy for regional-scale measurement and modelling. In: *Proceedings of the 8th International Conference on Permafrost. Zurich, Switzerland, 21–25 July*, (edited by Phillips, M., Springman, S., and Arenson, L.), pp. 325–330.

Gruber, S., Hoelzle, M., and Haeberli, W. (2004a). Rock-wall temperatures in the Alps: modelling their topographic distribution and regional differences. *Permafrost and Periglacial Processes*, 15(3) (1): 299–307. doi: 10.1002/ppp.501.

Gruber, S., King, L., Kohl, T., Herz, T., Haeberli, W., and Hoelzle, M. (2004b). Interpretation of geothermal profiles perturbed by topography: the alpine permafrost boreholes at Stockhorn Plateau, Switzerland. *Permafrost and Periglacial Processes*, 15: 349–357. doi: 10.1002/ppp.503.

Gubler, S., Fiddes, J., Keller, M., and Gruber, S. (2011). Scale-dependent measurement and analysis of ground surface temperature variability in alpine terrain. *The Cryosphere*, 5 (2): 431–443. doi: 10.5194/tc-5-431-2011.

Gubler, S., Endrizzi, S., Gruber, S., and Purves, R. S. (2013). Sensitivities and uncertainties of modeled ground temperatures in mountain environments. *Geoscientific Model Development Discussions*, 6 (1): 791–840. doi: 10.5194/gmdd-6-791-2013.

Guglielmin, M., Aldighieri, B., and Testa, B. (2003). PERMACLIM: a model for the distribution of mountain permafrost, based on climatic observations. *Geomorphology*, 51 (4): 245–257. doi: 10.1016/S0169-555X(02)00221-0.

Gurney, S. D. (1998). Aspects of the genesis and geomorphology of pingos: perennial permafrost mounds. *Progress in Physical Geography*, 22 (3): 307–324. doi: 10.1177/030913339802200301.

Gurney, S. D. (2001). Aspects of the genesis, geomorphology and terminology of palsas: perennial cryogenic mounds. *Progress in Physical Geography*, 25 (2): 249–260. doi: 10.1177/030913330102500205.

Haeberli, W. (1973). Die Basis-Temperatur der winterlichen Schneedecke als möglicher Indikator für die Verbreitung von Permafrost in den Alpen. *Zeitschrift für Gletscherkunde und Glazialgeologie*, IX/1/2: 221–227.

Haeberli, W. (1975). Untersuchungen zur Verbreitung von Permafrost zwischen Flüelapass und Piz Grialetsch (Graubünden). *Mitteilungen der Versuchsanstalt für Wasserbau, Hydrologie und Glaziologie der ETH Zürich, Zurich, Switzerland*, 17: 221 p.

Haeberli, W. (1976). Eistemperaturen in den Alpen. *Zeitschrift für Gletscherkunde und Glazialgeologie*, 11 (2): 203–220.

Haeberli, W. (1978). Special aspects of high mountain permafrost methodology and zonation in the Alps. In: *Proceedings of the 3th International Conference on Permafrost. Edmonton, Canada, 10–13 July*, (edited by Brown, R.), pp. 379–384.

Haeberli, W. (1979). Holocene push-moraines in Alpine permafrost. *Geografiska Annaler. Series A, Physical Geography*, 61 (1/2): pp. 43–48.

Haeberli, W. (1985). Creep of mountain permafrost: internal structure and flow of alpine rock glaciers. *Mitteilungen der VAW/ETH Zürich*, 77.

Haeberli, W. (1992). Construction, environmental problems and natural hazards in periglacial mountain belts. *Permafrost and Periglacial Processes*, 3 (2): 111–124. doi: 10.1002/ppp.3430030208.

Haeberli, W. and Alean, J. (1985). Temperature and accumulation of high altitude firn in the Alps. *Annals of Glaciology*, 6: 161–163.

Haeberli, W., Wegmann, M., and Vonder Mühll, D. (1997). Slope stability problems related to glacier shrinkage and permafrost degradation in the alps. *Eclogae geologicae Helvetiae*, 90: 407–414.

Haeberli, W., Hallet, B., Arenson, L., Elconin, R., Humlum, O., Kääb, A., Kaufmann, V., Ladanyi, B., Matsuoka, N., Springman, S., and Vonder Mühll, D. (2006). Permafrost creep and rock glacier dynamics. *Permafrost and Periglacial Processes*, 17 (3): 189–214. doi: 10.1002/ppp.561.

Haeberli, W., Noetzli, J., Arenson, L., Delaloye, R., Gartner-Roer, I., Gruber, S., Isaksen, K., Kneisel, C., Krautblatter, M., and Phillips, M. (2011). Mountain permafrost: development and challenges of a young research field. *Journal of Glaciology*, 56 (200): 1043–1058.

Haeberli, W., Paul, F., and Zemp, M. (in press, 2013). Vanishing glaciers in the European Alps. In: *The Pontifical Academy of Sciences, Scripta Varia 118, Fate of Mountain Glaciers in the Anthropocene, Working Group 2–4 April 2011, Vatican City*.

Hall, K., Lindgren, B. S., and Jackson, P. (2005). Rock albedo and monitoring of thermal conditions in respect of weathering: some expected and some unexpected results. *Earth Surface Processes and Landforms*, 30 (7): 801–811. doi: 10.1002/esp.1189.

Hand, D. J. (1997). *Construction and assessment of classification rules*. Wiley Series in Probability and Statistics, John Wiley & Sons, Chichester.

Hanson, S. and Hoelzle, M. (2005). Installation of a shallow borehole network and monitoring of the ground thermal regime of a high alpine discontinuous permafrost environment, Eastern Swiss Alps. *Norsk Geografisk Tidsskrift - Norwegian Journal of Geography*, 59 (2): 84–93. doi: 10.1080/00291950510020664.

Harris, C. and Isaksen, K. (2008). Recent warming of European permafrost: evidence from borehole monitoring. In: *Proceedings of the 9th International Conference on Permafrost. Fairbanks, Alaska, 30 June–3 July*, (edited by Kane, D. and Hinkel, K.), pp. 655–661.

Harris, C., Mühll, D. V., Isaksen, K., Haeberli, W., Sollid, J. L., King, L., Holmlund, P., Dramis, F., Guglielmin, M., and Palacios, D. (2003). Warming permafrost in European

mountains. *Global and Planetary Change*, 39 (3-4): 215–225. doi: 10.1016/j.gloplacha.2003.04.001.

Harris, C., Arenson, L. U., Christiansen, H. H., Etzelmüller, B., Frauenfelder, R., Gruber, S., Haeberli, W., Hauck, C., Hölzle, M., Humlum, O., Isaksen, K., Kääb, A., Kern-Lütschg, M. A., Lehning, M., Matsuoka, N., Murton, J. B., Nötzli, J., Phillips, M., Ross, N., Seppälä, M., Springman, S. M., and Mühll, D. V. (2009). Permafrost and climate in Europe: Monitoring and modelling thermal, geomorphological and geotechnical responses. *Earth-Science Reviews*, 92 (3–4): 117–171. doi: 10.1016/j.earscirev.2008.12.002.

Harris, S. and Brown, R. (1978). Plateau Mountain: a case study of alpine permafrost in the Canadian Rocky Mountains. In: *Proceedings of the 3th International Conference on Permafrost. Edmonton, Canada, 10–13 July*, (edited by Brown, R.), pp. 386–391.

Harris, S. and Pedersen, D. (1998). Thermal regimes beneath coarse blocky materials. *Permafrost and Periglacial Processes*, 9 (2): 107–120. doi: 10.1002/(SICI)1099-1530(199804/06)9:2<107::AID-PPP277>3.0.CO;2-G.

Hasler, A., Talzi, I., Tschudin, C., and Gruber, S. (2008). Wireless sensor networks in permafrost research - concept, requirements, implementation and challenges. In: *Proceedings of the 9th International Conference on Permafrost. Fairbanks, Alaska, 30 June–3 July*, (edited by Kane, D. and Hinkel, K.), pp. 669–674.

Hasler, A., Gruber, S., Font, M., and Dubois, A. (2011a). Advective heat transport in frozen rock clefts: Conceptual model, laboratory experiments and numerical simulation. *Permafrost and Periglacial Processes*, 22 (4): 378–389. doi: 10.1002/ppp.737.

Hasler, A., Gruber, S., and Haeberli, W. (2011b). Temperature variability and offset in steep alpine rock and ice faces. *The Cryosphere*, 5 (4): 977–988. doi: 10.5194/tc-5-977-2011.

Hasler, A., Gruber, S., and Beutel, J. (2012). Kinematics of steep bedrock permafrost. *Journal of Geophysical Research*, 117 (F1): F01016. doi: 10.1029/2011JF001981.

Hauck, C. (submitted). New concepts of geophysical surveying and data interpretation in permafrost terrain - a review. *Submitted to Permafrost and Periglacial Processes*.

Hauck, C. and Kneisel, C. (2008). *Quantifying the ice content in low-altitude scree slopes using geophysical methods*. Applied Geophysics in Periglacial Environments, Cambridge University Press. doi: 10.1017/CBO9780511535628.

Hauck, C., Vonder Mühll, D., and Maurer, H. (2003). Using dc resistivity tomography to detect and characterize mountain permafrost. *Geophysical Prospecting*, 51 (4): 273–284. doi: 10.1046/j.1365-2478.2003.00375.x.

Hausmann, H., Krainer, K., Brückl, E., and Mostler, W. (2007). Internal structure and ice content of Reichenkar rock glacier (Stubai Alps, Austria) assessed by geophysical investigations. *Permafrost and Periglacial Processes*, 18 (4): 351–367. doi: 10.1002/ppp.601.

Hayakawa, Y., Oguchi, T., and Lin, Z. (2008). Comparison of new and existing global digital elevation models: ASTER G-DEM and SRTM-3. *Geophysical Research Letters*, 35 (17): L17404. doi: 10.1029/2008GL035036.

Heggem, E., Juliussen, H., and Etzelmüller, B. (2005). Mountain permafrost in central-eastern Norway. *Norsk Geografisk Tidsskrift - Norwegian Journal of Geography*, 59 (2): 94–108. doi: 10.1080/00291950510038377.

Heggem, E. S. F., Etzelmüller, B., Anarmaa, S., Sharkhuu, N., Goulden, C. E., and Nandinsetseg, B. (2006). Spatial distribution of ground surface temperatures and active layer depths in the Hövsgöl area, northern Mongolia. *Permafrost and Periglacial Processes*, 17: 357–369. doi: 10.1002/ppp.568.

Heginbottom, J. (1995). Report of the IPA data workshop. *Frozen Ground*, 18: 12–13.

Heginbottom, J. (2002). Permafrost mapping: a review. *Progress in Physical Geography*, 26 (4): 623. doi: 10.1191/0309133302pp355ra.

Hiebl, J., Auer, I., Böhm, R., Schöner, W., Maugeri, M., Lentini, G., Spinoni, J., Brunetti, M., Nanni, T., Perčec Tadić, M., Bihari, Z., Dolinar, M., and Müller-Westermeier, G. (2009). A high-resolution 1961–1990 monthly temperature climatology for the greater Alpine region. *Meteorologische Zeitschrift*, 18 (5): 507–530. doi: 10.1127/0941-2948/2009/0403.

Hinkel, K. M. and Nicholas, J. R. J. (1995). Active layer thaw rate at a boreal forest site in central Alaska, U.S.A. *Arctic and Alpine Research*, 27 (1): 72–80.

Hinzman, L., Kane, D., Yoshikawa, K., Carr, A., Bolton, W., and Fraver, M. (2003). Hydrological variations among watersheds with varying degrees of permafrost. In: *Proceedings of the 8th International Conference on Permafrost. Zurich, Switzerland, 21–25 July*, (edited by Phillips, M., Springman, S., and Arenson, L.), pp. 407–411.

Hinzman, L. D., Goering, D. J., and Kane, D. L. (1998). A distributed thermal model for calculating soil temperature profiles and depth of thaw in permafrost regions. *Journal of Geophysical Research: Atmospheres*, 103 (D22): 28975–28991. doi: 10.1029/98JD01731.

Hipp, T., Etzelmüller, B., Farbrot, H., Schuler, T. V., and Westermann, S. (2012). Modelling borehole temperatures in Southern Norway, insights into permafrost dynamics during the 20th and 21st century. *The Cryosphere*, 6 (3): 553–571. doi: 10.5194/tc-6-553-2012.

Hjort, J. and Marmion, M. (2008). Effects of sample size on the accuracy of geomorphological models. *Geomorphology*, 102 (3-4): 341–350. doi: DOI:10.1016/j.geomorph.2008.04.006.

Hoelzle, M. (1992). Permafrost occurrence from BTS measurements and climatic parameters in the Eastern Swiss Alps. *Permafrost and Periglacial Processes*, 3 (2): 143–147. doi: 10.1002/ppp.3430030212.

Hoelzle, M. (1998). Rock glaciers, Upper Engadin, Switzerland. Boulder. *CO: National Snow and Ice Data Center/World Data Center for Glaciology. Digital Media*.

Hoelzle, M. and Gruber, S. (2008). Borehole and ground surface temperatures and their relationship to meteorological conditions in the Swiss Alps. In: *Proceedings of the 9th International Conference on Permafrost. Fairbanks, Alaska, 30 June–3 July*, (edited by Kane, D. and Hinkel, K.), pp. 723–728.

Hoelzle, M., Haeberli, W., and Keller, F. (1993). Application of BTS-measurements for modelling permafrost distribution in the Swiss Alps. In: *Proceedings of the 6th International Conference on Permafrost. Beijing, China, 5–9 July*, (edited by Brown, J.), pp. 272–277.

Hoelzle, M., Mittaz, C., Etzelmüller, B., and Haeberli, W. (2001). Surface energy fluxes and distribution models of permafrost in European mountain areas: an overview of current developments. *Permafrost and Periglacial Processes*, 12: 53–68. doi: 10.1002/ppp.385.

Hoelzle, M., Mühll, D. V., and Haeberli, W. (2002). Thirty years of permafrost research in the Corvatsch-Furtschellas area, Eastern Swiss Alps: a review. *Norsk Geografisk Tidsskrift - Norwegian Journal of Geography*, 56 (2): 137–145. doi: 10.1080/00291950276005646 8.

Hosmer, D. and Lemeshow, S. (2000). *Applied logistic regression*. Wiley-Interscience, New York.

Huete, A. (1988). A soil-adjusted vegetation index (SAVI). *Remote Sensing of Environment*, 25 (3): 295–309. doi: 10.1016/0034-4257(88)90106-X.

Humlum, O. (1997). Active layer thermal regime at three rock glaciers in Greenland. *Permafrost and Periglacial Processes*, 8 (4): 383–408. doi: 10.1002/(SICI)1099-1530(199710/12)8:4<383::AID-PPP265>3.0.CO;2-V.

Ikeda, A. and Matsuoka, N. (2002). Degradation of talus-derived rock glaciers in the Upper Engadin, Swiss Alps. *Permafrost and Periglacial Processes*, 13 (2): 145–161. doi: 10.1002/ppp.413.

Imhof, M. (1996). Modelling and verification of the permafrost distribution in the Bernese Alps, Switzerland. *Permafrost and Periglacial Processes*, 17: 267–280. doi:

10.1002/(SICI)1099-1530(199609)7:3<267::AID-PPP221>3.0.CO;2-L.

Imhof, M. (1998). Rock glaciers, Bernese Alps, western Switzerland. *Boulder CO: National Snow and Ice Data Center/World Data Center for Glaciology. Digital Media*.

Ingersoll, L., Zobel, O., and Ingersoll, A. (1954). *Heat conduction*. The University of Wisconsin Press.

International Organization for Standardization (1975). *International Standard Atmosphere*. Standard Atmosphere ISO 2533:1975.

IPCC (2007). *Climate Change 2007: The physical science basis. Contribution of Working Group I to the Fourth Assessment Report of the Intergovernmental Panel on Climate Change*. Cambridge University Press, Cambridge, United Kingdom and New York, NY, USA,.

Isaksen, K., Heggem, E., Bakkehøi, S., Ødegård, R., Eiken, T., Etzelmüller, B., and Sollid, J. (2003). Mountain permafrost and energy balance on Juvvasshøe, southern Norway. In: *Proceedings of the 8th International Conference on Permafrost. Zurich, Switzerland, 21–25 July*, (edited by Phillips, M., Springman, S., and Arenson, L.), pp. 467–472.

Janke, J. R. (2001). Rock glacier mapping: A method utilizing Enhanced TM data and GIS modeling techniques. *Geocarto International*, 16 (3): 5–15. doi: 10.1080/10106040108542199.

Janke, J. R. (2004). The occurrence of alpine permafrost in the Front Range of Colorado. *Geomorphology*, 67: 375–389. doi: 10.1016/j.geomorph.2004.11.005.

Janke, J. R. (2005). Photogrammetric analysis of Front Range rock glacier flow rates. *Geografiska Annaler: Series A, Physical Geography*, 87 (4): 515–526. doi: 10.1111/j.0435-3676.2005.00275.x.

Julian, A. and Chueca, J. (2007). Permafrost distribution from BTS measurements (Sierra de Telera, Central Pyrenees, Spain): assessing the importance of solar radiation in a mid-elevation shaded mountainous area. *Permafrost and Periglacial Processes*, 18 (2): 137–149. doi: 10.1002/ppp.576.

Juliussen, H. and Humlum, O. (2007). Towards a TTOP ground temperature model for mountainous terrain in central-eastern Norway. *Permafrost and Periglacial Processes*, 18 (2): 161–184. doi: 10.1002/ppp.586.

Juliussen, H. and Humlum, O. (2008). Thermal regime of openwork block fields on the mountains Elgåhogna and Sølen, central-eastern Norway. *Permafrost and Periglacial Processes*, 19 (1): 1–18. doi: 10.1002/ppp.607.

Kääb, A. (2008). Remote sensing of permafrost-related problems and hazards. *Permafrost and Periglacial Processes*, 19 (2): 107–136. doi: 10.1002/ppp.619.

Kääb, A. and Kneisel, C. (2006). Permafrost creep within a recently deglaciated glacier forefield: Muragl, Swiss Alps. *Permafrost and Periglacial Processes*, 17 (1): 79–85. doi:

10.1002/ppp.540.

Kääb, A., Haeberli, W., and Gudmundsson, G. H. (1997). Analysing the creep of mountain permafrost using high precision aerial photogrammetry: 25 years of monitoring Gruben rock glacier, Swiss Alps. *Permafrost and Periglacial Processes*, 8 (4): 409–426. doi: 10.1002/(SICI)1099-1530(199710/12)8:4<409::AID-PPP267>3.0.CO;2-C.

Kääb, A., Frauenfelder, R., and Roer, I. (2007). On the response of rockglacier creep to surface temperature increase. *Global and Planetary Change*, 56: 172–187. doi: 10.1016/j.gloplacha.2006.07.005. <ce:title>Climate Change Impacts on Mountain Glaciers and Permafrost</ce:title>.

Kane, D. L., Hinkel, K. M., Goering, D. J., Hinzman, L. D., and Outcalt, S. I. (2001). Non-conductive heat transfer associated with frozen soils. *Global and Planetary Change*, 29: 275–292. doi: 10.1016/S0921-8181(01)00095-9.

Keller, F. (1992). Automated mapping of mountain permafrost using the program PERMAKART within the geographical information system ARC/INFO. *Permafrost and Periglacial Processes*, 3 (2): 133–138. doi: 10.1002/ppp.3430030210.

Keller, F. and Gubler, H. (1993). Interaction between snow cover and high mountain permafrost, Murtel-Corvatsch, Swiss Alps. In: *Proceedings of the 6th International Conference on Permafrost. Beijing, China, 5–9 July*, (edited by Brown, J.), pp. 332–337.

Keller, F., Frauenfelder, R., Hoelzle, M., Kneisel, C., Lugon, R., Phillips, M., Reynard, E., and Wenker, L. (1998). Permafrost map of Switzerland. In: *Proceedings of the 7th International Conference on Permafrost. Nordicana, Yellowknife, Canada, 23–27 June*, (edited by Lewkowicz, A. and Allard, M.), pp. 557–562.

Keusen, H. and Haeberli, W. (1983). Site investigation and foundation design aspects of cable car construction in Alpine permafrost at the "Chli Matterhorn", Wallis, Swiss Alps. In: *Proceedings of the 4th International Conference on Permafrost. Fairbanks, Alaska, USA, 18–22 July*, pp. 601–605.

King, L. (1986). Zonation and ecology of high mountain permafrost in Scandinavia. *Geografiska Annaler. Series A. Physical Geography*, 68 (3): 131–139.

Kneisel, C. (1998). Occurrence of surface ice and ground ice/permafrost in recently deglaciated glacier forefields, St. Moritz area, Eastern Swiss Alps. In: *Proceedings of the 7th International Conference on Permafrost. Nordicana, Yellowknife, Canada, 23–27 June*, (edited by Lewkowicz, A. and Allard, M.), pp. 575–581.

Kneisel, C. (2004). New insights into mountain permafrost occurrence and characteristics in glacier forefields at high altitude through the application of 2D resistivity imaging. *Permafrost and Periglacial Processes*, 15 (3): 221–227. doi: 10.1002/ppp.495.

Kneisel, C. and Kääb, A. (2007). Mountain permafrost dynamics within a recently exposed glacier forefield inferred by a combined geomorphological, geophysical and photogrammetrical approach. *Earth Surface Processes and Landforms*, 32 (12): 1797–1810. doi: 10.1002/esp.1488.

Kneisel, C., Haeberli, W., and Baumhauer, R. (2000a). Comparison of spatial modelling and field evidence of glacier/permafrost relations in an Alpine permafrost environment. *Annals of Glaciology*, 31 (1): 269–274. doi: 10.3189/172756400781820093.

Kneisel, C., Hauck, C., and Mühll, D. V. (2000b). Permafrost below the timberline confirmed and characterized by geoelectrical resistivity measurements, Bever Valley, eastern Swiss Alps. *Permafrost and Periglacial Processes*, 11 (4): 295–304. doi: 10.1002/1099-1530(200012)11:4<295::AID-PPP353>3.0.CO;2-L.

Kneisel, C., Rothenbühler, C., Keller, F., and Haeberli, W. (2007). Hazard assessment of potential periglacial debris flows based on GIS-based spatial modelling and geophysical field surveys: a case study in the Swiss Alps. *Permafrost and Periglacial Processes*, 18 (3): 259–268. doi: 10.1002/ppp.593.

Kneisel, C., Hauck, C., Fortier, R., and Moorman, B. (2008). Advances in geophysical methods for permafrost investigations. *Permafrost and Periglacial Processes*, 19 (2): 157–178. doi: 10.1002/ppp.616.

Kohl, T. (1999). Transient thermal effects below complex topographies. *Tectonophysics*, 306: 311–324. doi: 10.1016/S0040-1951(99)00063-3.

Kohl, T., Signorelli, S., and Rybach, L. (2001). Three-dimensional (3-D) thermal investigation below high Alpine topography. *Physics of the Earth and Planetary Interiors*, 126: 195–210. doi: 10.1016/S0031-9201(01)00255-2.

Kremer, M., Lewkowicz, A. G., Bonnaventure, P. P., and Sawada, M. C. (2011). Utility of classification and regression tree analyses and vegetation in mountain permafrost models, Yukon, Canada. *Permafrost and Periglacial Processes*, 22 (2): 163–178. doi: 10.1002/ppp.719.

Lambiel, C. and Baron, L. (2008). Two-dimensional geoelectrical monitoring in an alpine frozen moraine. In: *Proceedings of the 9th International Conference on Permafrost. Fairbanks, Alaska, 30 June–3 July*, (edited by Kane, D. and Hinkel, K.).

Lambiel, C. and Pieracci, K. (2008). Permafrost distribution in talus slopes located within the alpine periglacial belt, Swiss Alps. *Permafrost and Periglacial Processes*, 19 (3): 293–304. doi: 10.1002/ppp.624.

Lambiel, C. and Reynard, E. (2001). Regional modelling of present, past and future potential distribution of discontinuous permafrost based on a rock glacier inventory in the Bagnes–Hérémence area (Western Swiss Alps). *Norsk Geografisk Tidsskrift - Norwegian Journal of Geography*, 55 (4): 219–223.

Lawrence, D. M. and Slater, A. G. (2005). A projection of severe near-surface permafrost degradation during the 21st century. *Geophysical Research Letters*, 32 (24): L24401. doi: 10.1029/2005GL025080.

Lehmkuhl, F., Stauch, G., and Batkhishig, O. (2003). Rock glacier and periglacial processes in the Mongolian Altai. In: *Proceedings of the 8th International Conference on Permafrost. Zurich, Switzerland, 21–25 July*, (edited by Phillips, M., Springman, S., and Arenson, L.), pp. 639–644.

Lehning, M., Voelksch, I., Gustafsson, D., Nguyen, T. A., Staehli, M., and Zappa, M. (2006). Alpine3D: a detailed model of mountain surface processes and its application to snow hydrology. *Hydrological Processes*, 20 (10): 2111–2128. doi: 10.1002/hyp.6204.

Leung, Y., Ma, J.-H., and Goodchild, M. F. (2004). A general framework for error analysis in measurement-based GIS Part 1: The basic measurement-error model and related concepts. *Journal of Geographical Systems*, 6: 325–354. doi: 10.1007/s10109-004-0141-4.

Levermann, A., Bamber, J. L., Drijfhout, S., Ganopolski, A., Haeberli, W., Harris, N. R. P., Huss, M., Krüger, K., Lenton, T. M., Lindsay, R. W., Notz, D., Wadhams, P., and Weber, S. (2012). Potential climatic transitions with profound impact on Europe: review of the current state of six 'tipping elements of the climate system'. *Climatic Change*, 110 (3-4): 845–878. doi: 10.1007/s10584-011-0126-5.

Lewkowicz, A. and Bonnaventure, P. (2008). Interchangeability of mountain permafrost probability models, northwest Canada. *Permafrost and Periglacial Processes*, 19 (1): 49–62. doi: 10.1002/ppp.612.

Lewkowicz, A. G. and Ednie, M. (2004). Probability mapping of mountain permafrost using the BTS method, Wolf Creek, Yukon Territory, Canada. *Permafrost and Periglacial Processes*, 15: 67–80. doi: 10.1002/ppp.480.

Li, J., Sheng, Y., Wu, J., Chen, J., and Zhang, X. (2009). Probability distribution of permafrost along a transportation corridor in the northeastern Qinghai province of China. *Cold Regions Science and Technology*, 59 (1): 12–18. doi: 10.1016/j.coldregions.2009.05.012.

Lilleoren, K. and Etzelmüller, B. (2011). A regional inventory of rock glaciers and ice-cored morains in Norway. *Geografiska Annaler: Series A, Physical Geography*, 93 (3): 175–191. doi: 10.1111/j.1468-0459.2011.00430.x.

Luetscher, M., Jeannin, P.-Y., and Haeberli, W. (2005). Ice caves as an indicator of winter climate evolution: a case study from the Jura Mountains. *The Holocene*, 15 (7): 982–993. doi: 10.1191/0959683605hl872ra.

Luetschg, M. and Haeberli, W. (2005). Permafrost evolution in the Swiss Alps in a changing climate and the role of the snow cover. *Norsk Geografisk Tidsskrift - Norwegian Journal of Geography*, 59: 78–83. doi: 10.1080/00291950510020583.

Luetschg, M., Stoeckli, V., Lehning, M., Haeberli, W., and Ammann, W. (2004). Temperatures in two boreholes at Flüela Pass, Eastern Swiss Alps: the effect of snow redistribution on permafrost distribution patterns in high mountain areas. *Permafrost and Periglacial Processes*, 15 (3): 283–297. doi: 10.1002/ppp.500.

Luetschg, M., Lehning, M., and Haeberli, W. (2008). A sensitivity study of factors influencing warm/thin permafrost in the Swiss Alps. *Journal of Glaciology*, 54 (187): 696–704. doi: 10.3189/002214308786570881.

Lunardini, V. (1991). *Heat transfer with freezing and thawing*. Developments in Geotechnical Engineering, Elsevier Sscience Publishers B.V., Amsterdam, Netherlands.

Luoto, M. and Hjort, J. (2004). Generalized linear modelling in periglacial studies: terrain parameters and patterned ground. *Permafrost and Periglacial Processes*, 15 (4): 327–338. doi: 10.1002/ppp.482.

Luoto, M. and Seppälä, M. (2002). Modelling the distribution of palsas in Finnish Lapland with logistic regression and GIS. *Permafrost and Periglacial Processes*, 13 (1): 17–28. doi: 10.1002/ppp.404.

Lüthi, M. and Funk, M. (2001). Modelling heat flow in a cold, high-altitude glacier: Interpretation of measurements from Colle Gnifetti, Swiss Alps. *Journal of Glaciology*, 47 (157): 314–324. doi: 10.3189/172756501781832223.

Luthin, J. and Guymon, G. (1974). Soil moisture-vegetation-temperature relationships in central Alaska. *Journal of Hydrology*, 23 (3/4): 233–246. doi: 10.1016/0022-1694(74)90005-5.

Mahaney, W. C., Miyamoto, H., Dohm, J. M., Baker, V. R., Cabrol, N. A., Grin, E. A., and Berman, D. C. (2007). Rock glaciers on Mars: Earth-based clues to Mars' recent paleoclimatic history. *Planetary and Space Science*, 55: 181–192. doi: 10.1016/j.pss.2006.04.016.

Mair, V., Zischg, A., Lang, D., K. andTonidandel, Krainer, K., Kellerer-Pirklbauer, A., Deline, P., Schoeneich, P., Cremonese, E., Pogliotti, P., Gruber, S., and Boeckli, L. (2011). PermaNET - Permafrost Long-term Monitoring Network. 1, Report 3. Klagenfurt. *Synthesis report. Interpraevent Journal series*, 1.

Marchenko, S., Romanovsky, V., and Tipenko, G. (2008). Numerical modeling of spatial permafrost dynamics in Alaska. In: *Proceedings of the 9th International Conference on Permafrost. Fairbanks, Alaska, 30 June–3 July*, (edited by Kane, D. and Hinkel, K.), pp. 190–204.

Mason, S. and Graham, N. (2002). Areas beneath the relative operating characteristics (roc) and relative operating levels (rol) curves: Statistical significance and interpretation. *Quarterly Journal of the Royal Meteorological Society*, 128 (584): 2145–2166. doi: 10.1256/003590002320603584.

Matsuoka, N. (2001a). Direct observation of frost wedging in alpine bedrock. *Earth Surface Processes and Landforms*, 26 (6): 601–614. doi: 10.1002/esp.208.

Matsuoka, N. (2001b). Solifluction rates, processes and landforms: a global review. *Earth-Science Reviews*, 55: 107–134. doi: 10.1016/S0012-8252(01)00057-5.

Maurer, H. and Hauck, C. (2007). Instruments and methods geophysical imaging of alpine rock glaciers. *Journal of Glaciology*, 53: 110–120.

Morard, S., Delaloye, R., and Dorthe, J. (2008). Seasonal thermal regime of a mid-latitude ventilated debris accumulation. In: *Proceedings of the 9th International Conference on Permafrost. Fairbanks, Alaska, 30 June–3 July*, (edited by Kane, D. and Hinkel, K.), pp. 1233–1238.

Mott, R., Faure, F., Lehning, M., Löwe, H., Hynek, B., Michlmayr, G., Prokop, A., and Schöner, W. (2008). Simulation of seasonal snow cover distribution for glacierized sites on Sonnblick, Austria, with Alpine3D model. *Annals of Glaciology*, 49: 155–160. doi: 10.3189/172756408787814924.

Mottaghy, D. and Rath, V. (2006). Latent heat effects in subsurface heat transport modeling and their impact on paleotemperature reconstructions. *Geophysical Journal International*, 164 (1): 236–245.

Nelson, F. E., Shiklomanov, N. I., Mueller, G. R., Hinkel, K. M., Walker, D. A., and Bockheim, J. G. (1997). Estimating active-layer thickness over a large region: Kuparuk River Basin, Alaska, U.S.A. *Arctic and Alpine Research*, 29 (4): 367–378.

Nicolsky, D. J., Romanovsky, V. E., Alexeev, V. A., and Lawrence, D. M. (2007). Improved modeling of permafrost dynamics in a GCM land-surface scheme. *Geophysical Research Letters*, 34 (8): L08501. doi: 10.1029/2007GL029525.

Niu, L., Ye, B., Li, J., and Sheng, Y. (2011). Effect of permafrost degradation on hydrological processes in typical basins with various permafrost coverage in Western China. *Science China Earth Sciences*, 54: 615–624. doi: 10.1007/s11430-010-4073-1.

Noetzli, J. (2008). Modeling transient three-dimensional temperature fields in mountain permafrost. Ph.D. thesis, Department of Geography, University of Zurich, Zurich, 150 pp.

Noetzli, J. and Gruber, S. (2009). Transient thermal effects in Alpine permafrost. *The Cryosphere*, 3 (1): 85–99. doi: 10.5194/tc-3-85-2009.

Nyenhuis (2005). Permafrost und Sedimenthaushalt in einem alpinen Geosystem. Ph.D. thesis, Rheinischen Friedrich–Wilhelms–Universität Bonn.

Nyenhuis, M., Hoelzle, M., and Dikau, R. (2005). Rock glacier mapping and permafrost distribution modelling in the Turtmanntal, Valais, Switzerland. *Zeitschrift für Geomorphologie*, 49: 275–292.

Oelke, C., Zhang, T., Serreze, M. C., and Armstrong, R. L. (2003). Regional-scale modeling of soil freeze/thaw over the Arctic drainage basin. *Journal of Geophysical Research: Atmospheres*, 108 (D10). doi: 10.1029/2002JD002722.

Oke, T. (1988). *Boundary layer climates*. Routledge, Taylor and Francis Group.

Osterkamp, T. and Burn, C. (2003). Permafrost. In: *Encyclopedia of Atmospheric Sciences*, pp. 1717 – 1729. Academic Press. doi: 10.1016/B0-12-227090-8/00311-0.

Panda, S. K., Prakash, A., Solie, D. N., Romanovsky, V. E., and Jorgenson, M. T. (2010). Remote sensing and field-based mapping of permafrost distribution along the Alaska Highway corridor, interior Alaska. *Permafrost and Periglacial Processes*, 21 (3): 271–281. doi: 10.1002/ppp.686.

Paul, F., Frey, H., and Le Bris, R. (2011). A new glacier inventory for the European Alps from Landsat TM scenes of 2003: Challenges and results. *Annals of Glaciology*, 52: 144–152.

Permafrance (2010). Permafrost in France. Schoeneich, P., Bodin, X., Krysiecki, JM., Deline, P. and Ravanels, L. (eds.). *Permafrance Network, Report Nr. 1*, p. 68 p.

PERMOS (2010). Permafrost in Switzerland 2006/2007 and 2007/2008. Noetzli, J. and Vonder Muehll, D. (eds.). *Glaciological report (Permafrost) No. 8/9 of the Cryospheric Commission of the Swiss Academy of Sciences, Zurich, Switzerland*, p. 68 pp.

Phillips, M. (2006). Avalanche defence strategies and monitoring of two sites in mountain permafrost terrain, Pontresina, Eastern Swiss Alps. *Natural Hazards*, 39: 353–379. doi: 10.1007/s11069-005-6126-x.

Phillips, M., Mutter, E. Z., Kern-Luetschg, M., and Lehning, M. (2009). Rapid degradation of ground ice in a ventilated talus slope: Flüela Pass, Swiss Alps. *Permafrost and Periglacial Processes*, 20 (1): 1–14. doi: 10.1002/ppp.638.

Pogliotti, P. (2010). Influence of snow cover on MAGST over complex morphologies in mountain permafrost regions. Ph.D. thesis, Earth Science Department, University of Turin, Italy.

Pollard, W. H. and French, H. M. (1980). A first approximation of the volume of ground ice, Richards Island, Pleistocene Mackenzie delta, Northwest Territories, Canada. *Canadian Geotechnical Journal*, 17 (4): 509–516. doi: 10.1139/t80-059.

Quinton, W., Hayashi, M., and Chasmer, L. (2011). Permafrost-thaw-induced land-cover change in the Canadian subarctic: implications for water resources. *Hydrological Processes*, 25 (1): 152–158. doi: 10.1002/hyp.7894.

Ravanel, L., Allignol, F., Deline, P., Gruber, S., and Ravello, M. (2010). Rock falls in the Mont Blanc Massif in 2007 and 2008. *Landslides*, 7: 493–501. doi: 10.1007/s10346-010-0206-z.

Rebetez, M., Lugon, R., and Baeriswyl, P. A. (1997). Climatic change and debris flows in high mountain regions: The case study of the Ritigraben torrent (Swiss Alps). *Climatic Change*, 36 (3-4): 371–389. doi: 10.1023/A:1005356130392.

Reynard, E. and Morand, S. (1998). Rock glacier inventory, Printse Valley, Valais, Switzerland. *Boulder CO: National Snow and Ice Data Center/World Data Center for Glaciology. Digital Media*.

Ridefelt, H., Etzelmüller, B., Boelhouwers, J., and Jonasson, C. (2008). Statistic-empirical modelling of mountain permafrost distribution in the Abisko region, sub-Arctic northern Sweden. *Norsk Geografisk Tidsskrift - Norwegian Journal of Geography*, 62 (4): 278–289. doi: 10.1080/00291950802517890.

Rigon, R., Bertoldi, G., and Over, T. M. (2006). GEOtop: A distributed hydrological model with coupled water and energy budgets. *Journal of Hydrometeorology*, 7: 371–377. doi: 10.1175/JHM497.1.

Riseborough, D. (2007). The effect of transient conditions on an equilibrium permafrost-climate model. *Permafrost and Periglacial Processes*, 18 (1): 21–32. doi: 10.1002/ppp.579.

Riseborough, D., Shiklomanov, N., Etzelmüller, B., Gruber, S., and Marchenko, S. (2008). Recent advances in permafrost modeling. *Permafrost and Periglacial Processes*, 19 (2) (1): 137–156,. doi: 10.1002/ppp.615.

Romanovsky, V. E., Smith, S. L., and Christiansen, H. H. (2010). Permafrost thermal state in the polar Northern Hemisphere during the international polar year 2007–2009: a synthesis. *Permafrost and Periglacial Processes*, 21 (2): 106–116. doi: 10.1002/ppp.689.

Roulet, N. T. and Woo, M.-K. (1986). Hydrology of a wetland in the continuous permafrost region. *Journal of Hydrology*, 89: 73–91. doi: 10.1016/0022-1694(86)90144-7.

Ruiz, L. and Liaudat, D. (2012). Mountain permafrost distribution in the Andes of Chubut (Argentina) based on a statistical model. In: *Proceedings of the 10th International Conference on Permafrost, Salekhard, Russia, 25–29 June*, (edited by Hinkel, K.), pp. 365–370.

Sazonova, T. S., Romanovsky, V. E., Walsh, J. E., and Sergueev, D. O. (2004). Permafrost dynamics in the 20th and 21st centuries along the East Siberian transect. *Journal of Geophysical Research: Atmospheres*, 109 (D1). doi: 10.1029/2003JD003680.

Scapozza, C., Lambiel, C., Baron, L., Marescot, L., and Reynard, E. (2011). Internal structure and permafrost distribution in two alpine periglacial talus slopes, Valais, Swiss Alps. *Geomorphology*, 132 (3–4): 208–221. doi: 10.1016/j.geomorph.2011.05.010.

Scherler, M., Hauck, C., Hoelzle, M., Stähli, M., and Völksch, I. (2010). Meltwater infiltration into the frozen active layer at an alpine permafrost site. *Permafrost and Periglacial Processes*, 21 (4): 325–334. doi: 10.1002/ppp.694.

Schmid, M.-O., Gubler, S., Fiddes, J., and Gruber, S. (2012). Inferring snowpack ripening and melt-out from distributed measurements of near-surface ground temperatures. *The Cryosphere*, 6 (5): 1127–1139. doi: 10.5194/tc-6-1127-2012.

Schneider, S., Hoelzle, M., and Hauck, C. (2012). Influence of surface and subsurface heterogeneity on observed borehole temperatures at a mountain permafrost site in the Upper Engadine, Swiss Alps. *The Cryosphere*, 6 (2): 517–531. doi: 10.5194/tc-6-517-2012.

Schoeneich, P., Lambiel, C., and Wenker, L. (1998). Rock glaciers, Prealps, Vaud, Switzerland. *Boulder CO: National Snow and Ice Data Center/World Data Center for Glaciology. Digital Media*.

Schöner, W., Boeckli, L., Hausmann, H., Otto, J., Reisenhofer, S., Riedl, C., and Seren, S. (2012). Spatial patterns of permafrost at Hoher Sonnblick (Austrian Alps) - Extensive field-measurements and modelling approaches. *Austrian Journal of Earth Sciences*, 105(2): 154–168.

Serrano, E., Agudo, C., Delaloye, R., and Gonzalez-Trueba, J. (2001). Permafrost distribution in the Posets massif, Central Pyrenees. *Norsk Geografisk Tidsskrift - Norwegian Journal of Geography*, 55 (4): 245–252. doi: 10.1080/00291950152746603.

Shiklomanov, N. and Nelson, F. (2003). Statistical representation of landscape-specific active-layer variability. In: *Proceedings of the 8th International Conference on Permafrost. Zurich, Switzerland, 21–25 July*, (edited by Phillips, M., Springman, S., and Arenson, L.), pp. 1039–1044.

Smith, M. W. and Riseborough, D. W. (1996). Permafrost monitoring and detection of climate change. *Permafrost and Periglacial Processes*, 7 (4): 301–309. doi: 10.1002/(SICI)1099-1530(199610)7:4<301::AID-PPP231>3.0.CO;2-R.

Smith, M. W. and Riseborough, D. W. (2002). Climate and the limits of permafrost: a zonal analysis. *Permafrost and Periglacial Processes*, 13 (1): 1–15. doi: 10.1002/ppp.410.

Stendel, M., Romanovsky, V. E., Christensen, J. H., and Sazonova, T. (2007). Using dynamical downscaling to close the gap between global change scenarios and local permafrost dynamics. *Global and Planetary Change*, 56: 203 – 214. doi: 10.1016/j.gloplacha.2006.07.014.

Strozzi, T., Kääb, A., and Frauenfelder, R. (2004). Detecting and quantifying mountain permafrost creep from in situ inventory, space-borne radar interferometry and airborne digital photogrammetry. *International Journal of Remote Sensing*, 25 (15): 2919–2931. doi: 10.1080/0143116042000192330.

Tanarro, L., Hoelzle, M., García, A., Ramos, M., Gruber, S., Gómez, A., Piquer, M., and Palacios, D. (2001). Permafrost distribution modelling in the mountains of the Mediterranean: Corral del Veleta, Sierra Nevada, Spain. *Norsk Geografisk Tidsskrift -*

Norwegian Journal of Geography, 55 (4): 253–260. doi: 10.1080/00291950152746612.

Tarnocai, C., Mark Nixon, F., and Kutny, L. (2004). Circumpolar–Active–Layer–Monitoring (CALM) sites in the Mackenzie Valley, northwestern Canada. *Permafrost and Periglacial Processes*, 15 (2): 141–153. doi: 10.1002/ppp.490.

Thies, H., Nickus, U., Mair, V., Tessadri, R., Tait, D., Thaler, B., and Psenner, R. (2007). Unexpected response of high alpine lake waters to climate warming. *Environmental Science & Technology*, 41 (21): 7424–7429. doi: 10.1021/es0708060.

Todd, A., Manning, A., Verplanck, P., Crouch, C., McKnight, D., and Dunham, R. (2012). Climate-change-driven deterioration of water quality in a mineralized watershed. *Environmental Science & Technology*, 46: 9324–9332. doi: 10.1021/es3020056.

U.S. Geological Survey (1997). GTOPO30 documentation (README file). *last access: 2012-12-20, http://webgis.wr.usgs.gov/globalgis/gtopo30/gtopo30.htm*.

USGS, METI, and NASA (2009). ASTER Global DEM validation. *Summary Report*, p. 28 pp. Last access March 2011.

van Everdingen, R. O. (1998). *Multi-Language Glossary of Permafrost and Related Ground-Ice Terms*. 25 International Permafrost Association, University of Calgary.

Venables, W. and Ripley, B. (2002). *Modern applied statistics with S*. Springer Verlag, New York.

Vonder Mühll, D. and Holub, P. (1992). Borehole logging in alpine permafrost, upper Engadin, Swiss Alps. *Permafrost and Periglacial Processes*, 3 (2): 125–132. doi: 10.1002/ppp.3430030209.

Vonder Mühll, D., Hauck, C., and Lehmann, F. (2000). Verification of geophysical models in alpine permafrost using borehole information. *Annals of Glaciology*, 31 (1): 300–306. doi: doi:10.3189/172756400781820057.

Vonder Mühll, D., Noetzli, J., and Roer, I. (2008). PERMOS – a comprehensive monitoring network of mountain permafrost in the Swiss Alps. In: *Proceedings of the 9th International Conference on Permafrost. Fairbanks, Alaska, 30 June–3 July*, (edited by Kane, D. and Hinkel, K.), pp. 1869–1874.

Wegmann, M. and Keusen, H. (1998). Recent geophysical investigations at a high alpine permafrost construction site in Switzerland. In: *Proceedings of the 7th International Conference on Permafrost. Nordicana, Yellowknife, Canada, 23–27 June*, (edited by Lewkowicz, A. and Allard, M.), pp. 1119–1123.

Westermann, S., Boike, J., Langer, M., Schuler, T. V., and Etzelmüller, B. (2011). Modeling the impact of wintertime rain events on the thermal regime of permafrost. *The Cryosphere*, 5 (4): 945–959. doi: 10.5194/tc-5-945-2011.

Williams, P. and Smith, M. (1989). *The frozen earth: fundamentals of geocryology*, vol. 306. Cambridge University Press Cambridge.

Woo, M.-K. and Winter, T. C. (1993). The role of permafrost and seasonal frost in the hydrology of northern wetlands in North America. *Journal of Hydrology*, 141: 5 – 31. doi: 10.1016/0022-1694(93)90043-9.

Woo, M.-K., Kane, D. L., Carey, S. K., and Yang, D. (2008). Progress in permafrost hydrology in the new millennium. *Permafrost and Periglacial Processes*, 19 (2): 237–254. doi: 10.1002/ppp.613.

Wu, Q., Lu, Z., Tingjun, Z., Ma, W., and Liu, Y. (2008). Analysis of cooling effect of crushed rock-based embankment of the Qinghai-Xizang Railway. *Cold Regions Science and Technology*, 53 (3): 27–282. doi: 10.1016/j.coldregions.2007.10.004.

Yang, Z., Ou, H., Xu, X., Zhao, L., Song, M., and Zhou, C. (2010). Effects of permafrost degradation on ecosystems. *Acta Ecologica Sinica*, 30 (1): 33–39. doi: 10.1016/j.chnaes.2009.12.006.

Ye, B., Yang, D., Zhang, Z., and Kane, D. L. (2009). Variation of hydrological regime with permafrost coverage over Lena Basin in Siberia. *Journal of Geophysical Research*, 114: 12 pp. doi: 10.1029/2008JD010537.

Yi, S., Woo, M.-K., and Arain, A. M. (2007). Impacts of peat and vegetation on permafrost degradation under climate warming. *Geophysical Research Letters*, 34: L16504+. doi: 10.1029/2007GL030550.

Zhang, T. (2005). Influence of the seasonal snow cover on the ground thermal regime: An overview. *Reviews of Geophysics*, 43 (4): RG4002. doi: 10.1029/2004RG000157.

Zhang, T., Heginbottom, J. A., Barry, R. G., and Brown, J. (2000). Further statistics on the distribution of permafrost and ground ice in the Northern Hemisphere. *Polar Geography*, 24: 126–131. doi: 10.1080/10889370009377692.

Zhang, T., Frauenfeld, O., Serreze, M., Etringer, A., Oelke, C., McCreight, J., Barry, R., Gilichinsky, D., Yang, D., Ye, H., *et al.* (2005). Spatial and temporal variability in active layer thickness over the Russian Arctic drainage basin. *Journal of Geophysical Research*, 110 (D16): D16101. doi: 10.1029/2004JD005642.

Zhang, T., Barry, R. G., Knowles, K., Heginbottom, J. A., and Brown, J. (2008a). Statistics and characteristics of permafrost and ground-ice distribution in the Northern Hemisphere. *Polar Geography*, 31 (1-2): 47–68. doi: 10.1080/10889370802175895.

Zhang, Y., Chen, W., and Riseborough, D. W. (2006). Temporal and spatial changes of permafrost in Canada since the end of the Little Ice Age. *Journal of Geophysical Research: Atmospheres*, 111 (D22): n/a–n/a. doi: 10.1029/2006JD007284.

Zhang, Y., Carey, S. K., and Quinton, W. L. (2008b). Evaluation of the algorithms and parameterizations for ground thawing and freezing simulation in permafrost regions. *Journal of Geophysical Research*, 113: 17 pp. doi: 10.1029/2007JD009343.

Zhang, Y., Wang, X., Fraser, R., Olthof, I., Chen, W., Mclennan, D., Ponomarenko, S., and Wu, W. (2012). Modelling and mapping climate change impacts on permafrost at high spatial resolution for a region with complex terrain. *The Cryosphere Discussions*, 6 (6): 4599–4636. doi: 10.5194/tcd-6-4599-2012.

Part II

Research papers

Paper I

Brief communication: "An inventory of permafrost evidence for the European Alps".

Cremonese, E., Gruber, S., Phillips, M., Pogliotti, P., Boeckli, L., Noetzli, J., Suter, C., Bodin, X., Crepaz, A., Kellerer-Pirklbauer, A., Lang, K., Letey, S., Mair, V., Morra di Cella, U., Ravanel, L., Scapozza, C., Seppi, R., and Zischg, A. (2011). Brief Communication: "An inventory of permafrost evidence for the European Alps". *The Cryosphere*, 5 (3): 651–657. doi: 10.5194/tc-5-651-2011

The author's contributions to this article:

- Contributed substantially to the development of the methodology.
- Substantial contribution to data pre- and post-processing.
- Homogenized and entered parts of the Swiss permafrost data.

The Cryosphere, 5, 651–657, 2011
www.the-cryosphere.net/5/651/2011/
doi:10.5194/tc-5-651-2011

The Cryosphere

Brief Communication: "An inventory of permafrost evidence for the European Alps"

E. Cremonese[1], S. Gruber[2], M. Phillips[3], P. Pogliotti[1], L. Boeckli[2], J. Noetzli[2], C. Suter[3], X. Bodin[4], A. Crepaz[5], A. Kellerer-Pirklbauer[6,7], K. Lang[8], S. Letey[1], V. Mair[8], U. Morra di Cella[1], L. Ravanel[4], C. Scapozza[9], R. Seppi[10], and A. Zischg[11]

[1]Environmental Protection Agency of Aosta Valley, ARPA Valle d'Aosta, Saint Christophe, Italy
[2]Glaciology, Geomorphodynamics and Geochronology, Department of Geography, University of Zurich, Zurich, Switzerland
[3]WSL Institute for Snow and Avalanche Research SLF, Davos, Switzerland
[4]Laboratoire EDYTEM, CNRS, Université de Savoie, Le Bourget du Lac, France
[5]Arabba Avalanche Center, Environmental Protection Agency of Veneto, ARPAV, Arabba di Livinallongo, Italy
[6]Department of Geography and Regional Science, University of Graz, Graz, Austria
[7]Institute of Remote Sensing and Photogrammetry, Graz University of Technology, Graz, Austria
[8]Autonomous Province of Bolzano, Geological Service, Bolzano, Italy
[9]Institute of Geography, University of Lausanne, Lausanne, Switzerland
[10]Earth Science Department, University of Pavia, Pavia, Italy
[11]Abenis Alpinexpert Srl, Bozen/Bolzano, Italy

Received: 28 March 2011 – Published in The Cryosphere Discuss.: 18 April 2011
Revised: 3 August 2011 – Accepted: 4 August 2011 – Published: 22 August 2011

Abstract. The investigation and modelling of permafrost distribution, particularly in areas of discontinuous permafrost, is challenging due to spatial heterogeneity, remoteness of measurement sites and data scarcity. We have designed a strategy for standardizing different local data sets containing evidence of the presence or absence of permafrost into an inventory for the entire European Alps. With this brief communication, we present the structure and contents of this inventory. This collection of permafrost evidence not only highlights existing data and allows new analyses based on larger data sets, but also provides complementary information for an improved interpretation of monitoring results.

1 Introduction

In mountain areas, permafrost distribution is spatially heterogeneous and there is a scarcity of direct permafrost measurements and observations. In the European Alps, numerous local permafrost distribution models have been developed (e.g. Keller, 1992; Hoelzle, 1996; Imhof, 1996; Gruber and Hoelzle, 2001; Lambiel and Reynard, 2001), but are usually based on a small number of data points (often proxies) from rather restricted regions. Similarly, statistical analyses of permafrost distribution patterns taking into account topography, mean annual air temperature (MAAT) or precipitation face the challenge of assembling heterogeneous data. In order to make the most of the potential of existing data, an Alpine-wide standardized collection of permafrost evidence has been carried out and is described here. We define a permafrost evidence to be a point or an area where permafrost is known to be present during a certain time or where the absence of permafrost can be ascertained. The wide variety of relevant field measurements and observations (e.g. temperature in boreholes or near the ground surface, rock glacier mapping, geophysics), and their different spatial scale of reference, make the process of data standardization challenging. Permafrost experts from several European Alpine countries have contributed to the inventory presented here (Appendix B). It was compiled within the framework of the project PermaNET and combines results obtained by many researchers and data assembled by national or regional monitoring programmes such as PERMOS (Noetzli and Vonder Muehll, 2010), PermaFRANCE (Schoeneich et al., 2010)

Correspondence to: E. Cremonese
(e.cremonese@arpa.vda.it)

Published by Copernicus Publications on behalf of the European Geosciences Union.

or PROALP (Mair et al., 2008). With this brief communication we aim to present the first version of the concept, structure and data of the inventory. In addition, we hope this brief communication will also contribute to the further improvement of the inventory through peer-review, to widen its usage and to improve its integration in the context of national and international monitoring and measurement programs.

2 Structure and organization of the inventory

The design and implementation of the inventory is based on the following principles: the inventory has to be simple in structure and technical implementation and the number of parameters must be kept small. This allows researchers to register their existing data within the newly standardized scheme in a user-friendly manner. For important variables, at least a qualitative uncertainty is assigned. After insertion, data are verified in order to remove obvious errors. Basic information on the origin of each evidence point is required, such as a published reference or the measurement method applied. The inventory contains the following types of evidence: borehole temperature (BH), ground surface temperature (GST), rock fall scar (SC), trench or construction site (TR), surface movement (SM), geophysical prospecting (GP), other indirect evidence (OIE) and rock glaciers (RG). SC and TR are considered to be evidence of permafrost only if ice has been seen (e.g. on photographs or in-situ) and can be excluded to be seasonal. The criterion to exclude seasonal ice is a depth exceeding five meters from the surface. SM is usually based on field observations, terrestrial surveys, photogrammetric analyses or DInSAR data. GP include primarily geoelectrics, seismics, ground penetrating radar and electromagnetic prospecting. OIE provides room for further types of evidence such as thermokarst depressions.

For all types of evidence, general information concerning for example location and the person responsible are required. Additionally, contributors can use the optional fields available for comments and further specification of criteria. BH, GST and SM have additional specific data fields. The complete list and description of information contained in the inventory are presented in Appendix A.

The rock glacier inventory (RG) is managed separately from the point types of evidence. Individual RG inventories are supplied as a collection of polygons and/or centroids (shapefiles) in local coordinate systems and then transformed to the common coordinate system WGS84. The contribution of an inventory requires the addition of common data fields into the GIS attribute table and supplying separate meta-information about the inventory. The estimation of RG activity is based on field observation or image interpretation (e.g. aerial photography, satellite imagery) of typical morphological characteristics (e.g. steepness of the front, absence of vegetation) and then classified as being "intact" (i.e. active or inactive landform with permafrost) or "relict" (i.e. without permafrost) and minimal information explaining the grounds for this assessment is included (Appendix A).

3 Data collection, verification and homogenization

The inventory was completed using four "calls for evidence" accompanied by a spreadsheet and detailed instructions. Thirty-five individuals or institutions provided data. Contributors provided information from their own research areas, consisting of existing data and knowledge adapted to the common data format used in this inventory. This was complemented by specific investigations in collaboration with regional/local geological services, ski resort operators, engineering companies or alpine guide societies. The design and administration of the inventory was carried out jointly by ARPA Valle d'Aosta (Italy), the WSL Institute for Snow and Avalanche Research SLF and the Department of Geography of the University of Zurich (Switzerland).

To avoid errors in spatial positioning introduced during data entry or coordinate transformation, the assembled inventory was sent as a KML file to all contributors for visual verification of the provided information using Google Earth. An updated version of the inventory was released using the feedback from the contributors after verification.

As the dataset is characterized by a high degree of heterogeneity, the issue of data homogenization is very important and still under development. A first step towards homogenization has been made for GST data measured on steep rock walls: as their inter-annual variation is similar to that of MAAT, a normalization procedure (Allen et al., 2009) to estimate mean annual ground surface temperature (MAGST) for the period 1961–1990 has been applied to make measurements from differing years comparable. Based on the resulting temperatures and considering possible mechanisms of thermal offset, GST points were classified into the categories "presence" or "absence" of permafrost with differing degrees of certainty (permafrost presence: MAGST $< -2\,^{\circ}C$ medium certainty; $-2\,^{\circ}C <$ MAGST $< 0\,^{\circ}C$ low certainty; permafrost absence: $0\,^{\circ}C <$ MAGST $< 2\,^{\circ}C$ low certainty; MAGST $> 2\,^{\circ}C$ medium certainty).

4 Content of the inventory

The total number of point type permafrost evidence is 408 (October 2010), extending from 44.29 to 47.47° N and from 5.91 to 14.88° E and covering all Alpine countries except Monaco, Liechtenstein and Slovenia. The rock glacier dataset includes seven inventories from Italy, Austria, Switzerland and France with a total of 4795 rock glaciers (Fig. 1). The seven inventories are regional (Valle d'Aosta, Piemonte, Veneto, Trentino Alto Adige in Italy, Massif du Combeynot in France, Ticino in Switzerland and central and eastern Austria) and thus do not cover the entire European Alps.

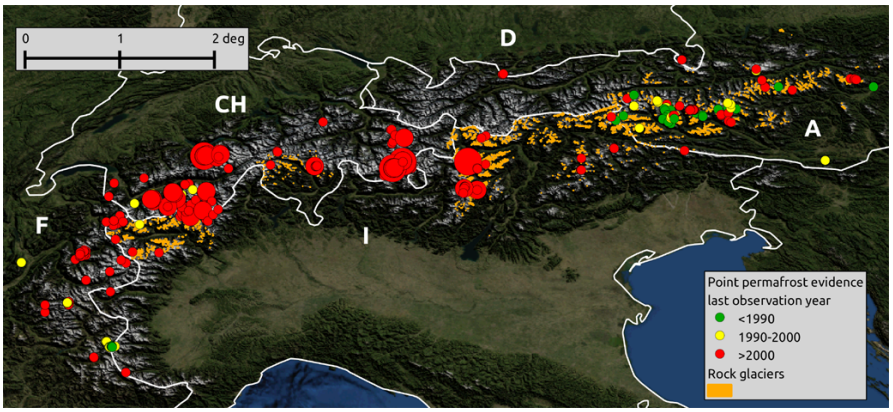

Fig. 1. Map of the permafrost evidence acquired in the Alps. The dots represent point permafrost evidence. The colors of dots represent the classes of last observation dates confirming permafrost state (before 1990, between 1900 and 2000, after 2000). The size of the dots indicates 3 classes (<3 yr, 3–8 yr, >8 yr) representing the length of observations/measured data associated with each evidence. Orange polygons represent rock glacier inventories.

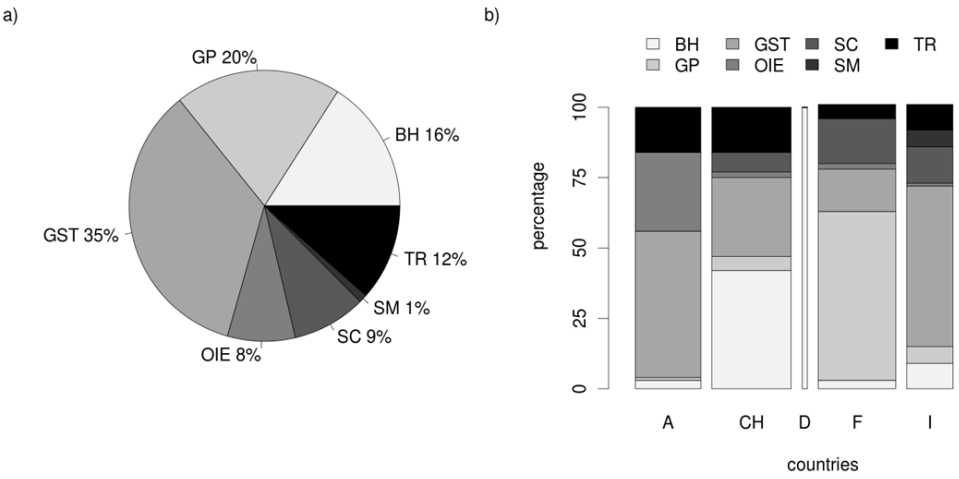

Fig. 2. **(a)** Relative amounts of point evidence types (borehole (BH), geophysical prospecting (GP), ground surface temperature (GST), other indirect evidence (OIE), rock fall scar (SC), surface movement (SM), trench or construction site (TR)) in the entire inventory and **(b)** by country. Bar width represents the relative abundance of evidence in each country: A–24 %, CH–29 %, D–0.5 %, F–28 %, I–17 %; for graphical reasons, Germany bar width has been increased (tripled).

GST, BH and GP are the most common types of point evidence. Most of the points are located in Switzerland, France and Italy (Fig. 2). The elevation of the permafrost evidence ranges from 1000 m a.s.l. in a cold talus slope in central Austria (Toteisboden) to 4120 m a.s.l. for a GST point in the Mont Blanc Massif (Grandes Jorasses); however, the majority (>60 %) are situated between 2500 and 3000 m a.s.l. (Fig. 3). Most of the points have slope angles in the range 10–45°. GST and SC also exist in near-vertical conditions and even some BH (Zugspitze (D), Aiguille du Midi (F), Gemsstock (CH), Grawand (IT)) are located in steep rock faces. GP, TR and SM mostly occur on gently inclined slopes. The distribution of slope aspects is slightly biased towards the North (36 %) and West (24 %) with fewer points (20 % each) in the South and East. The majority (85 %) of points have no or only sparse vegetation cover and few have partial or complete coverage (15 %, mostly of type TR). Most (44 %) of the evidence are located in coarse debris, the others are in bedrock (33 %) and in fine material (23 %). Evidently, types such as SC and TR are biased towards a certain surface type. About 20 % of BH and GST are situated on plateaus or ridges, while 10–15 % of TR are located in depressions.

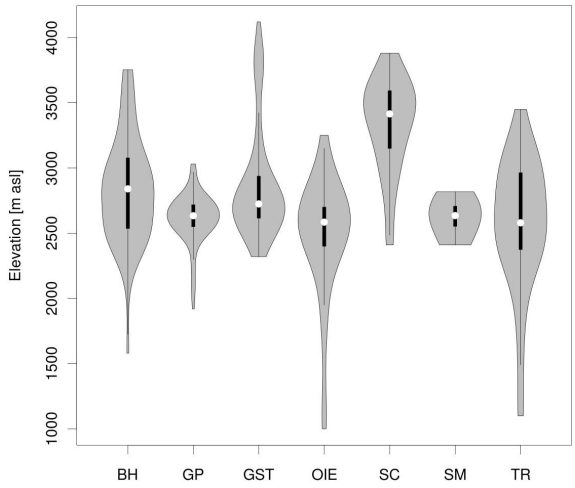

Fig. 3. Elevation range of each type of evidence (except rock glaciers). The plot shown is a combination of a box plot (the white dot is the median, the black boxes range from the lower to upper quartile, and the thin black lines represent the whiskers) and a kernel density plot super-imposed in a mirror image fashion (grey shaded areas).

The depth of BH ranges from 5 to 133 m with a mean of 33 m. Most boreholes are equipped with temperature sensor chains and data loggers but some require manual measurements. For each BH, active layer depth as well as mean annual ground temperature (MAGT) of the coldest sensor is reported as the mean of all available measurement years. As BH have variable depths, the MAGST of the coldest sensor is used as an indication for permafrost conditions. GST is mostly measured at a depth of around 10 cm (55 %), with some measurements being shallower (25 % at 0–2 cm) and others deeper (20 % at 15–55 cm). GST is reported as the mean of all full measurement years with durations ranging from 3 to 5 yr.

Evidence of the absence of permafrost is also relevant: whilst 75 % of the rock glaciers presented in the inventory are relict forms, only 23 % of the point types of evidence indicate the absence of permafrost. 61 % of point evidence where permafrost absence has been ascertained are ground surface temperature, 17 % are boreholes and 22 % are represented by geophysical investigations and trenches. Points of permafrost absence have a mean elevation of 2600 m a.s.l. but can reach also elevations higher than 3500 m a.s.l. in particularly unfavourable conditions (e.g. south exposed rock walls).

5 Data access

The October 2010 version of the inventory is available digitally at www.geo.uzh.ch/microsite/cryodata/. A compressed version of the inventory can be downloaded containing point types of evidence in ASCII format. Since the rationale behind the inventory is data sharing, point evidence publication policy are classified in two categories: "Usage without restriction" and "Inform before publication". Data belonging to the first category can be downloaded without any feedback to the owner while in the latter case, an automatic email reporting the contact person and the intended use of the data, will be sent to the owner when a download occurs.

6 Conclusions

We have established an inventory of permafrost evidence for the Alps and made its contents freely available to other scientists and practitioners. This inventory complements monitoring programmes in which changes in permafrost terrain are measured at individual locations with great precision and over long time spans (e.g. PERMOS, PermaFRANCE or NorPerm, Juliussen et al., 2010) by providing a solid basis to advance the understanding of the spatial distribution of permafrost and its evolution in heterogeneous mountain environments. While the homogenized contents and public availability of the inventory increase the value of the data contained, the synopsis of data over a larger region additionally enables analyses that were previously not possible, as larger environmental gradients are covered and more data points available. Future experience with data homogenization, scientific analyses, gathering of evidence, re-interpretation of existing data for inclusion in the inventory and with merging differing inventories and monitoring systems into higher-level products will likely require or inspire changes to the structure and strategy outlined here. In addition, the provision of proper user interfaces for the input, validity checking and output of data as well as strategies to ensure correct scientific governance and data stewardship are important to maximize the acceptance and utility of inventories such as the one presented here.

Appendix A

Inventory structure

1. General Information (required for all types of evidence)
   - Evidence Type: Borehole (BH), Geophysics (GP), Rock fall scar (SC), Ground surface temperature (GST), Surface movement (SM), Trench or construction site (TR), Other indirect evidence (OIE);
   - Country ID: Austria (A), Germany (D), France (F), Italy (I), Switzerland (CH), Liechtenstein (FL), Slovenia (SLO);

- Evidence ID: progressive code to identify the single evidence;
- Site name: established name for site;
- Responsible name: first and last name of responsible person/data owner. This person is to be contacted for any questions and also for impending publications;
- Responsible email: e-mail address of responsible person/data owner;
- Longitude: coordinates of the evidences (WGS84, decimal degrees);
- Latitude: coordinates of the evidences (WGS84, decimal degrees);
- Coordinate accuracy: approximate accuracy of coordinates (m);
- Position method: method used for locating site (e.g. GPS, MAP, Google Earth, others);
- Orientation method: method used for determining slope and aspect (e.g. field, GIS, other);
- Elevation: elevation of the evidence point (m);
- Slope: slope, expressed in degrees, of the evidence point (°);
- Aspect: aspect, expressed in degrees, of the evidence point (90° for East, 180° for South, 270° for West, 360° for North);
- Vegetation: degree of vegetation cover: none, sparse, partly covered, complete coverage;
- Surface type: coarse debris (no fines at surface), fine grained debris (fines at surface) or bedrock;
- Permafrost YES/NO: permafrost presence or absence (Yes/No);
- Permafrost certainty: degree of certainty related to permafrost presence or absence: high certainty (i.e.definite proof), medium certainty, low certainty;
- Justification: explanation and justification of the permafrost degree of certainty given;
- Ice: indication of the presence of ice below active layer depth or visible in rock fall scar (Yes/No/Unknown);
- Ice depth: depth of visible ice (m);
- Date last: last observation confirming permafrost state;
- Permafrost comments: any additional comments on permafrost;
- Terrain characteristics: indication of the type of terrain: slope, ridge, peak, plateau, depression, slope base;
- Source type: source of the information related to the evidence: literature, field observation, personal communication;
- Source comment: any additional comment on the source type;
- Publication policy: Usage without restriction, Inform before publication.

2. Additional information (not obligatory)
   - Additional data: indication of any additional measurement existing at this site (e.g. snow depth, air temperature, ...);
   - Comments general: any other information about the site that may be important;
   - Publications: indication of publications where the site and its permafrost condition are discussed (specifically).
3. Boreholes (specific information required for boreholes)
   - Borehole name: established local borehole name;
   - Borehole depth: maximum depth of the borehole (m);
   - Borehole ALT: mean of maximum annual active layer thickness (m);
   - Borehole ALT years: years used for the calculation of average active layer depth;
   - Borehole MAGT min: minimum mean annual temperature in the borehole (i.e. the mean annual temperature of the coldest sensor) (°C);
   - Borehole MAGT min depth: depth of the sensor used for the minimum mean annual temperature (m);
   - Borehole MAGT period: years used for the calculation of the minimum mean annual temperature;
   - Borehole MAGT accuracy: accuracy of the temperature sensors installed in the borehole;
   - Borehole GST: mean annual ground surface temperature; indicates if a measurement is available near the borehole not in the same thermistor chain (°C);
   - Borehole comments: any additional information: e.g. borehole with/without tubing, depth of Zero-annual amplitude (ZAA), angle of drilling (relative to ground surface) if borehole is not vertical.
4. Ground Surface Temperatures (specific information required for GST)
   - GST mean: mean ground surface temperature (°C);
   - GST period: years used for the calculation of the mean ground surface temperature;

- GST measurement depth: maximum depth of measurement from surface (cm);
- GST accuracy: accuracy of the temperature sensors;

5. Surface Displacement (specific information required for SD)
   - Displacement method: indication of the method used to measure displacement: field observation, air photo observation, photogrammetric analysis, terrestrial survey, InSAR, ...;
   - Movement rate: cm day^{-1}, cm $month^{-1}$ or cm yr^{-1};
   - Movement date: date of measurement.
6. Rock glacier inventory (required for each rock glacier inventory)
   - RGI ID: number of the rock glacier inventory;
   - RGI name: name of the inventory;
   - RGI file name: filename of the corresponding shapefile;
   - RGI coordinate system: coordinate system of the inventory;
   - RGI delineation base: specification of the delineation method used (e.g. air photo, map, field observation etc.);
   - RGI mapping strategy: specification of the mapping strategy used to compile the inventory (e.g. random sample of rock glaciers/all rock glaciers/only large rock glaciers etc.);
   - RGI year: date of the rock glacier inventory;
   - RGI responsible name: first and last name of responsible person/data owner;
   - RGI responsible email: e-mail address of responsible person/data owner;
   - RGI publication: indication of publications where the rock glacier inventory is discussed (specifically).
7. Rock glacier (required for each rock glacier)
   - Degree of activity: definition of the degree of activity using two classes: Intact (Active/inactive) or Relict;
   - RG field evidence: presence of field evidence for the rock glacier (e.g. Measurements)? Yes/No;
   - RG activity data: presence of InSAR (A), geodetic (B), photogrammetric (C), GPS (D) or other (E) data for the rock glacier: no data, activity, no activity;
   - RG vegetation front: presence of vegetation on the front of the rock glacier: Yes, No, Unknown;
   - RG glacier above: presence of a glacier or perennial snow field in the root zone of the rock glacier: Glacier, Perennial snow field, No.

Appendix B

List of contributing institutions

- Austria
  1. ZentralAnstalt für Meteorologie und Geodynamik – ZAMG
  2. Universität Graz
- France
  1. Conservatoire National des Arts et Métiers – CNAM
  2. Université Joseph Fourier
  3. Université de Savoie
  4. Centre national de la recherche scientifique – CNRS
- Germany
  1. Bayerisches Landesamt für Umwelt – LfU
- Italy
  1. Agenzia Regionale per la Protezione dell'Ambiente del Piemonte – ARPA Piemonte
  2. Agenzia Regionale per la Protezione dell'Ambiente della Valle d'Aosta – ARPA VdA
  3. Fondazione Montagna Sicura
  4. Provincia Autonoma di Bolzano
  5. Provincia Autonoma di Trento
  6. Regione Veneto
- Switzerland
  1. Bundesamt für Umwelt – BAFU
  2. Université de Lausanne – UNIL
  3. Universität Freiburg
  4. WSL Institute for Snow and Avalanche Research – SLF
  5. Universität Zürich – UZH

Acknowledgements. The project PermaNET is part of the European Territorial Cooperation and is co-funded by the European Regional Development Fund (ERDF) in the scope of the Alpine Space Programme (http://www.alpine-space.eu). We are grateful to all data contributors: Broccard A., Crittin C., Curtaz M., Delaloye R., Fabre D., Garcia S., Hölzle M., Keusen H. R., Kroisleitner C., Krysiecki J. M., Lambiel C., Lieb G., Mari S., Monnier S., Paro L., Riedl C., Rovera G., Schoeneich P., Springman S., Walcher J., Zampedri G., as well as the Swiss Permafrost Monitoring Network (PERMOS). Alexander Brenning has contributed to designing the initial structure of the inventory.

Edited by: R. Rigon

References

Allen, S., Gruber, S., and Owens, I.: Exploring steep bedrock permafrost and its relationship with recent slope failures in the Southern Alps of New Zealand, Permafrost Periglac., 20, 345–356, 2009.

Gruber, S. and Hoelzle, M.: Statistical modelling of mountain permafrost distribution: local calibration and incorporation of remotely sensed data, Permafrost Periglac., 12, 69–77, 2001.

Hoelzle, M.: Mapping and modelling of mountain permafrost distribution in the Alps, Norsk Geogr. Tidsskr., 50, 11–15, 1996.

Imhof, M.: Modelling and verification of the permafrost distribution in the Bernese Alps (Western Switzerland), Permafrost Periglac., 7, 267–280, 1996.

Juliussen, H., Christiansen, H. H., Strand, G. S., Iversen, S., Midttømme, K., and Rnning, J. S.: NORPERM, the Norwegian Permafrost Database – a TSP NORWAY IPY legacy, Earth Syst. Sci. Data, 2, 235–246, doi:10.5194/essd-2-235-2010, 2010.

Keller, F.: Automated mapping of mountain permafrost using the program PERMAKART within the geographical information system ARC/INFO, Permafrost Periglac., 3, 133–138, 1992.

Lambiel, C. and Reynard, E.: Regional modelling of present, past and future potential distribution of discontinuous permafrost based on a rock glacier inventory in the Bagnes-Hérémence area (Western Swiss Alps), Norsk. Geogr. Tidsskr., 55, 219–223, 2001.

Mair, V., Zischg, A., Krainer, K., Stötter, J., Zilger, J., Belitz, K., Schenk, A., Damm, B., Kleindienst, H., Bucher, K., Lang, K., Tagnin, S., and Munari, M.: PROALP Rilevamento e monitoraggio dei fenomeni permafrost. Esperienze della Provincia di Bolzano, Neve e Valanghe, 64, 50–59, 2008.

Noetzli, J. and Vonder Muehll, D. (Eds.): PERMOS 2010. Permafrost in Switzerland 2006/2007 and 2007/2008, Glaciological Report Permafrost No. 8/9, Cryospheric Commission of the Swiss Academy of Sciences, 2010.

Schoeneich, P., Bodin, X., Krysiecki, J., Deline, P., and Ravanel, L.: Permafrost in France. Report No. 1, Institute of Alpine Geography, University of Grenoble, 2010.

Paper II

A statistical approach to modeling permafrost distribution in the European Alps

Boeckli, L., Brenning, A., Gruber, S., and Noetzli, J. (2012a). A statistical approach to modelling permafrost distribution in the European Alps or similar mountain ranges. *The Cryosphere*, 6 (1): 125–140. doi: 10.5194/tc-6-125-2012

The author's contributions to this article:

- Contributed substantially to the development of the methodology.
- Implementation, testing and refinement of model.
- Designed and performed all data processing and analysis.
- Main author of entire article, except for Section 3.

The Cryosphere, 6, 125–140, 2012
www.the-cryosphere.net/6/125/2012/
doi:10.5194/tc-6-125-2012

The Cryosphere

A statistical approach to modelling permafrost distribution in the European Alps or similar mountain ranges

L. Boeckli[1], **A. Brenning**[2], **S. Gruber**[1], **and J. Noetzli**[1]

[1]Department of Geography, University of Zurich, Switzerland
[2]Department of Geography and Environmental Management, University of Waterloo, Ontario, Canada

Correspondence to: L. Boeckli (lorenz.boeckli@geo.uzh.ch)

Received: 26 April 2011 – Published in The Cryosphere Discuss.: 9 May 2011
Revised: 6 December 2011 – Accepted: 13 January 2012 – Published: 26 January 2012

Abstract. Estimates of permafrost distribution in mountain regions are important for the assessment of climate change effects on natural and human systems. In order to make permafrost analyses and the establishment of guidelines for e.g. construction or hazard assessment comparable and compatible between regions, one consistent and traceable model for the entire Alpine domain is required. For the calibration of statistical models, the scarcity of suitable and reliable information about the presence or absence of permafrost makes the use of large areas attractive due to the larger data base available.

We present a strategy and method for modelling permafrost distribution of entire mountain regions and provide the results of statistical analyses and model calibration for the European Alps. Starting from an integrated model framework, two statistical sub-models are developed, one for debris-covered areas (debris model) and one for steep bedrock (rock model). They are calibrated using rock glacier inventories and rock surface temperatures. To support the later generalization to surface characteristics other than those available for calibration, so-called offset terms have been introduced into the model that allow doing this in a transparent and traceable manner.

For the debris model a generalized linear mixed-effect model (GLMM) is used to predict the probability of a rock glacier being intact as opposed to relict. It is based on the explanatory variables mean annual air temperature (MAAT), potential incoming solar radiation (PISR) and the mean annual sum of precipitation (PRECIP), and achieves an excellent discrimination (area under the receiver-operating characteristic, AUROC = 0.91). Surprisingly, the probability of a rock glacier being intact is positively associated with increasing PRECIP for given MAAT and PISR conditions. The rock model is based on a linear regression and was calibrated with mean annual rock surface temperatures (MARST). The explanatory variables are MAAT and PISR. The linear regression achieves a root mean square error (RMSE) of 1.6 °C. The final model combines the two sub-models and accounts for the different scales used for model calibration.

The modelling approach provides a theoretical basis for estimating mountain permafrost distribution over larger mountain ranges and can be expanded to more surface types and sub-models than considered, here. The analyses performed with the Alpine data set further provide quantitative insight into larger-area patterns as well as the model coefficients for a later spatial application. The transfer into a map-based product, however, requires further steps such as the definition of offset terms that usually contain a degree of subjectivity.

1 Introduction

Many models already exist for estimating the spatial distribution of mountain permafrost in regions of the European Alps (Hoelzle, 1992; Keller, 1992; Imhof, 1996; Gruber and Hoelzle, 2001; Lambiel and Reynard, 2001; BAFU, 2005). These models are difficult to compare or combine because they have different empirical or statistical approaches and differing types of indices as output. Their extrapolation is difficult as they are usually calibrated for specific regions and, as a consequence, no estimation of permafrost distribution exists in large regions of the European Alps to date.

First estimations of permafrost occurrence in the Alps were based on the "rules of thumb" (Haeberli, 1975), which use basic relations of permafrost occurrence with

topographic attributes and surface characteristics. These relationships were first implemented within a GIS environment by Keller (1992) and later incorporated in further studies to predict spatial permafrost occurrence (Imhof, 1996; Frauenfelder et al., 1998; BAFU, 2005; Ebohon and Schrott, 2008). Besides topographic variables, climatic information and other direct proxy variables of the surface energy balance (such as MAAT and PISR) are often used in statistical or empirical permafrost models. The basal temperature of snow (BTS), introduced by Haeberli (1973) as an indicator of permafrost occurrence, has been widely used for model calibration (Hoelzle, 1992; Keller et al., 1998; Riedlinger and Kneisel, 2000; Gruber and Hoelzle, 2001; Stocker-Mittaz et al., 2002; Lewkowicz and Ednie, 2004; Brenning et al., 2005). Measurements in boreholes and near the ground surface have been used for model evaluation (Gruber et al., 2004; Heggem et al., 2005; Etzelmüller et al., 2006, 2007; Allen et al., 2009). Other studies used rock glacier inventories to infer the occurrence of permafrost (Janke, 2004), to identify the lower boundary of discontinuous permafrost (Nyenhuis et al., 2005), or for model assessment (Imhof, 1996; Gruber and Hoelzle, 2001).

Existing permafrost distribution models typically do not distinguish between different surface characteristics such as fine or coarse-grained debris slopes or steep bedrock, even though their differences in snow-cover and material characteristics can cause strongly differing ground temperatures. Because the amount and type of available permafrost data differs between the various surface types this often results in an unknown degree of extrapolation. Models based on BTS for example are also used to predict permafrost occurrence in bedrock without snow or on ground that is nearly always blown free of snow. Similarly, models based on rock glacier occurrence are used to predict permafrost also in fine-grained substrate. The output of most established models consists of permafrost zonation classes such as "probable permafrost" or an index that is then related to a qualitative probability. These quantities are usually defined beforehand (e.g. rules of thumb (Haeberli, 1975); the BTS relationship (Haeberli, 1973); or based on the concept of permafrost zonation limits (Lambiel and Reynard, 2001)) and cannot be validated quantitatively later on. A notable exception is the work by Lewkowicz and Ednie (2004) but applied to more diverse terrain, extrapolation to differing surface conditions may again be problematic.

With this paper we aim to base a statistical model on reliable permafrost data for a larger area and to make the extrapolation to surface types for which no suitable calibration data is available transparent by introducing dedicated offset terms. While this does not solve the problem of difficult validation due to strong heterogeneity and little data, it provides a basis for better model calibration with the data available and for better separation of quantitative statistical analysis and of subjective adjustment. The objectives of the present study are thus to (a) introduce a suitable strategy and method for statistic-based modelling the permafrost distribution for large mountain regions, (b) to discuss generic difficulties of such models regarding model application to an entire landscape, and (c) to provide the results of our statistical analysis (i.e. model coefficients) for the European Alps.

2 Conceptual background

The lack of sufficient and reliable data for calibration and validation probably is one of the most important limitations for permafrost modeling and it is important to devise strategies for the efficient use of existing data. While much progress has been made in therms of physics-based modelling of mountain permafrost in recent years (cf. Riseborough et al., 2008; Harris et al., 2009), also those methods are challenged in terms of their validation for diverse conditions and we therefore decided to use a statistical approach. To benefit from a large data basis, the presented model is based on an Alpine-wide collection of permafrost evidence (Cremonese et al., 2011). Overall, only MARST measurements and the rock glacier inventories offer enough data to support the fitting of statistical models. The other permafrost observations described by Cremonese et al. (2011) were not used for model calibration because, (a) they are not sufficient in number to allow consistent statistical analysis; (b) the integration and homogenization of heterogeneous permafrost observations are subject to large uncertainty and subjectivity, and (c) observations are strongly biased towards permafrost existence and less observation in non-permafrost conditions are available. The evidence collection is subject to some degree of homogenization, especially the rock glacier inventories in it may be subject to differences due to slightly differing conventions and data used that must be accounted for in statistical models. To utilize rock glacier inventories and MARST data, a combination of two sub-models is required: one for debris-covered areas and one for steep bedrock. With the term "steep bedrock" we refer to terrain that (a) is not or only marginally affected by a snow cover in wintertime, (b) does not contain large amounts of blocks and/or debris, and (c) is without vegetation coverage. The statistical models are calibrated based on rock glacier activity status as a binary variable, and rock temperatures as a continuous variable, respectively. While this model combination results in probabilities sensu strictu, their application to areas that are not rock glaciers or steep bedrock is difficult. Because we only have limited evidence for permafrost occurrence or absence, this extrapolation is an integral part of permafrost modeling. To make this transparent, we use offset terms that we embed in the model to allow later subjective adjustment. Because the measurements of MARST used for model calibration are representative on a scale of few tens of centimeters only, the application of results in a model based on a DEM of several tens of meters is difficult and requires dedicated attention. Because MAAT has regional trends besides its local

dependance on elevation, we prefer to use MAAT instead of elevation as an explanatory variable. The modelling approach we present is suitable for large mountain regions and is here demonstrated for application to the European Alps (43°–49° N, 4°–16° E).

2.1 Debris model

In debris slopes, intact (active and inactive) rock glaciers are a diagnostic and well visible geomorphological feature to detect the presence of permafrost whereas relict forms indicate its absence (e.g. Haeberli, 1985). Active and inactive rock glaciers are grouped as "intact" rock glaciers because of their existing ice content (cf. Haeberli, 1985; Ikeda and Matsuoka, 2002; Roer and Nyenhuis, 2007; Lilleoren and Etzelmüller, 2011) and the reliable indication of permafrost they offer. Relict rock glaciers do no longer contain ice, show a collapsed surface due to melting of the ice, and they often have a vegetation cover (Roer and Nyenhuis, 2007).

The possibility of mapping rock glaciers from e.g. aerial photographs or field observations makes this an attractive and unique data source. The existence of rock glaciers depends on suitable debris production and transport mechanisms, implying that permafrost can also exist in areas where rock glaciers are absent (Imhof, 1996). Because here, no visible features indicate permafrost, a model-based estimation is especially valuable. Due to a cooling effect of the coarse block surface (Harris and Pedersen, 1998) and the creeping of rock glaciers, an estimation of permafrost distribution based on rock glacier activity generally results in an overestimation of the amount of permafrost below surfaces that are not rock glaciers. This effect may be compensated by offset terms to describe the permafrost status of those surfaces relative to the status of rock glaciers.

The debris model is calibrated using status information of rock glaciers resulting in a binary response (permafrost yes/no). While generalized linear models (GLMs) are commonly used to model binary response variables such as presence/absence of permafrost (Lewkowicz and Bonnaventure, 2008), an extension of this model that is able to account for random inventory effects is required here. Such random effects may be related to different observation techniques and interpretation criteria being applied in the compilation of inventories by different research groups, which may result in an inventory-specific bias. The generalized linear mixed model (GLMM; Venables and Ripley, 2002) is able to account for such random inventory effects and is therefore applied in this study. It is implemented as "glmmPQL" in the R package "MASS" (Venables and Ripley, 2002). GLMs and GLMMs for binary response variables can be specified using either the probit or, more commonly, the logistic link function (Hosmer and Lemeshow, 2000; Gelman and Hill, 2007). While both are nearly identical (Aldrich and Nelson, 1984; Gelman and Hill, 2007), a probit link function is preferred in this study due to mathematical advantages in the combined framework, as outlined in Sect. 3.1.

2.2 Rock model

Near-surface temperatures in steep bedrock have been observed in the Alps since 2002 (Gruber et al., 2003; PERMOS, 2010). Based on this data and other analyses (Gruber et al., 2004; Allen et al., 2009), it was shown that short-wave radiation is the major controlling factor for the lateral variability of MARST in steep and homogeneous rock making it suitable for a linear statistical model. Because this is based on near vertical slopes that have no blocky layer and no snow, the extrapolation into the most common type of rock slope that is heterogeneous, fractured and partly snow-covered requires special attention. Differing mechanisms and effects have been postulated (Gruber and Haeberli, 2007; Noetzli et al., 2008) and measured (Hasler et al., 2011), and require an offset term for their inclusion in a permafrost distribution model. Measurements of ground surface temperatures (GST) or BTS in less steep terrain were not included in our analysis because of their large inter-annual variability caused by the strong influence of the snow cover (Hoelzle et al., 2003; Brenning et al., 2005).

2.3 Model combination

In our case of Alpine-wide permafrost distribution modelling, we wish to integrate two models that are fitted separately in two different model domains: debris surfaces and steep bedrock. While the debris model is based on an Alpine-wide digital elevation model (DEM) with coarse grid spacing, the rock model is calibrated using locally measured terrain attributes, which refer to fine-scale topographic information. When combining these two models we have to consider scale effects with particular emphasis on the situation where an empirical model developed using fine-scale in situ measurements is applied at a coarser resolution for regional-scale application.

3 Statistical method

The introduction of our statistical approach for permafrost modeling starts by using the probit model formulation to show the formal equivalence between permafrost probabilities derived from temperature as a continuous random variable, and presence/absence as a binary one (Sect. 3.1). This lays the foundations of the proposed approach, because this allows us to establish a unified framework for the rock model and debris model, which are based on these two different types of response variables. A simple approach for combining permafrost probabilities from rock and debris models is then proposed (Sect. 3.2). This may result in scale issues, which require further attention (Sect. 3.3). Two practical aspects of the application of our approach are then

discussed, the discrimination between rock and debris surfaces (Sect. 3.4), and the assessment of the models' goodness of fit (Sect. 3.5).

3.1 Model formulation

Permafrost is defined thermally by the permanent presence of zero or negative ground temperatures (°C) over two entire years (van Everdingen, 1998). Because we are interested in depths where the variability of annual ground temperatures can be neglected, we assume maximum and mean ground temperatures to be equal. We therefore express the probability p of permafrost occurrence at a given location by the probability of mean ground temperature ϑ being ≤ 0°C:

$$p = P(\vartheta \leq 0). \quad (1)$$

If the ground temperature ϑ is modeled linearly (as we will later do in the rock model),

$$\vartheta = \widetilde{\alpha} + \widetilde{\Delta} + \sum_{i=1}^{k} \widetilde{\beta}_i x_i + \widetilde{\varepsilon} = \widetilde{\vartheta} + \widetilde{\varepsilon}, \quad (2)$$

where $\widetilde{\varepsilon}$ is a normally distributed residual error term with mean 0 and variance $\widetilde{\sigma}^2$, the x_i and $\widetilde{\beta}_i$ are the model's k explanatory variables and their coefficients, and $\widetilde{\alpha} + \widetilde{\Delta}$ represents an intercept term that is explained in detail in Sect. 3.3. Throughout this work, model coefficients with a tilde refer to the temperature scale as in Eq. (2), while model coefficients at the probit scale will carry no tilde.

In a predictive situation, this model will allow us to predict $\widetilde{\vartheta}$ with a variance $\widetilde{\sigma}^2_{\text{pred}} \geq \widetilde{\sigma}^2$, which can be estimated from the model. In this situation, the permafrost probability p is therefore predicted to be

$$p = \Phi(-\widetilde{\vartheta}/\widetilde{\sigma}_{\text{pred}}), \quad (3)$$

where Φ is the cumulative standard normal distribution function. The negative sign is due to the fact that we are interested in the probability of negative rather than positive temperatures.

On the other hand, direct evidence of permafrost presence or absence (debris model) allows us to model the permafrost probability p directly using generalized linear models. The probit link function is used in this study, because of its relation to the cumulative normal distribution function (Aldrich and Nelson, 1984; Gelman and Hill, 2007). Here, the probability of permafrost presence is modeled linearly not at the probability scale but at the probit scale, which is obtained from an inverse cumulative distribution function of the standard normal distribution:

$$\text{probit}(p) = \Phi^{-1}(p) \quad (4)$$

Thus, and if we introduce an additional (thermal) offset term Δ (Sect. 3.2) into the probit model, we write the debris model as

$$\text{probit}(p) = \alpha + \Delta + \sum_{i=1}^{k} \beta_i x_i, \quad (5)$$

where the x_i and β_i are the model's k explanatory variables and their corresponding coefficients, and α is the model intercept.

From Eqs. (3), (4) and (5) it becomes evident that a linear regression of ϑ is equivalent to a probit regression of p with scaled coefficients:

$$-\widetilde{\vartheta}/\widetilde{\sigma}_{\text{pred}} = \alpha + \Delta + \sum_{i=1}^{k} \beta_i x_i \quad (6)$$

This relationship between the temperature-based model and the model based on rock glacier presence/absence allows us to convert the temperature-based model in Eq. (2) into a probit-based probability model (Eq. 5). It will later be shown that in this specific context, this is relatively insensitive to the estimation of the prediction variance, and we will therefore use a conservative variance estimator $\widehat{\widetilde{\sigma}}^2_{\text{pred}}$, which will later be specified. The above equivalence allows us to integrate continuous- and binary-response permafrost distribution models within the formal framework of a linear model with comparable model coefficients.

3.2 Integration of continuous- and binary-response models

The coefficients of model M_{d} (debris surface) are derived from the debris model, resulting in the coefficients $\alpha_{\text{d}}, \beta_{\text{d},1}, \beta_{\text{d},2}$ adopted from Eq. (5). Δ_{d} is introduced into this model as a fixed offset value that can be used for adjusting effects such as rock glacier movement; this value is not estimated from the data but represents the possibility to later introduce an expert-defined adjustment term.

Model M_{r} (rock surface), by contrast, is derived from the rock model (Eq. 2) and partly uses the same explanatory variables as model M_{d}, with the exception of a difference in spatial scale (discussed in Sect. 3.3). It is important to note that in this model formulation, the adjustment offset $\widetilde{\Delta}_{\text{r}}$ can be directly interpreted as a thermal offset of the near-surface ground temperature (MARST) minus the temperature at the top of permafrost (TTOP). Given this model's prediction variance $\widehat{\widetilde{\sigma}}^2_{\text{pred,r}}$, we estimate the probit-scale coefficients of M_{r} from Eq. (6), i.e. by dividing all temperature-scale model coefficients by $-\widehat{\widetilde{\sigma}}_{\text{pred,r}}$.

In practice, the spatial distribution of different surface types is usually not well known and may exhibit transitions such as spatially varying debris or snow cover thicknesses. We represent this in a simple way through a (spatially varying) degree of membership in a land cover class, m_τ, with values between 0 and 1 that sum up to 1 at each location. The integrated model is then defined to be

$$\text{probit}(p_{\text{d}}, p_{\text{r}}; m_{\text{d}}, m_{\text{r}}) = m_{\text{d}}\text{probit}(p_{\text{d}}) + m_{\text{r}}\text{probit}(p_{\text{r}}), \quad (7)$$

which has an obvious generalization to more than two land cover classes. Probabilities of permafrost occurrence can be

obtained from this integrated probit value by applying the inverse probit transformation, and probit-scale prediction variances are integrated in a similar way as the weighted sum of each model's prediction variances.

3.3 Scaling issues

With scale effects we refer to the fact that model coefficients may change at different scales or levels of aggregation as coarser-scale explanatory variables tend to show a smaller range of values and less scatter. This situation is related to the change of support problem (e.g. Gotway and Young, 2002), but instead of a geostatistical interpolation setting we need a solution that is tailored to the situation of integrating two linear models.

We start by looking at the scaling problem encountered in the situation where the rock model is fitted at a fine scale (parameters with index "F") and applied at a coarser scale (index "C") and consider initially only a linear model with one explanatory variable ($k = 1$) and no offset term $\widetilde{\Delta}_\mathrm{F} = 0$.

Thus, from Eq. (2),

$$\vartheta_\mathrm{F} = \widetilde{\alpha}_\mathrm{F} + \widetilde{\beta}_\mathrm{F} x_\mathrm{F} + \widetilde{\varepsilon}_\mathrm{F}, \tag{8}$$

where the residual variance is $\mathrm{var}\widetilde{\varepsilon}_\mathrm{F} = \widetilde{\sigma}^2_\mathrm{F}$.

In a predictive situation, we have to approximate the fine-scale x_F with its coarse-scale equivalent x_C. We therefore predict x_F using a scaling model,

$$x_\mathrm{F} = f(x_\mathrm{C}) + \varepsilon_\mathrm{C}, \tag{9}$$

where the residuals shall be assumed to be independent and identically distributed according to a normal distribution with mean 0 and variance $\mathrm{var}\varepsilon_\mathrm{C} = \sigma^2_\mathrm{C}$. The function f represents an arbitrary predictive model, such as a linear regression in x_C. More generally, we could approximate x_F using a model built on multiple variables other than x_C.

Thus,

$$\vartheta_\mathrm{F} = \widetilde{\alpha}_\mathrm{F} + \widetilde{\beta}_\mathrm{F} f(x_\mathrm{C}) + \varepsilon', \tag{10}$$

where the residuals are

$$\varepsilon' = \widetilde{\varepsilon}_\mathrm{F} + \widetilde{\beta}_\mathrm{F} \varepsilon_\mathrm{C}. \tag{11}$$

Since the spatial predicitons are to be made at the coarse scale, where one grid cell is composed of N fine-scale grid cells, we have

$$\vartheta_\mathrm{C} = \frac{1}{N} \sum_{i=1}^{N} \vartheta_\mathrm{F} \tag{12}$$

$$= \alpha_\mathrm{F} + \widetilde{\beta}_\mathrm{F} f(x_\mathrm{C}) + \frac{1}{N} \sum_i \widetilde{\varepsilon}_{\mathrm{F,i}} + \frac{\widetilde{\beta}_\mathrm{F}}{N} \sum_i \varepsilon_{\mathrm{C,i}}, \tag{13}$$

where we make use of the fact that x_C does not vary within a coarse-resolution grid cell. We refer to the last two terms, which involve the fine- and coarse-scale residuals, as the residual of ϑ_C.

The estimation of the residual variance of ϑ_C is not an easy task because the within-cell residuals $\widetilde{\varepsilon}_{\mathrm{F,i}}$ and $\varepsilon_{\mathrm{C,i}}$, respectively, can certainly not be considered to be independent due to the likely presence of (positive) spatial autocorrelation over these short distances. The variances of the partial residual terms would be expected to decrease proportionally to N^{-1} under the assumption of independent within-cell replication. The estimation variance of the mean value of positively autocorrelated random variables, by contrast, decreases more slowly with increasing sample size. In the extreme case of perfect within-cell dependence, averaging over N identical pseudo-replications would not reduce estimation variance compared to using only one replication. We adopt this conservative approach by assuming that averaging over N finer-scale grid cells does not reduce the uncertainty $\mathrm{var}\varepsilon'$ in the statistical model ground temperature at the aggregate scale (Hurlbert, 1984). In addition, we replace β^2_F with the square of a one-sided (upper) 95-% confidence limit of $|\beta_\mathrm{F}|$, $\beta^2_{\mathrm{F,cl}}$. Thus, as a conservative estimator for $\mathrm{var}\varepsilon'$, we use

$$\sigma'^2 := \sigma^2_\mathrm{F} + \beta^2_{\mathrm{F,cl}} \sigma^2_\mathrm{C}. \tag{14}$$

Consequently, the residual variance of the scaling model adds to the residual variance of the scaled model, using the regression coefficient for variance weighting, and the equation would be expanded by additional $\beta^2_{i,\mathrm{F,cl}} \sigma^2_{i,\mathrm{C}}$ for each additional explanatory variable to be scaled. Estimates of β_F and σ^2_F can be obtained from the fine-scale rock temperature model, and an estimate of σ_C from the scaling model.

In a predictive situation, σ^2_F can be replaced with the corresponding prediction variance of the rock temperature model, which is generally slightly greater than σ^2_F. The prediction variance varies, however, slightly between samples. In the present study, the prediction variance is inflated only by 6 % on average, with a maximum of 11 %, and we therefore increase σ^2_F by 6 % in general in this study as a first-order approximation.

3.4 Surface types

To distinguish between the two model domains (debris vs. bedrock) one of the following approaches can be applied: (1) an index describing the degree of membership in the exposed bedrock rock surface class, (2) a statistical model of land cover such as a logistic regression or generalized additive model (Hastie and Tibshirani, 1990) or (3) remotely-sensed or map-based land cover products.

3.5 Model evaluation

To assess the accuracy of the debris model, the area under the receiver-operating characteristics curve, which is known as AUROC, was calculated. This value ranges between 0.5 (random model behavior) and 1.0 (perfect model; Hosmer and Lemeshow, 2000). AUROC values reported in this study

Table 1. Overview of data used for model calibration (RG Rock glacier; AT Austria, CH Switzerland, DE Germany, FR France, IT Italy).

Response variable	Country	Region	N (intact/relict)	Source
RG status	AT, CH, FR, IT	Various regions	1625/3916	Cremonese et al. (2011)
RG status	CH	Entremont, Valais	115/137	Delaloye et al. (1998)
RG status	CH	Engadina, Graubünden	115/137	Frauenfelder et al. (2001); Frauenfelder (2005)
RG status	CH	Engadina, Graubünden	18/6	Hoelzle (1998)
RG status	CH	Aletsch region, Bern	11/13	Imhof (1998)
RG status	CH	Printse valley, Valais	115/137	Reynard and Morand (1998)
RG status	CH	Fletschhorn area, Valais	50/22	Frauenfelder (1998)
RG status	CH	Prealps, Vaud	0/25	Schoeneich et al. (1998)
MARST	CH, DE, FR, IT	Various regions	49	Cremonese et al. (2011)
MARST	CH	Matterhorn, Jungfraujoch	8	Hasler et al. (2011)

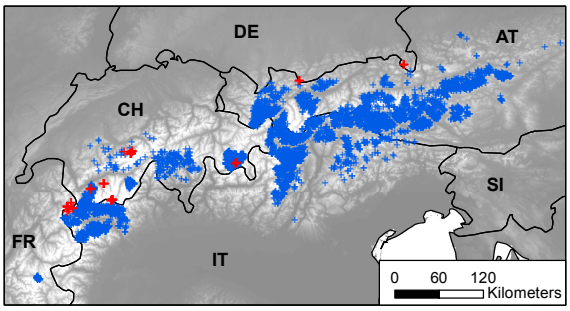

Fig. 1. Spatial distribution of intact/relict rock glaciers (blue crosses) and the locations of the rock surface temperature loggers (red crosses).

are based on model predictions that include the inventory random effect.

A 10-fold cross-validation was performed to assess how transferrable to independent test data sets the model is (Hand, 1997). The original data set was randomly partitioned into 10 sub-samples. Of these 10 sub-samples, a single sub-sample was retained for testing the model, and the remaining 9 sub-samples were used as training data. This process was repeated 10 times using each of the 10 sub-samples exactly once as the validation data. The 10 results from the folds were combined to produce a single estimation which then was used to measure the AUROC.

The goodness-of-fit for the rock model was obtained by calculating the R^2 and the root mean square error (RMSE). Furthermore, the RMSE resulting from a 10-fold cross-validation was calculated.

4 Data

4.1 Response variables

Most of the rock glacier inventories used to fit the debris model were provided by the permafrost observation collection of the PermaNET project (Cremonese et al., 2011). This collection was complemented by inventories from Switzerland published at the Seventh International Conference on Permafrost ("Yellowknife inventories"; ICP Yellowknife, Canada, 23–27 June 1998; Delaloye et al., 1998; Frauenfelder, 1998; Hoelzle, 1998; Imhof, 1998; Reynard and Morand, 1998; Schoeneich et al., 1998) and an inventory from the Upper Engadine, Switzerland (Frauenfelder et al., 2001; Frauenfelder, 2005). The final data set used as basis for the model development includes 2184 intact and 4218 relict rock glaciers from Austria, France, Italy and Switzerland (Table 1, Fig. 1).

For each rock glacier, information concerning its activity is available. The activity information from the different inventories was reclassified into the two classes (1) intact and (2) relict. The inventories from the PermaNET data contain polygon information for each rock glacier. From this inventories a stratified random sample was selected that resulted in one random point within the polygon for each rock glacier. For the Yellowknife inventories the centroids of the rock glaciers were used instead, because polygon information was unavailable. Finally, from each of the inventories an equal number of intact and relict rock glacier samples was drawn randomly in order to obtain balanced samples.

MARST data from France, Germany, Italy and Switzerland contained in the PermaNET inventory were used (Pogliotti, 2006; Pogliotti et al., 2008; PERMOS, 2010; Cremonese et al., 2011) and complemented with additional measurements from Switzerland (Hasler et al., 2011, Table 1, Fig. 1). All 57 sensors were located in rock walls $> 55°$ steep and several meters above flat ground to ensure snow-free conditions. The data originate from eight areas (Fig. 1) within which a wide range of aspects and elevations has been

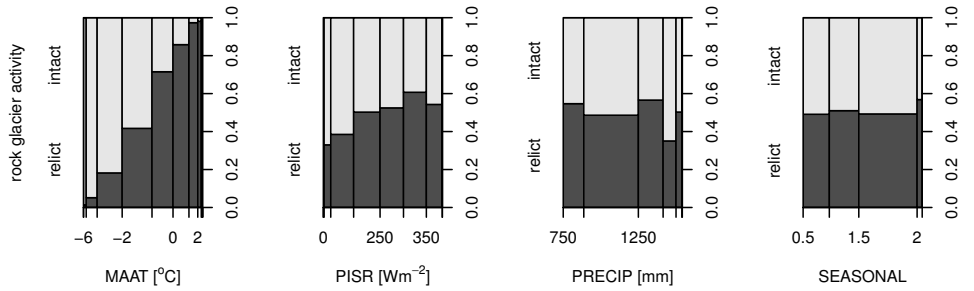

Fig. 2. Frequencies of intact as opposed to relict rock glaciers conditional on potential explanatory variables. Bar widths in these spinograms are proportional to the empirical frequency of the given interval of values of explanatory variable. The figure does not account for random inventory effects.

sampled. Measurement depths are on the order of 10 cm. The rock types sampled vary between areas and include limestone, granite and gneiss. The attribute data for each logger contains elevation, slope angle and aspect (measured in the field) as well as the observation period (logger years) taken for the calculation of MARST values. With this information MARST measurements of single or few years duration were adjusted to longer-term temperature trends according to Allen et al. (2009): longer-term MAAT from Piz Corvatsch (Upper Engadina, MeteoSchweiz, 2010) for the period 1961–1990 (MAAT $= -6\,^{\circ}$C) were compared with MAAT of the period corresponding to the specific logger years. The difference between these temperatures was used to correct the MARST values. The underlying assumption is that the difference of MAAT to its longer-term mean and the difference of MARST to its longer-term mean are equal (cf. Fig. 3.1 of PERMOS, 2010). By using the period of 1961–1990 as reference, the air temperature warming especially in the past decade due to climate change is neglected. This leads to an optimistic estimation (biased towards an overestimation of permafrost distribution) of MARST, but is in line with the debris model that also follows an optimistic approach. In comparison with the high number of rock glaciers available, 57 measurement points are few. They are, however, used for describing a system that is much less complicated than rock glaciers because the influence of snow, phase change, a mixed-media active layer and the downslope displacement of ice-rich material is minimal or non-existent.

4.2 Explanatory variables

As potential explanatory variables we consider PISR, MAAT, PRECIP, and a seasonal precipitation index (SEASONAL). PISR was derived from the Global Digital Elevation Model (GDEM; Hayakawa et al., 2008) with a grid spacing of $1''$ (approximately 30 m) using RSAGA (Brenning, 2008) and the algorithm of Wilson and Gallant (2000). PISR was calculated for one year with an hourly temporal resolution and clear sky conditions (100 % atmospheric transmittance) and is calculated for a latitudinal extent of 1° (6 bands according to the total latitudinal extent of our study area). ASTER GDEM covers the entire Alpine arc and shows an overall vertical accuracy on a global basis of approximately 20 m at 95 % confidence (USGS et al., 2009).

Alpine-wide MAAT data for the period 1961–1990 (Hiebl et al., 2009) was provided by the Central Institute for Meteorology and Geodynamics (ZAMG, Austria). MAAT is based on the GTOPO30 elevation model (Center, 1997) with an approximate resolution of 1000 m and shows a monthly standard error of less then 1 °C (Hiebl et al., 2009). A constant lapse rate of 0.65 °C 100 m^{-1} was used to interpolate the coarse MAAT based on more precise elevation information from the ASTER GDEM.

Alpine-wide monthly precipitation data (Efthymiadis et al., 2006) is available for 1800–2003, gridded at $10'$ resolution (approximately 15 km, available from ALP-IMP, http://www.cru.uea.ac.uk/cru/data/alpine/). Based on this data, PRECIP for the period 1961–1990 was calculated. As potential explanatory variable for the debris model, PRECIP was centered (cPRECIP) by subtracting its mean value of 1271 mm. Centering PRECIP allows to directly compare the coefficients of the different models including and excluding PRECIP as explanatory variable. Additionally, an index describing the seasonality of precipitation (SEASONAL) was computed by dividing the mean sum of summer precipitation (May–October) by the mean sum of winter precipitation (November–April).

For the locations of the MARST loggers, the usage of locally measured terrain parameters is necessary for the characterization of MARST, because they strongly depend on micro-topographic radiation effects such as sun exposure or terrain shading (the resolution of the ASTER GDEM is too coarse for this purpose.). For increased accuracy, PISR was therefore calculated following Corripio (2003) based on local measurements of elevation, slope angle and aspect. Additionally, for the Swiss locations (except the one published by Hasler et al., 2011) local horizons affecting the obstruction of solar irradiation were determined using a camera with

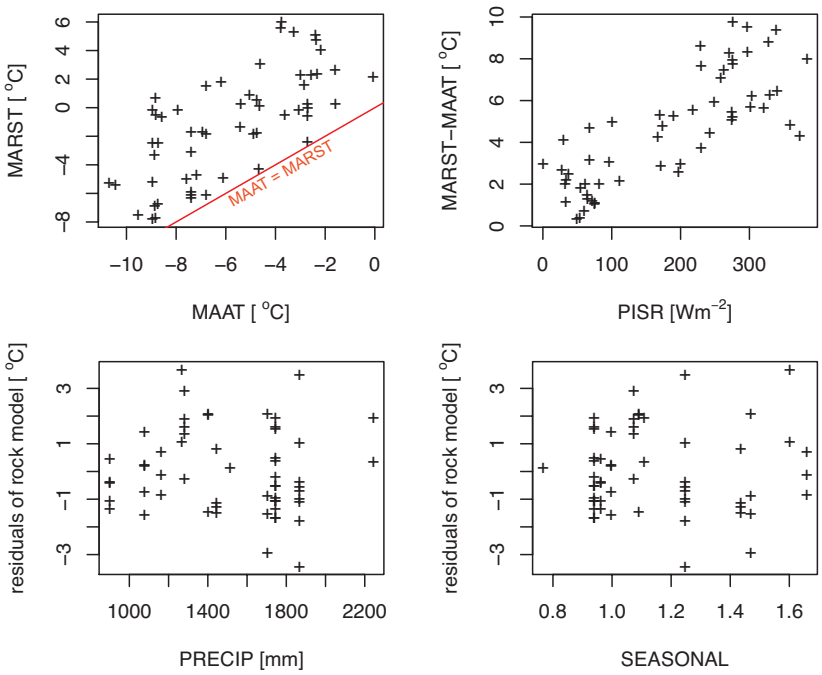

Fig. 3. Scatterplots illustrating the relation of MARST to MAAT (top left) and of the difference between MARST and MAAT to PISR (top right) for the 57 MARST values. In the lower panels, the model residuals (mean = 0 °C, standard deviation = 1.52 °C) of the rock model are plotted against PRECIP and SEASONAL to visualize possible relations of these two variables.

Table 2. Summary statistics of the randomly sampled points representing potential explanatory variables for the debris model (Q25 lower quantile, Q75 upper quantile).

	Intact rock glaciers ($N = 1790$)				Relict rock glaciers ($N = 1790$)			
	Mean	Median	Q25	Q75	Mean	Median	Q25	Q75
Altitude [m]	2641	2646	2523	2770	2302	2323	2140	2484
MAAT [°C]	−2.13	−2.17	−2.86	−1.44	−0.12	−0.20	−1.19	0.84
PISR [W m^{-2}]	248	240	188	307	268	270	211	329
PRECIP [mm]	1239	1188	1028	1464	1212	1178	1021	1358
SEASONAL	1.44	1.54	1.07	1.72	1.46	1.54	1.07	1.75

fish eye lens (Gruber et al., 2003) and considered in the PISR calculations. Further, the MAAT provided by ZAMG was adjusted for the logger locations using local elevation information measured in the field.

5 Alpine-wide permafrost model

This section contains the model calibration and interpretation for the debris and the rock model. For each sub-model, three different sets of explanatory variables were used to compute regression models. Afterwards, the final model was chosen based on goodness-of-fit-statistics. In the last subsection of this chapter, the combination of the sub-models is presented.

5.1 Debris model

A total of 3580 rock glacier points (Table 2) were used for model calibration. While MAAT and PISR in the debris model show a clear relation to the activity of rock glaciers, the correlation with precipitation is less obvious in a univariate analysis (Fig. 2). Nevertheless, cPRECIP was included in the final model based on the high significance of the Wald test (Table 3). The seasonality of precipitation (SEASONAL)

Table 3. Model coefficients (and standard errors in parentheses) of debris models using different sets of explanatory variables, and the corresponding goodness-of-fit statistics. Debris model 1 was chosen as final model. (The units for the explanatory variables are given in square brackets for each coefficient.)

	Debris model 1	Debris model 2	Debris model 3
Intercept	0.817 (0.192)***	0.821 (0.182)***	1.366 (0.320)***
MAAT [°C]	−0.906 (0.046)***	−0.882 (0.035)***	−0.885 (0.035)***
PISR [W m^{-2}]	−0.007 (0.001)***	−0.007 (0.001)***	−0.007 (0.001)***
cPRECIP [mm]	0.001 (0.0002)***	–	–
SEASONAL	–	–	−0.391 (0.187)*
AUROC	0.91	0.90	0.90
AUROC$_{cv}$	0.91	0.91	0.90
Inventory-level standard deviation	0.212	0.413	0.442
Residual standard deviation	1.758	1.377	1.372

Significance of Wald test: * < 0.05, ** < 0.01, *** < 0.001

shows no significant contribution within the debris model and was therefore omitted for the final model.

The chosen GLMM includes MAAT, PISR and cPRECIP as fixed effects and the membership of each point in the different inventories as random effects (Table 3). All explanatory variables show a high significance (p-value). When considering random effects, the debris model achieves an AUROC of 0.91, respective 0.91 for the 10-fold cross-validation (AUROC$_{cv}$), which both are "outstanding" discriminations according to Hosmer and Lemeshow (2000).

The coefficients of the final model indicate: a difference in cPRECIP of 400 mm is identical with a change of 0.52 on the probit scale. A difference in MAAT of 1 °C is equivalent to a probit-change of 0.91. Thus, a change in cPRECIP of 400 mm is identical to a difference in MAAT of 0.57 °C and leads to a dislocation of the limit between intact and relict rock glaciers of 88 m (assuming a constant lapse rate of 0.65 °C 100 m^{-1}). An increase of 240 W m^{-2} (approximate difference in PISR of a south vs. north exposed slope with an angle of 30°) is associated with a decrease of 1.78 on the probit scale. This change is equivalent to an increase in MAAT by 1.96 °C or approximately 300 m in elevation.

5.2 Rock model

For all 57 locations, MARST are higher than MAAT (Table 4, Fig. 3, top left) and the difference between MARST and MAAT increases with higher PISR (Fig. 3, top right). PRECIP was not included in the rock model, because the variable showed no high significance and it deteriorates the Akaike Information Criterion (AIC), which measures model fit while penalizing for model size (Table 5; Gelman and Hill, 2007). SEASONAL was omitted from the final model because its range of values on the present training sample was too narrow (from 0.76 to 1.66) to allow for an Alpine-wide application of this empirical relationship (SEASONAL between 0.50 and 2.47).

Table 4. Summary statistics and Pearson correlations between MARST and potential explanatory variables for all MARST locations for the rock model (Q25 lower quantile, Q75 upper quantile).

	Mean	Median	Q25	Q75	Pearson correlation
MARST [°C]	−1.21	−0.57	−4.70	1.49	–
MAAT [°C]	−5.78	−6.11	−8.58	−3.07	0.70
PISR [W m^{-2}]	183	197	68	275	0.44
PRECIP [mm]	1514	1704	1267	1745	−0.38
SEASONAL	1.15	1.07	0.94	1.25	0.16

The coefficients of the chosen model indicate that MARST are generally warmer than the corresponding MAAT. An increase in PISR of 240 W m^{-2} is associated with a decrease in MARST of 4.6 °C and is equivalent to a change in MAAT of 4.2 °C. Thus, a change in slope aspect from south to north has a similar influence on MARST as a change in elevation of approximately 650 m.

5.3 Scaling model and model combination

A LIDAR DEM covering South Tyrol (data provided by Autonomous Province of Bolzano – South Tyrol, Italy) with a resolution of 2.5 m was used to estimate the prediction variance of the scaling model. The other variance component was estimated from the rock model. PISR derived from the LIDAR DEM refers to local, "real world" estimates and can be compared with PISR values calculated for the rock logger locations.

The following linear regression was fitted to a random sample of 28 640 points within South Tyrol above 2000 m and relates finer-scale (2.5 m, LIDAR DEM) PISR to coarse-scale values calculated from a reduced-resolution and reduced quality (30 m, ASTER GDEM) equivalent:

Table 5. Model coefficients (and standard errors in parentheses) of rock models using different sets of explanatory variables, and the corresponding goodness-of-fit statistics. Rock model 2 was chosen as final model. (The units for the explanatory variables are given in square brackets for each coefficient.)

	Rock model 1	Rock model 2	Rock model 3
Intercept	2.506 (1.006)*	1.677 (0.573)**	2.000 (0.573)***
MAAT [°C]	1.055 (0.091)***	1.096 (0.081)***	1.160 (0.083)***
PISR [W m^{-2}]	0.019 (0.002)***	0.019 (0.002)***	0.019 (0.002)***
PRECIP [mm]	−0.001 (0.001)	–	–
SEASONAL	–	–	−2.87 (0.943)*
R^2	0.82	0.82	0.83
R^2_{adj}	0.81	0.81	0.82
RMSE [°C]	1.56	1.57	1.50
$RMSE_{cv}$ [°C]	1.69	1.676	1.65
AIC	222.32	221.39	218.361
Residual standard error [°C]	1.616	1.616	1.561

Significance of Wald test: * < 0.05, ** < 0.01, *** < 0.001

Table 6. Variance components used for combining the rock and debris models.

	Estimate
$\sigma^2_F = \text{average}\sigma^2_{pred}$	2.76
$\beta_{F,cl}$	0.022
σ^2_C	2108
σ'^2	3.80

$$PISR_F = 3.704 + 0.931 PISR_C \quad (15)$$

This model resulted in an $R^2 = 0.72$ and a residual standard error of 46 W m^{-2}.

For the two other explanatory variables (MAAT and cPRECIP), no scaling correction was necessary because both variables show negligible spatial variation within ASTER GDEM grid cells.

The conservative estimation of σ' (Eq. 14) obtained a value of 1.95 °C and was used for converting predicted MARST into the corresponding probit-based values (Eq. 6). The individual variance components are displayed in Table 6. The adjustment parameters Δ_r (Eq. 2) and the Δ_d (Eq. 5) were set to zero. Both models (debris and rock model) were then combined using Eq. (7). Probabilities of a rock glacier being intact as opposed to relict, respectively probabilities of MARST ≤ 0 °C in steep bedrock, were obtained by applying the inverse probit transformation (Fig. 4). A sample application of the model showing a map-based output product is presented in Fig. 5.

6 Discussion

6.1 Use and limitations of the model

The presented model approach is based on statistical relations and thus limited in the ability to represent physical processes such as snow redistribution by avalanche and wind that is known to have an impact on mountain permafrost occurrence (Haeberli, 1975; Hoelzle et al., 2001). To account for the different thermal responses related to surface conditions in two domains (debris and rock cover) an adjustment-offset Δ can be applied in our model for each sub-domain model individually (Sect. 3.1). Identifying suitable average adjustment parameters for each domain is challenging because of the large spatial variation of the offsets between different locations (Hoelzle and Gruber, 2008).

The explanatory variables MAAT and cPRECIP are derived from existing data sources (Sect. 4.2). PISR estimates are based on a DEM. For an Alpine-wide model application, the ASTER GDEM can be used to calculate PISR values. For regional model application (e.g. South Tyrol, Italy), where more precise DEM data is available, this could be used to derive the PISR values. Functions similar to Eq. (15) are then needed to address the scaling from fine to coarse resolution for the debris model. The prediction is also possible based on two different DEMs: a coarse elevation model (e.g. ASTER GDEM) for the debris model representing the mesoscale characteristics of rock glaciers, and a more precise DEM for the rock model because MARST values more strongly depend on accurate PISR estimates. The ASTER GDEM, which is used in this study to calculate PISR and to rescale MAAT for the debris model, shows limitations in the Alps when compared to a more reliable DEM (Frey and Paul, 2011). However, no better DEM is available at the moment for the entire Alps.

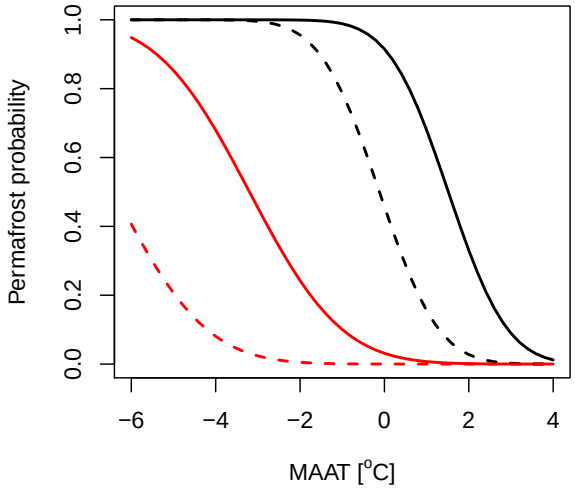

Fig. 4. Predicted probabilities of a rock glacier being intact (black) and of MARST $\leq 0\,^{\circ}$C in steep bedrock (red) for PISR = 100 W m^{-2} (solid line) and PISR = 300 W m^{-2} (dashed line). A precipitation value of 1271 mm (cPRECIP = 0 mm) was used for this figure.

The spatial distribution of the rock glaciers used for model calibration (debris model) nearly covers the entire Alps. In contrast, only 57 MARST measurements mostly from the central part of the Alps were available. This inevitably requires a strong generalization of the rock model, especially regarding the precipitation (Sect. 6.2). The temporal extrapolation of MARST values to the period 1961–1990 was addressed by using long-term MAAT measurements. However, the corrected data is sensible to inter-annual variability, because some of the measurement series were only one year long.

The transition zone between debris covered slopes and steep bedrock requires further investigation. Some ground surface temperature (GST) measurements exist in this zone but as mention in Sect. 2 the large inter-annual variability makes this data unsuitable for statistical modelling.

6.2 Influence of precipitation

The precipitation variable in the debris model can be seen as a simple proxy for the amount of snow in a regional context or the reduction of short wave insolation by cloud cover. The positive coefficient of precipitation in the regression model (Sect. 5.1) implies that in areas with higher precipitation, rock glaciers are more likely to be intact, or equivalently, the limit between intact and relict rock glaciers tends to shift towards lower elevations. According to our model, this means that for given MAAT (or elevation in a local context) and PISR conditions, the boundaries of permafrost occurrence in debris-covered and wet areas of the Alps are on average approximately 220 m lower than in relatively dry areas with 1000 mm lower PRECIP. This contrasts with several studies that state that permafrost boundaries are lower in dry or continental areas (e.g. Barsch, 1978; King, 1986), but it is consistent with regional-scale trends in the lower limit of intact rock glacier distribution in the Andes of Central Chile (Brenning, 2005; Azócar and Brenning, 2010). Debris rock glaciers, referring to rock glaciers developed in strong relation to a glacier (e.g. Barsch, 1996; Hughes et al., 2003), may offer an explanation for the positive coefficient of PRECIP in the debris model. However, their precise definition is difficult and as a consequence their influence on the debris model cannot be assessed.

The positive influence of precipitation regarding the intactness of a rock glacier is also shown in Fig. 6, where three different models without precipitation as explanatory variable for drier, normal and relatively wet areas are compared. The three models were calibrated using three subsamples of the entire data set representing drier, normal and relatively wet inventories (drier: mean PRECIP = 1105 mm, normal: mean PRECIP = 1291 mm, and relatively wet: mean PRECIP = 1679 mm). The variable precipitation is not just significant, but also relevant regarding possible model prediction as shown in Fig. 7. The predicted values modelled with cPRECIP as explanatory variable differ with a maximum of 1.5 °C (or approximately 200 m of elevation) from the model prediction without cPRECIP included as explanatory variable.

To further investigate possible relationships between precipitation and the spatial density of rock glaciers, we compared data from two different rock glacier inventories, for which the inventory perimeters were manually digitized (IGUL, Tecino, Switzerland and GEOL,Trentino, Italy); inventory boundaries are currently not available for the other inventories. The results show that rock glacier density in the Alps tends to be higher in areas with less precipitation (Fig. 8). This could explain the widespread notion that also permafrost boundaries occur at lower elevation in dry areas.

The correlation of MARST and precipitation is weak (Fig. 3, bottom right) and PRECIP shows no significance in the rock model (Table 5). However, the observed significance and magnitude of the influence of SEASONAL suggests that further research on the physical relationship of precipitation seasonality on rock temperatures would be desirable, and that a larger rock temperature data basis would allow us to incorporate an additional relevant predictor variable into the model. According to Gruber et al. (2004) the influence of PISR is larger in dry areas compared to wet areas, especially in south facing rock walls, but seasonal precipitation patterns were not included in the study of Gruber et al..

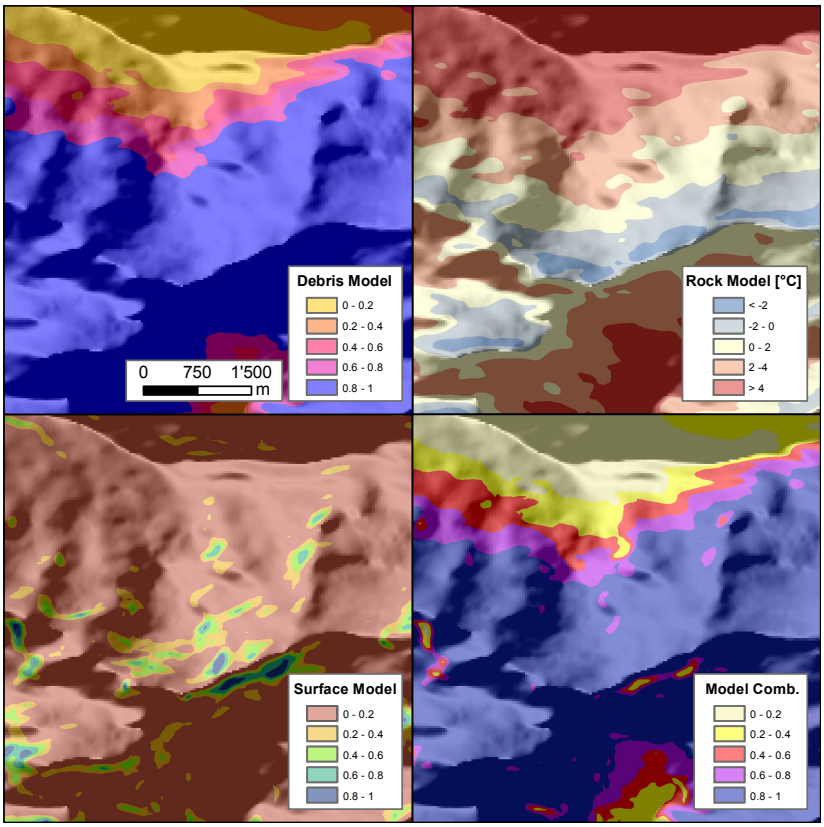

Fig. 5. Example of the application of the different models. Top left: Prediction of the debris model showing probabilities of permafrost occurrence. Top right: Predicted MARST values of the rock model. Bottom left: Prediction of an arbitrary surface model (here: probabilities of steep bedrock occurrence depending on slope angle only). Bottom right: Combination of the three models showing probabilities of permafrost occurrence.

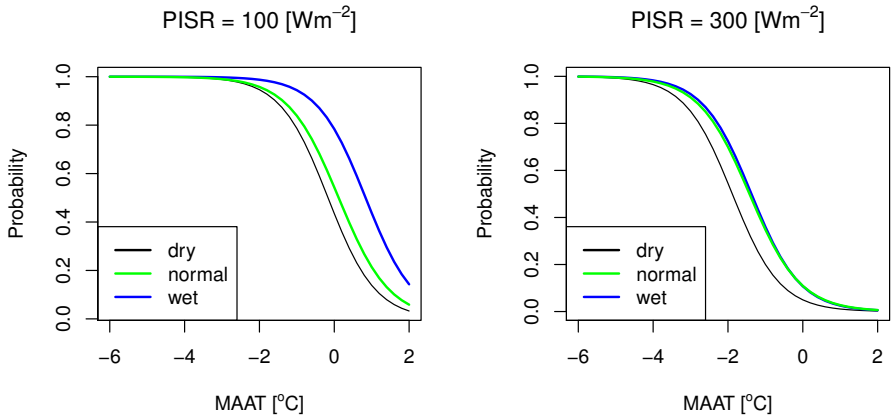

Fig. 6. Probabilities of a rock glacier being intact as opposed to relict for drier (mean PRECIP = 1105 mm), normal (mean PRECIP = 1291 mm) and relatively wet (mean PRECIP = 1679 mm) inventories using three different models (dry, mean, wet). The three models do not include cPRECIP as explanatory variable.

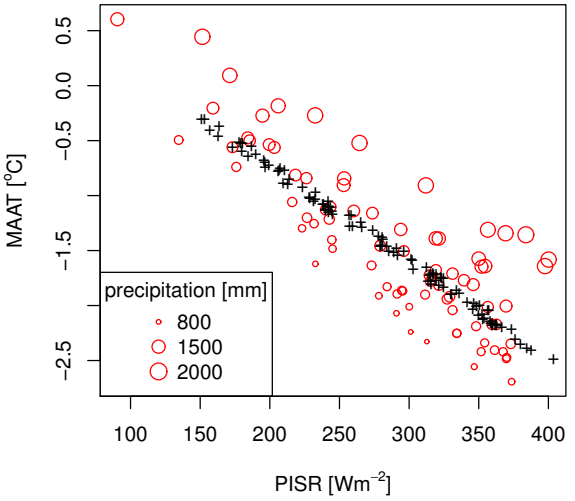

Fig. 7. Prediction values for the two first models from Table 3 calculated for a randomly selected probability range of 0.475–0.525 for intact rock glacier occurrence. Black crosses: debris model without cPRECIP as explanatory variable, red bubbles: debris model including cPRECIP as explanatory variable.

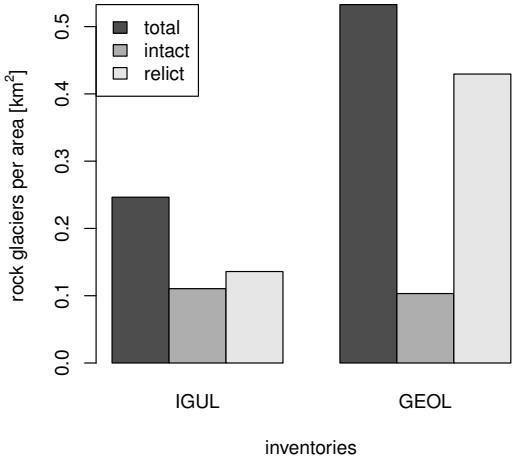

Fig. 8. Spatial density of rock glacier occurrence in inventories with high (IGUL Tecino, Switzerland; mean PRECIP = 1900 mm) and low (GEOL, Trentino, Italy; mean PRECIP = 1072 mm) precipitation. The relevant area is calculated for areas above 2000 m of elevation excluding glaciered areas (data provided by Paul et al., 2009) and steep slopes (slope angle $< 50°$).

7 Conclusions

We have presented an approach and statistical model designed to cater for the specific needs of permafrost distribution estimation for entire mountain regions. Based on this, rock glacier inventories and MARST measurements were used to calibrate model coefficients for the European Alps. By using intact and relict rock glaciers as calibration data, the prediction of the debris model is biased towards and overestimation of the permafrost distribution, while the rock model generally underestimates the current permafrost distribution. Current data does not permit extending the statistical analyses to other types of surface cover with the same statistical rigor, as a high number of observations would be required. This is a fundamental challenge to all statistical permafrost distribution modelling, and equally to the validation of physically-based numerical models. However, the quantitative statistical model presented already contains offset terms to allow later subjective adjustment for the extension to other surface types.

By allowing analyses (i.e. model calibration) in larger areas, more robust and new insight can be derived because of more available data and due to larger environmental gradients covered by one analysis. In this way, a shift of the limit between intact and relict rock glaciers towards lower elevation has been detected to coincide with increasing precipitation. This influence of precipitation needs further investigation because it conflicts with previous but less quantitative studies. However, this is the first investigation known to the authors, which systematical analyses the spatial rock glacier distribution in relation to precipitation patterns with a large data sample in the Alps.

The model presented is build on reliable data and subjective adjustment is clearly separated from statistical analysis. In this sense, this paper is a step towards an Alpine permafrost map, but the model and coefficients presented cannot be directly applied to an entire landscape and they require subjective adjustments of the offsets Δ_d and $\widetilde{\Delta}_r$. The following steps are needed to use the presented approach for Alpine-wide model application and to provide a map-based output product: (a) the definition of offsets terms for surfaces other than steep bedrock and rock glaciers; (b) the derivation of scaling functions to correct PISR estimates derived from different DEMs; (c) the preparation of gridded land cover maps quantifying the membership in the two classes debris and bedrock slopes as well as any other surface type considered with an offset term; and (d) the establishment of a legend and interpretation guidelines for map users. After the inclusion of offset terms, model results are no longer probabilities but should be considered to be an index, which describes the permafrost occurrence per grid cell and than can be shown in a map (cf. Boeckli et al., 2012).

Acknowledgements. Funding of this study was partly provided by the Alpine Space Program project PermaNET, the Bavarian Environment Agency (Bayerisches Landesamt für Umwelt, LfU), the Swiss Federal Office for the Environment (Bundesamt für Umwelt, BAFU), the Autonomous Province of Bolzano and the Region of Veneto, Geological Survey. Special thanks go to Arthur Lutz and Christian Gschwend for support with data preprocessing. The Swiss Society of Snow, Ice and Permafrost (SEP) as well as the

Swiss Geomorphological Society (SGmG) financially supported a research exchange without which this publication would not been possible.

Edited by: R. Rigon

References

Aldrich, J. and Nelson, F.: Linear probability, logit, and probit models, Sage Publications, Inc., 1984.

Allen, S., Gruber, S., and Owens, I.: Exploring steep bedrock permafrost and its relationship with recent slope failures in the Southern Alps of New Zealand, Permafrost and Periglacial Processes, 20, 345–356, doi:10.1002/ppp.658, 2009.

Azócar, G. and Brenning, A.: Hydrological and geomorphological significance of rock glaciers in the dry Andes, Chile (27–33 S), Permafrost and Periglacial Processes, 21, 42–53, doi:10.1002/ppp.669, 2010.

BAFU: Hinweiskarte der potentiellen Permafrostverbreitung in der Schweiz, Bundesamt für Umwelt (BAFU)/Swiss Federal Office for the Environment, 2005.

Barsch, D.: Active rock glaciers as indicators for discontinuous alpine permafrost. An example from the Swiss Alps, in: Proceedings of the 3th International Conference on Permafrost. Edmonton, Canada, 10–13 July, vol. 1, pp. 349–352, 1978.

Barsch, D.: Rock Glaciers: Indicators for the present and former geoecology in high mountain environments, Springer-Verlag: Berlin, 1996.

Boeckli, L., Gruber, S., and Brenning, A.: Estimated permafrost distribution in the European Alps, The Cryosphere, in preparation, 2012.

Brenning, A.: Climatic and geomorphological controls of rock glaciers in the Andes of Central Chile: Combining statistical modelling and field mapping, Ph.D. thesis, Humboldt-Universität Berlin, 2005.

Brenning, A.: Statistical geocomputing combining R and SAGA: The Example of Landslide susceptibility Analysis with generalized additive Models, SAGASeconds Out, 19, 23–32, 2008.

Brenning, A., Gruber, S., and Hoelzle, M.: Sampling and statistical analyses of BTS measurements, Permafrost and Periglacial Processes, 16, 383–393, doi:10.1002/ppp.541, 2005.

Center, U.: GTOPO30 documentation (README file), Land Processes Distributed Active Archive Center. Available in: http://edcdaac.usgs.gov/GTOPO30/README.asp, 1997.

Corripio, J.: Vectorial algebra algorithms for calculating terrain parameters from DEMs and solar radiation modelling in mountainous terrain, International Journal of Geographical Information Science, 17, 1–23, 2003.

Cremonese, E., Gruber, S., Phillips, M., Pogliotti, P., Boeckli, L., Noetzli, J., Suter, C., Bodin, X., Crepaz, A., Kellerer-Pirklbauer, A., Lang, K., Letey, S., Mair, V., Morra di Cella, U., Ravanel, L., Scapozza, C., Seppi, R., and Zischg, A.: Brief Communication: "An inventory of permafrost evidence for the European Alps", The Cryosphere, 5, 651–657, doi:10.5194/tc-5-651-2011, 2011.

Delaloye, R., Reynard, E., and Wenker, L.: Rock glaciers, Entremont, Valais, Switzerland, Boulder CO: National Snow and Ice Data Center/World Data Center for Glaciology. Digital Media, 1998.

Ebohon, B. and Schrott, L.: Modeling mountain permafrost distribution: A new map of Austria, in: Proceedings of the 9th International Conference on Permafrost. Fairbanks, Alaska, 30 June–3 July, pp. 397–402, 2008.

Efthymiadis, D., Jones, P., Briffa, K., Auer, I., Böhm, R., Schöner, W., Frei, C., and Schmidli, J.: Construction of a 10-min-gridded precipitation data set for the Greater Alpine Region for 1800–2003, J. Geophys. Res., 110, D01105, doi:10.1029/2005JD006120, 2006.

Etzelmüller, B., Heggem, E., Sharkhuu, N., Frauenfelder, R., Kääb, A., and Goulden, C.: Mountain permafrost distribution modelling using a multi-criteria approach in the Hövsgöl area, northern Mongolia, Permafrost and Periglacial Processes, 17, 91–104, doi:10.1002/ppp.554, 2006.

Etzelmüller, B., Farbrot, H., Gudhmundsson, A., Humlum, O., Tveito, O., and Björnsson, H.: The regional distribution of mountain permafrost in Iceland, Permafrost and Periglacial Processes, 18, 185–199, doi:10.1002/ppp.583, 2007.

Frauenfelder, R.: Rock glaciers, Fletschhorn Area, Valais, Switzerland, International Permafrost Association, Data and Information Working Group, NSIDC, University of Colorado at Boulder, 1998.

Frauenfelder, R.: Regional-scale modelling of the occurrence and dynamics of rockglaciers and the distribution of paleopermafrost, PhD thesis, Geographisches Institut der Universität Zürich, 2005.

Frauenfelder, R., Allgöwer, B., Haeberli, W., and Hoelzle, M.: Permafrost investigations with GIS – a case study in the Fletschhorn area, Wallis, Swiss Alps, in: Proceedings of the 7th International Conference on Permafrost. Nordicana, Yellowknife, Canada, pp. 551–556, 1998.

Frauenfelder, R., Haeberli, W., Hoelzle, M., and Maisch, M.: Using relict rockglaciers in GIS-based modelling to reconstruct Younger Dryas permafrost distribution patterns in the Err-Julier area, Swiss Alps, Norsk Geografisk Tidsskrift-Norwegian Journal of Geography, 55, 195–202, 2001.

Frey, H. and Paul, F.: On the suitability of the SRTM DEM and ASTER GDEM for the compilation of topographic parameters in glacier inventories, International Journal of Applied Earth Observation and Geoinformation, doi:10.1016/j.jag.2011.09.020, http://www.sciencedirect.com/science/article/pii/S0303243411001437, 2011.

Gelman, A. and Hill, J.: Data analysis using regression and multilevel/hierarchical models, vol. 648, Cambridge University Press: Cambridge, UK, 2007.

Gotway, C. A. and Young, L. J.: Combining Incompatible Spatial Data, Journal of the American Statistical Association, 97, pp. 632–648, http://www.jstor.org/stable/3085677, 2002.

Gruber, S. and Haeberli, W.: Permafrost in steep bedrock slopes and its temperature-related destabilization following climate change, J. Geophys. Res., 112, F02S18, doi:10.1029/2006JF000547, 2007.

Gruber, S. and Hoelzle, M.: Statistical modelling of mountain permafrost distribution: local calibration and incorporation of remotely sensed data, Permafrost Periglacial Processes, 12, 69–77, doi:10.1002/ppp.374, 2001.

Gruber, S., Peter, M., Hoelzle, M., Woodhatch, I., and Haeberli, W.: Surface temperatures in steep Alpine rock faces – a strategy for regional-scale measurement and modelling, in: Proceedings of the 8th International Conference on Permafrost. Zurich, Switzer-

land, 21–25 July, vol. 1, pp. 325–330, 2003.

Gruber, S., Hoelzle, M., and Haeberli, W.: Rock-wall temperatures in the Alps: modelling their topographic distribution and regional differences, Permafrost and Periglacial Processes, 15, 299–307, doi:10.1002/ppp.501, 2004.

Haeberli, W.: Die Basis-Temperatur der winterlichen Schneedecke als möglicher Indikator für die Verbreitung von Permafrost in den Alpen, Zeitschrift für Gletscherkunde und Glazialgeologie, IX/1/2, 221–227, 1973.

Haeberli, W.: Untersuchungen zur Verbreitung von Permafrost zwischen Flüelapass und Piz Grialetsch (Graubünden), Mitteilungen der Versuchsanstalt für Wasserbau, Hydrologie und Glaziologie der ETH Zürich, Zurich, Switzerland, 17, 221 pp, 1975.

Haeberli, W.: Creep of mountain permafrost: internal structure and flow of alpine rock glaciers, Mitteilungen der VAW/ETH Züric, 77, 1985.

Hand, D. J.: Construction and assessment of classification rules, Wiley Series in Probability and Statistics, John Wiley & Sons, Chichester, 1997.

Harris, S. and Pedersen, D.: Thermal regimes beneath coarse blocky materials, Permafrost and Periglacial Processes, 9, 107–120, doi:10.1002/(SICI)1099-1530(199804/06)9:2<107::AID-PPP277>3.0.CO;2-G, 1998.

Harris, C., Arenson, L. U., Christiansen, H. H., Etzelmüller, B., Frauenfelder, R., Gruber, S., Haeberli, W., Hauck, C., Hölzle, M., Humlum, O., Isaksen, K., Kääb, A., Kern-Lütschg, M. A., Lehning, M., Matsuoka, N., Murton, J. B., Nötzli, J., Phillips, M., Ross, N., Seppälä, M., Springman, S. M., and Mühll, D. V.: Permafrost and climate in Europe: Monitoring and modelling thermal, geomorphological and geotechnical responses, Earth-Science Rev., 92, 117–171, doi:10.1016/j.earscirev.2008.12.002, 2009.

Hasler, A., Gruber, S., and Haeberli, W.: Temperature variability and offset in steep alpine rock and ice faces, The Cryosphere, 5, 977–988, doi:10.5194/tc-5-977-2011, 2011.

Hastie, T. and Tibshirani, R.: Generalized additive models, Chapman & Hall/CRC, 1990.

Hayakawa, Y., Oguchi, T., and Lin, Z.: Comparison of new and existing global digital elevation models: ASTER G-DEM and SRTM-3, Geophys. Res. Lett., 35, L17404, doi:10.1029/2008GL035036, 2008.

Heggem, E., Juliussen, H., and Etzelmüller, B.: Mountain permafrost in central-eastern Norway, Norsk Geografisk Tidsskrift-Norwegian Journal of Geography, 59, 94–108, doi:10.1080/00291950510038377, 2005.

Hiebl, J., Auer, I., Böhm, R., Schöner, W., Maugeri, M., Lentini, G., Spinoni, J., Brunetti, M., Nanni, T., Perčec Tadić, M., Bihari, Z., Dolinar, M., and Müller-Westermeier, G.: A high-resolution 1961–1990 monthly temperature climatology for the greater Alpine region, Meteorologische Zeitschrift, 18, 507–530, doi:10.1127/0941-2948/2009/0403, 2009.

Hoelzle, M.: Permafrost occurrence from BTS measurements and climatic parameters in the Eastern Swiss Alps, Permafrost and Periglacial Processes, 3, 143–147, doi:10.1002/ppp.3430030212, 1992.

Hoelzle, M.: Rock glaciers, Upper Engadin, Switzerland. Boulder, CO: National Snow and Ice Data Center/World Data Center for Glaciology. Digital Media, 1998.

Hoelzle, M. and Gruber, S.: Borehole and ground surface temperatures and their relationship to meteorological conditions in the Swiss Alps, in: Proceedings of the 9th International Conference on Permafrost. Fairbanks, Alaska, 30 June–3 July, pp. 723–728, 2008.

Hoelzle, M., Mittaz, C., Etzelmüller, B., and Haeberli, W.: Surface energy fluxes and distribution models of permafrost in European mountain areas: an overview of current developments, Permafrost and Periglacial Processes, 12, 53–68, doi:10.1002/ppp.385, 2001.

Hoelzle, M., Haeberli, W., and Stocker-Mittaz, C.: Miniature ground temperature data logger measurements 2000–2002 in the Murtèl-Corvatsch area, Eastern Swiss Alps, in: Proceedings of the 8th International Conference on Permafrost. Zurich, Switzerland, 21–25 July, pp. 419–424, 2003.

Hosmer, D. and Lemeshow, S.: Applied logistic regression, Wiley-Interscience, New York, 2000.

Hughes, P. D., Gibbard, P. L., and Woodward, J. C.: Relict rock glaciers as indicators of Mediterranean palaeoclimate during the Last Glacial Maximum (Late Würmian) in northwest Greece, J. Quaternary Science, 18, 431–440, doi:10.1002/jqs.764, 2003.

Hurlbert, S.: Pseudoreplication and the design of ecological field experiments, Ecological monographs, 54, 187–211, 1984.

Ikeda, A. and Matsuoka, N.: Degradation of talus-derived rock glaciers in the Upper Engadin, Swiss Alps, Permafrost and Periglacial Processes, 13, 145–161, doi:10.1002/ppp.413, 2002.

Imhof, M.: Modelling and verification of the permafrost distribution in the Bernese Alps, Switzerland, Permafrost and Periglacial Processes, 17, 267–280, doi:10.1002/(SICI)1099-1530(199609)7:3<267::AID-PPP221>3.0.CO;2-L, 1996.

Imhof, M.: Rock glaciers, Bernese Alps, western Switzerland, Boulder CO: National Snow and Ice Data Center/World Data Center for Glaciology. Digital Media, 1998.

Janke, J. R.: The occurrence of alpine permafrost in the Front Range of Colorado, Geomorphology, 67, 375–389, doi:10.1016/j.geomorph.2004.11.005, 2004.

Keller, F.: Automated mapping of mountain permafrost using the program PERMAKART within the geographical information system ARC/INFO, Permafrost and Periglacial Processes, 3, 133–138, doi:10.1002/ppp.3430030210, 1992.

Keller, F., Frauenfelder, R., Hoelzle, M., Kneisel, C., Lugon, R., Phillips, M., Reynard, E., and Wenker, L.: Permafrost map of Switzerland, in: Proceedings of the 7th International Conference on Permafrost. Nordicana, Yellowknife, Canada, 23–27 June, pp. 557–562, 1998.

King, L.: Zonation and ecology of high mountain permafrost in Scandinavia, Geografiska Annaler. Series A. Physical Geography, 68, 131–139, 1986.

Lambiel, C. and Reynard, E.: Regional modelling of present, past and future potential distribution of discontinuous permafrost based on a rock glacier inventory in the Bagnes–Heé reé mence area (Western Swiss Alps), Norsk Geografisk Tidsskrift-Norwegian Journal of Geography, 55, 219–223, 2001.

Lewkowicz, A. and Bonnaventure, P.: Interchangeability of mountain permafrost probability models, northwest Canada, Permafrost and Periglacial Processes, 19, 49–62, doi:10.1002/ppp.612, 2008.

Lewkowicz, A. G. and Ednie, M.: Probability mapping of mountain permafrost using the BTS method, Wolf Creek, Yukon Ter-

ritory, Canada, Permafrost and Periglac. Process, 15, 67–80, doi:10.1002/ppp.480, 2004.

Lilleoren, K. and Etzelmüller, B.: A regianl inventory of rock glaciers and ice-cored morains in Norway, Geografiska Annaler: Series A, Physical Geography, 93, 175–191, doi:10.1111/j.1468-0459.2011.00430.x, 2011.

MeteoSchweiz: Standardnormwerte 1961–1990: Lufttemperatur 2m, Schweiz, http://www.meteoschweiz.admin.ch/web/de/klima/klima_schweiz/tabellen.Par.0004.DownloadFile.ext.tmp/temperaturmittel.pdf, 2010.

Noetzli, J., Hilbich, C., Hoelzle, M., Hauck, C., Gruber, S., and Krauer, M.: Comparison of transient 2D temperature fields with time-lapse electrical resistivity data at the Schilthorn Crest, Switzerland, in: Proceedings of the 9th International Conference on Permafrost. Fairbanks, Alaska, 30 June–3 July, pp. 1293–1298, 2008.

Nyenhuis, M., Hoelzle, M., and Dikau, R.: Rock glacier mapping and permafrost distribution modelling in the Turtmanntal, Valais, Switzerland, Zeitschrift für Geomorphologie, 49, 275–292, 2005.

Paul, F., Barry, R., Cogley, J., Frey, H., Haeberli, W., Ohmura, A., Ommanney, C., Raup, B., Rivera, A., and Zemp, M.: Recommendations for the compilation of glacier inventory data from digital sources, Ann. Glaciol., 50, 119–126, doi:10.3189/172756410790595778, 2009.

PERMOS: Permafrost in Switzerland 2006/2007 and 2007/2008, edited by: Noetzli, J. and Vonder Muehll, D., Glaciological Report (Permafrost) No. 8/9 of the Cryospheric Commission of the Swiss Academy of Sciences, Zurich, Switzerland, p. 68 pp., 2010.

Pogliotti, P.: Analisi morfostrutturale e caratterizzazione termica di ammassi rocciosi recentemente deglaciati, Master's thesis, Earth Science Department, University of Turin, Italy, 2006.

Pogliotti, P., Cremonese, E., di Cella, U. M., Gruber, S., and Giardino, M.: Thermal diffusivity variability in alpine permafrost rock walls, in: Proceedings of the 9th International Conference on Permafrost. Fairbanks, Alaska, 30 June–3 July, vol. 2, pp. 1427–1432, 2008.

Reynard, E. and Morand, S.: Rock glacier inventory, Printse Valley, Valais, Switzerland, Boulder CO: National Snow and Ice Data Center/World Data Center for Glaciology. Digital Media, 1998.

Riedlinger, T. and Kneisel, C.: Interaktionen von Permafrost und Ausaperung im Gletschervorfeld des Vadret da Rosatsch, Oberengadin, Schweiz., Trierer Geographische Studien, 23, 147–164, 2000.

Riseborough, D., Shiklomanov, N., Etzelmüller, B., Gruber, S., and Marchenko, S.: Recent advances in permafrost modeling, Permafrost and Periglacial Processes, 19, 137–156,, 2008.

Roer, I. and Nyenhuis, M.: Rockglacier activity studies on a regional scale: comparison of geomorphological mapping and photogrammetric monitoring, Earth Surface Processes and Landforms, 32, 1747–1758, doi:10.1002/esp.1496, 2007.

Schoeneich, P., Lambiel, C., and Wenker, L.: Rock glaciers, Prealps, Vaud, Switzerland, Boulder CO: National Snow and Ice Data Center/World Data Center for Glaciology. Digital Media, 1998.

Stocker-Mittaz, C., Hoelzle, M., and Haeberli, W.: Modelling alpine permafrost distribution based on energy-balance data: a first step, Permafrost Periglacial Processes, 13, 271–282, doi:10.1002/ppp.426, 2002.

USGS, METI, and NASA: ASTER Global DEM Validation, Summary Report, p. 28 pp., http://www.ersdac.or.jp/GDEM/E/image/ASTERGDEM_ValidationSummaryReport_Ver1.pdf, last access March 2011, 2009.

van Everdingen, R. O.: Multi-Language Glossary of Permafrost and Related Ground-Ice Terms, 25 International Permafrost Association, University of Calgary, 1998.

Venables, W. and Ripley, B.: Modern applied statistics with S, Springer Verlag, New York, 2002.

Wilson, J. and Gallant, J.: Terrain analysis: principles and applications, John Wiley & Sons, New York, 2000.

Paper III

Permafrost distribution in the European Alps: calculation and evaluation of an index map and summary statistics

Boeckli, L., Brenning, A., Gruber, S., and Noetzli, J. (2012b). Permafrost distribution in the European Alps: calculation and evaluation of an index map and summary statistics. *The Cryosphere*, 6 (4): 807–820. doi: 10.5194/tc-6-807-2012

The author's contributions to this article:

- Substantially contributed to the development of the methodology.
- Designed and performed all data processing and analysis.
- Main author of all sections in the article.

The Cryosphere, 6, 807–820, 2012
www.the-cryosphere.net/6/807/2012/
doi:10.5194/tc-6-807-2012

The Cryosphere

Permafrost distribution in the European Alps: calculation and evaluation of an index map and summary statistics

L. Boeckli[1], **A. Brenning**[2], **S. Gruber**[1], **and J. Noetzli**[1]

[1]Department of Geography, University of Zurich, Switzerland
[2]Department of Geography and Environmental Management, University of Waterloo, Ontario, Canada

Correspondence to: L. Boeckli (lorenz.boeckli@geo.uzh.ch)

Received: 7 February 2012 – Published in The Cryosphere Discuss.: 6 March 2012
Revised: 22 June 2012 – Accepted: 3 July 2012 – Published: 27 July 2012

Abstract. The objective of this study is the production of an Alpine Permafrost Index Map (APIM) covering the entire European Alps. A unified statistical model that is based on Alpine-wide permafrost observations is used for debris and bedrock surfaces across the entire Alps. The explanatory variables of the model are mean annual air temperatures, potential incoming solar radiation and precipitation. Offset terms were applied to make model predictions for topographic and geomorphic conditions that differ from the terrain features used for model fitting. These offsets are based on literature review and involve some degree of subjective choice during model building. The assessment of the APIM is challenging because limited independent test data are available for comparison and these observations represent point information in a spatially highly variable topography. The APIM provides an index that describes the spatial distribution of permafrost and comes together with an interpretation key that helps to assess map uncertainties and to relate map contents to their actual expression in the terrain. The map can be used as a first resource to estimate permafrost conditions at any given location in the European Alps in a variety of contexts such as research and spatial planning.

Results show that Switzerland likely is the country with the largest permafrost area in the Alps, followed by Italy, Austria, France and Germany. Slovenia and Liechtenstein may have marginal permafrost areas. In all countries the permafrost area is expected to be larger than the glacier-covered area.

1 Introduction

Permafrost in the European Alps is of practical and scientific interest, and the regional estimation of its distribution is described in numerous studies (e.g. Hoelzle, 1994; Imhof, 1996; Frauenfelder, 1998; Keller et al., 1998; Gruber and Hoelzle, 2001; Lambiel and Reynard, 2001; BAFU, 2005; Bodin, 2007; Ebohon and Schrott, 2008). Modelling strategies are not limited to the European Alps but have been developed for and applied to different mountain regions (e.g. Serrano et al., 2001; Tanarro et al., 2001; Janke, 2004; Lewkowicz and Ednie, 2004; Heggem et al., 2005; Etzelmüller et al., 2007; Lewkowicz and Bonnaventure, 2008; Li et al., 2009; Bonnaventure et al., 2012). Regional permafrost distribution models are typically based on empirical-statistical relationships and give indications of permafrost distribution, with limited accuracy demands (Harris et al., 2009). PERMAKART (Keller, 1992) and PERMAMAP (Hoelzle, 1992; Hoelzle et al., 1993) were the first modelling approaches in the Alps that related topographic and climatic variables to the existence of permafrost and that provided map-based products to visualize permafrost distribution. Both models have been applied to various regions, and the basic relationships have been used/adapted for the development of further models (Imhof, 1996; BAFU, 2005; Ebohon and Schrott, 2008). As output, both models provide gridded data spatially predicting permafrost occurrence by using discrete classification schemes.

The existing work for the European Alps cannot easily be compiled into an Alpine-wide permafrost map, because the relevant studies (a) usually are regionally calibrated, (b) rely on differing methods, and (c) exclude large parts of the Alps.

Published by Copernicus Publications on behalf of the European Geosciences Union.

The present study is aimed to overcome these limitations and to provide one coherent Alpine Permafrost Index Map (APIM).

Based on a systematic collection of permafrost evidence (Cremonese et al., 2011), an Alpine-wide Permafrost MODel (APMOD) has been developed recently (Boeckli et al., 2012). Compared to previous studies, APMOD has a unique data basis that is distributed over the entire Alps. However, the difficult challenge that all permafrost distribution models have to deal with is that permafrost as a subsurface phenomenon cannot easily be detected at the terrain surface, and direct evidence for its presence or absence is generally rare. Therefore, model development is strongly limited by the type of calibration data available. As a consequence, the derivation of a map-based product from statistical models requires the inference of permafrost conditions in morphological settings other than those used for calibration. This task involves some degree of subjective choice during model application, which often is not declared or described in detail in previous work. This paper complements the study of Boeckli et al. (2012) by describing the required steps towards and the first results of an application of the APMOD.

Building upon the formulation of an Alpine-wide permafrost distribution model by Boeckli et al. (2012), the aims of this paper are

- to create a permafrost map (APIM) displaying index values based on model-derived probabilities of permafrost presence;
- to evaluate the APIM using independent data and discuss the general challenges inherent in this evaluation;
- to develop a legend and interpretation key that allow the efficient use of the APIM as well as the communication of its most important uncertainties; and
- to provide summary statistics regarding permafrost distribution in the Alps.

2 A permafrost index based on a probability model

The statistical model that is applied in this study, APMOD, is described in detail by Boeckli et al. (2012). APMOD is based on an Alpine-wide evidence collection (Cremonese et al., 2011) and uses mean annual air temperatures (MAAT), potential incoming solar radiation (PISR) and the mean annual sum of precipitation (PRECIP) as explanatory variables. APMOD involves two sub-models for two different land cover classes: The debris model has been calibrated using rock glacier inventories and predicts the probability of rock glaciers being intact as opposed to relict. The rock model is based on mean annual rock surface temperatures (MARST) and predicts the probability of finding MARST $\leq 0\,^{\circ}\mathrm{C}$ in steep bedrock. Both models are combined based on fuzzy membership (linear function depending on slope angle, Sect. 3.1) to the land cover types rock and debris, and allow the inclusion of temperature offset terms. These offset terms are required to generalize APMOD to other surface characteristics than those used for model calibration. When applied to digital elevation models (DEMs) of differing resolution, scaling functions improve the coherence and comparability of the results.

The probabilities of permafrost occurrence derived from APMOD are translated into permafrost index values, because the term "probability" is misleading and does not communicate the uncertainties and assumptions that are integrated in the final map-based product: The calibration of APMOD was not possible for many surface types, because permafrost observations are not available in sufficient quality and quantity. To derive a map-based product, we need to infer conditions where we have no data and the uncertainty of such predictions is difficult to assess. The term permafrost index thus avoids the notion of probability as we introduce some estimated additional factors (temperature offsets) and cannot evaluate true probability or extent. We suggest that the index represents an indicator of the probability for permafrost occurrence, the spatial percentage of permafrost per cell and/or the thickness of the permafrost body for current climatic conditions. The index can also be interpreted as a proxy of the mean annual ground temperature. However, permafrost extent, thickness or temperature cannot be allocated directly with the values of the index, because various local and regional processes are neglected or only approximated by the model.

3 Data and methods

The topographic and climatic variables that are required to apply APMOD are calculated according to Boeckli et al. (2012). In the following, data and methods are combined to derive an Alpine-wide surface cover that is considered in APIM (Sect. 3.1), and to prepare evaluation data for APIM (Sect. 3.2). Section 3.3 describes the method to derive Alpine-wide summary statistics.

The software R (version 2.14.1; R Development Core Team, 2010) was used for all statistical analyses. Terrain and geodata analyses were conducted with SAGA GIS (Olaya, 2004), "RSAGA" (Brenning, 2008) and "raster" (Hijmans and van Etten, 2012) packages for R.

3.1 Surface types

A land cover map defining the two surface types (debris cover and steep bedrock) for the application of the two sub-models is required for APMOD. A transition zone with varying degree of membership for the two surface types is used where APMOD is applied using a combination of the two sub-models (debris and rock model). In this paper, additional surface types are introduced as a spatial basis for addressing

the offsets and assumptions described in Sect. 4. The following land surface types are differentiated and described below: debris cover, steep bedrock, vegetation and glacier coverage.

3.1.1 Steep bedrock and debris cover

The distinction between these two model domains is based on slope angle alone: We define an index m_r by

$$m_r' = \frac{S - S_{\min}}{S_{\max} - S_{\min}}, \quad (1)$$

$$m_r = \begin{cases} 0 & \text{if } m_r' \leq 0 \\ 1 & \text{if } m_r' \geq 1 \\ m_r' & \text{otherwise,} \end{cases}$$

which describes the degree of membership in the steep bedrock surface class, where S is the slope angle of the grid cell, $S_{\min}$ is a fixed threshold angle up to which only debris cover occurs, and $S_{\max}$ is the assumed maximum slope angle up to which the surface may be debris-covered. To be consistent and applying the rock model to the same surface-cover domain as it was calibrated for, we use the same definition of steep bedrock as in Boeckli et al. (2012): "Steep bedrock" is defined as terrain that (a) is not or only marginally affected by a snow cover in wintertime, (b) does not contain large amounts of blocks and/or debris, and (c) is without vegetation coverage. Based on a literature review, Pogliotti (2010) summarizes that slope angles of 35–37° represent the upper limit of usually well snow-covered areas ($S_{\min}$) and slope angles of 55–60° define the upper limit of snow accumulation ($S_{\max}$). Analysing the distribution of slope angle values within training areas representing debris respectively, bedrock cover (Fig. 1) indicates similar values for the two thresholds based on the data used here. The training areas were derived from the land cover map of Switzerland (Vector25, swisstopo, 2007) using randomly distributed points ($N = 4029$ for rock and $N = 4381$ for debris cover). Here, the distribution of slope angle values is biased because bedrock is also possible in flat terrain (e.g. glacier forefields), and the points that are used for this analysis are sparse for very steep slopes.

Finally, $S_{\min}$ was set to 35°, which coincides with the start of a strong increase in the presence of exposed bedrock (Fig. 1) and $S_{\max}$ was set to 55°. Slopes with greater slope angles in the DEM rarely present debris surfaces (Fig. 1), and these can likely be attributed to errors in the DEM. To address point (c) above, we assume a debris cover ($m_r = 0$) if the surface is covered by vegetation (see below).

3.1.2 Vegetation

The discrimination of vegetation from vegetation-free surfaced areas is based on the soil-adjusted vegetation index (SAVI; Huete, 1988) and is derived from Landsat Thematic Mapper (Landsat 5) and Landsat Enhanced Thematic Mapper (Landsat 7) images using red and near-infrared (NIR) wavelengths. SAVI accounts for the soil-induced influences on vegetation index values and involves an additional constant L to the formula of the normalized difference vegetation index (NDVI):

$$\text{SAVI} = \frac{\text{NIR} - \text{red}}{\text{NIR} + \text{red} + L}(1 + L). \quad (2)$$

L was set to 1, since this value is suitable for characterizing low vegetation densities (Huete, 1988) present in mountainous vegetation. Thirteen scenes cover the entire Alpine region. Only images taken in August/September/October were used, since vegetation is still well-developed as evidenced by remotely sensed phenology (cf. Fontana et al., 2008) and snow cover is likely near its annual minimum. For each of the 13 scene locations, the scene with lowest cloud cover was chosen (Table 1). After calculating the SAVI values, all 13 grids were merged (by using the maximum SAVI value in areas of overlap) and resampled with bilinear interpolation to the resolution of ASTER GDEM.

A threshold for discriminating vegetation from vegetation-free surfaced areas was chosen by analysing SAVI values in training areas derived from Vector25. The training data consist of randomly distributed points: 42 797 for vegetation and 8419 for vegetation-free areas. The Vector25 land cover classes rock and debris were treated as vegetation-free areas, while forest, open forest, bush land and remaining areas were classified as vegetation. Finally, optimizing the κ coefficient (Cohen, 1960) as a function of the SAVI threshold, pixels with SAVI < 0.335 are considered free of vegetation,

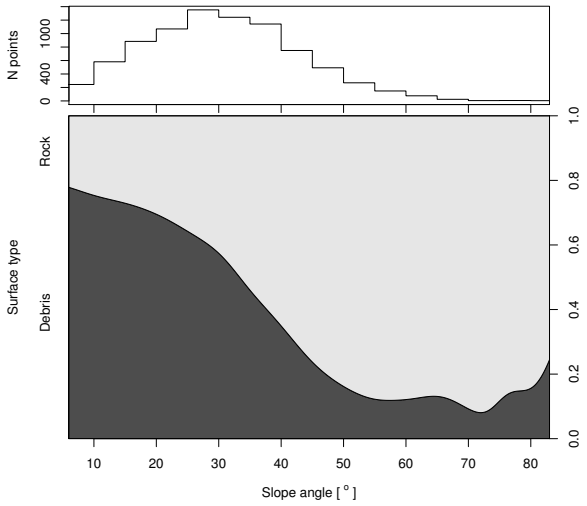

Fig. 1. Conditional density plot for the two surface classes debris and rock (derived from Vector25) in relation to slope angle. Above, the number of points that are used for this analysis are shown in relation to slope angle.

Table 1. Landsat scenes used to calculate the SAVI.

Path	Row	Date (d/m/y)	Sensor
191	27	14/10/2006	Landsat 5
191	28	14/10/2006	Landsat 5
192	27	05/10/2006	Landsat 5
192	28	22/08/2007	Landsat 5
193	27	20/10/2003	Landsat 5
193	28	34/08/2003	Landsat 5
194	27	21/08/2000	Landsat 7
194	28	32/10/2002	Landsat 7
195	27	24/08/2006	Landsat 5
195	28	18/10/2003	Landsat 5
195	29	06/09/2002	Landsat 7
196	28	23/08/2003	Landsat 5
196	29	23/08/2003	Landsat 5

and pixels with SAVI ≥ 0.335 are classified as vegetation. Further, a median filter (3×3 cells) was applied to remove artifacts, and all pixels where $m_r = 1$ (steep bedrock) were considered free of vegetation.

3.1.3 Glaciers

Glacier outlines derived from Landsat images were provided by Paul et al. (2011). The outlines represent glacier extent in the year 2003, manually corrected for debris-covered glacier parts.

3.2 Evaluation of a permafrost index map

The evaluation data are based on rock glaciers and point observations of permafrost presence and absence. Status information (intact vs. relict) of rock glaciers can be used to evaluate the output of APMOD in areas covered by rock glaciers. As a result of matched sampling, Boeckli et al. (2012) excluded 394 intact and 2403 relict rock glaciers from model fitting. They are available for model evaluation in the debris cover domain (Fig. 2). Further 352 observation points are available within the permafrost evidence collection (Fig. 2; Cremonese et al., 2011) that were not used for model calibration. These observations are based on different methods and were classified as permafrost presence or absence by each individual data contributor. This classification was also rated by the data contributor with an index that describes the certainty of this classification (PF_{cert}). The point observations allow to evaluate the map for other types of surfaces.

An additional measure describing the agreement of the terrain attributes (PF_{loc}) was calculated for each observation point. This is necessary because some observation points are not suitable for model evaluation and needed to be excluded beforehand, which will be discussed in Sect. 6.2. However, the weighting scheme applied to derive PF_{loc} is based on subjective thresholds.

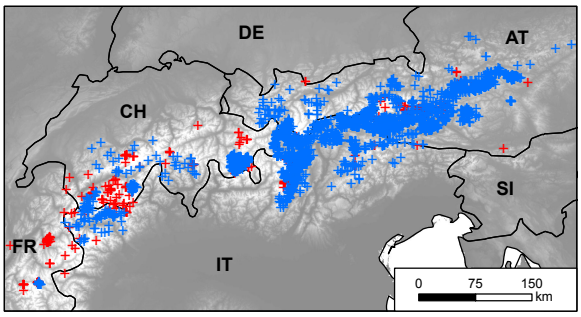

Fig. 2. Spatial distribution of permafrost evidence data (Cremonese et al., 2011), which were not used for model calibration in Boeckli et al. (2012) and are thus available for evaluation. Blue dots represent rock glaciers, and red crosses represent evidence points (summarized in Table 3).

Table 2. Thresholds and corresponding weights per variable that were used to characterize the agreement of the terrain attributes (PF_{loc}) for the evaluation data. The weight for the variable aspect for slope angles $\leq 15°$ (derived from ASTER GDEM) was fixed to 2, because uncertainties in this variable are large for flat terrain.

Weights	Elevation (m)	Slope angle (°)	Aspect (°)*
2	< 100	< 10	< 25
1	100–250	10–25	25–50
0	> 250	> 25	> 50

* Only applied to observations with a slope angle $> 15°$.

The terrain variable elevation, slope angle and aspect were derived from the digital elevation model ASTER GDEM (Hayakawa et al., 2008) for all 352 observation points and then compared to the values that were manually entered by the data provider into the permafrost evidence database. It is not possible to automatically differentiate errors in the evidence metadata from the effects of sub-grid variability with this method. It is, however, useful to have this index of topographical agreement for the interpretations of differences in the comparison and for further investigating possible errors in the evidence data. Differences in aspect values (Δ_A) were calculated using the absolute difference between aspect angles modulo 360° in the interval $(-180°, 180°)$. Absolute differences in elevation, slope and aspect angle (Fig. 3) were used to manually define thresholds and to weight these differences (Table 2). The weight of the variable aspect was disregarded for slope angles $\leq 15°$, because uncertainties in this variable are large for flat terrain. Multiplying the assigned weights for the three measures elevation, slope angle and aspect for each observation results in values ranging from 0 to 8, where a value ≥ 4 is classified as "agree", a value of 1–2 "disagree" and a value of 0 "strongly disagree" (Table 3). The multiplication of the three weights implies that an

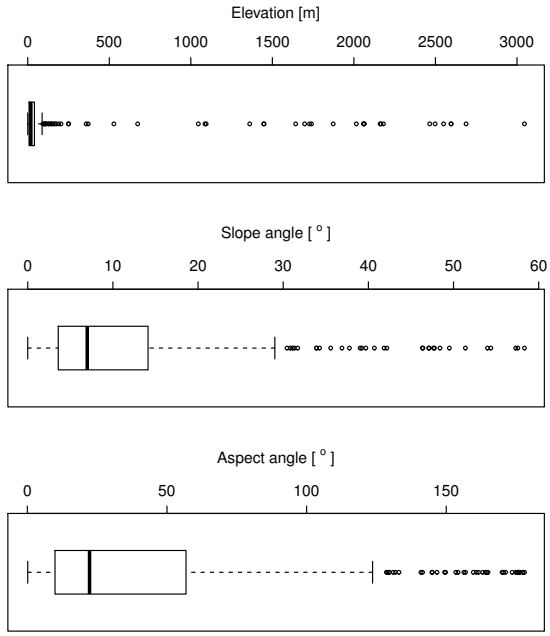

Fig. 3. Absolute difference between terrain variables calculated based on ASTER GDEM and the ones provided by the data contributor into the permafrost evidence collection (Cremonese et al., 2011).

observation with one of the three measures = 0 is classified as "strongly disagree", whatever the other two measures are.

Permafrost point-observations with PF_{cert} equals "quite likely" and PF_{loc} equals "strongly disagree" are not considered for model evaluation, and the following evidence types from Table 3 were also excluded from evaluation: (a) ground surface temperatures were not considered because of the large inter-annual variability caused by the influence of the snow cover (Hoelzle et al., 2003; Brenning et al., 2005); (b) rock fall scars were excluded because only 4 observations remained after removing observations with PF_{loc} equals "strongly disagree"; (c) surface movements were not considered because only four observations are available; and (d) other indirect evidence was excluded because no additional information regarding measurement or observation type is available.

To assess the discrimination of the permafrost index, the area under the receiver-operating characteristics curve (AUROC, Mason and Graham, 2002) was measured. This measure ranges from 0.5 (random discrimination) and 1 (perfect discrimination).

3.3 Calculation of summary statistics

The term "permafrost index area" will be used to present the result and refers to the area having an index equal to or higher than a specified threshold. Glaciers are excluded from the permafrost index areas. It is important to note the difference to permafrost area that would be defined as the surface actually underlain by permafrost (cf. Zhang et al., 2000; Gruber, 2012). The index area is the unit of interest for decision-making ("Where do I need to consider permafrost?") and the actual result of the model presented. Permafrost area may be important, e.g. for estimating water storage in subsurface ice, but is more difficult to support by reliable data.

Pixel area of the unprojected ASTER GDEM grid depends on latitude (ϕ) and the mean radius of the Earth ($R = 6371\,\mathrm{km}$). North–south (Δy) and west–east (Δx) for the $1''$ spherical grid were used to calculate the area:

$$\Delta y = \frac{\pi R}{648\,000} \text{ and } \Delta x = \cos(\phi)\Delta y \tag{3}$$

4 Estimation of offset terms

The MARST used for model calibration were measured in homogenous rock following the procedure outlined in Gruber et al. (2003). This provides a quantification of the influence of topography on rock temperatures, but likely temperatures at greater depth in most rock faces are lower due to effects of snow, debris and fracturing (Gruber and Haeberli, 2007). To address this, a temperature-offset term is included in the rock model that is based on literature: Measurements in the Swiss Alps showed that the spatial variation of temperature offset in rock faces is large and mainly depends on (a) radiation exposure (Hasler et al., 2011), (b) snow depth and its timing (cf. Pogliotti, 2010) and (c) the amount and characteristics of cleft systems at the rock surface (Hasler et al., 2011). Summarizing these three factors, Hasler et al. (2011) postulate that radiation-exposed steep rock faces with interspersed snow patches and/or large fractures are up to 3 °C colder at depth (i.e. in the order of a few meters) compared to MARST in snow-free and compact rock. In north-exposed situations, the effect of snow and/or fractures is less important, because short-wave radiation is less dominant. Based on these findings, the offset term Δ_R was implemented as a linear function of PISR and applied to the rock model:

$$\Delta_R = O_{min} + \mathrm{PISR}\frac{O_{max} - O_{min}}{350\,\mathrm{W\,m^{-2}}}, \tag{4}$$

where O_{min} is the minimal and O_{max} is the maximal offset for pixels where $\mathrm{PISR} = 350\,\mathrm{W\,m^{-2}}$. The percentile of $350\,\mathrm{W\,m^{-2}}$ is 0.88 in the cumulative distribution function of PISR values. O_{min} was set to -0.5 and $O_{max} = -2.5$. Spatial variation of Δ_R is not considered.

The debris model provides an optimistic estimate (biased towards an overestimation) of permafrost occurrence in debris surfaces because of three main rock glacier characteristics: (a) cooling effect of coarse block surface (e.g. Haeberli et al., 2006), (b) rock glacier movement towards lower elevations (e.g. Barsch, 1978), and (c) delayed response of ice-rich

Table 3. Overview of the different observation types (BH: borehole, GST: ground surface temperature, SC: rock fall scar, TR: trench and construction site, SM: surface movement, GP: geophysical investigation, OIE: other indirect evidence) that remain for evaluation. For each type, the number of permafrost-existence (PF_{yes}) and permafrost-absence (PF_{no}) observations is given (Certainty levels PF_{cert}: 1 definite proof, 2 quite certain, 3 quite likely; Agreement levels PF_{loc}: a agree, d disagree, s strongly disagree).

Type	PF_{yes}	PF_{cert} (1/2/3)	PF_{loc} (a/d/s)	PF_{no}	PF_{cert} (1/2/3)	PF_{loc} (a/d/s)
BH	45	36/6/3	22/3/20	16	11/5/0	11/1/4
GST	49	18/25/6	37/3/9	41	3/16/22	34/1/6
SC	36	6/30/0	3/1/32	–	–	–
TR	38	25/12/1	22/0/16	9	3/6/0	6/2/1
SM	4	2/2/0	3/ 0/1	–	–	–
GP	70	29/35/6	61/4/5	11	3/8/0	11/0/0
OIE	33	7/19/7	23/4/6	–	–	–

Table 4. Temperature offsets (°C) that were applied to the different surface types. A positive sign means a positive temperature offset is applied, which results in a more pessimistic permafrost estimate. A negative sign means a more optimistic permafrost estimate.

Surface cover	Δ_R	Δ_{Da}	Δ_{Db}	total offset
Steep bedrock	[−0.5, −2.5]	–	–	[−0.5, −2.5]
Debris cover	–	0.5	–	0.5
Vegetation	–	0.5	2	2.5

permafrost to climatic forcing (e.g. Frauenfelder et al., 2008). Consequently, it is desirable to find relationships to infer conditions below surfaces other than rock glaciers. The first two sources of bias are considered in this study, while the third remains unaccounted for due to a lack of information that would allow its estimation.

By moving down-slope, a rock glacier transports a cold and ice-rich mass from its rooting zone to conditions that may be less favourable for the formation of permafrost. The melting of ice as a result of an increase in active layer thickness can thus exert a cooling influence at depth and preserve permafrost where it would not form without the advection of ice-rich material. We approximate the magnitude of this effect by the altitudinal extent of rock glaciers, i.e. the difference in elevation between the lowest and highest point of each rock glacier, assuming that in the Alps only the rooting zone of a rock glacier shows conditions for the development of ice-rich permafrost. For the 5541 rock glaciers in the inventory of Cremonese et al. (2011), the mean altitudinal extent is 139 m. In APMOD, a random point within each rock glacier is taken for model calibration (Boeckli et al., 2012), which, on average, corresponds to the centroid of the rock glacier. Accordingly, the altitudinal extent is divided by two resulting in a bias correction of 70 m, which corresponds to an approximate difference in MAAT of 0.5 °C (assumed surface temperature lapse rate 0.0065 °C m^{-1}, cf. International Organization for Standardization, 1975). This value is chosen for the movement-related offset (Δ_{Da}) and applied to the debris model.

A surface cover of coarse blocks with no or little infill by fine material usually results in markedly colder MAGT than, for example, fine moraine-derived soil or solid bedrock. This effect has been measured and discussed by several researchers (e.g. Humlum, 1997; Harris and Pedersen, 1998; Gorbunov et al., 2004; Hanson and Hoelzle, 2005; Gruber and Hoelzle, 2008; Gubler et al., 2011). Ground temperatures of coarse blocks in comparison to finer grained material may be 1.3–2 °C (Juliussen and Humlum, 2008) to 4–7 °C (Harris and Pedersen, 1998) colder. 1.6 °C to 2.2 °C reduction of MAGT with respect to finer grained material was observed during one year at Corvatsch (Switzerland) for a large data set containing 390 temperature sensors distributed in 39 footprints (Gubler et al., 2011). Accordingly, an offset of 2 °C (Δ_{Db}) is implemented in the debris model to address the effect of coarse blocks.

While Δ_{Da} is applied to the whole domain of the debris model, Δ_{Db} is applied to vegetated areas only, because these areas are normally characterized by fine-grained debris and can be detected by remote sensing for the entire Alps. Several studies indicate that, in the European Alps, a closed vegetation cover usually indicates the absence of permafrost (Haeberli, 1975; Hoelzle et al., 1993). This relationship is not necessarily true in all situations (e.g. Delaloye et al., 2003), but provides a valuable indication. In the context of APIM, we regard a closed vegetation cover to be indicative of fine material and thus the absence of open-work block cover. Therefore, the above-mentioned offset (Δ_{Db}) addressing coarse blocks is applied to account for thermal differences between non-vegetated and vegetated areas.

5 Results

5.1 Interpretation key for the permafrost index

A sample map of APIM is shown for the entire Alps (Fig. 4) and the Rimpfischhorn in Switzerland (Fig. 5). The map

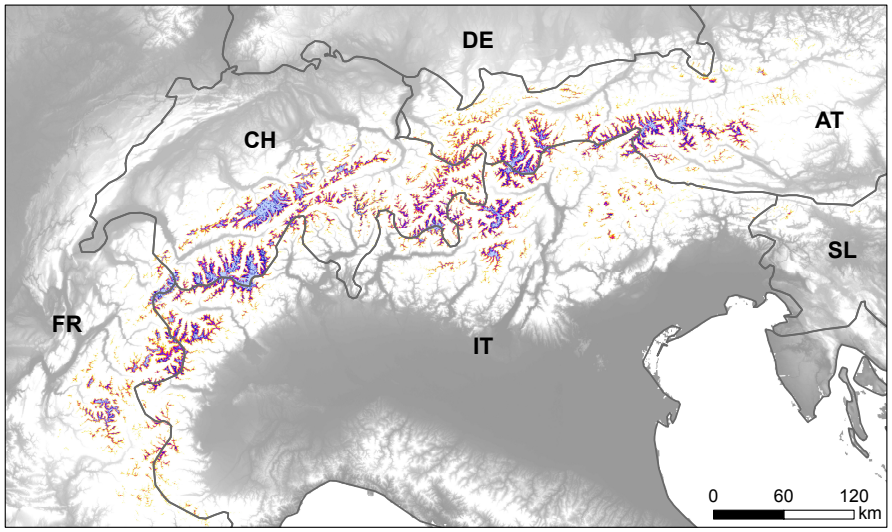

Fig. 4. Alpine Permafrost Index Map (APIM) shown for the European Alps (AT: Austria, CH: Switzerland, DE: Germany, FR: France, IT: Italy, SL: Slovenia). The map should be interpreted together with the legend and interpretation key (Fig. 10).

should be used with the provided legend and interpretation key (Fig. 10). An additional map showing the surface types (Fig. 6) is necessary in order to understand the statistical model parameters and to interpret the shown index value more accurately.

The aim of the interpretation key provided with the permafrost index map is to allow efficient use and understanding of the map and to communicate the most important uncertainties for practical use, e.g. by public authorities or for infrastructure planning and maintenance. It consists of three parts: (a) the legend itself and an accompanying text, (b) an interpretation key that allows to refine the estimate shown in the map based on additional surface cover observations (e.g. based on air photo interpretation), and (c) a description and a legend explaining the auxiliary surface-cover map provided (Fig. 10). The index varies from "permafrost in nearly all conditions" to "permafrost only in very favourable conditions" and describes semi-quantitatively the occurrence of permafrost. The term "very favourable conditions" refers to a situation (topography and ground characteristics) that locally modifies favourably conditions for permafrost presence. The terms used in the legend communicate to some degree an uncertainty in the map, and they consequently allow for further interpretations.

A different map signature is used for glaciers, which are by definition not permafrost, although cold glaciers can have permafrost conditions at their bed (e.g. Haeberli, 1976; Luthi and Funk, 2001) and the development of permafrost after the disappearance of temperate glaciers is possible (Kneisel et al., 2000).

The accompanying text describes the most important limitations of the map and explains the usage of the interpretation key. Based on the pictures and the text of the interpretation key, the map user should be able to understand and apply this additional information. A "call for feedback" was sent to several permafrost researchers in Europe. Seven replies helped improve the legend and interpretation key.

5.2 Evaluation of the permafrost index map

Comparing the final map index with the distribution of intact and relict rock glaciers shows the model performance in debris-covered areas (Fig. 7). 1863 of the 2403 relict rock glaciers and 42 of the 395 intact rock glaciers show no index value and permafrost is expected to be absent. The majority (68 %) of the remaining 540 relict rock glaciers lies within a permafrost index < 0.4, whereas most (63 %) of the remaining 353 intact rock glaciers are located in areas with an index > 0.5 (mean index equals 0.58). The discrimination of rock glacier status based on predicted permafrost index values results in an AUROC of 0.78 that is an acceptable value according to Hosmer and Lemeshow (2000).

The predicted permafrost index values for borehole temperatures, geophysical investigations and trench or construction sites cover the entire range from 0 to 1 for permafrost-existence observations (Fig. 8) with mean index values of: 0.80 (borehole temperatures), 0.32 (geophysical investigations) and 0.38 (trench or construction sites). The index values of the permafrost-absence observations range from 0 to 0.44, except for one construction site. The discrimination for these tree observations types shows an AUROC $= 0.6$. When neglecting the offset terms discussed in Sect. 4, the

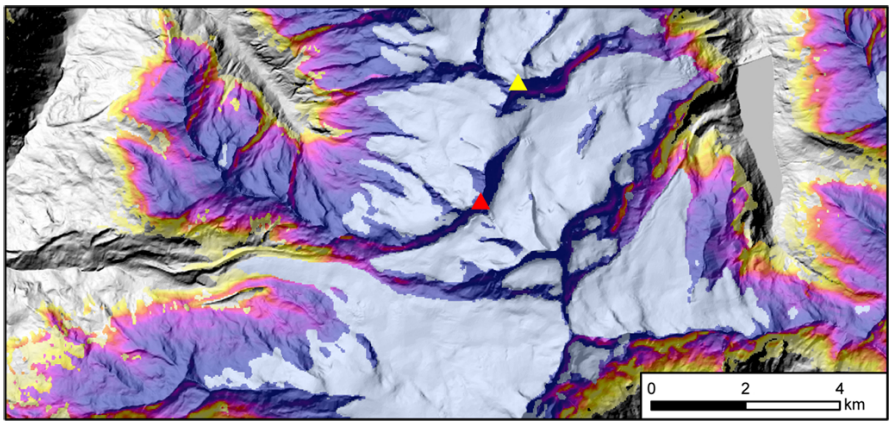

Fig. 5. Alpine Permafrost Index Map (APIM) shown for the area surrounding Rimpfischhorn (4199 m, red triangle) and Allalinhorn (4027 m, yellow triangle) in Switzerland. The map should be interpreted together with the legend and interpretation key (Fig. 10).

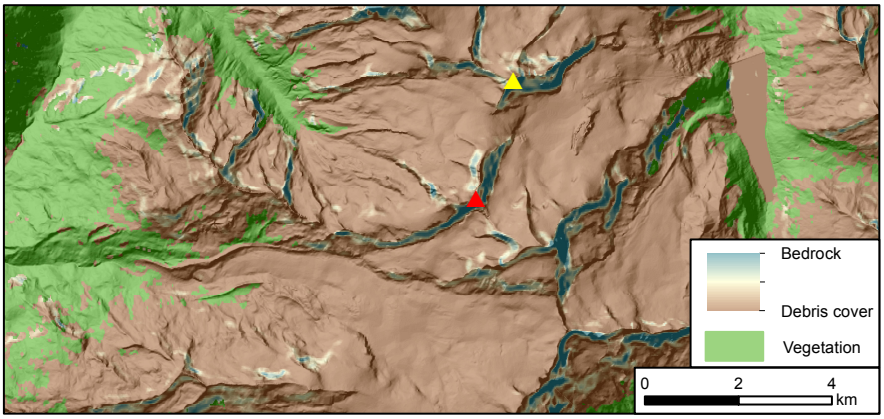

Fig. 6. Surface cover map showing the vegetation mask and the surface class index m_r (Eq. 1) for the same area as Fig. 5. To grid cells with a slope angle $\leq 35°$ the debris model, for slope angles $\geq 55°$ the rock model is used. In between, a fuzzy membership (linear function depending on slope angle) is applied in order to provide a complete spatial coverage of APIM.

AUROC results in 0.56. If the offset term Δ_{Db} is applied based on local terrain and vegetation information provided by Cremonese et al. (2011) instead of vegetation information derived from SAVI, the AUROC results in 0.67.

5.3 Calculation of summary statistics

The area potentially influenced by permafrost in the Alps (43°–49° N, 4°–16° E) ranges from 2000–12 000 km^2 (Table 5), and the meaning of this range will be discussed in Sect. 6. The largest extent of permafrost is between 2600 and 3000 m depending on the index chosen as threshold, whereas the largest area of glaciers is located above 3000 m (Fig. 9). The offset Δ_{Db} that is applied to the debris model for all vegetated pixels plays an important role regarding the final output map or summary statistic. Neglecting Δ_{Db} increases the potential permafrost area in the entire Alps by approximately 20 %, respectively 3147 km^2 (calculated for an index ≥ 0.1, Table 6).

Table 5. Estimated permafrost index areas for the entire Alps. The relative area refers to the total area of the Alps (ca. 200 000 km^2).

Permafrost index	Total area (km^2)	Relative area (%)
≥ 0.1	11 627	6
≥ 0.5	6220	3
≥ 0.9	2007	1
Glaciers	2056	1

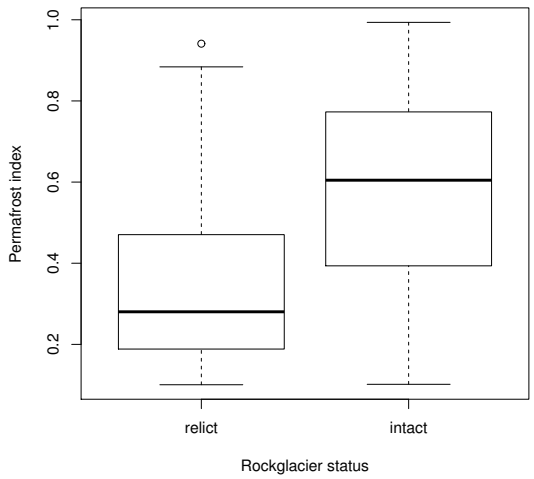

Fig. 7. Permafrost index values for intact and relict rock glaciers that were not used for model calibration. A random point within each rock glacier polygon was used for this figure.

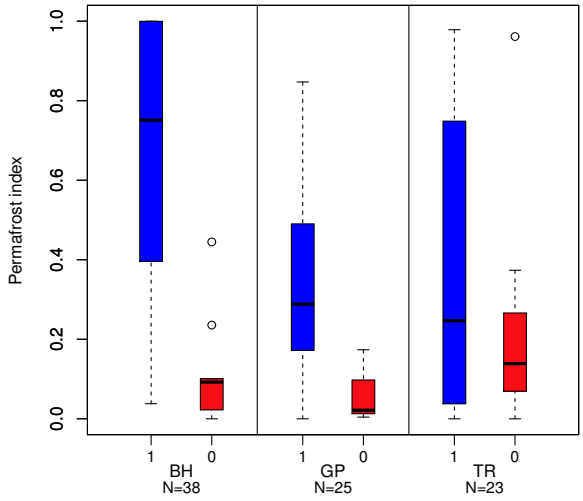

Fig. 8. Box plots showing predicted permafrost index values for the evidence types "Borehole temperatures" (BH), "Geophysical investigations" (GP) and "Trench or construction sites" (TR) for permafrost-existence (1) and permafrost-absence observations (0).

According to this analysis, Switzerland is the country that contains the largest permafrost area (Table 7). In Italy and Austria also large permafrost areas exist.

6 Discussion

APIM is based on a larger calibration data set in comparison with other map-based products. Further, existing permafrost distribution models are calibrated for a specific spatial domain or surface type (e.g. using basal temperature of snow (BTS, Haeberli, 1973) measurements in gentle terrain) but later applied to a whole mountain range. This spatial extrapolation that is required for every spatially distributed permafrost model is done in a transparent manner in this work by introducing temperature offsets (Sect. 4).

Table 6. Estimated permafrost index areas for the Alps calculated without the offset $\Delta_{Db} = 2\,°C$ for vegetated areas. ΔA refers to the difference in area between estimated permafrost distribution calculated with (Table 5) and without offset Δ_{Db}.

Permafrost index	Total area (km^2)	ΔA (km^2)
≥ 0.1	14 774	3147
≥ 0.5	6566	346
≥ 0.9	2011	4

6.1 Interpretation of permafrost index area

The comparison of permafrost index areas obtained in this study with estimates from the literature is complicated by differences in terminology and methods used. Considering index values ≥ 0.5 is one possible assumption to estimate the area affected by permafrost (see Table 7). For Switzerland, the estimated permafrost area then results in 2163 km^2. For comparison, Keller et al. (1998) estimated the permafrost area in Switzerland to range from 4–6 %, which corresponds to approximately 1651–2477 km^2. In Austria, 1600 km^2 were assigned to mountain permafrost by Ebohon and Schrott (2008) and our estimate is 1557 km^2. For France, a value of 1200 km^2 is published (PERMAFRANCE, 2010), whereas our estimate is 703 km^2.

These estimates are consistent but subject to uncertainties and face the problem of differing or missing definitions for "permafrost area" as described in Sect. 3.3.

6.2 Evaluation of APMOD

Existing data (Sect. 3.2) allow to evaluate the map for different surface types, but the following challenges remain: (a) the number of observations is very small compared to the study area, and the observations are strongly biased towards permafrost existence; (b) even less evidence in steep bedrock as well as in intermediate slopes between debris cover and steep bedrock is available; (c) when combing data of different research groups, based on different techniques and coordinate systems, the quality and consistency of the data is a major challenge and errors (e.g. shift in coordinates) cannot be excluded; (d) while the output of APMOD is grid-based with cells having an area of approximately 900 m^2, the observations represent point information within a complex, spatially variable mountain topography. This problem relates

Table 7. Estimated permafrost index areas (km^2) for the Alpine countries using different index values, and comparison to glacier area (CH: Switzerland, IT: Italy, AT: Austria, FR: France, DE: Germany, SLO: Slovenia, FL: Liechtenstein).

Country	Index ≥ 0.1	Index ≥ 0.5	Index ≥ 0.9	Glaciers
CH	3710	2163	754	1010
IT	3353	1786	569	441
AT	2907	1557	484	340
FR	1587	703	199	265
DE	44.1	7.6	0.8	0.6
SLO	25.7	3.6	0.1	0.0
FL	0.3	0.0	0.0	0.0
Total	11 626	6220	2007	2056

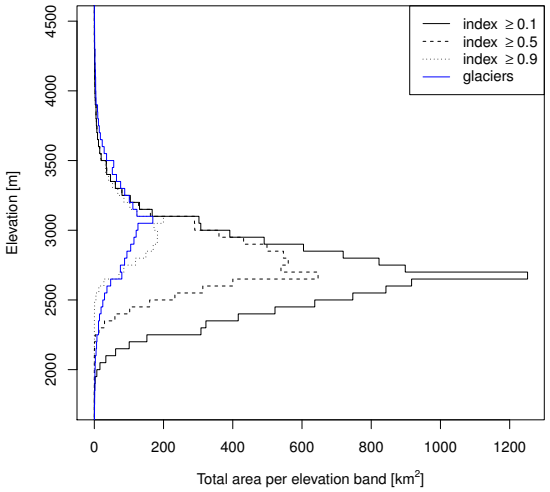

Fig. 9. Altitudinal distribution of permafrost index areas in the Alps, calculated for elevation bands of 50 m.

to sub-grid variability and scaling issues (cf. Gubler et al., 2011). To address point (c) and (d), PF_{loc} was introduced in Sect. 3.2 to exclude unsuitable evaluation data in this context.

The evaluation of APMOD shows that the prediction of the model is reasonable for rock glaciers and boreholes. For "trench or construction sites" as well as for "geophysical investigations," the predicted permafrost index values are in general too low for permafrost presence, but the discrimination of permafrost absence and presence is correct. All three observation types show low index values for permafrost presence, which means that permafrost is also possible at low index values. Partly, this distribution of index values can be explained by the bias towards permafrost existence observations (mean index value of all observations from Fig. 8 = 0.35) induced by the tendency of permafrost researchers to choose locations that do have permafrost. The discrimination of the model is slightly worse when the offset terms are not included, which supports our chosen strategy to include them. Further, the model performance increases when introducing local terrain and vegetation information to apply the offset terms. This highlights the importance of small-scale heterogeneity and the potential to improve the model's prediction by using the interpretation key and site observations.

6.3 Uncertainties and limitations of APMOD

The temperature offsets used in this study are based on a qualitative assessment of recent literature and on the assumption of spatial and temporal invariance in the model domain. We consider these assumptions and estimates to be the best possible guess given the information available at this time.

The radiation dependent offset (Δ_R) that is included in the rock model ranges from $-0.5\,^\circ$C (minimal PISR) to $-2.84\,^\circ$C (maximal PISR), which corresponds to an altitudinal shift of 77–437 m (assumed surface temperature lapse rate of $0.0065\,^\circ\mathrm{C\,m^{-1}}$). Minimal and maximal offset terms are based on investigations by Hasler et al. (2011), but the dependencies based on radiation represent a strong simplification because no information of the surface and subsurface characteristics is available here. Therefore, the maximal uncertainty of the offset within the rock model is derived from the difference between minimal and maximal offset terms and is estimated to be 2.34 °C (e.g. an altitudinal shift of the lower permafrost limit of ±360 m).

The movement-related offset within the debris model is $+0.5\,^\circ$C, respectively 70 m, and is based on the mean altitudinal extent of the analysed rock glaciers. The standard error of this mean value is given by the standard deviation of the sample (81 m) divided by the square root of its quantity ($N = 5541$) and results in 1.1 m. However, local variability of rock glacier extent is not accounted for with this movement-related offset.

The effect of coarse blocks is addressed in the debris model with an offset of 2 °C. Here, we assume that the surface characteristics of rock glaciers are constant and we neglect the fact that rock glaciers with fine-grained material also exist in the Alps (e.g. Matsuoka et al., 2005). As discussed in Sect. 4, published values for this cooling effect range from 1.3 °C (Juliussen and Humlum, 2008) to 7 °C (Harris and Pedersen, 1998). Thus, we assume this temperature offset to vary between $-0.7\,^\circ$C and $+5\,^\circ$C, corresponding to an altitudinal variation of the order of −153 to +770 m.

The discussed uncertainties in the offset terms are large and influence the final permafrost distribution on the map. However, the interpretation key allows the map user to capture some of these extreme topographical situations and to refine the estimate of the map. Isolated permafrost patches in densely vegetated areas and/or below tree line (cf. Gruber and Haeberli, 2009) are not considered in APMOD, but are

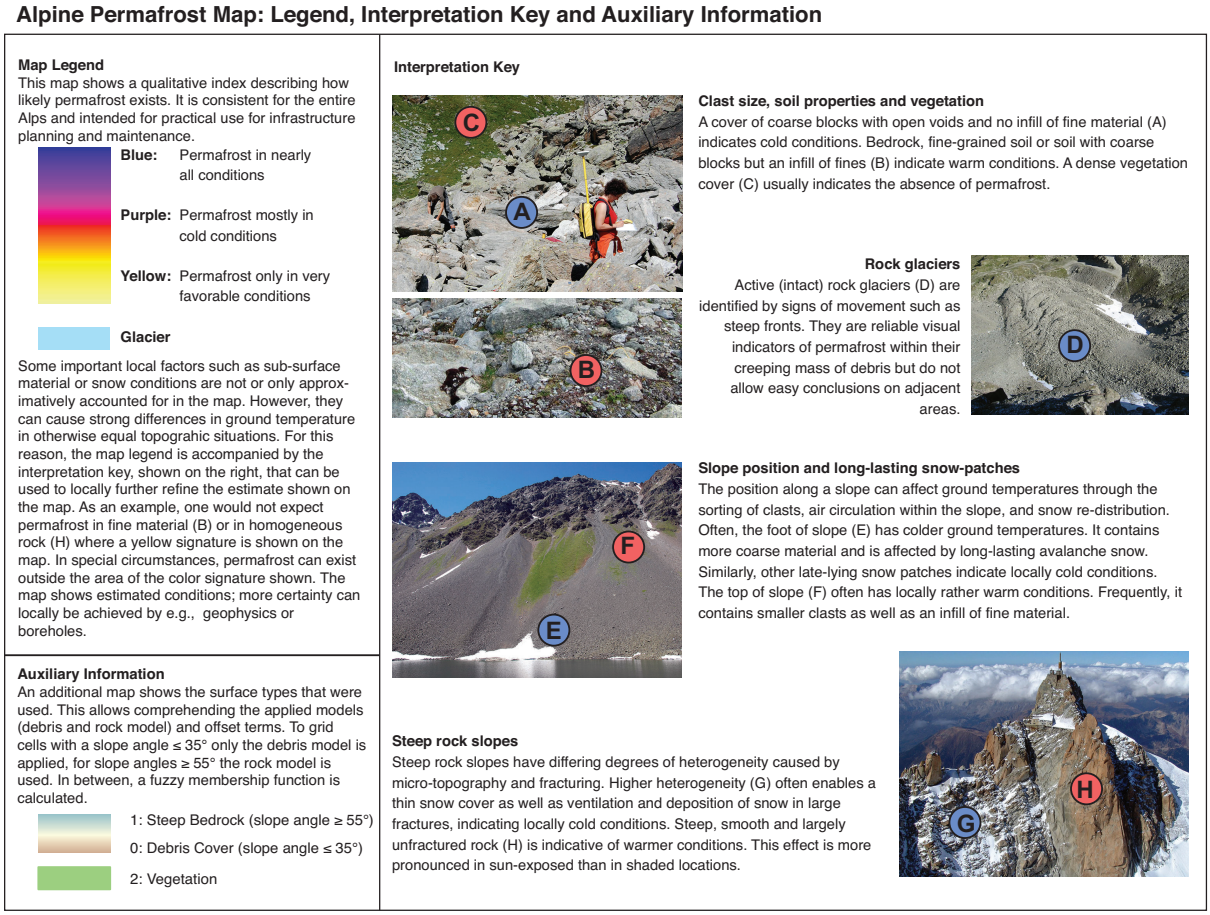

Fig. 10. Legend, interpretation key and auxiliary information that is provided with the Alpine Permafrost Index Map (APIM). This information helps to assess map uncertainties, to relate map contents to their actual expression in terrain and to comprehend the applied models and offset terms.

of minor importance for an Alpine permafrost distribution map.

The classification of the surface types as described in Sect. 3.1 is based on simple approaches, and we distinguish between rock, debris, vegetation and glacier cover. Especially the first two surface types are often hard to differentiate, and all kinds of mixture forms exist in reality. The chosen approach allows classifying these surface types Alpine-wide. For local model application, a more accurate land surface map could be used instead.

APMOD does not account for the recent warming in air temperatures due to climate change and represents a static snapshot of potential permafrost distribution. This is justified because the deviation of an updated and transient permafrost distribution would require knowledge of subsurface ice content that can preserve permafrost conditions for decades. For the purposes of this map ("Where do I need to consider permafrost?"), a steady-state distribution is therefore sufficient and will likely remain relevant in the coming decades.

The rock model was adjusted with longer-term mean annual air temperatures for the period 1961–1990, and predicted MARST values correspond to the same period. Rock wall temperatures react rapidly to climate change (Gruber and Haeberli, 2007), whereas rock glaciers respond with delayed air temperatures due to high ice content (e.g. Haeberli et al., 2006) and coarse blocky surface. Additionally, transient effects, as well as three-dimensional topographical effects, can be responsible for colder temperatures at larger depth than expected based on today's climate conditions (Noetzli and Gruber, 2009). In the final map (APIM), glacier outlines from the year 2003 were used. Because glaciers are subject to fast changes, recently de-glaciated areas need be assessed with caution (cf. Kneisel, 2004; Kneisel and Kääb, 2007).

7 Conclusions

The statistical model of Boeckli et al. (2012) was applied to estimate the current permafrost distribution in the European Alps. This is the first uniform modelling approach that includes all Alpine countries. The Alpine Permafrost Index Map (APIM) uses a grid spacing of approximately 30 m and an index ranging from 0 to 1. A high index value points to permafrost in nearly all conditions, and a low index value means permafrost exists only in locally very favourable conditions. Together with the legend and interpretation key, this product should be useful for both researchers and stakeholders to estimate the permafrost distribution for a given region in the European Alps. The main conclusions from this study are the following:

- The transition of a statistical permafrost distribution model to a permafrost map requires a generalization of the model to other surface types than those used for model calibration. Therefore, additional offset terms were defined qualitatively based on the literature; however, they involve some degree of subjectivity. That is why the map is based on index values and not on pure probabilities.
- Evaluation of spatially distributed models predicting permafrost is challenging because test data are limited and its distribution biased towards permafrost presence. For future model calibration and evaluation, ground truth data need to be collected using a suitable sampling design in order to avoid site selection bias inherent in convenience sampling.
- Calculated permafrost index areas provide an indication of possible permafrost extents in different subregions of the Alps. The relative area of permafrost occurrence in relation to the total area of the Alps is estimated to be 3% when considering an index ≥ 0.5.

8 Data availability

The APIM is freely available for download at: http://doi.pangaea.de/10.1594/PANGAEA.784450 in georeferenced png format. Additionally, the interpretation key (Fig. 10) and the surface-cover map (cf. Fig. 6), which define the used vegetation mask as well as the distinction of debris cover and bedrock based on slope angle, are available. Alternatively, all data are available as a kmz overlay for Google Earth and as a Web Mapping Service for use in a GIS environment (accessible at: http://www.geo.uzh.ch/microsite/cryodata/PF_map_explanation.html).

Acknowledgements. Funding of this study was partly provided by the Alpine Space Program project PermaNET, the Bavarian Environment Agency (Bayerisches Landesamt für Umwelt, LfU), the Swiss Federal Office for the Environment (Bundesamt für Umwelt, BAFU), the Autonomous Province of Bolzano and the Region of Veneto, Geological Survey. The precipitation data were provided by the ALP-IMP project (http://www.cru.uea.ac.uk/cru/data/alpine/). Landsat scenes are available online (GLOVIS, http://glovis.usgs.gov). Vector25 was provided by the Federal Office of Topography, swisstopo. We thank Wilfried Haeberli for his input on a previous version of this manuscript. Constructive comments on the interpretation key by several colleagues are gratefully acknowledged.

Edited by: D. Riseborough

References

BAFU: Hinweiskarte der potentiellen Permafrostverbreitung in der Schweiz, Swiss Federal Office for the Environment (FOEN), 2005.

Barsch, D.: Active rock glaciers as indicators for discontinuous alpine permafrost, An example from the Swiss Alps, in: Proceedings of the 3th International Conference on Permafrost, Edmonton, Canada, 10–13 July, 1, 349–352, 1978.

Bodin, X.: Géodynamique du Pergélisol Alpin: Fonctionnement, distribution et évolution récente, L'Exemple du Massif du Combeynot (Hautes Alpe), Ph.D. thesis, Université Denis Diderot Paris 7, France, 2007.

Boeckli, L., Brenning, A., Gruber, S., and Noetzli, J.: A statistical approach to modelling permafrost distribution in the European Alps or similar mountain ranges, The Cryosphere, 6, 125–140, doi:10.5194/tc-6-125-2012, 2012.

Bonnaventure, P. P., Lewkowicz, A. G., Kremer, M., and Sawada, M. C.: A Permafrost Probability Model for the Southern Yukon and Northern British Columbia, Canada, Permafrost Periglac., 23, 52–68, doi:10.1002/ppp.1733, 2012.

Brenning, A.: Statistical geocomputing combining R and SAGA: The example of landslide susceptibility analysis with generalized additive models, SAGA-Seconds Out, 19, 23–32, 2008.

Brenning, A., Gruber, S., and Hoelzle, M.: Sampling and statistical analyses of BTS measurements, Permafrost Periglac., 16, 383–393, doi:10.1002/ppp.541, 2005.

Cohen, J.: A Coefficient of Agreement for Nominal Scales, Educ. Psychol. Meas., 20, 37–46, doi:10.1177/001316446002000104, 1960.

Cremonese, E., Gruber, S., Phillips, M., Pogliotti, P., Boeckli, L., Noetzli, J., Suter, C., Bodin, X., Crepaz, A., Kellerer-Pirklbauer, A., Lang, K., Letey, S., Mair, V., Morra di Cella, U., Ravanel, L., Scapozza, C., Seppi, R., and Zischg, A.: Brief Communication: "An inventory of permafrost evidence for the European Alps", The Cryosphere, 5, 651–657, doi:10.5194/tc-5-651-2011, 2011.

Delaloye, R., Reynard, E., Lambiel, C., Marescot, L., and Monnet, R.: Thermal anomaly in a cold scree slope (Creux du Van, Switzerland), in: Proceedings of the 8th International Conference on Permafrost, Zurich, Switzerland, 1, 175–180, 2003.

Ebohon, B. and Schrott, L.: Modeling mountain permafrost distribution: A new map of Austria, in: Proceedings of the 9th Interna-

tional Conference on Permafrost, Fairbanks, Alaska, 30 June–3 July, 397–402, 2008.

Etzelmüller, B., Farbrot, H., Gudhmundsson, A., Humlum, O., Tveito, O., and Björnsson, H.: The regional distribution of mountain permafrost in Iceland, Permafrost Periglac., 18, 185–199, doi:10.1002/ppp.583, 2007.

Fontana, F., Rixen, C., Jonas, T., Aberegg, G., and Wunderle, S.: Alpine Grassland Phenology as Seen in AVHRR, VEGETATION, and MODIS NDVI Time Series – a Comparison with In Situ Measurements, Sensors, 8, 2833–2853, doi:10.3390/s8042833, 2008.

Frauenfelder, R.: Rock glaciers, Fletschhorn Area, Valais, Switzerland, International Permafrost Association, Data and Information Working Group, NSIDC, University of Colorado at Boulder, 1998.

Frauenfelder, R., Schneider, B., and Kääb, A.: Using dynamic modelling to simulate the distribution of rockglaciers, Geomorphology, 93, 130–143, doi:10.1016/j.geomorph.2006.12.023, 2008.

Gorbunov, A. P., Marchenko, S. S., and Seversky, E. V.: The thermal environment of blocky materials in the mountains of Central Asia, Permafrost Periglac., 15, 95–98, doi:10.1002/ppp.478, 2004.

Gruber, S.: Derivation and analysis of a high-resolution estimate of global permafrost zonation, The Cryosphere, 6, 221–233, doi:10.5194/tc-6-221-2012, 2012.

Gruber, S. and Haeberli, W.: Permafrost in steep bedrock slopes and its temperature-related destabilization following climate change, J. Geophys. Res., 112, F02S18, doi:10.1029/2006JF000547, 2007.

Gruber, S. and Haeberli, W.: Mountain permafrost, in: Permafrost Soils, edited by: Margesin, R., Biology Series, Springer, 16, 33–44, doi:10.1007/978-3-540-69371-0_3, 2009.

Gruber, S. and Hoelzle, M.: Statistical modelling of mountain permafrost distribution: local calibration and incorporation of remotely sensed data, Permafrost Periglac., 12, 69–77, doi:10.1002/ppp.374, 2001.

Gruber, S. and Hoelzle, M.: The cooling effect of coarse blocks revisited: a modeling study of a purely conductive mechanism, in: Proceedings of the 9th International Conference on Permafrost, Fairbanks, Alaska, 30 June–3 July, 1, 557–561, 2008.

Gruber, S., Peter, M., Hoelzle, M., Woodhatch, I., and Haeberli, W.: Surface temperatures in steep Alpine rock faces – a strategy for regional-scale measurement and modelling, in: Proceedings of the 8th International Conference on Permafrost, Zurich, Switzerland, 21–25 July, 1, 325–330, 2003.

Gubler, S., Fiddes, J., Keller, M., and Gruber, S.: Scale-dependent measurement and analysis of ground surface temperature variability in alpine terrain, The Cryosphere, 5, 431–443, doi:10.5194/tc-5-431-2011, 2011.

Haeberli, W.: Die Basis-Temperatur der winterlichen Schneedecke als möglicher Indikator für die Verbreitung von Permafrost in den Alpen, Zeitschrift für Gletscherkunde und Glazialgeologie, IX/1/2, 221–227, 1973.

Haeberli, W.: Untersuchungen zur Verbreitung von Permafrost zwischen Flüelapass und Piz Grialetsch (Graubünden), Mitteilungen der Versuchsanstalt für Wasserbau, Hydrologie und Glaziologie der ETH Zürich, Zurich, Switzerland, 17, 221 pp., 1975.

Haeberli, W.: Eistemperaturen in den Alpen, Zeitschrift für Gletscherkunde und Glazialgeologie, 11, 203–220, 1976.

Haeberli, W., Hallet, B., Arenson, L., Elconin, R., Humlum, O., Kääb, A., Kaufmann, V., Ladanyi, B., Matsuoka, N., Springman, S., and Mühll, D. V.: Permafrost creep and rock glacier dynamics, Permafrost Periglac., 17, 189–214, doi:10.1002/ppp.561, 2006.

Hanson, S. and Hoelzle, M.: Installation of a shallow borehole network and monitoring of the ground thermal regime of a high alpine discontinuous permafrost environment, Eastern Swiss Alps, Norsk Geogr. Tidsskr., 59, 84–93, doi:10.1080/00291950510020664, 2005.

Harris, C., Arenson, L. U., Christiansen, H. H., Etzelmüller, B., Frauenfelder, R., Gruber, S., Haeberli, W., Hauck, C., Hölzle, M., Humlum, O., Isaksen, K., Kääb, A., Kern-Lütschg, M. A., Lehning, M., Matsuoka, N., Murton, J. B., Nötzli, J., Phillips, M., Ross, N., Seppälä, M., Springman, S. M., and Mühll, D. V.: Permafrost and climate in Europe: Monitoring and modelling thermal, geomorphological and geotechnical responses, Earth-Sci. Rev., 92, 117–171, doi:10.1016/j.earscirev.2008.12.002, 2009.

Harris, S. and Pedersen, D.: Thermal regimes beneath coarse blocky materials, Permafrost Periglac., 9, 107–120, doi:10.1002/(SICI)1099-1530(199804/06)9:2<107::AID-PPP277>3.0.CO;2-G, 1998.

Hasler, A., Gruber, S., and Haeberli, W.: Temperature variability and offset in steep alpine rock and ice faces, The Cryosphere, 5, 977–988, doi:10.5194/tc-5-977-2011, 2011.

Hayakawa, Y., Oguchi, T., and Lin, Z.: Comparison of new and existing global digital elevation models: ASTER G-DEM and SRTM-3, Geophys. Res. Lett., 35, L17404, doi:10.1029/2008GL035036, 2008.

Heggem, E., Juliussen, H., and Etzelmüller, B.: Mountain permafrost in central-eastern Norway, Norsk Geogr. Tidsskr., 59, 94–108, doi:10.1080/00291950510038377, 2005.

Hijmans, R. J. and van Etten, J.: raster: Geographic analysis and modeling with raster data, R package version 1.9-64, The R Foundation for Statistical Computing, Vienna, 2012.

Hoelzle, M.: Permafrost occurrence from BTS measurements and climatic parameters in the Eastern Swiss Alps, Permafrost Periglac., 3, 143–147, doi:10.1002/ppp.3430030212, 1992.

Hoelzle, M.: Permafrost und Gletscher im Oberengadin: Grundlagen und Anwendungsbeispiele für automatisierte Schätzverfahren, Mitteilungen der VAW-ETH Zurich, 132, 121 pp., 1994.

Hoelzle, M., Haeberli, W., and Keller, F.: Application of BTS-measurements for modelling permafrost distribution in the Swiss Alps, in: Proceedings of the 6th International Conference on Permafrost, South China University Technology Press, Beijing, 272–277, 1993.

Hoelzle, M., Haeberli, W., and Stocker-Mittaz, C.: Miniature ground temperature data logger measurements 2000–2002 in the Murtèl-Corvatsch area, Eastern Swiss Alps, in: Proceedings of the 8th International Conference on Permafrost. Zurich, Switzerland, 21–25 July, 419–424, 2003.

Hosmer, D. and Lemeshow, S.: Applied logistic regression, Wiley-Interscience, New York, 2000.

Huete, A.: A soil-adjusted vegetation index (SAVI), Remote Sens. Environ., 25, 295–309, doi:10.1016/0034-4257(88)90106-X, 1988.

Humlum, O.: Active layer thermal regime at three rock glaciers in Greenland, Permafrost Periglac., 8, 383–408, doi:10.1002/(SICI)1099-1530(199710/12)8:4<383::AID-PPP265>3.0.CO;2-V, 1997.

Imhof, M.: Modelling and verification of the permafrost distribution in the Bernese Alps, Switzerland, Permafrost Periglac., 17, 267–280, doi:10.1002/(SICI)1099-1530(199609)7:3<267::AID-PPP221>3.0.CO;2-L, 1996.

International Organization for Standardization: International Standard Atmosphere, Standard Atmosphere ISO 2533:1975, 1975.

Janke, J. R.: The occurrence of alpine permafrost in the Front Range of Colorado, Geomorphology, 67, 375–389, doi:10.1016/j.geomorph.2004.11.005, 2004.

Juliussen, H. and Humlum, O.: Thermal regime of openwork block fields on the mountains Elgåhogna and Sølen, central-eastern Norway, Permafrost Periglac., 19, 1–18, doi:10.1002/ppp.607, 2008.

Keller, F.: Automated mapping of mountain permafrost using the program PERMAKART within the geographical information system ARC/INFO, Permafrost Periglac., 3, 133–138, doi:10.1002/ppp.3430030210, 1992.

Keller, F., Frauenfelder, R., Hoelzle, M., Kneisel, C., Lugon, R., Phillips, M., Reynard, E., and Wenker, L.: Permafrost map of Switzerland, in: Proceedings of the 7th International Conference on Permafrost, Nordicana, Yellowknife, Canada, 23–27 June, 557–562, 1998.

Kneisel, C.: New insights into mountain permafrost occurrence and characteristics in glacier forefields at high altitude through the application of 2D resistivity imaging, Permafrost Periglac., 15, 221–227, doi:10.1002/ppp.495, 2004.

Kneisel, C. and Kääb, A.: Mountain permafrost dynamics within a recently exposed glacier forefield inferred by a combined geomorphological, geophysical and photogrammetrical approach, Earth Surf. Proc. Landforms, 32, 1797–1810, doi:10.1002/esp.1488, 2007.

Kneisel, C., Haeberli, W., and Baumhauer, R.: Comparison of spatial modelling and field evidence of glacier/permafrost relations in an Alpine permafrost environment, Ann. Glaciol., 31, 269–274, 2000.

Lambiel, C. and Reynard, E.: Regional modelling of present, past and future potential distribution of discontinuous permafrost based on a rock glacier inventory in the Bagnes–Heé reé mence area (Western Swiss Alps), Norsk Geogr. Tidsskr., 55, 219–223, 2001.

Lewkowicz, A. and Bonnaventure, P.: Interchangeability of mountain permafrost probability models, northwest Canada, Permafrost Periglac., 19, 49–62, doi:10.1002/ppp.612, 2008.

Lewkowicz, A. G. and Ednie, M.: Probability mapping of mountain permafrost using the BTS method, Wolf Creek, Yukon Territory, Canada, Permafrost Periglac., 15, 67–80, doi:10.1002/ppp.480, 2004.

Li, J., Sheng, Y., Wu, J., Chen, J., and Zhang, X.: Probability distribution of permafrost along a transportation corridor in the northeastern Qinghai province of China, Cold Regions Sci. Technol., 59, 12–18, doi:10.1016/j.coldregions.2009.05.012, 2009.

Luthi, M. P. and Funk, M.: Modelling heat flow in a cold, high-altitude glacier: interpretation of measurements from Colle Gnifetti, Swiss Alps, J. Glaciol., 47, 314–324, doi:10.3189/172756501781832223, 2001.

Mason, S. and Graham, N.: Areas beneath the relative operating characteristics (roc) and relative operating levels (rol) curves: Statistical significance and interpretation, Q. J. Royal Meteorol. Soc., 128, 2145–2166, doi:10.1256/003590002320603584, 2002.

Matsuoka, N., Ikeda, A., and Date, T.: Morphometric analysis of solifluction lobes and rock glaciers in the Swiss Alps, Permafrost Periglac., 16, 99–113, doi:10.1002/ppp.517, 2005.

Noetzli, J. and Gruber, S.: Transient thermal effects in Alpine permafrost, The Cryosphere, 3, 85–99, doi:10.5194/tc-3-85-2009, 2009.

Olaya, V.: A gentle introduction to SAGA GIS, edition 1.1, user's guide, University of Göttingen, Göttingen, Germany, available at: http://www.saga-gis.org/en/index.html(last access: 25 July 2012), 2004.

Paul, F., Frey, H., and Le Bris, R.: A new glacier inventory for the European Alps from Landsat TM scenes of 2003: Challenges and results, Ann. Glaciol., 52, 144–152, 2011.

PERMAFRANCE: Permafrost in France, edited by: Schoeneich, P., Bodin, X., Krysiecki, J. M., Deline, P., and Ravanels, L., Permafrance Network, Report Nr. 1, 68 pp., 2010.

Pogliotti, P.: Influence of snow cover on MAGST over complex morphologies in mountain permafrost regions, Ph.D. thesis, Earth Science Department, University of Turin, Italy, 2010.

R Development Core Team: Development Core Team: R: a language and environment for statistical computing, R Foundation for Statistical Computing, Vienna, Austria, ISBN 3-900051-07-0, available at: http://www.R-project.org, 2010.

Serrano, E., Agudo, C., Delaloye, R., and Gonzalez-Trueba, J.: Permafrost distribution in the Posets massif, Central Pyrenees, Norsk Geogr. Tidsskr., 55, 245–252, 2001.

swisstopo: Vector25 – das digitale Landschaftsmodell der Schweiz, Bundesamt für Landestopographie, Wabern (CH), 2007.

Tanarro, L., Hoelzle, M., García, A., Ramos, M., Gruber, S., Gómez, A., Piquer, M., and Palacios, D.: Permafrost distribution modelling in the mountains of the Mediterranean: Corral del Veleta, Sierra Nevada, Spain, Norsk Geogr. Tidsskr., 55, 253–260, 2001.

Zhang, T., Heginbottom, J. A., Barry, R. G., and Brown, J.: Further statistics on the distribution of permafrost and ground ice in the Northern Hemisphere, Polar Geography, 24, 126–131, doi:10.1080/10889370009377692, 2000.

Paper IV

Estimated permafrost ice content at the regional scale: Method and application to the European Alps

---

Boeckli, L., Gruber, S., Noetzli, J., and Brenning, A. (submitted). Estimated permafrost ice content at the regional scale: Method and application to the European Alps. *submitted to Permafrost and Periglacial Processes*

The author's contributions to this article:

- Developed methodology.
- Designed and performed all data processing and analysis.
- Main author of all sections in the article.

Estimation of permafrost ice content at the regional scale: Methods and application to the European Alps

Lorenz Boeckli*[1], Stephan Gruber[1], Jeannette Noetzli[1], and Alexander Brenning[2]

[1]Department of Geography, University of Zurich, Switzerland
[2]Department of Geography and Environmental Management, University of Waterloo, Ontario, Canada

January 18, 2013

Abstract

The ice content of permafrost in the European Alps is largely unknown and with it the relevance of permafrost as a water storage. In this study a simple approach to estimate the total amount of permafrost ice in the European Alps is presented. It distinguishes between three different surface types (bedrock, debris and intact rock glaciers), and for each surface type an average depth profile of its characteristics is defined. Based on mean annual ground surface temperature, the permafrost thickness is estimated using an analytical solution to the heat conduction equation and a solution to compute the depth of the freezing front (Stefan Solution) for bedrock and debris. The estimation of the ice content of intact rock glaciers is based on average rock glacier characteristics (depth and volumetric ice content) from the literature. The areal extent of bedrock and debris cover is distinguished using slope angle thresholds and satellite imagery. The spatial density of intact rock glacier occurrence is estimated using eight rock glacier inventories. The total water equivalent of permafrost ice in the European Alps is estimated to be 24–28 km^3, which is approximately one-fourth of the glacier ice volume. According to a sensitivity analysis, the final estimate of permafrost ice in the Alps mainly depends on the physical parameterization of debris and the calculation of near ground surface temperature.

*lorenz.boeckli@geo.uzh.ch

130

1 Introduction

The ice content of permafrost and seasonally frozen ground influences water storage and runoff processes. To assess its relevance in a regional or global (i.e. contribution to sea level rise) context, first the total amount of permafrost ice needs to be estimated. For most regions, the amount of ice stored in permafrost is insufficiently known and its evolution in time remains unclear. This is especially true for mountain regions, which have an increased spatial heterogeneity of ground composition and permafrost extent. Existing studies focus on (a) the estimation of ice content in high or low latitude permafrost (Vtyurin, 1973; Pollard and French, 1980; Seguin and Frydecki, 1990; Couture and Pollard, 1998; Ermolin et al., 2004; Zhang et al., 2008), and (b) the ice content of rock glaciers for an entire mountain range (Barsch, 1977; Brenning, 2005; Bolch and Marchenko, 2006; Azócar and Brenning, 2010). The former studies (a) are mostly based on rough estimations of the areal extent of permafrost and the distinction of morphological landforms with a high-volumetric ice content such as pingos. Furthermore, averaged ground-ice versus depth profiles are assumed based on borehole information or geophysical investigations and then applied to an entire landscape to derive the total ice content. The ice content of rock glaciers (b) is estimated by assuming averaged thickness and volumetric ice content, and the areal extent of rock glacier is derived based on satellite imagery, existing inventories or statistical mapping methods.

The general aim of this study is to estimate the ice content of permafrost for an entire mountain range at the example of the European Alps and to reveal the important influences on and sensitivities of such an estimate. This is a difficult task, as mountain permafrost is characterized by a high spatial variability and varying volumetric ice content. The latter is highly dependent on surface and subsurface characteristics for which reason the distinction of different surface types is needed. The analysis of the uncertainties inherent in the estimate is important because the spatial generalization of surface and ground conditions is performed over large areas. To estimate the ice content for a mountain range, we a) distinguish between different surface cover and ground types as they differ in their possible ice contents, b) estimate the relevant area of each surface type, c) assume a typical stratigraphy per surface type characterizing the thermal properties and its potential ice content, and d) estimate permafrost thickness depending on spatially distributed mean annual ground surface temperatures (MAGST). The approach is described in the context of the European Alps, but can be adapted to other regions.

The following section contains a review of existing information of permafrost ice content documented in individual studies in the Alps. Section 3 provides the methods to a) estimate the area of the considered surface types, b) to derive an Alpine-wide gridded MAGST data set, c) to calculate the depth of the permafrost base and active layer thickness, and d) to estimate thermal conductivity and thermal diffusivity based on ground properties. In section 4, the relevant ground properties are described characterizing the different ground types. Section 5 contains the results of the sensitivity analysis and the final estimates of

the total ice content in the European Alps. Finally, the results and methods are discussed (Sect. 5) and the conclusions are drawn (Sect. 6).

2 Background: Ice content in Alpine permafrost

Permafrost is defined as ground that remains at or below 0 °C for at least two consecutive years (van Everdingen, 1998), irrespective of the presence or absence of ice. Problems of the definition of permafrost arise especially in continental climates where the distinction of permafrost and glacier is not always obvious, because transitions of cold/polythermal glaciers, ice-cored moraines and perennially frozen sediments are possible (Kneisel et al., 2000; Haeberli et al., 2006). In this study, glacier ice is restricted to occur within glacier outlines published by Paul et al. (2011), and only the non-glacierized area, outside the glacier outlines, is considered to possibly contain permafrost ice.

The best-investigated ice-rich permafrost features in the Alps are rock glaciers, ice-debris landforms that indicate the existence of present or past permafrost. Intact (active and inactive) rock glaciers point to permafrost presence due to their ice content (e.g. Haeberli and Hoelzle, 1995; Roer and Nyenhuis, 2007) while relict rock glaciers do no longer contain ice, and are indicators for today's permafrost absence. The hydrological significance of rock glaciers has been analyzed by Barsch (1977); Bolch and Marchenko (2006); Brenning (2005); Azócar and Brenning (2010) in a regional context. Boreholes and geophysical investigations point to a high volumetric ice content in rock glaciers (Haeberli, 1985; Vonder Mühll and Holub, 1992; Evin and Fabre, 1990; Burger et al., 1999; Arenson et al., 2002; Hausmann et al., 2007). In the European Alps, the spatial distribution of rock glaciers has been analyzed by various studies for single regions (Barsch, 1977; Delaloye et al., 1998; Frauenfelder, 1998; Hoelzle, 1998; Imhof, 1998; Phillips, 1998; Reynard and Morand, 1998; Schoeneich et al., 1998; Nyenhuis et al., 2005). However, no studies so far focus on the entire European Alps.

Next to rock glaciers, talus slopes without signs of movement have the potential to contain ice-rich permafrost (examples are shown in Fig. 1). A number of recent studies focus on the thermal regime of ventilated talus slopes (e.g. Delaloye et al., 2003; Delaloye and Lambiel, 2005; Morard et al., 2008; Phillips et al., 2009) but little information about their internal structure and volumetric ice content is available. Typical debris thicknesses in talus slopes range from 15 to 50 m (Sass, 2007). Scapozza et al. (2011) analyzed the internal structure and ice content of two talus slopes in the Valais, Swiss Alps. Three boreholes in one of these talus slopes indicate ice-rich layers up to 50 % per volume. Ground ice occurrence of around 20% and saturated conditions were modeled by Hauck and Kneisel (2008) using geophysical methods at an Alpine scree slope in Val Bever, Switzerland. To our knowledge, analyses of the spatial distribution of ice-rich talus slopes and their ice content in a regional context have not been published.

Moraines often have high ground ice contents and therefore need to be considered here

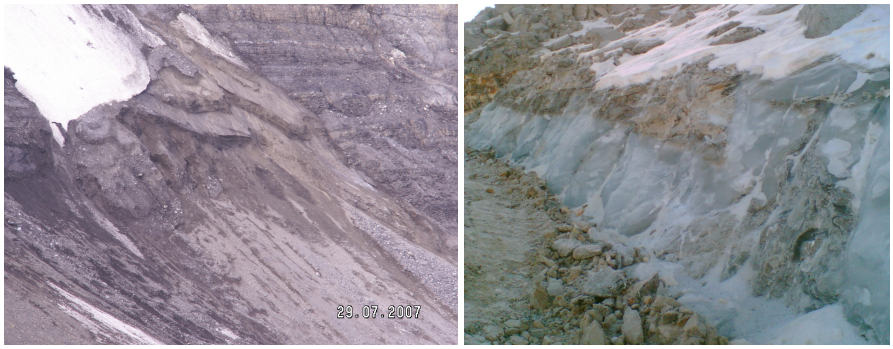

Figure 1: Evidence of ground ice in debris covered-area. Left: Exposed ice-cemented permafrost at 2400 m below the 2005 Dents Blanches (Switzerland) rock fall (photograph by B. Rey-Bellet), right: buried firn in debris cover at Hoetaelli (3270 m), near Stockhorn, Switzerland (photograph by O. Wild).

irrespective of the formation mechanism of the ground ice. Ice-cored moraines were first systematically described and mapped in Scandinavia (Østrem, 1964). A frozen moraine next to the 'Unterer Theodulgletscher, Chli Matterhorn' (Switzerland) showed an estimated overall ice content of 75% and a depth of approximately 30 m at the location where a pylon for a cable car was built (Keusen and Haeberli, 1983). The frozen moraine 'Col des Gentianes' near the Tortin glacier in the Swiss Alps is characterized by a very heterogeneous internal structure (Lambiel and Baron, 2008) and massive ice lenses were found that probably extend down to 10 m depth. In an ice-cored moraine near Zermatt (Switzerland) a 2 m thick active layer was observed, underlain by 20–30 m of frozen sedimentary material (Hauck et al., 2003). High resistivity values in geoelectrical soundings were interpreted to indicate the presence of massive ice within this moraine (Hauck et al., 2003). Further, dead-ice in recently deglaciated glacier forefields has been analyzed in the European Alps by Kneisel (1998); Kääb and Kneisel (2006); Kneisel and Kääb (2007). In such areas, permafrost is expected to occur in isolated patches only. The areal extent of recently deglaciated glacier forefields can be estimated using glacier inventories from different years (e.g. Paul et al., 2011); however, hardly any field evidence of ground ice occurrence is available. Subglacial permafrost is less relevant as ice storage than the glaciers covering it. Additionally, only few cold-based glaciers exist in the Alps that would allow permafrost occurrence within their bed (Haeberli, 1976; Lüthi and Funk, 2001).

A review of massive ice in bedrock for the European Alps by Gruber and Haeberli (2007) lists individual observations (examples are shown in Fig. 2), but no estimates of bedrock ice content for a larger area are available. Ice in bedrock is contained in fractures and matrix porosity. The fracture porosity (or degree of jointing) is highly heterogeneous

Figure 2: Evidence of permafrost ice in bedrock. Left: Ice-filled crack in bedrock that has been exposed during construction activities at Stockhorn, Switzerland, right: massive ice visible in a rock fall detachment zone after a rock fall at Liongrat, Matterhorn, Italy (photograph by L. Trucco).

and difficult to measure and estimate (Palmstrom, 2005; Tiab and Donaldson, 2012).

Beside the above described typical permafrost locations, extrazonal permafrost exists in Europe and has been analyzed by various studies (e.g. Christian, 1987; Kneisel et al., 2000; Luetscher et al., 2005; Morard et al., 2008; PERMOS, 2010). However, its spatial occurrence and total ice content is assumed not to be relevant when compared to the involved uncertainties of our approach.

3 Approach and methods

In general, the ice volume (ICE) of permafrost for a homogeneous spatial unit can be calculated as:

$$ICE = A(Z_P - Z_{ALD})I, \tag{1}$$

where A is the planimetric area (m^2), Z_P the depth of the permafrost base (m), Z_{ALD} the active layer depth (m), and I the volumetric ice content (m^3/m^3). Z_P and Z_{ALD} are defined as depth in direction to the Earth's center. Z_{ALD} defines the seasonal depth of thawing and is required to estimate the permafrost thickness ($Z_P - Z_{ALD}$). A homogeneous spatial unit represents individual areas (e.g. grid cells) that are characterized by a given surface type and assumed ground properties.

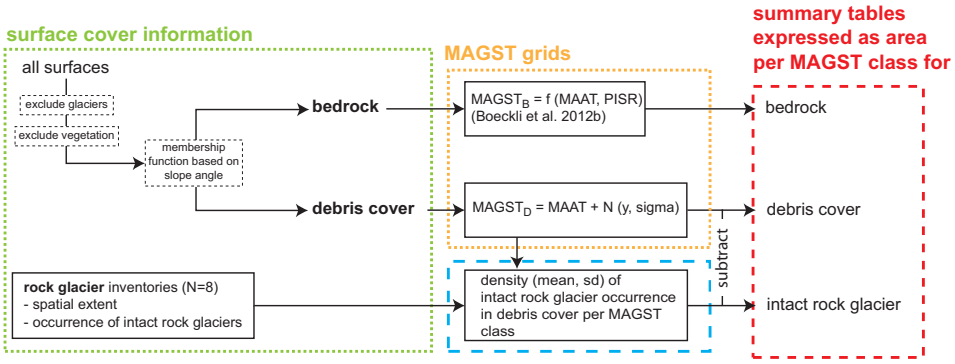

Figure 3: Flowchart illustrating the calculation of the areas for bedrock, debris cover and intact rock glaciers. Some surface information could be mapped (dotted squares), while for other surface types only estimates of their areal proportion are available (dashed squares). For the calculations and the sensitivity analysis, summary tables that express the area of a given surface type per MAGST class were used.

As surface types, we distinguish between bedrock, debris cover and intact rock glaciers (Sect. 3.1). We then characterize and summarize ground ice contents for bedrock and debris cover within 2 °C intervals of MAGST (Sect. 3.2) based on Z_P and Z_{ALD} (Sect. 3.3) and assumed average ground characteristics (Sect. 4.1). The ice content of intact rock glaciers is calculated independently of MAGST using estimated average values for Z_P, Z_{ALD} and I from the literature (Sect. 4.2).

Ground characteristics are estimated using a 'best guess' parameterization and lower and upper bounds per parameter. Based on that, the influence of the individual parameters on the final result is assessed with a sensitivity analyses. The subscripts used are summarized in Table 1.

3.1 Areal extent of individual surface types

Estimates of fractional bedrock and debris area were derived using a) glacier coverage, b) a vegetation mask, and c) slope angle thresholds. First, the glaciated area and vegetation cover is excluded from the analysis (Fig. 3). The underlying assumption is that permafrost is mostly absent in densely vegetated areas (Haeberli, 1975; Hoelzle et al., 1993). The used vegetation mask is based on the soil-adjusted vegetation index (SAVI; Huete, 1988) and is derived from Landsat Thematic Mapper (Landsat 5) and Landsat Enhanced Thematic Mapper (Landsat 7) images as described in Boeckli et al. (2012b). Glacier cover is based on glacier outlines derived from Landsat images provided by Paul et al. (2011). The outlines represent glacier extent of the year 2003, manually corrected for debris-covered glacier

parts. In a next step, fractional bedrock and debris-covered area are distinguished for each grid cell. Here, slope angle dependent probabilities of bedrock occurrence (vs. debris cover) are used based on a membership function (Fig. 1 and Eq. (1) in Boeckli et al., 2012b).

To estimate the area of intact rock glaciers, eight inventories compiled during the Alpine-space project PermaNET (Cremonese et al., 2011) were used. Each inventory contains polygon information of intact and relict rock glaciers. If not available, perimeters were manually digitized in a GIS for individual rock glacier inventories using the hill shade of the ASTER G-DEM as imagery background. The matching (or direct comparison) of each inventory with gridded and $MAGST_d$ (subscript $_D$ indicates debris) allows to derive a density of intact rock glacier occurrence per $MAGST_d$ class within the perimeter of the inventory. By applying this to all inventories individually, a mean density of intact rock glacier occurrence in debris cover and the corresponding quartiles were calculated per $MAGST_d$ class. This allows to derive the area of intact rock glaciers per $MAGST_d$ class Alpine-wide. Here we assume that the spatial density of intact rock glacier occurrence is dependent on MAGST only and its dependence on slope angle or suitable catchments are neglected (cf. Brenning and Trombotto, 2006; Brenning and Azócar, 2010). In a last step, the area of intact rock glaciers was subtracted from the debris area for each $MAGST_d$ class.

3.2 MAGST values for bedrock and debris cover

For debris-covered areas, no surface temperature model is available for the entire European Alps. Here, the mean temperature difference (D) between $MAGST$ and mean annual air temperature ($MAAT$) is used:

$$MAGST_d = MAAT + D, \tag{2}$$

D and its standard deviation σ_D are estimated by comparing $MAGST_d$ values at 36 monitoring sites from the permafrost monitoring network of Switzerland (PERMOS) with MAAT values. Gridded MAAT for the period 1960–1990 (Hiebl et al., 2009) is based on the GTOPO30 elevation model (U.S. Geological Survey, 1997) with an approximate resolution of 1000 m and shows a monthly standard error of less then 1 °C (Hiebl et al., 2009). A constant lapse rate of 0.65 °C 100 m^{-1} (cf. International Organization for Standardization, 1975) was used to interpolate the coarse MAAT based on more precise elevation information from the ASTER GDEM. To refer the longer-term MAAT for each monitoring site to the time interval the observations are available, the difference of MAAT 1961–1990 to the observation period is calculated for Piz Corvatsch (Switzerland) and then used to derive a MAAT value for the same time period as measurements are available for each monitoring site individually. Here, we assume the difference of MAAT for a specific region to its longer-term value to be spatially uniform.

$MAGST_d$ data include measurements of 19 boreholes located in the Swiss Alps (for more details, see PERMOS, 2010) and 17 ground surface temperature loggers located in

debris cover at Schilthorn, Switzerland. In the case of boreholes, the uppermost thermistors were chosen having depths that span 0.1–2 m. $MAGST_d$ is usually warmer than MAAT (Fig. 4), however some boreholes located in talus slopes show colder $MAGST_d$ than the longterm MAAT, indicating that an effective cooling of the ground is present (e.g. Delaloye et al., 2003; Hanson and Hoelzle, 2004). Estimates for D range between 1.0–3.5 °C (Table 2) and correspond to the mean of all measurements per surface type. Considering that the measurements are probably affected by a bias towards colder and permafrost favorable conditions because site-selection was done for permafrost research, we assume D=3 °C (lower bound: D=2 °C, upper bound: D=4 °C) in this study. This value is slightly lower than used as norm case (D=4.8 °C) in a modeling study to derive global permafrost zonation (Gruber, 2012), which can be explained by the exclusion of vegetated areas in our analysis. σ_D is assumed to be 2 °C and is used in Sect 3.3.3 to derive $MAGST_d$ for aggregated $MAGST_d$ classes.

MAGST estimates for steep bedrock ($MAGST_b$) are based on a statistical model described by Boeckli et al. (2012a): The model predicts $MAGST_b$ using a linear regression based on mean annual air temperatures (MAAT) and potential incoming solar radiation (PISR) for the entire Alps with a grid resolution of approximately 30 m (details are given by Boeckli et al., 2012a). The prediction is based on the climate standard period 1961–1990 and the model coefficients of 'rock model 2' given in Table 5 in Boeckli et al. (2012a). The explanatory variables, gridded MAAT and PISR, are calculated according to Boeckli et al. (2012a). σ_b that is required in Sect. 3.3.3 can be estimated from the regression model ($\sigma_b = 1.6\ ^\circ C$, Table 5 in Boeckli et al. (2012a)).

3.3 Estimation permafrost thickness in debris cover and bedrock

Z_P and Z_{ALD} (Fig. 5) are estimated based on $MAGST$ using an analytical solution to the heat conduction equation for an assumed steady state environment without phase change. Z_{ALD} was additionally determined using a simplified solution of the Stefan Problem (Lunardini, 1991), which is a widely used analytical solution for the freezing (or thawing) front (Sect. 3.3.2).

3.3.1 Z_P and Z_{ALD} based on heat conduction

Under the assumptions of steady state conditions and a two-layered ground, Z_P is given by temperature gradients (GG_A for layer A, and GG_B for layer B) and $MAGST$ (Williams and Smith, 1989):

$$Z_P = \begin{cases} -MAGST/GG_A & \text{if } GT(Z_L) \geq 0 \\ Z_L - GT(Z_L)/GG_B & \text{if } GT(Z_L) < 0\ , \end{cases} \quad (3)$$

We calculate Z_P using Eq. (3) and $GT(Z_L)$, the ground temperature at the layer boundary depth Z_L (Fig. 5), is given by:

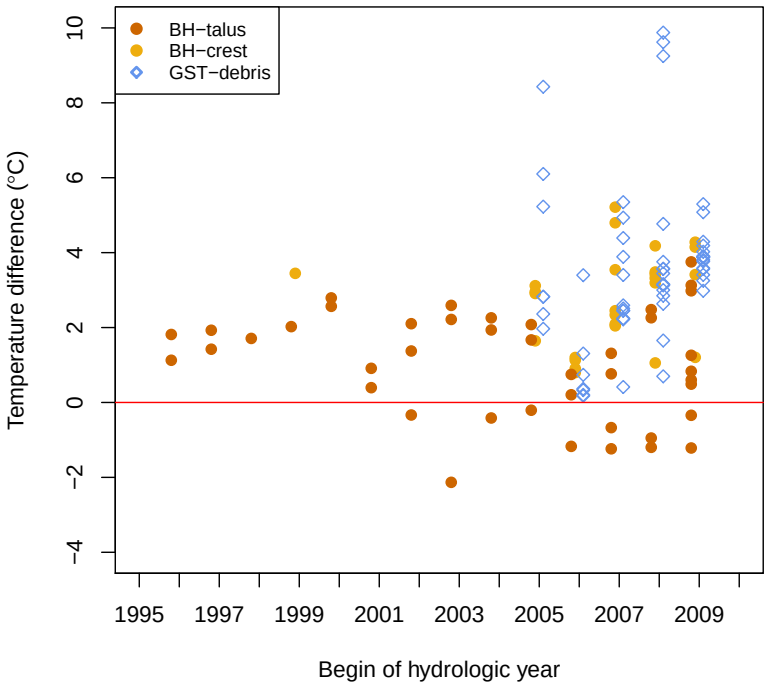

Figure 4: $MAGST_d$ relative to long-term MAAT for the period 1961–1990 for ground surface temperatures at Schilthorn (GST debris), for boreholes drilled at crest (BH crest) and talus slope (BH talus) locations.

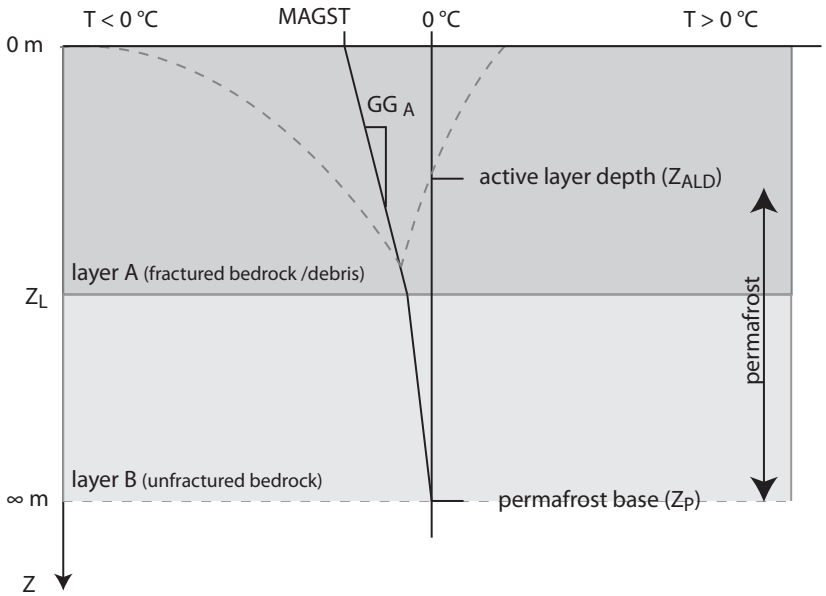

Figure 5: Schematic permafrost profile based on $MAGST$ and a two-layered ground. In each layer (A and B), the mean temperature gradient (GG) is assumed to be constant. The lower layer starts at depth Z_L and is considered to be unfractured bedrock.

$$GT(Z_L) = MAGST + GG_A Z_L \tag{4}$$

GG_A and GG_B are given by the geothermal heat flux Qg ($\mathrm{Wm^{-2}}$) divided by the thermal conductivities K_A and K_B ($\mathrm{WK^{-1}m^{-1}}$).

We disregard advective and multi-annual transient effects and assume Z_{ALD} to be controlled by the seasonal fluctuation of surface temperature and ground properties such as thermal conductivity. Maximum ground temperature (GT_{max}) at any depth (z) can be approximated by using the heat conduction equation according to Ingersoll et al. (1954):

$$GT_{max}(z) = MAGST + GG_A z + AS\, e^{(-z\sqrt{\omega/2\kappa})}, \tag{5}$$

where the amplitude of the temperature wave at depth z is defined by the amplitude of the surface wave AS (°C), the period of the wave ω ($\mathrm{s^{-1}}$, i.e. $\omega = 2\pi/31536000$ s for one year), the thermal diffusivity κ ($\mathrm{m^2 s^{-1}}$) and depth z (m). Here, only the ground properties of the upper layer A are considered as we assume $Z_{ALD} < Z_L$ and that different thermophysical properties of layer B have no substantial influence on thermal regime in layer A. The effect of latent heat is not accounted for in Eq. (5).

AS was estimated based on mean monthly air temperature (MMAT) values and mean monthly ground surface temperatures (MMGST). AS derived from MMAT of MeteoSwiss stations measured at Piz Corvatsch (3305 m a.s.l.) and Jungfraujoch (3580 m a.s.l., Switzerland) is around 7.9 °C. AS in gentle terrain, where ground surface temperatures are influenced by snow cover in wintertime is estimated to be 4.5 °C (calculation based on MMGST of 17 loggers located at Schilthorn, Switzerland, PERMOS, 2010). In this study, AS was set to 6.2 °C (mean of 7.9 and 4.5 °C) and 4.5 °C respective 7.9 °C for the lower respective upper bound.

Eq. (5) was numerically solved for $GT_{max}(z) = 0$ using the 'uniroot' routine (Brent, 1973) implemented within the software R (R Development Core Team, 2010). The roots (i.e., zeros) of this function in a given interval represent Z_{ALD} and Z_P, respectively. Finally, the ice content of permafrost, expressed in the following as water equivalent WE (mm), can be calculated for the ground profile using a) the permafrost thickness $Z_P - Z_{ALD}$, b) the assumed average ice content of the profile, and c) a constant ice density of 900 kg $\mathrm{m^{-3}}$.

3.3.2 Z_{ALD} based on Stefan Solution

An alternative solution to derive Z_{ALD} is a simplified solution of the Stefan Problem. According to Hinkel and Nicholas (1995), Z_{ALD} is:

$$Z_{ALD} = \sqrt{\frac{2K_{AL}}{L\rho\Theta_o}}\sqrt{ADDT}, \tag{6}$$

where L is the latent heat of fusion of water (0.334 MJ $\mathrm{kg^{-1}}$), ρ is the density of ice, Θ_o is the soil porosity (matrix porosity), and $ADDT$ is the accumulated degree days of thaw.

$ADDT$ is a partial temperature integral over time, calculated by summing the average daily temperatures (°C) beginning with start of the surface thaw (i.e., 0° C) to the end of surface thaw. $ADDT$ is here calculated by assuming a sinusoidal surface temperature wave:

$$TS(t) = TS(0) + AS * sin(\omega * t) \tag{7}$$

with period $\omega = 2\pi/365$ days, amplitude $AS = 6.2\,°C$ (Sect. 3.3.1) and an offset $TS_{t=0}$ (TS: surface temperature, $_t$: time) corresponding to the MAGST. $TS(0)$ defines the beginning and end of surface thaw. The partial integral of $TS(t)$ to calculate $ADDT$ was calculated by adaptive quadrature as implemented in the 'integrate' function of R (Piessens et al., 1983; R Development Core Team, 2010).

3.3.3 WE for aggregated MAGST classes

In order to reduce computational effort, WE is calculated for different MAGST classes separately, and not for each individual grid cell. We assume MAGST to be normally distributed within each class with a mean value equal to the class mean itself and a standard deviation (σ) that can be estimated from the MAGST model (Sect. 3.2). The probability density function defines the distribution of MAGST values per class and is given by

$$MAGST(x) = \frac{1}{\sqrt{2\pi\sigma^2}} e^{-\frac{1}{2}\frac{(x-MAGST_C)^2}{\sigma^2}}. \tag{8}$$

Based on Eq. 8 a random sample was drawn ($N = 100$) for each MAGST class individually, to obtain a MAGST value distribution per class. Based on these MAGST distributions, WE for each sample per class was calculated. The total water equivalent of permafrost ice WE_{tot} for a MAGST class is then calculated as the arithmetic mean of the samples.

3.4 Thermal conductivity and volumetric heat capacity

To calculate the thermal conductivity for fractured bedrock and debris, the approach of de Vries (1963) as suggested by Zhang et al. (2008) was adopted:

$$K = \frac{\Theta_w K_w + f_a \Theta_a K_a + f_s \Theta_s K_s}{\Theta_w + f_a \Theta_a + f_s \Theta_s}, \tag{9}$$

where K is the thermal conductivity and Θ is the volume fraction of the soil's constituents water ($_w$), air ($_a$), and solid soil ($_s$). The sum of Θ_w, Θ_a and Θ_s is 1, and the soil porosity (Θ_o) is equal to the sum of Θ_w and Θ_a. The factors f_s and f_a are defined as:

$$f_s = \frac{1}{3}\Big(\frac{2}{1 + (K_s/K_w - 1)0.125} + \frac{1}{1 + (K_s/K_w - 1)0.75}\Big) \tag{10}$$

$$f_a = \frac{1}{3}\Big(\frac{2}{1+(K_a/K_w-1)g_a)} + \frac{1}{1+(K_a/K_w-1)(1-2g_a)}\Big), \tag{11}$$

and g_a is :

$$g_a = \begin{cases} 0.333 - (0.333 - 0.035)\Theta_a/\Theta_o & \text{if } \Theta_w > 0.09 \\ 0.013 + 0.944\Theta_w & \text{if } \Theta_w \leq 0.09 \end{cases} \tag{12}$$

According to de Vries and Afgan (1975), K_w (liquid) is 0.57 $\mathrm{WK^{-1}m^{-1}}$ and K_a is 0.025 $\mathrm{WK^{-1}m^{-1}}$. The thermal conductivity of K_w in frozen state (ice) is much higher and assumed to be 2.4 $\mathrm{WK^{-1}m^{-1}}$ (Clauser, 2012). Accordingly, K_w for the lower ground layer (layer B, Fig. 5) was set to 2.4 $\mathrm{WK^{-1}m^{-1}}$ and for layer A the mean value of the thermal conductivity for liquid and frozen state of water is assumed ($K_w = 1.5\,\mathrm{WK^{-1}m^{-1}}$). K_s was chosen as defined for unfractured bedrock (Sect. 4.1).

The volumetric heat capacity is calculated over all constituents multiplied by their respective volumetric fractions. The thermal diffusivity (κ) is then given by the thermal conductivity divided by the volumetric heat capacity. The following heat capacity values (given in $\mathrm{Jm^{-3}K^{-1}}$) according to de Vries and Afgan (1975) were used: 4.2 10^3 (liquid water), 1.25 10^3 (air), and 2.5 10^6 (bedrock). The heat capacity of frozen water is 1.8 $10^3\mathrm{Jm^{-3}K^{-1}}$ (Clauser, 2012). Similar as for the thermal conductivities, the heat capacity value of the layer B was chosen for frozen state, while the heat capacity of layer A is assumed to be the mean of the values for liquid and frozen state (3 $10^3\mathrm{Jm^{-3}K^{-1}}$).

4 Ground properties

4.1 Characteristics of bedrock and debris cover

The lower of the two layers considered (layer B) is assumed to be unfractured bedrock. The upper layer, which is often characterized by a higher ice content (Osterkamp and Burn, 2003), is assumed to be fractured bedrock or debris. This results in three different ground types for which average physical properties need to be defined: a) unfractured bedrock, b) fractured bedrock, and c) debris. For each ground type, the thermal properties are defined based on typical values reported in the literature. We start by looking at unfractured bedrock as it is further used to derive the thermal characteristics for the other two ground types.

Cermak and Rybach (2012) list thermal conductivity values (in $\mathrm{WK^{-1}m^{-1}}$) for different rock types: granite 1.3–2.5, gneiss 1.2–3.1, and sedimentary rocks 2.09 (limestone) – 5.8 (dolomite). Thermal conductivity values between 2 and 3 $\mathrm{WK^{-1}m^{-1}}$ have been used in modeling studies for bedrock (Gruber et al., 2004; Noetzli and Gruber, 2009; Baston et al., 2010; Hipp et al., 2012) and the 'best guess' value was therefore set to 2.5 $\mathrm{WK^{-1}m^{-1}}$. As lower respective upper bounds 1.2 and 5.8 $\mathrm{WK^{-1}m^{-1}}$ are used (Table 3). Thermal

diffusivity values (in $10^{-7}m^2s^{-1}$) are 6.8–12.8 for granite, 6.0–15.7 for gneiss, and 10.1 for limestone (Cermak and Rybach, 2012).

In general, the matrix porosity of rocks is about 0.4–25 % (Schopper, 2012). Sedimentary rocks such as chalk are characterized by larger porosity up to 50 % (Matsuoka, 2001), whereas igneous and metamorphic rock show low porosity values of around 0.8–3% (Wegmann, 1998; Draebing and Krautblatter, 2012; Stöffler, 2012). For our analysis, a matrix porosity of 3% was used as 'best guess' value for unfractured bedrock, because it represents the upper bound of igneous and metamorphic rock, which form large parts of the Alps. The lower bound was set to 1% and the upper bound to 6%. The relative saturation, which is required to calculate ice content, depends on aspect angle and rock depth (Sass, 2005). Here, values according to Draebing and Krautblatter (2012) are assumed for unfractured bedrock: 0.9 (best guess), 0.8 (lower bound), and 1 (upper bound).

For fractured bedrock, the fracture porosity needs to be estimated first. Not much quantitative information for the European Alps is available and the deviation of an average fracture porosity used in this study is based on limited empirical evidence: Observations at Hörnliridge (Matterhorn, Switzerland) show typical cleft spacing of 0.2–2 m with apertures of 0.03–0.30 m and an extent of 3–40 m (Hasler et al., 2012). A mean cleft spacing of 0.9 m was measured in highly fractured rock at Hüttenberg, Austria (Hermann et al., 1983). In the Central Gotthard Massif, a mean cleft spacing at the surface of 0.47 m was measured at the Gamsboden (Zangerl et al., 2006). Based on these values we assume a mean cleft spacing of 0.5 m and a fracture aperture of 0.1 m for the European Alps. This results in a fracture porosity of 0.17 m^3/m^3 (0.1 m/0.6 m) for a 20 m deep layer A (Z_L = 20 m). The lower and upper bounds for Z_L were set to 5 m and 30 m, respectively. The relative saturation is considered to be different in the permafrost body and in the active layer: For the permafrost body, values similar as for unfractured bedrock are assumed and in the active layer we assume that moisture is absent in fractures and only present in pores (Table 4).

Arenson and Springman (2005) analyzed borehole samples from the rock glacier Muragl, Engiadina (Switzerland) and found porosity (Θ_o) values ranging from 0.4 to 0.8. For sandy loam and silt loam, Θ_o is around 0.34–0.67 (Ochsner et al., 2001). According to these two extreme values, Θ_w for debris was set to 0.5 (best guess value), 0.4 (lower bound), 0.6 (upper bound). Θ_w values for rock glaciers can range up to 1 (Arenson and Springman, 2005; Haeberli et al., 2006) for super-saturated conditions. For sandy loam and silt loam, Ochsner et al. (2001) measured Θ_w of 0.02–0.46. According to this, the relative saturation for debris cover was chosen to be 0.6 (best guess), 0.5 (lower bound), 0.7 (upper bound) for the permafrost body. The relative saturation in the active layer is assumed to be much smaller due to the mostly well drained situations in sloping terrain. Z_L values are mainly based on the investigation by Sass (2007) (Sect. 2).

The geothermal heat flux (Qg) is influenced by topography and transient effects leading to higher values in valleys and lower values for peaks (Kohl, 1999). However, we assume the geothermal heat flux to be spatially uniform with values ranging from 0.04–0.06 Wm^{-2}

(best guess: 0.05 Wm^{-2}. These values are lower than the geothermal heat flux at depth (around 0.8 Wm^{-2} according to Medici and Rybach, 1995) in order to account for the effect of lower geothermal heat flux values at higher elevations (Kohl, 1999), where permafrost is present in the Alps.

4.2 Characteristics of intact rock glaciers

The first layer underneath the active layer is mostly characterized by high ice content that ranges from 10–90% by volume (e.g. Haeberli et al., 1998; Arenson et al., 2002; Hausmann et al., 2007; Brenning, 2010). In this study we adopt the lower and upper bounds for average intact rock glacier ice contents of 47–70% obtained by Brenning (2010) based on a synthesis of published data. The depth of the ice-rich layer is often around 20–30 m (Barsch, 1996; Burger et al., 1999; Haeberli et al., 2006) and the depth of the active layer itself ranges from 1 to 5 m (Fig. 3.5 in PERMOS, 2010). Below this ice-rich layer, fine-grained debris or bedrock is typically located with a much lower ice content or without permafrost and is not considered in this study. The values that were used for estimation of WE are summarized in Table 5.

4.3 Sensitivity analysis

The sensitivity analysis is performed for all ground parameters individually by using lower respective upper bounds instead of best guess parameterization. Further, the sensitivity of the amplitude of the surface wave AS (Eqs. 5 and 7) is investigated. For debris cover, the offset term D (Eq. 2) is additionally considered in the sensitivity analyses because the estimation of total water equivalent is sensitive to it (Sect. 5). The relative deviation, which is used to quantify the sensitivity in this study, is calculated by dividing the absolute difference of results obtained by using lower and upper bounds by the value that is based on the best guess parameterization.

5 Results

The study area ranges from 43°–49° N and 4°–16° E and covers the entire European Alps. The area estimation is based on an ASTER Global Digital Elevation Model (G-DEM, Hayakawa et al., 2008) at a grid resolution of approximately 30 m.

5.1 Bedrock and debris cover

According to the best guess parameterizations used in this study, permafrost in bedrock is characterized by larger permafrost thickness Z_P compared to debris for given MAGST (Fig. 6, left). This is caused by higher thermal conductivity in layer A for bedrock. Maximum Z_{ALD} values calculated based on heat conduction (solid lines in Fig. 6, center) range

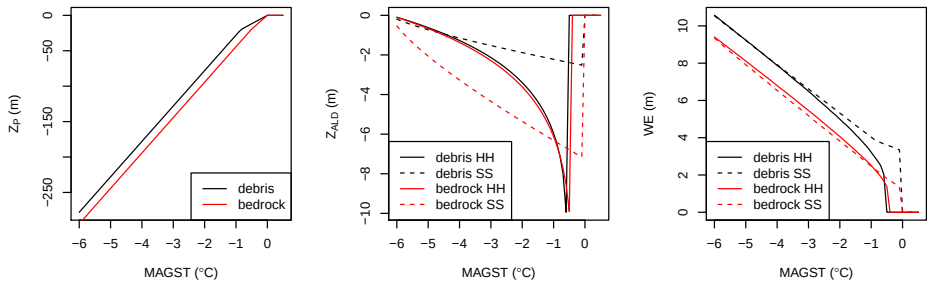

Figure 6: Z_P, Z_{ALD} and WE calculated for the two profiles bedrock and debris for different mean annual ground surface temperature $MAGST$. Two approaches ares used to calculate Z_{ALD} and WE respectively: a) analytical heat conduction without phase change (HH, solid line), and b) Stefan Solution (SS, dashed lines).

up to 10 m and the differences between debris and bedrock is small. The abrupt decrease in Z_{ALD} at MAGST of around -0.5 °C is due to the fact that here, maximum ground temperature is > 0 °C at any depth and thus, no permafrost is present. Z_{ALD} based on the Stefan Solution is dependent on the thermal conductivity and the soil porosity. Low thermal conductivity and a high soil porosity (i.e. debris) lead to lower Z_{ALD} values than a high thermal conductivity and a low porosity (i.e. bedrock). Based on the assumed ground properties, debris cover shows larger water equivalent WE for given MAGST values than bedrock (Fig. 6, left), caused by higher volumetric ice content and smaller active layer depths Z_{ALD}.

The estimated area of bedrock in the European Alps is 2984 km^2 (Table 6) and the corresponding total water equivalent of permafrost ice (TWE) is 1.7 km^3 calculated using heat conduction to determine Z_{ALD} and 1.8 km^3 calculated using the Stefan Solution to determine Z_{ALD} respectively. Z_{ALD} values based on the Stefan Solution are larger than using the heat condition approach. However, the difference of these two approaches in terms of the estimated TWE is small for bedrock areas. The largest contribution to TWE originates from the $MAGST_b$ range between -2 an 0 °C.

The debris area, whether frozen or unfrozen, is estimated to be 190 044 km^2 (Table 7). Resulting total water equivalent TWE range from 17.2 km^3 (based on heat conduction) to 21.4 km^3 (based on Stefan Solution). Again, the largest contribution to TWE comes from the $MAGST_d$ values between -2 and 0 °C.

The results of the sensitivity analysis for bedrock and debris are different (Table 8). For bedrock, the most sensitive parameters according to our parameterization are related to layer B (K_B and $\Theta_{o\,B}$), while for debris, the characteristics of layer A shows larger

sensitivities (K_A and $\Theta_{o\,A}$). For bedrock permafrost, the maximal relative deviation that is calculated by using upper respective and lower bounds is 94 % for the parameter K_B (thermal conductivity in the lower layer). For debris permafrost, the largest relative deviation is associated with the parameter D, which defines the difference in MAGST and MAAT (relative deviation = 104 %).

5.2 Intact rock glaciers

The relative area of intact rock glaciers per $MAGST_d$ class that is derived from the eight rock glacier inventories, is summarized in Table 9. Based on these values the total area of intact rock glaciers in the European Alps is estimated to be 223 km^2 (Table 9).

The total water equivalent of ice stored in intact rock glaciers in the European Alps is estimated to be 4.86 km^3. The analysis of the related sensitivities includes the parameters from Table 5 and lower and upper bounds of intact rock glacier area that are derived from the standard deviation from Table 9. Our results indicates that the most sensitive parameter in the estimation of TWE for intact rock glacier is its area (relative deviation = 62 %, Table 10).

6 Discussion

Summarizing the results of section 5, the total water equivalent of permafrost in the European Alps is in the order of 24–28 km^3 using the best guess parameterizations. Most of the ice is estimated to be present in debris-covered areas (around 74 %) and in areas with relatively warm MAGST (-2 – 0 °C) because of their large areal extent. According to our study, around 20 % of total water equivalent of permafrost ice in the Alps is stored in rock glaciers and the amount of ice in bedrock is small (6 %). The difference between the two approaches to determine Z_{ALD} (heat conduction and Stefan Solution) is not significant for bedrock (ΔTWE = 0.07 km^3). This is not the case for debris, where final estimates of TWE obtained by these two approaches differ significantly (ΔTWE = 4 km^3). The Stefan Solution is expected to reveal better results since effects of latent heat are important. However, suitable data of mean annual active layer thicknesses or moisture content would be required in order to evaluate which approach is more appropriate.

Existing studies in northern Canada assume averaged "ground ice versus depth" profiles for entire landscapes (Pollard and French, 1980; Couture and Pollard, 1998), independent of near-surface ground temperatures. This is not possible for the European Alps, because of the large spatial variability of near ground surface temperature. Additionally, the spatial characteristics of subsurface conditions are highly variable in the Alps and thus our approach cannot be compared to similar studies that focus on lowland permafrost.

6.1 Sensitivity analysis

The uncertainties of the values presented in this study are large but the aim was to reveal the magnitude of permafrost ice and to develop a framework that deals with the most important uncertainties. The ranges that are considered by the lower and upper bounds for the individual parameters represent extreme estimates as this paper deals with average behavior for an entire landscape. This is useful to quantify the maximal sensitivity of each parameter. The sensitivity analysis involves all relevant parameters, which were used to parameterize the required ground characteristics. Additionally, the amplitude of the surface wave AS that influence the active layer depth Z_{ALD}, and the temperature offset D that was used to derive mean annual ground surface temperatures in debris cover $MAGST_D$ are addressed in the sensitivity analysis. The results of the sensitivity analysis highlight the large uncertainties of the final estimate. Individual parameters influence the final estimate with a maximal deviation that is in the order of the estimate itself. In general, the parameterization of debris is most important because permafrost in debris contributes significantly more to the final TWE than permafrost below the other two surface types (bedrock and intact rock glacier). The following parameters show a very high sensitivity (relative deviation $> 60\%$ related to debris permafrost): D, K_A, Z_L, and $\Theta_{o\,A}$. The uncertainty of the predicted $MAGST_B$ values is not included in the sensitivity analysis. However, it is incorporated in the calculation of the results for aggregated $MAGST_B$ classes (Sect. 3.3.3) and is of minor importance because of the small contribution of bedrock permafrost to TWE.

6.2 Limitations of the modeling approach

To estimate MAGST for debris cover, constant differences between MAGST and MAAT were assumed. Differences in the warming effect that winter snow exerts on ground temperatures and the topographic differentiations between shady and sun-exposed slopes are not reproduced because neither precipitation nor solar radiation are taken into account. These effects are expected to be of minor relevance when looking at average values over an entire mountain range. However, it is assumed that the permafrost area in debris cover is overestimated in our analysis, because talus slopes often show permafrost absence at the top of the slope and permafrost presence at the foot of the slope (Haeberli, 1975; Lambiel and Pieracci, 2008; Phillips et al., 2009; Scapozza et al., 2011), which is not considered in our analysis. On the other hand, paleoclimatic effects from past cold periods can significantly influence the thermal regime at depth (Noetzli and Gruber, 2009) and thus, our approach based on current surface temperatures possibly underestimates current permafrost thicknesses and derived ice contents.

The total water equivalent of intact rock glaciers in this study area is of minor relevance when compared to the one of debris permafrost. However, the estimation of the spatial density of rock glacier occurrence could be improved by integrating more rock glacier

inventories or by using statistical methods (Azócar and Brenning, 2010). Compared to an estimated amount of 1.44 km^3 ice-rich permafrost in active rock glaciers in Switzerland Barsch (1977), our estimate of 4.86 km^3 is comparable considering active and inactive rock glaciers for the entire Alps.

6.3 Relevance of permafrost ice

Ice stored in permafrost represents a significant, but seldom recognized, ground water reservoir in alpine terrain (Clow et al., 2003). Permafrost controls drainage processes such as the groundwater storage capacity, which is minimal in spring when the ground is frozen (Roulet and Woo, 1986), or the amount of water infiltration into the active layer (Quinton et al., 2011). Existing studies highlights the importance of the hydrological significance of permafrost for single catchments and relate an increase in base flow to thawing of permafrost ice (Ye et al., 2009; Caine, 2010). The total water equivalent of permafrost TWE in the European Alps is approximately one-fourth of the TWE of Alpine glaciers (90 $\pm$ 30 km^3, Levermann et al., 2012). However, in other mountain ranges such as the dry Chilean Andes, the water equivalent of rock glaciers is estimated to be much larger than the glacier water equivalent (Azócar and Brenning, 2010) and the contribution of total permafrost is even larger. In contrast to glacier meltwater, however, which contributes mostly to stream discharge, a large portion of thawing permafrost ice would remain retained in pores within the saturated and unsaturated zone of soils and bedrock, especially where permafrost has low ice contents. Loss rates for permafrost ice are hardly known but are certainly much smaller than for glaciers (cf. Kääb et al., 1997). Consequently, the volume of glacier is assumed to vanish much more rapidly with a probable disappearance of most Alpine glacier ice during the coming decades (Haeberli et al., 2013). It is possible that already during the second half of the 21st century, more subsurface ice in permafrost may remain than surface ice in glaciers in the European Alps.

7 Conclusions

The total water equivalent of permafrost in the European Alps is in the order of 24–28 km^3. This estimate is based on a simple framework that distinguishes between three different surface and ground types (bedrock, debris and intact rock glaciers) and uses ground surface temperatures and analytical solutions to the heat equation to derive permafrost thicknesses and active layer depth. According to our calculations, 74 % of the total water equivalent of permafrost in the Alps is present in debris-covered areas, 19 % is stored in rock glaciers and the amount of ice in bedrock is 7 %. However, the uncertainties of these estimates are large, because little information of subsurface properties such as thermal conductivity, porosity or relative saturation is available and the extrapolation of this information is performed over large areas.

The total water equivalent of permafrost in the European Alps is approximately one-fourth of the glacier ice volume. Due to rapid glacier vanishing in the European Alps, it is probable that during the second half of the 21st century, more subsurface ice in permafrost may remain than in surface ice in glaciers. Therefore, the significance of permafrost as ground water reservoir or the influence of permafrost on drainage processes requires further attention.

The proposed modeling approach distinguishes between different surface types for which an average depth profile of their characteristics is defined. The sensitivities of the required input variables are estimated by defining lower and upper bounds for each variable. However, for lack of reference data a proper validation of the individual modeling results is currently not possible.

Acknowledgments

The precipitation data was compiled by the ALP-IMP project (`http://www.cru.uea.ac.uk/cru/data/alpine/`). Alpine-wide MAAT data (Hiebl et al., 2009) was provided by the Central Institute for Meteorology and Geodynamics (ZAMG), Austria. Landsat scenes are available online via the Global Visualization Viewer provided by the U.S. Geological Survey (http://glovis.usgs. gov). Thanks goes to the Swiss Permafrost Monitoring Network (PERMOS) for making available borehole and ground surface temperatures. Additionally, we thank Wilfried Haeberli for his input on a previous version of this manuscript.

References

Arenson, L., Hoelzle, M., and Springman, S. 2002. Borehole deformation measurements and internal structure of some rock glaciers in Switzerland. *Permafrost and Periglacial Processes* **13,** 117–135.

Arenson, L. U. and Springman, S. M. 2005. Triaxial constant stress and constant strain rate tests on ice-rich permafrost samples. *Canadian Geotechnical Journal* **42,** 412–430.

Azócar, G. and Brenning, A. 2010. Hydrological and geomorphological significance of rock glaciers in the dry Andes, Chile (27^o–33^o S). *Permafrost and Periglacial Processes* **21,** 42–53.

Barsch, D. 1977. Nature and importance of mass wasting by rock glaciers in alpine permafrost environments. *Earth Surface Processes* **2,** 231–245.

Barsch, D. 1996. *Rock Glaciers: Indicators for the present and former geoecology in high mountain environments*. Springer-Verlag: Berlin.

Baston, D. P., Falta, R. W., and Kueper, B. H. 2010. Numerical modeling of thermal conductive heating in fractured bedrock. *Ground Water* **48,** 836–843.

Boeckli, L., Brenning, A., Gruber, S., and Noetzli, J. 2012a. A statistical approach to modelling permafrost distribution in the European Alps or similar mountain ranges. *The Cryosphere* **6,** 125–140.

Boeckli, L., Brenning, A., Gruber, S., and Noetzli, J. 2012b. Permafrost distribution in the European Alps: calculation and evaluation of an index map and summary statistics. *The Cryosphere* **6,** 807–820.

Bolch, T. and Marchenko, S. 2006. Significance of glaciers, rockglaciers and ice-rich permafrost in the Northern Tien Shan as water towers under climate change conditions. In *Selected papers from the Workshop Assessment of Snow, Glacier and Water Resources in Asiaheld in Almaty, Kazakhstan*, pages 28–30.

Brenning, A. 2005. Geomorphological, hydrological and climatic significance of rock glaciers in the Andes of Central Chile. *Permafrost and Periglacial Processes* **16,** 231–240.

Brenning, A. 2010. The significance of rock glaciers in the dry Andes – reply to L. Arenson and M. Jakob. *Permafrost and Periglacial Processes* **21,** 286–288.

Brenning, A. and Azócar, G. 2010. Statistical analysis of topographic and climatic controls and multispectral signatures of rock glaciers in the dry Andes, Chile (27–33 S). *Permafrost and Periglacial Processes* **21,** 54–66.

Brenning, A. and Trombotto, D. 2006. Logistic regression modeling of rock glacier and glacier distribution: Topographic and climatic controls in the semi-arid Andes. *Geomorphology* **81,** 141–154.

Brent, R. 1973. *Algorithms for Minimization without Derivatives*. Englewood Cliffs, NJ: Prentice-Hall.

Burger, K., Degenhardt, J., and Giardino, J. 1999. Engineering geomorphology of rock glaciers. *Geomorphology* **31,** 93–132.

Caine, N. 2010. Recent hydrologic change in a colorado alpine basin: an indicator of permafrost thaw? *Annals of Glaciology* **51,** 130–134.

Cermak, V. and Rybach, L. 2012. Thermal conductivity and specific heat of minerals and rocks. *Landolt-Börnstein - Group V Geophysics Numerical Data and Functional Relationships in Science and Technology. SpringerMaterials - The Landolt-Börnstein Database* .

Christian, E. 1987. Composition and origin of underground arthropod fauna in an extrazonal permafrost soil of central Europe. *Biology and Fertility of Soils* **3,** 27–30.

Clauser, C. 2012. Geothermal energy. *Landolt-Börnstein – Group VIII Advanced Materials and Technologies. SpringerMaterials – The Landolt-Börnstein Database* .

Clow, D., Schrott, L., Webb, R., Campbell, D., Torizzo, A., and Dornblaser, M. 2003. Ground water occurrence and contributions to streamflow in an alpine catchment, colorado front range. *Ground Water* **41,** 937–950.

Couture, N. and Pollard, W. 1998. An assessment of ground ice volume near Eureka, Northwest Territories. In *Proceedings of the 7th International Conference on Permafrost. Nordicana, Yellowknife, Canada, 23–27 June.*

Cremonese, E., Gruber, S., Phillips, M., Pogliotti, P., Boeckli, L., Noetzli, J., Suter, C., Bodin, X., Crepaz, A., Kellerer-Pirklbauer, A., Lang, K., Letey, S., Mair, V., Morra di Cella, U., Ravanel, L., Scapozza, C., Seppi, R., and Zischg, A. 2011. Brief Communication: "An inventory of permafrost evidence for the European Alps". *The Cryosphere* **5,** 651–657.

de Vries, D. A. 1963. Thermal properties of soil. *In Physics of Plant Environment, edited by W. R. van Dijk, pp. 210 235, North Holland Publishing, Amsterdam* .

de Vries, D. A. and Afgan, N. H. 1975. *Heat and mass tranfer in the biosphere.* John Wiley and Sons.

Delaloye, R. and Lambiel, C. 2005. Evidence of winter ascending air circulation throughout talus slopes and rock glaciers situated in the lower belt of alpine discontinuous permafrost (Swiss Alps). *Norsk Geografisk Tidsskrift - Norwegian Journal of Geography* **59,** 194–203.

Delaloye, R., Reynard, E., Lambiel, C., Marescot, L., and Monnet, R. 2003. Thermal anomaly in a cold scree slope (Creux du Van, Switzerland). In Phillips, M., Springman, S., and Arenson, L., editors, *Proceedings of the 8th International Conference on Permafrost. Zurich, Switzerland, 21–25 July*, volume 1, pages 175–180.

Delaloye, R., Reynard, E., and Wenker, L. 1998. Rock glaciers, Entremont, Valais, Switzerland. *Boulder CO: National Snow and Ice Data Center/World Data Center for Glaciology. Digital Media* .

Draebing, D. and Krautblatter, M. 2012. P-wave velocity changes in freezing hard low-porosity rocks: a laboratory-based time-average model. *The Cryosphere Discussions* **6,** 793–819.

Ermolin, E., de Angelis, H., Skvarca, P., and Rau, F. 2004. Ground ice in permafrost on Seymour (Marambio) and Vega Islands, Antarctic Peninsula. *Annals of Glaciology* **39,** 373–378.

Evin, M. and Fabre, D. 1990. The distribution of permafrost in rock glaciers of the southern Alps (France). *Geomorphology* **3,** 57–71.

Frauenfelder, R. 1998. Rock glaciers, Fletschhorn Area, Valais, Switzerland. *International Permafrost Association, Data and Information Working Group, NSIDC, University of Colorado at Boulder* .

Gruber, S. 2012. Derivation and analysis of a high-resolution estimate of global permafrost zonation. *The Cryosphere* **6,** 221–233.

Gruber, S. and Haeberli, W. 2007. Permafrost in steep bedrock slopes and its temperature-related destabilization following climate change. *Journal of Geophysical Research* **112,** F02S18.

Gruber, S., Hoelzle, M., and Haeberli, W. 2004. Rock-wall temperatures in the Alps: modelling their topographic distribution and regional differences. *Permafrost and Periglacial Processes* **15(3),** 299–307.

Haeberli, W. 1975. Untersuchungen zur Verbreitung von Permafrost zwischen Flüelapass und Piz Grialetsch (Graubünden). *Mitteilungen der Versuchsanstalt für Wasserbau, Hydrologie und Glaziologie der ETH Zürich, Zurich, Switzerland* **17,** 221 p.

Haeberli, W. 1976. Eistemperaturen in den Alpen. *Zeitschrift für Gletscherkunde und Glazialgeologie* **11,** 203–220.

Haeberli, W. 1985. Creep of mountain permafrost: internal structure and flow of alpine rock glaciers. *Mitteilungen der VAW/ETH Zürich* **77,**.

Haeberli, W., Hallet, B., Arenson, L., Elconin, R., Humlum, O., Kääb, A., Kaufmann, V., Ladanyi, B., Matsuoka, N., Springman, S., and Mühll, D. V. 2006. Permafrost creep and rock glacier dynamics. *Permafrost and Periglacial Processes* **17,** 189–214.

Haeberli, W. and Hoelzle, M. 1995. Application of inventory data for estimating characteristics of and regional climate-change effects on mountain glaciers: a pilot study with the European Alps. *Annals of Glaciology* **21,** 206–212.

Haeberli, W., Hoelzle, M., Kääb, A., Keller, F., Vonder Mühll, D., and Wagner, S. 1998. Ten years after drilling through the permafrost of the active rock glacier Murtèl, Eastern Swiss Alps: answered questions and new perspectives. In *Proceedings of the 7th International Conference on Permafrost. Nordicana, Yellowknife, Canada, 23–27 June*, pages 403–410.

Haeberli, W., Paul, F., and Zemp, M. in press, 2013. Vanishing glaciers in the european alps. In *The Pontifical Academy of Sciences, Scripta Varia 118, Fate of Mountain Glaciers in the Anthropocene, Working Group 2–4 April 2011, Vatican City.*

Hanson, S. and Hoelzle, M. 2004. The thermal regime of the active layer at the Murtel rock glacier based on data from 2002. *Permafrost and Periglacial Processes* **15,** 273–282.

Hasler, A., Gruber, S., and Beutel, J. 2012. Kinematics of steep bedrock permafrost. *Journal of Geophysical Research* **117,** F01016.

Hauck, C. and Kneisel, C. 2008. *Quantifying the ice content in low-altitude scree slopes using geophysical methods*. Cambridge University Press.

Hauck, C., Vonder Mühll, D., and Maurer, H. 2003. Using dc resistivity tomography to detect and characterize mountain permafrost. *Geophysical Prospecting* **51,** 273–284.

Hausmann, H., Krainer, K., Brückl, E., and Mostler, W. 2007. Internal structure and ice content of Reichenkar rock glacier (Stubai Alps, Austria) assessed by geophysical investigations. *Permafrost and Periglacial Processes* **18,** 351–367.

Hayakawa, Y., Oguchi, T., and Lin, Z. 2008. Comparison of new and existing global digital elevation models: ASTER G-DEM and SRTM-3. *Geophysical Research Letters* **35,** L17404.

Hermann, W., Kohlbeck, F., and Scheidegger, A. 1983. In situ stress measurements in highly fractured rock at hüttenberg, austria. *Mitteilungen Österreichische Geologische Gesellschaft* **76,** 161–166.

Hiebl, J., Auer, I., Böhm, R., Schöner, W., Maugeri, M., Lentini, G., Spinoni, J., Brunetti, M., Nanni, T., Perčec Tadić, M., Bihari, Z., Dolinar, M., and Müller-Westermeier, G. 2009. A high-resolution 1961–1990 monthly temperature climatology for the greater Alpine region. *Meteorologische Zeitschrift* **18,** 507–530.

Hinkel, K. M. and Nicholas, J. R. J. 1995. Active layer thaw rate at a boreal forest site in central Alaska, U.S.A. *Arctic and Alpine Research* **27,** pp. 72–80.

Hipp, T., Etzelmüller, B., Farbrot, H., Schuler, T. V., and Westermann, S. 2012. Modelling borehole temperatures in Southern Norway, insights into permafrost dynamics during the 20th and 21st century. *The Cryosphere* **6,** 553–571.

Hoelzle, M. 1998. Rock glaciers, Upper Engadin, Switzerland. Boulder. *CO: National Snow and Ice Data Center/World Data Center for Glaciology. Digital Media* .

Hoelzle, M., Haeberli, W., and Keller, F. 1993. Application of BTS-measurements for modelling permafrost distribution in the Swiss Alps. In *Proceedings of the 6th International Conference on Permafrost. Beijing, China, 5–9 July*, pages 272–277.

Huete, A. 1988. A soil-adjusted vegetation index (SAVI). *Remote Sensing of Environment* **25,** 295–309.

Imhof, M. 1998. Rock glaciers, Bernese Alps, western Switzerland. *Boulder CO: National Snow and Ice Data Center/World Data Center for Glaciology. Digital Media* .

Ingersoll, L., Zobel, O., and Ingersoll, A. 1954. *Heat conduction*. The University of Wisconsin Press.

International Organization for Standardization 1975. *International Standard Atmosphere*. Standard Atmosphere ISO 2533:1975.

Kääb, A., Haeberli, W., and Gudmundsson, G. H. 1997. Analysing the creep of mountain permafrost using high precision aerial photogrammetry: 25 years of monitoring Gruben rock glacier, Swiss Alps. *Permafrost and Periglacial Processes* **8,** 409–426.

Kääb, A. and Kneisel, C. 2006. Permafrost creep within a recently deglaciated glacier forefield: Muragl, Swiss Alps. *Permafrost and Periglacial Processes* **17,** 79–85.

Keusen, H. and Haeberli, W. 1983. Site investigation and foundation design aspects of cable car construction in Alpine permafrost at the "Chli Matterhorn", Wallis, Swiss Alps. In *Proceedings of the 4th International Conference on Permafrost. Fairbanks, Alaska, USA, 18–22 July*, pages 601–605.

Kneisel, C. 1998. Occurrence of surface ice and ground ice/permafrost in recently deglaciated glacier forefields, St. Moritz area, Eastern Swiss Alps. In *Proceedings of the 7th International Conference on Permafrost. Nordicana, Yellowknife, Canada, 23–27 June*, pages 575–581.

Kneisel, C., Haeberli, W., and Baumhauer, R. 2000. Comparison of spatial modelling and field evidence of glacier/permafrost relations in an Alpine permafrost environment. *Annals of Glaciology* **31,** 269–274.

Kneisel, C., Hauck, C., and Mühll, D. V. 2000. Permafrost below the timberline confirmed and characterized by geoelectrical resistivity measurements, Bever Valley, eastern Swiss Alps. *Permafrost and Periglacial Processes* **11,** 295–304.

Kneisel, C. and Kääb, A. 2007. Mountain permafrost dynamics within a recently exposed glacier forefield inferred by a combined geomorphological, geophysical and photogrammetrical approach. *Earth Surface Processes and Landforms* **32,** 1797–1810.

Kohl, T. 1999. Transient thermal effects below complex topographies. *Tectonophysics* **306,** 311–324.

Lambiel, C. and Baron, L. 2008. Two-dimensional geoelectrical monitoring in an alpine frozen moraine. In *Proceedings of the 9th International Conference on Permafrost. Fairbanks, Alaska, 30 June – 3 July.*

Lambiel, C. and Pieracci, K. 2008. Permafrost distribution in talus slopes located within the alpine periglacial belt, Swiss Alps. *Permafrost and Periglacial Processes* **19,** 293–304.

Levermann, A., Bamber, J. L., Drijfhout, S., Ganopolski, A., Haeberli, W., Harris, N. R. P., Huss, M., Krüger, K., Lenton, T. M., Lindsay, R. W., Notz, D., Wadhams, P., and Weber, S. 2012. Potential climatic transitions with profound impact on europe: review of the current state of six 'tipping elements of the climate system'. *Climatic Change* **110,** 845–878.

Luetscher, M., Jeannin, P.-Y., and Haeberli, W. 2005. Ice caves as an indicator of winter climate evolution: a case study from the jura mountains. *The Holocene* **15,** 982–993.

Lunardini, V. 1991. *Heat transfer with freezing and thawing.* Developments in Geotechnical Engineering.

Lüthi, M. and Funk, M. 2001. Modelling heat flow in a cold, high-altitude glacier: Interpretation of measurements from Colle Gnifetti, Swiss Alps. *Journal of Glaciology* **47,** 314–324.

Matsuoka, N. 2001. Microgelivation versus macrogelivation: towards bridging the gap between laboratory and field frost weathering. *Permafrost and Periglacial Processes* **12,** 299–313.

Medici, F. and Rybach, L. 1995. Geothermal map of switzerland 1995 (heat flow density),. *Géophysique 30, Schweizerische Geophysikalische Kommission, 1995* .

Morard, S., Delaloye, R., and Dorthe, J. 2008. Seasonal thermal regime of a mid-latitude ventilated debris accumulation. In *Proceedings of the 9th International Conference on Permafrost. Fairbanks, Alaska, 30 June – 3 July*, pages 1233–1238.

Noetzli, J. and Gruber, S. 2009. Transient thermal effects in Alpine permafrost. *Cryosphere* **3,** 85–99.

Nyenhuis, M., Hoelzle, M., and Dikau, R. 2005. Rock glacier mapping and permafrost distribution modelling in the Turtmanntal, Valais, Switzerland. *Zeitschrift für Geomorphologie* **49,** 275–292.

Ochsner, T. E., Horton, R., and Ren, T. 2001. New perspective on soil thermal properties. *Soil Science Society of America Journal* **65,** 1641–1647.

Osterkamp, T. and Burn, C. 2003. Permafrost. In *Encyclopedia of Atmospheric Sciences*, pages 1717 – 1729. Academic Press.

Østrem, G. 1964. Ice-cored moraines in scandinavia. *Geografiska Annaler* **46,** 282–337.

Palmstrom, A. 2005. Measurements of and correlations between block size and rock quality designation (rqd). *Tunnelling and Underground Space Technology* **20,** 362 – 377.

Paul, F., Frey, H., and Le Bris, R. 2011. A new glacier inventory for the European Alps from Landsat TM scenes of 2003: Challenges and results. *Annals of Glaciology* **52,** 144–152.

PERMOS 2010. Permafrost in Switzerland 2006/2007 and 2007/2008. Noetzli, J. and Vonder Muehll, D. (eds.). *Glaciological report (Permafrost) No. 8/9 of the Cryospheric Commission of the Swiss Academy of Sciences, Zurich, Switzerland* page 68 pp.

Phillips, M. 1998. Rock glacier inventory, Hautes Alpes Calcaires, Switzerland. *CO: National Snow and Ice Data Center/World Data Center for Glaciology. Digital Media* .

Phillips, M., Mutter, E. Z., Kern-Luetschg, M., and Lehning, M. 2009. Rapid degradation of ground ice in a ventilated talus slope: Flüela Pass, Swiss Alps. *Permafrost and Periglacial Processes* **20,** 1–14.

Piessens, R., Doncker-Kapenga, D., Überhuber, C., and Kahaner, D. 1983. *QUADPACK, a subroutine package for automatic integration.* Springer Verlag.

Pollard, W. H. and French, H. M. 1980. A first approximation of the volume of ground ice, richards island, pleistocene mackenzie delta, northwest territories, canada. *Canadian Geotechnical Journal* **17,** 509–516.

Quinton, W., Hayashi, M., and Chasmer, L. 2011. Permafrost-thaw-induced land-cover change in the Canadian subarctic: implications for water resources. *Hydrological Processes* **25,** 152–158.

R Development Core Team 2010. Development core team: R: a language and environment for statistical computing. *R Foundation for Statistical Computing, Vienna, Austria, ISBN 3-900051-07-0, available at: http://www.R-project.org* .

Reynard, E. and Morand, S. 1998. Rock glacier inventory, Printse Valley, Valais, Switzerland. *Boulder CO: National Snow and Ice Data Center/World Data Center for Glaciology. Digital Media* .

Roer, I. and Nyenhuis, M. 2007. Rockglacier activity studies on a regional scale: comparison of geomorphological mapping and photogrammetric monitoring. *Earth Surface Processes and Landforms* **32,** 1747–1758.

Roulet, N. T. and Woo, M.-K. 1986. Hydrology of a wetland in the continuous permafrost region. *Journal of Hydrology* **89,** 73–91.

Sass, O. 2005. Rock moisture measurements: techniques, results, and implications for weathering. *Earth Surface Processes and Landforms* **30,** 359–374.

Sass, O. 2007. Bedrock detection and talus thickness assessment in the european alps using geophysical methods. *Journal of Applied Geophysics* **62,** 254 – 269.

Scapozza, C., Lambiel, C., Baron, L., Marescot, L., and Reynard, E. 2011. Internal structure and permafrost distribution in two alpine periglacial talus slopes, Valais, Swiss Alps. *Geomorphology* **132,** 208 – 221.

Schoeneich, P., Lambiel, C., and Wenker, L. 1998. Rock glaciers, Prealps, Vaud, Switzerland. *Boulder CO: National Snow and Ice Data Center/World Data Center for Glaciology. Digital Media* .

Schopper, J. R. 2012. Porosity of rocks. *Landolt-Börnstein - Group V Geophysics Numerical Data and Functional Relationships in Science and Technology. SpringerMaterials - The Landolt-Börnstein Database* .

Seguin, M. K. and Frydecki, J. 1990. Geophysical detection and possible estimation of ice content in permafrost in northern quebec. *The Leading Edge* **9,** 25–29.

Stöffler, D. 2012. Physical properties of rocks. *Landolt-Börnstein - Group V Geophysics Numerical Data and Functional Relationships in Science and Technology. SpringerMaterials - The Landolt-Börnstein Database* .

Tiab, D. and Donaldson, E. C. 2012. Chapter 8 - naturally fractured reservoirs. In *Petrophysics (Third Edition)*, pages 485 – 552. Gulf Professional Publishing, Boston, third edition edition.

U.S. Geological Survey 1997. GTOPO30 documentation (README file). *last access: 2012-12-20, http://webgis.wr.usgs.gov/globalgis/gtopo30/gtopo30.htm* .

van Everdingen, R. O. 1998. *Multi-Language Glossary of Permafrost and Related Ground-Ice Terms*. 25 International Permafrost Association, University of Calgary.

Vonder Mühll, D. and Holub, P. 1992. Borehole logging in alpine permafrost, upper Engadin, Swiss Alps. *Permafrost and Periglacial Processes* **3,** 125–132.

Vtyurin, B. 1973. Patterns of distribution and a quantitative estimate of the ground ice in the USSR. In *Proceedings Second International Conference on Permafrost, USSR Contributions, Yakutsk, USSR, 13–28 July*, pages 159–164.

Wegmann, M. 1998. *Frostdynamik in hochalpinen Felswänden am Beispiel der Region Jungfraujoch-Aletsch*. PhD thesis, VAW, ETH Zuerich, Switzerland.

WiIliams, P. and Smith, M. 1989. The frozen earth, chapter 4: The ground thermal regime. *Cambridge University Pres* .

Ye, B., Yang, D., Zhang, Z., and Kane, D. L. 2009. Variation of hydrological regime with permafrost coverage over lena basin in siberia. *Journal of Geophysical Research* **114,** 12 pp.

Zangerl, C., Loew, S., and Eberhardt, E. 2006. Structure, geometry and formation of brittle discontinuities in anisotropic crystalline rocks of the central gotthard massif, switzerland. *Eclogae Geologicae Helvetiae* **99,** 271–290.

Zhang, T., Barry, R. G., Knowles, K., Heginbottom, J. A., and Brown, J. 2008. Statistics and characteristics of permafrost and ground-ice distribution in the northern hemisphere. *Polar Geography* **31,** 47–68.

Zhang, Y., Carey, S. K., and Quinton, W. L. 2008. Evaluation of the algorithms and parameterizations for ground thawing and freezing simulation in permafrost regions. *J. Geophys. Res.* **113,** 17 pp.

158

Table 1: List of subscripts used.

subscript	meaning
P	base
PFB	permafrost body
AL	active layer
ALD	active layer depth
A	layer A
B	layer B
L	layer boundary
b	bedrock
uf	unfractured
f	fractured
d	debris
C	class
D	temperature difference MAGST-MAAT
max	maximum
t	time
w	water
a	air
s	solid soil
RG	rock glacier
HH	pure heat conduction
SS	Stefan Solution

Table 2: D and σ_D calculated from ground surface temperatures at Schilthorn (GST debris), for boreholes drilled at crest (BH crest) and talus slope (BH talus) locations. N describes the number of measurements available.

	N	D ($^\circ C$)	σ_D ($^\circ C$)
GST debris	17	3.5	2.1
BH crest	9	2.7	1.3
BH talus	10	1.0	1.4
all	36	2.5	2.0

160

Table 3: Ground properties for unfractured ($_{uf}$) bedrock (K: thermal conductivity, κ: thermal diffusivity , Θ_o: porosity, SR : relative saturation). K and κ values are used to derive the thermal properties of fractured bedrock and debris (Table 4). Lower and upper bounds are given in brackets.

	K $(WK^{-1}m^{-1})$	κ $(10^{-7}m^2s^{-1})$	Θ_o (m^3/m^3)	SR (m^3/m^3)
bedrock$_{uf}$	2.5 (1.2, 5.8)	10 (6.0, 15.7)	0.03 (0.01, 0.06)	0.9 (0.8, 1)

Table 4: Ground properties for fractured ($_f$) bedrock and debris (Θ_o: porosity, SR: relative saturation, Z_L: depth of layer). The relative saturation was estimated for permanently frozen ground in the permafrost body ($_{PFB}$) and for the active layer ($_{AL}$) separately. Lower and upper bounds are given in brackets. K and κ are calculated as described in Sect. 3.4

	Θ_o	SR_{PFB}	SR_{AL}	Z_L
(m^3/m^3)	(m^3/m^3)	(m)		
bedrock$_f$	0.17 (0.1, 0.2)	0.9 (0.8, 1)	0.7 (0.6, 0.9)	20 (5, 30)
debris	0.4 (0.3, 0.7)	0.6 (0.5, 0.7)	0.03 (0.02, 0.05)	20 (10, 30)

Table 5: Intact rock glacier characteristics and corresponding lower and upper bounds given in brackets. I represents the average volumetric ice-content of a intact rock glacier, and Z_{RG} the averaged depth. Permafrost underneath a rock glacier body is not considered in this study.

Z_{ALD} (m)	I (m^3/m^3)	Z_{RG} (m)
3 (1, 5)	0.55 (0.47, 0.7)	25 (20, 30)

Table 6: Results for bedrock permafrost (layer A: fractured bedrock, layer B: unfractured bedrock) and different $MAGST_b$ classes. $_{HH}$ refers to the calculation based on heat conduction, and $_{SS}$ refers to the calculation that uses the Stefan Solution to determine Z_{ALD}.

$MAGST_b$ °C	A (km^2)	Z_P (m)	$Z_{ALD\,HH}$ (m)	$Z_{ALD\,SS}$ (m)	WE_{HH} (m)	WE_{SS} (m)	TWE_{HH} (km^3)	TWE_{SS} (km^3)
< -8	0.63	448.00	0.02	0.07	13.14	13.13	0.01	0.01
-8,-6	5.86	348.00	0.22	0.59	10.68	10.63	0.06	0.06
-6,-4	24.87	248.00	1.08	2.26	8.14	7.97	0.20	0.20
-4,-2	88.25	149.00	2.36	4.21	5.38	5.22	0.47	0.46
-2,0	261.24	62.00	3.42	4.44	2.60	2.58	0.68	0.68
0,2	498.84	12.00	1.12	1.69	0.54	0.64	0.27	0.32
2,4	570.26	1.00	0.09	0.38	0.02	0.08	0.01	0.04
>4	1533.95	0.00	0.00	0.00	0.00	0.00	0.00	0.00
total	2983.9	-	-	-	-	-	1.70	1.77

Table 7: Results for debris cover (layer A: debris, layer B: unfractured bedrock) and different $MAGST_d$ classes. $_{HH}$ refers to the calculation based on heat conduction, and $_{SP}$ refers to the calculation that uses the Stefan Solution to determine Z_{ALD}. The area of intact rock glaciers was subtracted from the debris area per $MAGST_d$ class to derive A.

$MAGST_d$ °C	A (km^2)	Z_P (m)	$Z_{ALD\,HH}$ (m)	$Z_{ALD\,SS}$ (m)	WE_{HH} (m)	WE_{SS} (m)	TWE_{HH} (km^3)	TWE_{SS} (km^3)
< -8	1.38	439.00	0.08	0.08	14.48	14.48	0.02	0.02
-8,-6	7.19	339.00	0.39	0.30	11.99	12.01	0.09	0.09
-6,-4	44.45	239.00	1.10	0.80	9.30	9.40	0.41	0.42
-4,-2	357.70	145.00	2.11	1.37	6.40	6.76	2.29	2.42
-2,0	2335.97	65.00	2.89	1.46	3.40	4.03	7.94	9.42
0,2	5447.41	18.00	1.11	0.68	1.03	1.45	5.64	7.90
2,4	3632.53	3.00	0.47	0.17	0.24	0.31	0.89	1.13
4,6	1440.82	0.00	0.00	0.00	0.00	0.00	0.00	0.00
6,8	1647.90	0.00	0.00	0.00	0.00	0.00	0.00	0.00
>8	175128.86	0.00	0.00	0.00	0.00	0.00	0.00	0.00
total	190044	-	-	-	-	-	17.27	21.38

Table 8: Relative deviations (RD) per parameter in relation to total water equivalent for bedrock and debris permafrost ($_{HH}$: heat conduction, $_{SS}$: Stefan Solution).

	bedrock		debris	
parameter	RD_{HH} (%)	RD_{SS} (%)	RD_{HH} (%)	RD_{SS} (%)
Qg	27.9	26.0	25.3	17.3
K_A	30.3	21.9	68.6	32.2
K_B	94.4	91.1	66.7	53.9
K_{AL}	0.0	17.8	0.0	14.6
Z_L	51.6	51.8	68.1	66.9
κ	15.6	0.0	20.5	0.0
$\Theta o\ A$	28.6	35.9	63.7	76.0
$\Theta o\ B$	85.5	80.8	60.4	47.5
SR_A	10.8	11.5	21.2	23.8
SR_B	11.4	10.8	8.1	6.3
AS	6.0	9.9	9.8	3.9
D			104.4	96.2

Table 9: Debris and intact rock glacier areas for different $MAGST_d$ classes in the European Alps (A_d: area of debris cover including intact rock glaciers, A_{relRG}: relative area of intact rock glacier occurrence per $MAGST_d$ class inclusive lower and upper quartiles in parentheses, A_{absRG}: absolute area of intact rock glaciers inclusive lower and upper quartiles in parentheses).

$MAGST_d$ (°C)	A_d (km^2)	A_{relRG} (%)	A_{absRG} (km^2)
< -8	1.38	0 (0, 0)	0 (0, 0)
-8,-6	7.19	0 (0, 0)	0 (0, 0)
-6,-4	44.45	0 (0, 0)	0 (0, 0)
-4,-2	359.38	0.47 (0.01, 0.17)	1.68 (0.05, 0.62)
-2,0	2376.90	1.72 (1.28, 2.13)	40.93 (30.46, 50.51)
0,2	5579.35	2.36 (1.77, 2.91)	131.94 (98.79, 162.53)
2,4	3676.96	1.21 (0.57, 1.85)	44.43 (20.92, 68.03)
4,6	1444.95	0.29 (0.03, 0.48)	4.13 (0.41, 6.96)
6-8	1647.98	0 (0, 0)	0.07 (0, 0)
>8	175128.86	0 (0, 0)	0 (0, 0)
total	190267.41	6.05 (3.66, 7.54)	223.18 (150.64, 288.65)

Table 10: Relative deviation (RD) per parameter in relation to total water equivalent for intact rock glaciers.

parameter	RD (%)
area	62
Z_{ALD}	18
Z_{RG}	45
I	42

Part III

Appendix

Personal bibliography

Peer-reviewed publications

Cremonese, E., Gruber, S., Phillips, M., Pogliotti, P., Boeckli, L., Noetzli, J., Suter, C., Bodin, X., Crepaz, A., Kellerer-Pirklbauer, A., Lang, K., Letey, S., Mair, V., Morra di Cella, U., Ravanel, L., Scapozza, C., Seppi, R., and Zischg, A. (2011). Brief Communication: "An inventory of permafrost evidence for the European Alps". *The Cryosphere*, 5 (3): 651–657. doi: 10.5194/tc-5-651-2011.

Boeckli, L., Brenning, A., Gruber, S., and Noetzli, J. (2012a). A statistical approach to modelling permafrost distribution in the European Alps or similar mountain ranges. *The Cryosphere*, 6 (1): 125–140. doi: 10.5194/tc-6-125-2012.

Boeckli, L., Brenning, A., Gruber, S., and Noetzli, J. (2012b). Permafrost distribution in the European Alps: calculation and evaluation of an index map and summary statistics. *The Cryosphere*, 6 (4): 807–820. doi: 10.5194/tc-6-807-2012.

Schöner, W., Boeckli, L., Hausmann, H., Otto, J., Reisenhofer, S., Riedl, C., and Seren, S. (2012). Spatial patterns of permafrost at Hoher Sonnblick (Austrian Alps) - Extensive field-measurements and modelling approaches. *Austrian Journal of Earth Sciences*, 105(2): 154–168.

Publications without peer review

Mair, V., Zischg, A., Lang, D., K. andTonidandel, Krainer, K., Kellerer-Pirklbauer, A., Deline, P., Schoeneich, P., Cremonese, E., Pogliotti, P., Gruber, S., and Boeckli,

L. (2011). PermaNET - Permafrost Long-term Monitoring Network. 1, Report 3. Klagenfurt. *Synthesis report. Interpraevent Journal series*, 1.

Boeckli, L. and Noetzli, J. (2011). Wenn die Permafrostverbreitung auch für Laien fassbar wird. *Geosciences Actuel*, 4: 14–16.

Curriculum Vitae (short version)

Personal details

First names:	Lorenz Reto
Last name:	Böckli Wirz
Date of birth:	20 October, 1980
Place of birth:	Winterthur, Switzerland
Citizenship:	Swiss

Education

2008–2012	PhD student at the Department of Geography, University of Zurich
2006–2010	Higher education in Geography, University of Zurich Education for grammar school teacher in Geography
2011	Diploma in higher eduction for Geography, University of Zurich
2002–2008	Studies in Geography at the University of Zurich Specialization: Physical Geography, Glaciology, Remote Sensing and GIS Thesis: *Deposition of small and frequent avalanches* (in German)
2008	Master of Science in Geography, University of Zurich
1996–2001	Grammar School at the Kantonsschule im Lee, Winterthur, Switzerland
2001	Matura Typus Lehramt

Acknowledgements

During my PhD I have been supported and accompanied by numerous people I would like to thank here:

Stephan Gruber supported me from the beginning of my Diploma work to the end of my PhD. I am very thankful for the large amount of time he spent to help me during this period. I benefitted a great deal from his critical and constructive assistance and his general enthusiasm was very motivating. Jeannette Nötzli was an enormous help during my PhD and her door was always open for me. Numerous discussions with her helped me a lot to navigate trough my PhD and her critical view on my manuscripts helped to improve them significantly. Additionally, I am very grateful for the unforgettable moments I spent with Stephan and Jeannette at various research sites in the Swiss mountains.

Special thanks goes to Wilfried Haeberli. During my studies, my work as teaching assistant and my PhD, he always was a great support. His vast experience and knowledge helped me in various situations and his helping and motivating mind are deeply acknowledged.

Further, I would like to thank Alexander Brenning for his great support. His critical and very detailed review of my manuscripts as well as his general recommendations regarding scientific methods and writing are here appreciated. The visit at the University of Waterloo, Canada was one of the most exciting moments during my PhD.

My PhD was embedded in the European Alpine-space project PermaNET (`http://www.permanet-alpinespace.eu`), and I would like to thank all involved people. My special thanks go to Andreas von Poschinger, Claudia Riedl, Eduardo Cremonese, Paolo Pogliotti, Matteo Dall'Amico, and Marcia Phillips for their support and interest in my research. The field work in the 'Nationalpark Berchtesgaden' would not have been possible without the support of Helmut Franz and his ranger-team. Many thanks to Silvan Rieben, Martin Böckli and Marlene Scheel for their assistance during fieldwork.

A warm thanks goes to my office mates and the entire 3G-group for the great working atmosphere, many scientific discussions and amazing field trips. Particular thanks goes

to Andreas Hasler for interesting discussions and unforgettable moments at Jungfraujoch and Hörnli Ridge, to Stefanie Gubler and Joel Fiddes for an intensive collaboration, and Stefano Endrizzi for his support with GEOtop. Holger Frey provided me the latex template for this thesis, which saved me a lot of time, thanks a lot. Further, I would like to thank Ronald Schmidt for his help with the ArcGIS Server and the possibility to provide an online solution for the Alpine-wide permafrost index map.

Furthermore, I am grateful for the work of two internship students, Arthur Lutz and Christian Gschwend, who helped me a lot in data preprocessing for compiling the Alpine Permafrost Index Map (APIM).

Finally, the warmest thanks are addressed to my wife Vanessa, my parents, my brothers and my friends. They all supported me strongly during good and sometimes hard times and helped me to not forget the life beside the PhD.

The present study was funded by the Alpine Space project PermaNET by the following project partners: the Bavarian Environment Agency (LfU Bayern), Germany, the Central Institute for Meteorology and Geodynamics in Salzburg (ZAMG), Austria, and the Federeal Office for the Environment (FOEN), Switzerland. To finally finish the thesis, additional funding was provided by the Swiss permafrost monitoring network (PERMOS).